The University of Nottingham

Department of Civil Engineering

Division of Infrastructure and Geomatics

Modelling and Visualisation to Support Decision-making in Air Quality-related Transport Planning

by

El-Said Mamdouh Mahmoud Zahran

(BSc, MSc)

Thesis submitted to the University of Nottingham

for the degree of Doctor of Philosophy

November 2010

Abstract

This thesis introduces three main elements to support decision-making in air quality-related transport planning. The first are novel automatic collection and processing algorithms for traffic flow and geospatial data for input to air pollution models of transport schemes under analysis. The second is a novel strategy to improve the modelling of air quality by the calibration of input background concentrations. The third is a novel 3D air pollution dispersion interface for the 3D visualisation of the air quality predictions in 3D digital city models.

Four urban transport schemes were used for the initial development of, and for testing, the applicability and validation of future air quality predictions of the decision-support system based on the above three elements. The automation of the input data collection and processing reduced significantly the time and effort required to set up the air pollution model. The calibration of background concentrations significantly improved the accuracy of, not only the annual mean, but also the hourly, air quality predictions and effectively reduced the model runtime. The 3D air pollution dispersion interface provided an intuitive 3D visualisation of the air quality predictions at and above the ground surface in a single 3D virtual scene. The application of this decision-support system enabled the development of alternative future traffic scenarios so a proposed urban transport scheme might contribute to achieving certain air quality objectives. The validation of the future air quality predictions showed that the methods used for the future projection of air pollution input data slightly increase the error between the modelled and actual annual mean NO_2 future concentrations. They also significantly increase the error between the modelled and actual hourly NO_2 future concentrations.

Contents

List of Figures

List of Tables

List of Acronyms

AADT	Annual Average Daily Traffic
ADMS	Atmospheric Dispersion Modelling System
APDM	Air Pollution Dispersion Modelling
AQAP	Air Quality Action Plan
AQMA	Air Quality Management Area
AQMS	Air Quality Monitoring Station
AQO	Air Quality Objective
AURN	Automatic Urban and Rural Network
BPR	Bureau of Public Roads
CASA	Centre for Advanced Spatial Analysis
CERC	Cambridge Environmental Research Consultants
CRS	Chemical Reaction Scheme
DA	Detailed Assessment
DEFRA	Department for Environment, Food and Rural Affairs
DMRB	Design Manual for Roads and Bridges
DTM	Digital Terrain Model
ERG	Environmental Research Group
FAC	Monthly and Hourly Traffic Flow Factors

GIS	Geographic Information System
HCI	Human-Computer Interaction
HDV	Heavy Duty Vehicles
HGV	Heavy Good Vehicles
LDV	Light Duty Vehicles
LGV	Light Good Vehicles
LOD	Level of Details
LPS	Leica Photogrammetry Suite
LTP	Local Transport Plan
LURM	Land Use Regression Modelling
NAEI	National Atmospheric Emissions Inventory
NET	Nottingham Express Transit
PSV	Public Service Vehicles
QMC	Queens Medical Centre
RMSE	Root Mean Square Error
TIN	Triangular Irregular Network
USA	Updating and Screening Assessment
VBA	Visual Basic for Applications
VRM	Virtual Reality Modelling

Publications

ZAHRAN, E.S., BENNETT, L. and SMITH, M., 2010. An approach to represent air quality in 3D digital city models for air quality-related transport planning in urban areas. In Computing in Civil and Building Engineering, Proceedings of the International Conference, W. TIZANI (Editor), 30 June-2 July, Nottingham, UK, Nottingham University Press, Paper 10, p. 19, ISBN 978-1-907284-60-1.

The Young European Arena of Research (YEAR 2008), Ljubljana, Slovenia, Extended Abstract on "Modelling Air Pollution Impacts of Urban Traffic Management Schemes".

Acknowledgement

In the name of Allah, most Gracious, most merciful

First of all, I would like to acknowledge the financial support of the Ministry of Higher Education, Egypt. I also acknowledge the help of the IESSG in providing the Dunkirk and Nottingham City Centre's aerial photography, the Nottingham City Council for supplying air pollution input and monitoring data of the Dunkirk and Nottingham City Centre.

My extraordinary gratitude goes to my supervisors, Dr. Lloyd Bennett and Dr. Martin Smith, for guiding me through this research, Dr. Nikolaos Kokkas for sharing with me so much of his knowledge about GIS and 3D city modelling, the Pollution Control and Transport sections in Nottingham City Council for the help with the air pollution model set-up and the traffic flow data of the transport case studies and the Division of Geomatics and Infrastructure in the University of Nottingham for funding me to publish a research paper in the International Conference on Computing in Civil and Building Engineering 2010.

I want to thank CERC for giving me a trial license to ADMS-Urban and for helping with the technical issues of ADMS-Roads. I also like to thank my entire family for being there during the ups and downs of my research, and for making the time during my studies so enjoyable. Also, special thanks go to all the friends who provided support throughout the research project.

Chapter 1

Introduction

1.1 Background and Issues

The recent estimates for Great Britain have indicated a growth in urban motor traffic (excluding motorcycles) from 1996 to 2031 of 50% (DETR, 2006). The growth of urban traffic levels is associated with a broad range of problems such as traffic congestion, air pollution, traffic noise, reduced accessibility and community severance. However, tackling the traffic congestion is deemed the main contributing factor in resolving the other traffic growth-related problems (NCC and NCC, 2006). Without intervention, increased mobility and longer journeys due to the growth of cities were estimated to raise the levels of congestion in urban areas by 15% from 2000 to 2010 (NCC and NCC, 2006).

The predominance of the private car is a major contributor to the current and future congestion levels in urban areas (Pooley and Turnbull, 2005). The growth in incomes and the enhanced personal mobility, due to the personal freedom offered by the car, have resulted in high levels of private car ownership (Davison and Knowles, 2006). This has encouraged the dispersal of amenities and activity sites which has in turn motivated the greater use of private cars as access is no longer easily available by public transport. Therefore, those without access to a private car are often disadvantaged leading to social inequalities. However, those with access to a private car often lose time, miss opportunities and feel frustrated due to the traffic congestion.

Many urban transport schemes developed by local authorities involve changing the physical infrastructure to improve the traffic flow and/or to encourage the use of alternatives to the private car, in order to reduce traffic congestion and to reduce the associated problems resulting from traffic growth, such as worsening air pollution. Greater Nottingham constitutes one of the urban areas where a number of transport schemes have been implemented, and others will be implemented, as part of the local transport plan for Greater Nottingham (NCC and NCC, 2006). Further details about the transport schemes of Greater Nottingham can be found in Chapter 2Sections 2.6 and 2.7.

Road traffic is realised to be the major contributor to the air pollution in urban areas (Madsen et al., 2007). The air pollution in urban areas, where the population exposure to traffic emissions is the maximum, currently causes about 800,000 premature deaths per annum worldwide (Curtis et al., 2006). Jalaludin et al. (2004) have found that there are associations between particles of 10 micrometers or less (PM_{10}) levels and doctor visits for asthma. In addition, they have reported an association between Nitrogen Dioxide (NO_2) levels and the prevalence of wet cough amongst the Australian primary school children.

Sun et al. (2006) evaluated the relationship between air pollution and asthma exacerbation amongst children and adults. They found amongst children that there were significant positive correlations between NO_2, Carbon Monoxide (CO), PM_{10} levels and emergency visits for asthma. However, amongst adults, no significant correlation between any of these air pollutants and emergency visits for asthma was found. Sandstrom and Brunekreef (2007) have found that traffic-related air pollution is the primary cause of the reduction in the lung development of children.

Not only respiratory illnesses but also cancer has been found amongst children to be associated with traffic-related air pollution in urban areas (Ruchirawat et al., 2007). Polycyclic aromatic hydrocarbons and benzene are the most carcinogenic compounds found in urban traffic air pollution emissions. The exposure to these genotoxic substances adversely affected the DNA damage levels and repair capacity which has increased the incidence of cancer.

Furthermore, air pollution is closely intertwined with the climate change (Noyes et al., 2009). Climate change is primarily caused by the greenhouse gases, the majority of which are emitted by the road traffic. The climate change impacts on the human health comprise increased death and injury associated with more severe and frequent heat waves, extreme weather events, and enhanced vector-borne and allergic disease transmission. In addition, due to the climate change, ozone and PM levels are forecast to increase, particularly in urban areas which are polluted and subject to less precipitation and stagnant atmospheric circulation patterns.

This was further investigated by Athanassiadou et al. (2010) who used ADMS-Urban, an air pollution model, to predict the future impacts of climate change on air quality in London. The future air quality was predicted by using meteorological input data from simulation of a plausible future climate for the period ~2070 - 2090. The future rise in temperature and specific humidity due to climate change increased the future ozone and subtly increased the future PM_{10} levels in London. Meanwhile, such a rise in future temperatures exacerbates mortality and morbidity from cardio-respiratory disease in humans exposed to ozone and PM.

Air pollution dispersion modelling may be used to model the air quality impact of proposed urban transport schemes. The results of air pollution

dispersion modelling should be accurate enough to provide reliable air quality predictions. Some recent air pollution dispersion modelling research went into the validation of air pollution modelling results by the determination of the error between calculated and corresponding monitored air pollution concentrations. However, this recent research did not investigate potential sources of this error so that it could be minimised (Cai and Xie, 2010;Ginnebaugh et al., 2010;Majumdar et al., 2009;Parra et al., 2010;Namdeo et al., 2002;Namdeo and Colls, 1996).

Some additional challenges, identified in recent air pollution dispersion modelling research, include the labour-intensive processing of input data to air pollution dispersion models (Cheng and Chang, 2009;Wang et al., 2008;Wang, 2005). Also identified was the long air pollution model runtime which may extend to several days (Barrett and Britter, 2009, 2008). The long time-demanding input data processing and running of air pollution dispersion models tend to limit the number of design alternatives of the proposed urban transport scheme for which the air quality impacts may be investigated.

Visualisation of modelled air quality, both before and after scheme implementation, should help transport planners and decision-makers to select the transport scheme design alternative that maximises the air quality benefits and/or minimises the adverse air quality impacts. Having high quality visualisation of air pollution may be very helpful in public consultations which are nowadays an increasingly important part of the planning and decision-making processes. Currently, the results of air pollution dispersion modelling are usually displayed by overlaying 2D coloured contour maps of the air pollution concentrations over 2D digital maps of the interest area in a Geographic Information System (GIS) (PCS, 2010;CERC, 2010). However, this may not be intuitively meaningful for all

the different people who constitute the participants in the public consultations about proposed urban transport schemes.

Using the traditional 2D contour maps to recognise the change of pollution concentrations with height requires the creation of many scenes, one at each height. This has the potential to confuse the observer with such a large number of 2D scenes and may not provide the best understanding of the changes in pollution concentrations with height, as is explained in more detail in Section 7.1. Therefore, the full 3D visualisation of various air pollution concentrations at and above the ground surface in a single 3D virtual scene may achieve improvements in relation to two important factors regarding Human-Computer Interaction (HCI), namely increased information retention and shortened comprehension time (Sears and Jacko, 2008).

1.2 Research Questions

Considering the issues discussed in Section 1.1, the following research questions naturally arise:

- How can the processing of input data to air pollution dispersion models be improved, in order to reduce the processing time and effort?
- How can the error between modelled and corresponding monitored air pollution concentrations be minimised, while reducing the air pollution model runtime?
- Can an air pollution dispersion model and a 3D digital city model be integrated so that modelled air quality, at and above the ground surface, can be visualised intuitively in a single 3D scene, in order to overcome the 2D visualisation issues, increase information retention and shorten comprehension time?

If all the above three questions can be answered positively, then logical fourth and fifth questions are:

- Can the resulting modelling capability provide, with acceptable levels of statistical confidence, estimates of future air quality predictions?
- Is this resulting modelling capability transferrable to a wide range of urban transport schemes in different geographical locations?

1.3 Aim and Objectives

With the research questions presented in Section 1.2 in mind, the overall aim of this research was an investigation into an effective decision-support system to assist air quality-related transport planning based on the deep integration between an air pollution dispersion modelling system and a 3D digital city model. Repeatability and flexibility are required to allow for the application to different urban transport schemes. The effectiveness of such a decision-support system depends on the calibration and validation of the air pollution dispersion modelling system, so that it enables decision-makers and transport planners to predict accurately, and hence reliably, the air quality impacts of the proposed urban transport schemes. This effectiveness is increased by automating the processing of the traffic, and geospatial, data input to the air pollution dispersion modelling system. This decreases the time required for setting up the air pollution dispersion modelling system, and hence may facilitate the investigation of the air quality impacts of numerous design alternatives for the transport scheme. Such automation of the processing may also eliminate inconsistency in air pollution modelling results, which usually arises from having different levels of confidence in data measurement, and vulnerability to error, among individuals involved in the manual input and data processing, and allow increased resolution, leading to more accurate air quality predictions.

Furthermore, the effectiveness of this decision-support system arises from the representation of the air quality impacts of the proposed urban transport scheme in a 3D digital city model (a 3D georeferenced virtual environment). The link to GIS assigns the air pollution data the true 3D spatial extension at and above the ground surface in this 3D georeferenced virtual environment. This provides an intuitive 3D visualisation opportunity and may improve the communications and ideas exchange among participants with different types and/or levels of expertise during transport planning consultation exercises. Consequently, this decision-support system may support the stakeholders to select the design alternative of a proposed urban transport scheme that maximises its air quality benefits and/or minimises its adverse air quality impacts.

To meet this aim the objectives were as follows:

1. Investigation into current challenges in air pollution dispersion modelling and visualisation.
2. Research into algorithms to automate the processing of large files of high resolution traffic, and geospatial, data for input to the air pollution dispersion model.
3. Research into the optimum set-up of the air pollution model.
4. Calibration of the air pollution dispersion model, and development of a validation strategy for the air quality predictions, against air quality monitoring data, before and after the implementation of a transport scheme, based on the application of ADMS-Roads.
5. Development of a 3D air pollution dispersion interface based on the representation of the output results of ADMS-Roads, before and after the implementation of the transport scheme, in a 3D digital city model.
6. Investigating the feasibility of using the decision-support system to determine the future traffic flow/speed changes needed, in addition to

those anticipated due to a proposed transport scheme, in order to increase its air quality benefits.

7. Testing the transferability of the developed decision-support system to a range of transport schemes.

1.4 Methodology

In order to achieve the research aim and objectives presented in Section 1.3, the following individual tasks were undertaken:

- A review of the published research literature relating to transport-induced air pollution modelling and visualisation. (objective 1)
- The identification of urban transport schemes which could be used for the initial development of the research decision-support system, testing its transferability as shown in Chapter 9 and validating its future air quality predictions as shown in Chapter 10, by the application of a number of identified selection criteria. (objectives 2, 3, 4, 5, 6 and 7)
- The identification of the air pollution model application area for the initial development of the research decision-support system. (objectives 2, 3, 4 and 5)
- The development, and computer programming implementation of, mathematical algorithms to automate the processing of the traffic, and geospatial, data of the modelled road network in the air pollution model application area. (objective 2)
- The identification of the air pollutant to model, the collection of other input data to the air pollution model, trying many alternatives for the output grid design and output heights above the ground surface and the evaluation of these design alternatives. (objective 3).

- The calibration and validation of the air pollution model base case scenario using the available monitoring data. (objective 4)
- The representation of the air quality predictions of the air pollution model base case scenario in the 3D city model in order to build the 3D air pollution dispersion interface of the base case. (objective 5)
- The identification of criteria to develop the 3D air pollution dispersion interface based on research in the literature and personal communications as well as the principles and guidelines of HCI. (objective 5)
- The projection of the traffic input data to create two future traffic scenarios for with and without the proposed urban transport scheme. (objectives 4 and 5)
- The projection of background air pollution concentrations using the Year Adjustment Calculator (AEA, 2008), and traffic emission rates using the 2003 DMRB traffic emission factors (DMRB, 2007), to the modelling year of the future traffic scenarios, and the running of the air pollution model to predict the air quality for the two future air quality scenarios. (objectives 4 and 5)
- Updating the 3D city model to represent the future additional features associated with the implementation of the planned urban transport scheme. (objective 5)
- The creation of 3D air pollution dispersion interfaces for the two future air quality scenarios. (objective 5)
- The application of the research decision-support system to develop alternative future traffic scenarios for the proposed urban transport scheme that maximise its air quality benefits and/or minimise its adverse air quality impacts. (objective 6)

- The assessment of the transferability of the research decision-support system to two more proposed urban transport schemes. (objective 7)
- The application of the research decision-support system to an already implemented urban transport scheme in order to attempt to validate the future air quality predictions of the decision-support system. (objective 4)

1.5 Contribution to Knowledge

The overarching contribution to knowledge of this research project is the deep integration between traffic-induced air pollution dispersion models and 3D digital city models to create and develop an effective decision-support system for air quality-related transport planning.

This research project developed two new GIS tools which were implemented by computer programming to automate the collection and processing of the geospatial data input to the air pollution dispersion model. This data represents the geographical coordinates of the centreline vertices of the road network in the air pollution model application area. Furthermore, these new GIS tools introduce the concept of 'level-of-details' to the science of air pollution dispersion modelling. This was accomplished by the implementation of a novel mathematical algorithm to impose a minimum allowable distance between the vertices of each section of road centreline that are considered in the air pollution model (see Sections 9.4 and 10.4 for details).

The accuracy, and thus reliability, of air quality predictions and the runtime of the air pollution model have been improved in this research project by the introduction of four new concepts to the science of air pollution dispersion modelling, namely macro-calibration, macro-validation, micro-

calibration and micro-validation. The iterative application of the macro-calibration mathematical model to background concentrations minimises the error between the annual means of the hourly sequential monitored and calculated concentrations (see Section 6.4.1 for more details). The macro-validation is the determination process of such an error after each iteration of the macro-calibration. The macro-calibration is an easy and quick alternative if the modeller is only interested in getting reliable predictions for the annual mean air pollution concentrations.

The iterative mathematical model of micro-calibration builds upon the results of the macro-calibration to minimise the error between not only the annual means but also the hourly sequential monitored and calculated air pollution concentrations. Micro-validation is the process of the evaluation of such an error between the hourly sequential monitored and calculated air pollution concentrations and this process is used to decide the final acceptable iteration of the micro-calibration (see Figure 6.4 for details).

This research project has introduced a novel approach to generate and represent the output air pollution concentrations of air pollution dispersion models in 3D digital city models. This has resulted in a 3D air pollution dispersion interface that shows the air pollution at and above the ground surface in a single 3D virtual scene. Firstly, the air pollution has been visualised as a 3D point array, with each point as a colour reflecting the air pollution concentration value at this point, as shown in Figures 7.13 to 7.16. However this development was found not to be particularly intuitively meaningful, so the design of the interface has been developed through the specification and application of suitable customisation criteria for the 3D digital features of this interface, in order to attain an intuitive visualisation of air pollution dispersion in the 3D city model. The final development stage of the 3D air pollution dispersion interface rendered the air pollution

as volumetric grey clouds, using ordinary people's (negative) perceptions of grey clouds representing poor weather: the darker the clouds, the worse is the weather (see Section 7.5 for details).

This research has introduced a new strategy to help develop alternative future traffic scenarios for a proposed urban transport scheme to maximise its air quality benefits. These traffic scenarios have been developed by altering the traffic flow and/or speed in order to eliminate the exceedance of the national air quality objective for the annual mean of NO_2 concentrations, after the implementation of the transport scheme, in the air pollution model application area. This provides some additional insight for transport planners into the correlation between traffic flow, traffic speed and air quality (see Section 8.4 for details).

This research project has introduced a novel approach to validation of future air quality predictions after the projection of emissions in the future which was identified as being impossible by Smit et al. (2010). This approach is based on the application of the air pollution dispersion model to an area in which the air quality is affected by an already completed transport scheme, which involved a significant reduction in the amount of traffic (except buses) on certain roads in Nottingham City Centre, as explained in section 2.6.3. Relevant air quality monitoring data were available for before and after the implementation of the completed transport scheme. The monitoring data before the implementation of the transport scheme is used for the calibration and validation of a past base case scenario for the air pollution model, corresponding to a base year (before scheme implementation) some years ago. Then, this base case scenario is projected into the future, to after the implementation of the transport scheme, in order to predict the air quality at a more recent past

time. The available monitoring data at this more recent past time is then used for the validation of the air pollution model future air quality predictions (see Chapter 10 for details). This may help to identify the contribution of each projected item of the air pollution input data to the error between monitored and calculated concentrations due to the projection. Consequently, this may lead to developing calibration strategies for the future projection methods.

1.6 Thesis Outline

This thesis outline is provided in order to assist the reader's understanding of the presentation of the various stages of this research.

Chapter 1 gives an introduction about the research project.

Chapter 2 contains a literature review about the national air quality standards and geographical areas in Greater Nottingham in which the air pollution levels exceed the standards. This gives the reader the required information about the air pollution model application areas which are considered in this research project. In addition, this chapter provides a background about the urban transport schemes in Greater Nottingham that could be considered in this research project.

Chapter 3 compares different air pollution modelling options in order to select the most suitable option and system for this research. The chapter then continues to address the limitations in recent air pollution modelling validation and verification. Moreover, this chapter reviews the current visualisation strategies of air pollution dispersion data and addresses limitations of, and challenges identified by, these strategies.

Chapter 4 gives the selection criteria applied to Greater Nottingham's transport schemes which are considered in this research. Then the urban transport schemes to be used as case studies in the different stages of this research project are selected.

Chapter 5 presents the details of processing traffic data for input to the air pollution model during the initial development stage of this research decision-support system. Also, this chapter explains the adopted strategy to project the processed traffic input data into the future, to after the implementation of the urban transport scheme identified for this development stage.

Chapter 6 presents the set-up of the air pollution model 'base case scenario' (details of the area where a transport scheme may be implemented, and all the modelling input data required, for a base year before the scheme's implementation, for which relevant air pollution monitoring data is available) and discusses the development of the calibration methodology. The chapter then presents the mathematical model of macro-calibration and micro-calibration and describes the methodology of macro-validation and micro-validation. Furthermore, this chapter explains the horizontal and vertical design of the air pollution model output grid in order to allow the generation and representation of the air quality output data of the base case scenario in the 3D city model.

Chapter 7 develops customisation criteria to design a good interface. Then this chapter illustrates the design of the 3D air pollution dispersion interface and applies the customisation criteria to develop this design.

Chapter 8 projects the air pollution input data of the air pollution model base case scenario into the future, to after the implementation of the

identified urban transport scheme for the initial development of this research decision-support system. Then, the developed decision-support system is applied to predict and visualise the future air quality impacts of this transport scheme. The chapter also investigates the use of this research decision-support system for developing alternative future traffic scenarios for this transport scheme that may increase its air quality benefits.

Chapter 9 evaluates the transferability of this research decision-support system to other urban transport schemes. This comprises the illustration of the development, and computer programming implementation, of the first new GIS tool that automates the collection and processing of geospatial data for input to the air pollution dispersion model.

Chapter 10 investigates the validation of future air quality predictions of this research decision-support system. This includes the description of the development, and computer programming implementation, of the second new GIS tool that automates the collection and processing of geospatial data for input to the air pollution dispersion model.

Chapter 11 summarises and critically evaluates the findings of this research project, in order to present the merits, and specify the limitations, of the developed methods for air pollution modelling and visualisation. Then, the chapter identifies possible directions for further research.

Chapter 2

Air Quality and Transportation Policies of Greater Nottingham

2.1 Introduction

This chapter contains a literature review about the air quality management policy of Greater Nottingham. This involves a background about the UK national air quality standards and the geographical areas in Greater Nottingham in which the air pollution levels exceed these standards. The background covering some of these areas supplies an overview of the transport case studies for the air pollution modelling undertaken in this research project. The chapter also reviews the air quality monitoring in the City of Nottingham. The review of this information provides the necessary background concerning the monitoring stations whose data is subsequently used for the calibration and validation of the air pollution models used in this research.

This chapter also provides a background about the recent local transport plan for Greater Nottingham. This includes a review of the urban transport schemes that are implemented, and will be implemented, in Greater Nottingham during the period April 2006 - March 2011, from which the transport case studies of this research project are subsequently selected.

2.2 Air Quality Policy of Greater Nottingham

According to The Air Quality (England) Regulations 2000, the local authorities in Greater Nottingham are required to review and assess the local air quality against seven pollutants (PCS, 2001). The Air Quality (England) Regulations 2000, as amended, specify the Air Quality Objectives (AQOs) for the seven pollutants, to be attained by the due date for each pollutant as shown in Table 2.1 (PCS, 2003).

Table 2.1 The Air Quality (England) Regulations 2000 (as amended) Source: (PCS, 2003)

Substance	Air quality objective levels	Air quality objective dates
Benzene	16.25 micrograms per cubic metre or less, when expressed as a running annual mean 5 micrograms per cubic metre or less, when expressed as an annual mean	31st December 2003 31st December 2010
1,3 Butadiene	2.25 micrograms per cubic metre or less, when expressed as a running annual mean	31st December 2003
Carbon Monoxide	10 milligrams per cubic metre or less, when expressed as a maximum daily running 8 hour mean	31st December 2003
Lead	0.5 micrograms per cubic metre or less, when expressed as an annual mean 0.25 micrograms per cubic metre or less, when expressed as an annual mean	31st December 2004 31st December 2008
Nitrogen Dioxide	200 micrograms per cubic metre, when expressed as an hourly mean, not to be exceeded more than 18 times a year 40 micrograms per cubic metre or less, when expressed as an annual mean	31st December 2005 31st December 2005

PM_{10}	50 micrograms per cubic metre or less, when expressed as a 24 hour mean, not to be exceeded more than 35 times a year	31st December 2004
	40 micrograms per cubic metre or less, when expressed as an annual mean	31st December 2004
Sulphur Dioxide	125 micrograms per cubic metre or less, when expressed as a 24 hour mean, not to be exceeded more than 3 times a year	31st December 2004
	350 micrograms per cubic metre or less, when expressed as an hourly mean, not to be exceeded more than 24 times a year	31st December 2004
	266 micrograms per cubic metre or less, when expressed as a 15 minute mean, not to be exceeded more than 35 times a year	31st December 2005

In order to assess the air quality against the required objectives, three elements should be delivered sequentially over a period of three years as follows (PCS, 2004):

- An Updating and Screening Assessment (USA) for identifying those aspects that have changed since the preceding round of reviews and assessments.
- A Detailed Assessment (DA) of those pollutants and specific locations that are identified in the USA as requiring further work.
- A Progress Report detailing developments and changes in the authority's area that may affect air quality and progress made towards improving air quality.

According to the regulations, the review and assessment process should take place in areas of likely public exposure to the air pollution (PCS, 2004). In terms of the 24-hour objectives, the relevant assessment locations are those where members of the public are probably exposed for

8 hours or more in a day. For the annual mean objectives this might be where people are exposed for a cumulative period of 6 months in a year (PCS, 2004).

2.3 Air Quality Management Areas in Greater Nottingham

According to section 83 of the Environment Act 1995, the local authorities are required to specify Air Quality Management Areas (AQMAs) where an AQO will not be achieved by the due date (PCS, 2003). In addition, it requires the local authorities corresponding to specify Air Quality Action Plans (AQAPs) to the declared AQMAs. These plans present the actions to be taken to achieve the AQOs in the declared AQMAs along with a timetable for implementing the plans (PCS, 2003).

The detailed assessment and progress report produced by Nottingham City Council in September 2001 identified three AQMAs. These three areas were identified by using the Atmospheric Dispersion Modelling System (ADMS-Urban) as follows (PCS, 2001):

1. Area comprising, and to the east of, the City Hospital (sulphur dioxide).
2. City centre north, east and south (nitrogen dioxide).
3. Dunkirk / Clifton Boulevard encompassing the Queen's Medical Centre site (nitrogen dioxide).

The pollutant of concern for the first AQMA is sulphur dioxide which principally emerges from the major combustion plant at the Nottingham City Hospital. The pollutant of concern for both the second and third AQMAs is Nitrogen Dioxide (NO_2) which is emitted primarily from the road traffic

(PCS, 2001). Figure 2.1, Figure 2.2 and Figure 2.3 depict the three declared AQMAs.

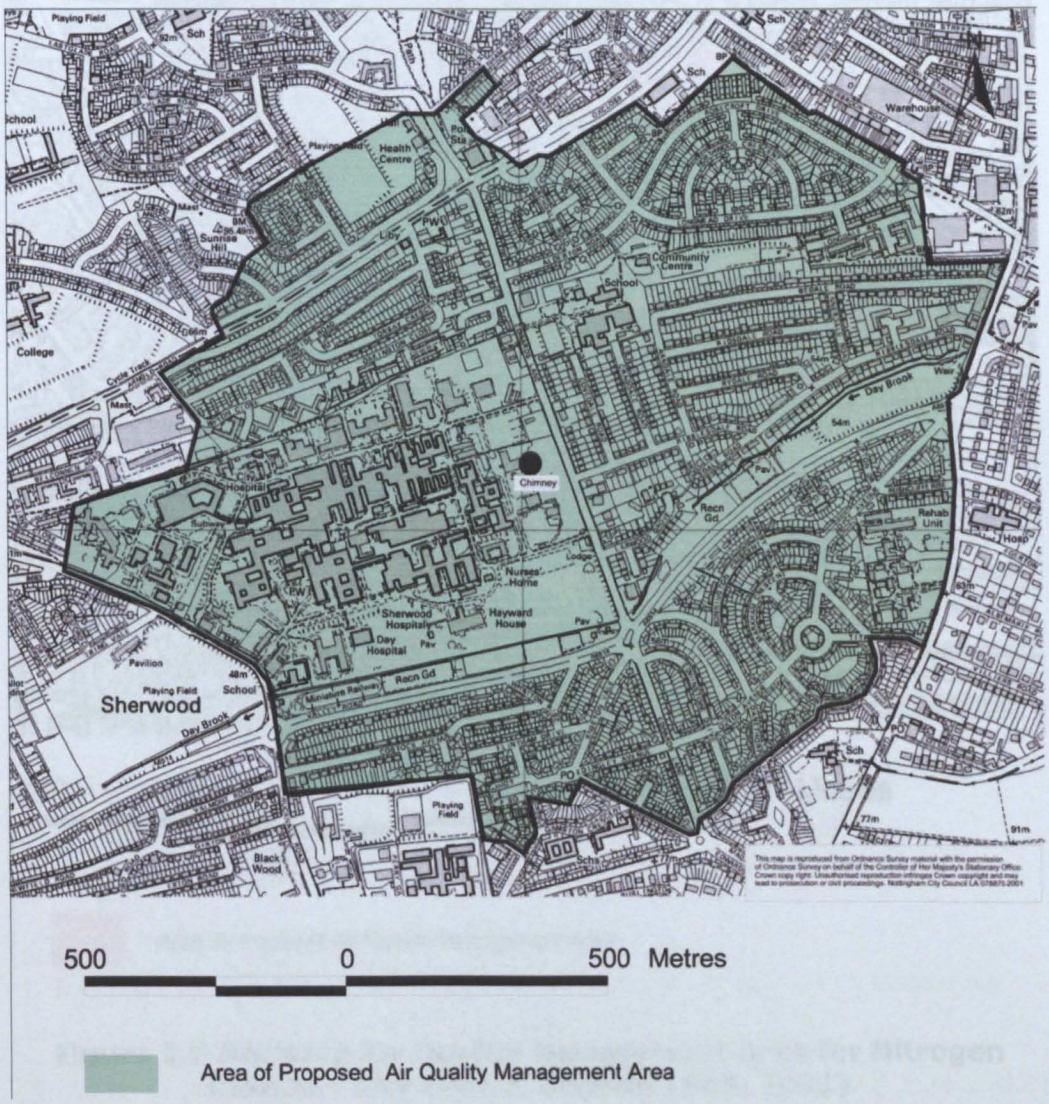

Figure 2.1 Declared Air Quality Management Area for Sulphur Dioxide, Source: (PCS, 2001)

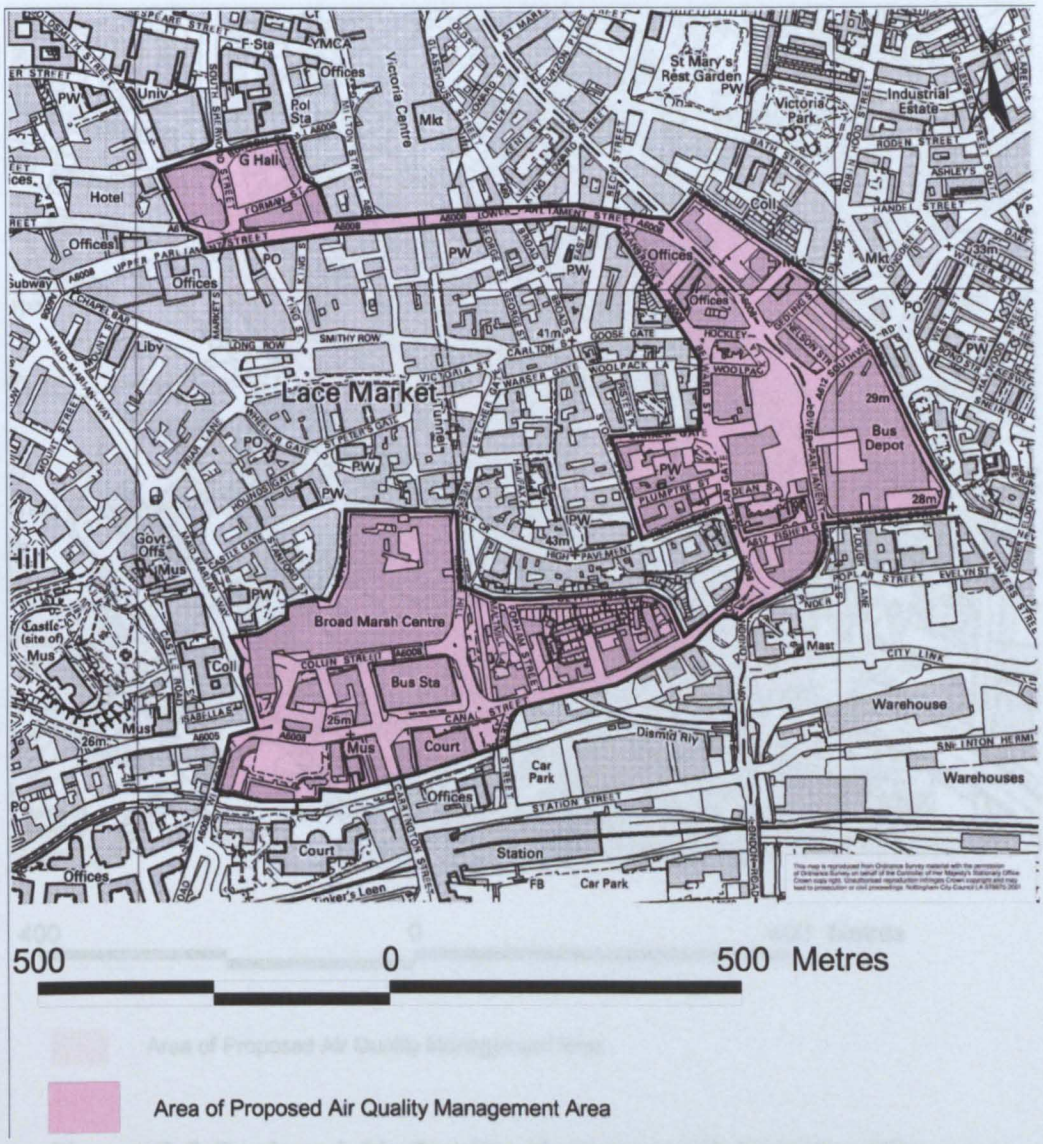

Figure 2.2 Declared Air Quality Management Area for Nitrogen Dioxide - City Centre, Source: (PCS, 2001)

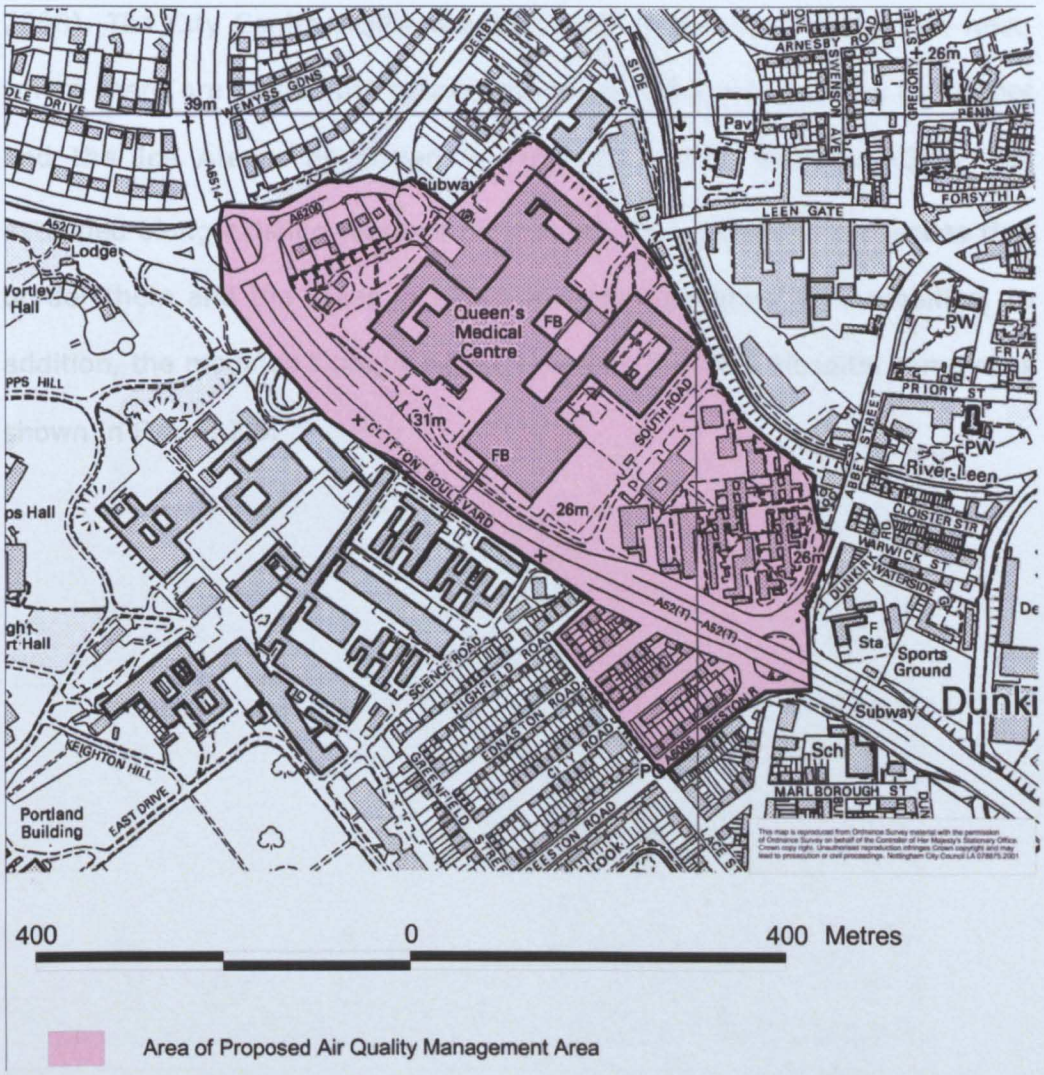

Figure 2.3 Declared Air Quality Management Area for Nitrogen Dioxide – Dunkirk, Source: (PCS, 2001)

The USA accomplished by Nottingham City Council in 2006 has resulted in revoking the City Hospital AQMA for Sulphur Dioxide (PCS, 2006). Consequently, it was recommended that there is no need to proceed to a detailed assessment for sulphur dioxide. On the other hand, it was recommended that it is necessary to keep declaring the AQMAs for NO_2 and hence, proceeding to a subsequent DA for NO_2 within these areas was recommended (PCS, 2006).

The DA accomplished by Nottingham City Council in 2008 modified the declared AQMAs for NO_2 according to the findings of the modelling and diffusion tube monitoring in respect of the NO_2 annual mean AQO (PCS,

2008). The City Centre AQMA was extended to the north and north-west, where there are residential properties, but no longer included a bus depot and the Ice Arena, as shown in Figure 2.4. The Dunkirk AQMA was extended along existing roads to incorporate the residential properties that border them and the areas included at major junctions were modified. In addition, the modified Dunkirk AQMA excluded the QMC Hospital campus as shown in Figure 2.5.

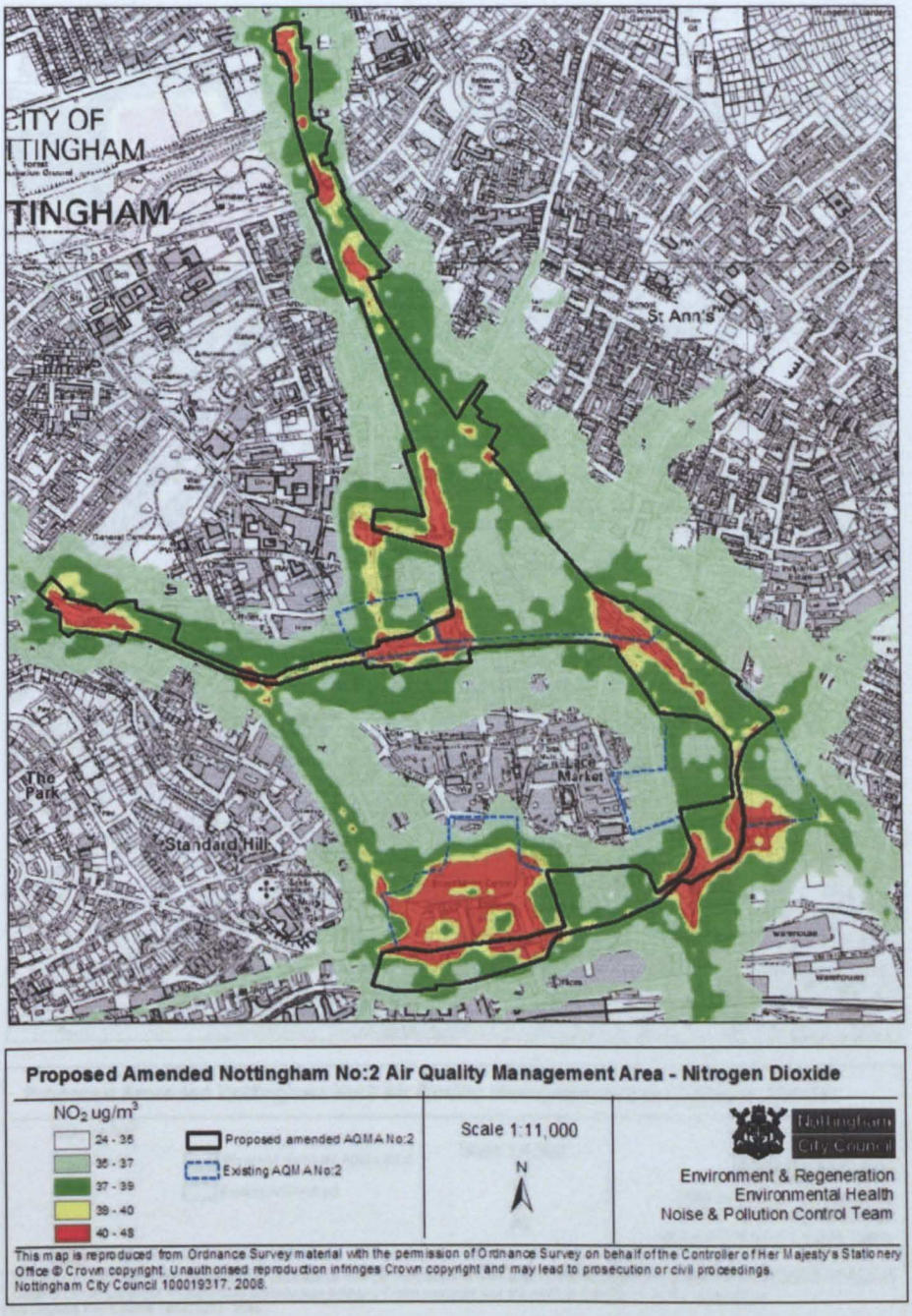

Figure 2.4 Modified AQMA in Nottingham City Centre
Source: (PCS, 2008)

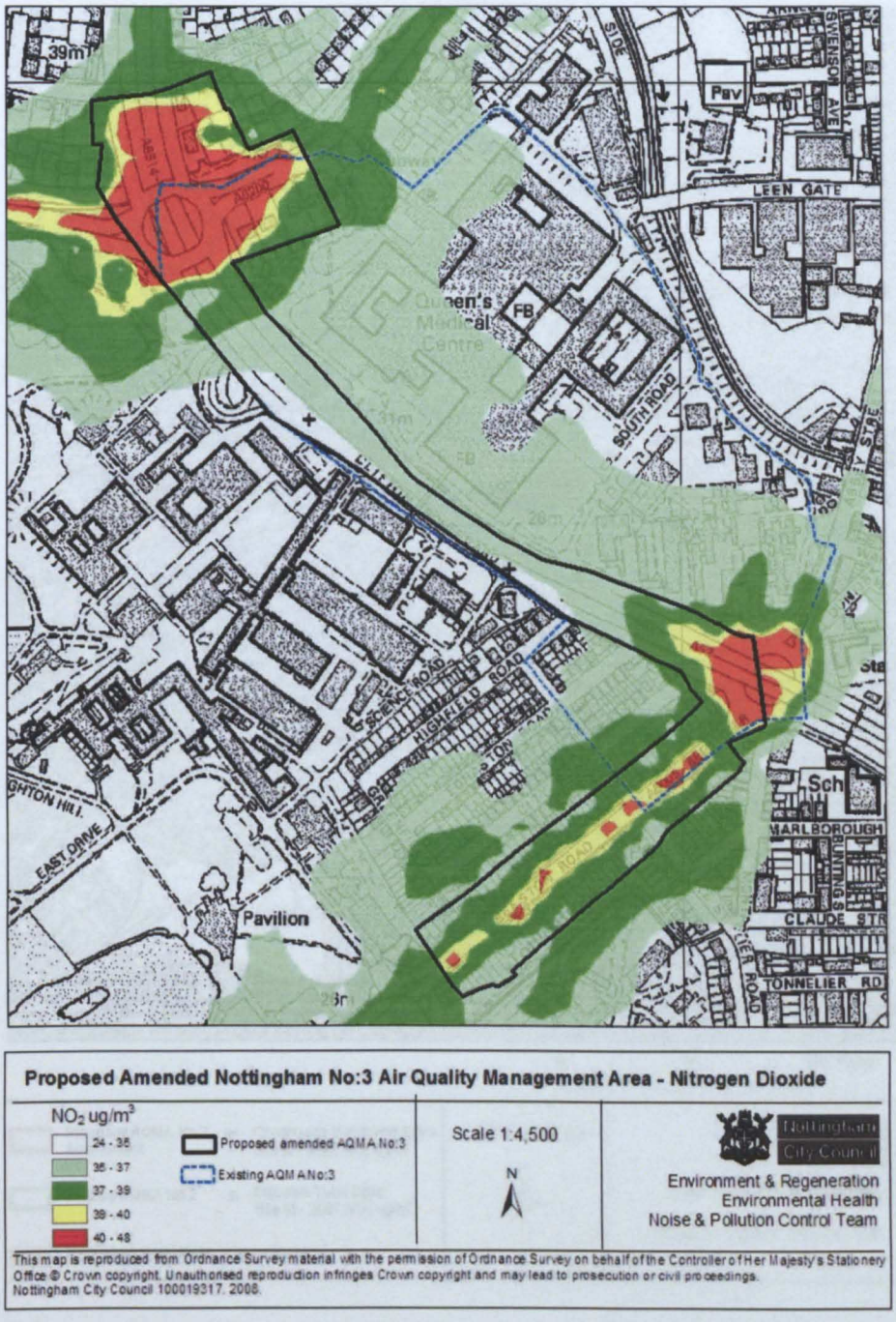

Figure 2.5 Modified AQMA in Dunkirk
Source: (PCS, 2008)

The DA undertaken by Nottingham City Council in 2009 modified further the declared AQMAs for NO_2 according to the findings of the modelling and monitoring (PCS, 2010). Figure 2.6 and Figure 2.7 show the modified AQMAs as proposed in 2010.

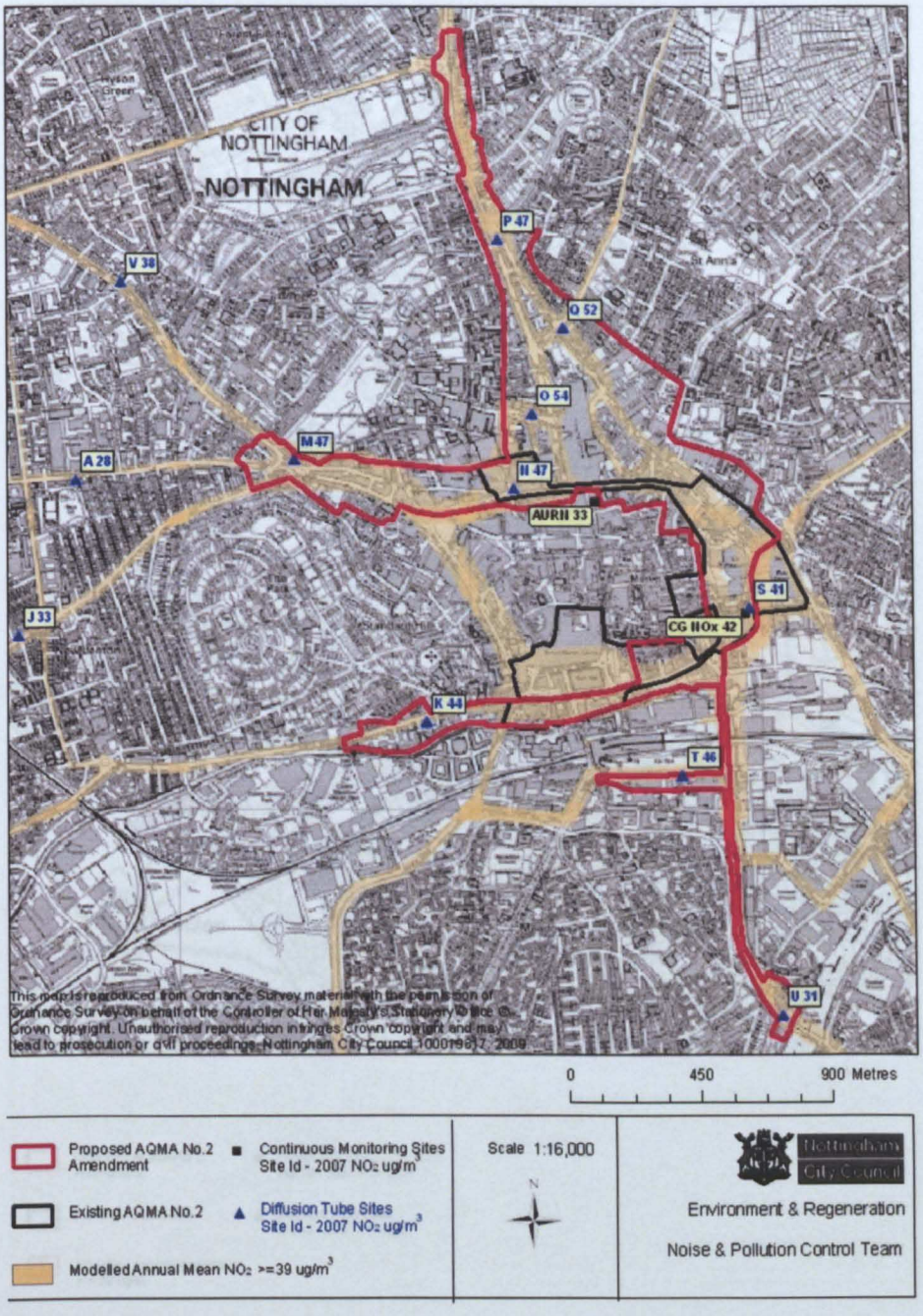

Figure 2.6 Proposed 2010 Variations in Nottingham City Centre's AQMA, Source: (PCS, 2010)

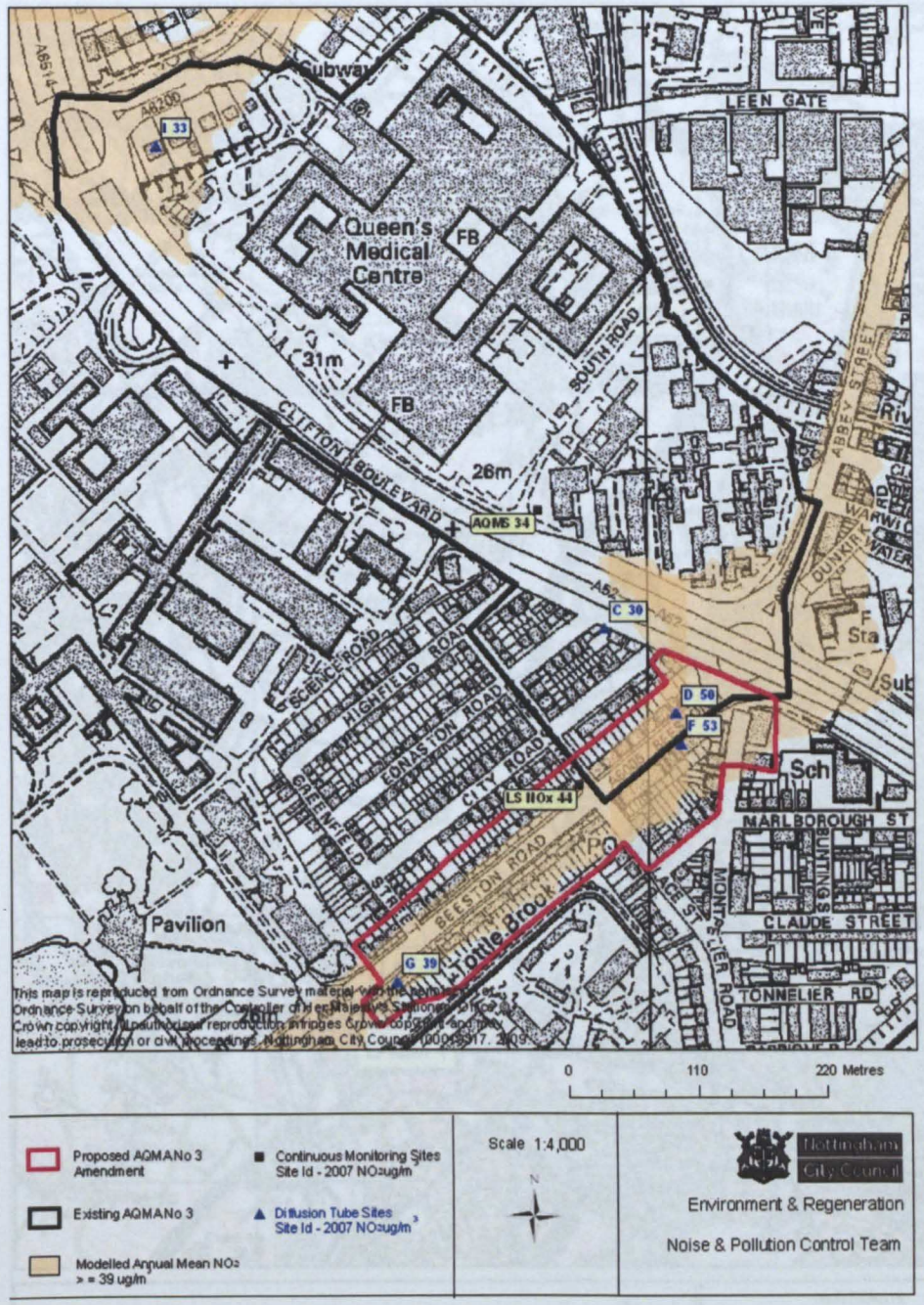

Figure 2.7 Proposed 2010 Variations in Dunkirk AQMA
Source: (PCS, 2010)

The DA and progress report published by Broxtowe Borough Council in May 2005 identified a likelihood of narrow exceedance of the standards for NO_2 (BBC, 2006). This was identified at four locations along the M1 corridor where there are residents subject to exposure. Consequently, four traffic-related AQMAs were declared in Broxtowe Borough Area as depicted in Figure 2.8.

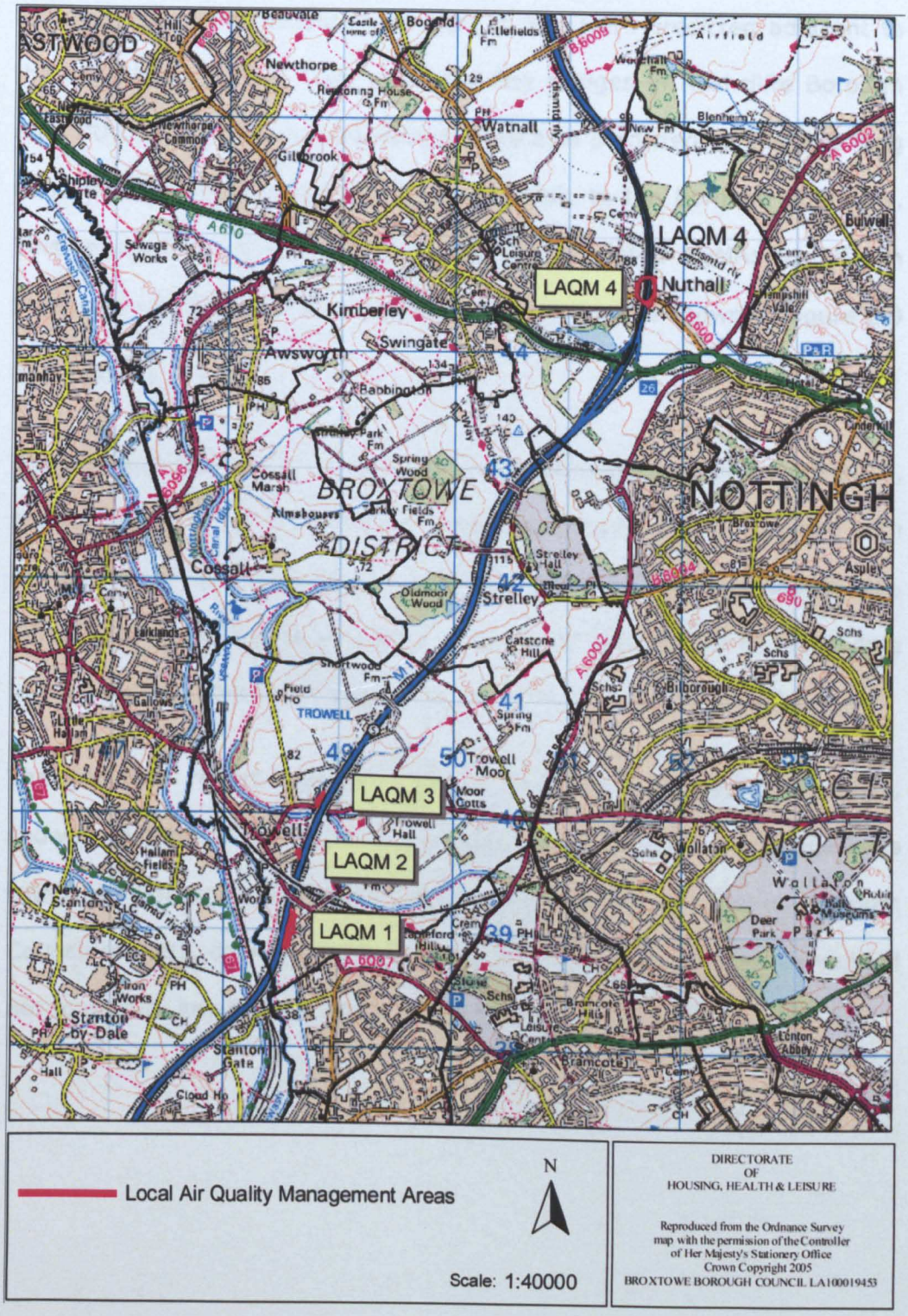

Figure 2.8 Broxtowe Air Quality Management Areas
Source: (BBC, 2010)

The USA undertaken by Broxtowe Borough Council in 2009 revealed that the annual mean AQO of NO_2 is being met within the declared AQMAs (BBC, 2009). Therefore, it was recommended to proceed to a DA for NO_2 within these areas with a view to revoking them.

Exceedances of the annual mean AQO of NO_2 were predicted adjacent to the approaches to the Trent and Lady Bay bridges in Rushcliffe Borough area (RBC, 2005). Such exceedances were also predicted on the A52 Ring Road from the Nottingham Knight roundabout to the Borough boundary. This resulted in the declaration of two traffic-related AQMAs for NO_2 in September 2005 within the Rushcliffe Borough area as shown in Figure 2.9 and Figure 2.10.

The progress report, published by Rushcliffe Borough Council in April 2010, recommended to keep the AQMA 1 area unchanged and to continue with monitoring in this area. The report also recommended continuing NO_2 diffusion tube monitoring in AQMA 2 over 2010 with a view to proceeding to a DA for NO_2 which may lead to revoking this area (RBC, 2010b).

The progress report, published by Gedling Borough Council in 2003, showed that there would be no exceedance for the air quality objectives within the Borough (GBC, 2003). The DA, undertaken for Gedling Borough Council in 2007, confirmed the progress report findings and recommended not to declare any AQMAs within Gedling Borough area (GBC, 2007).

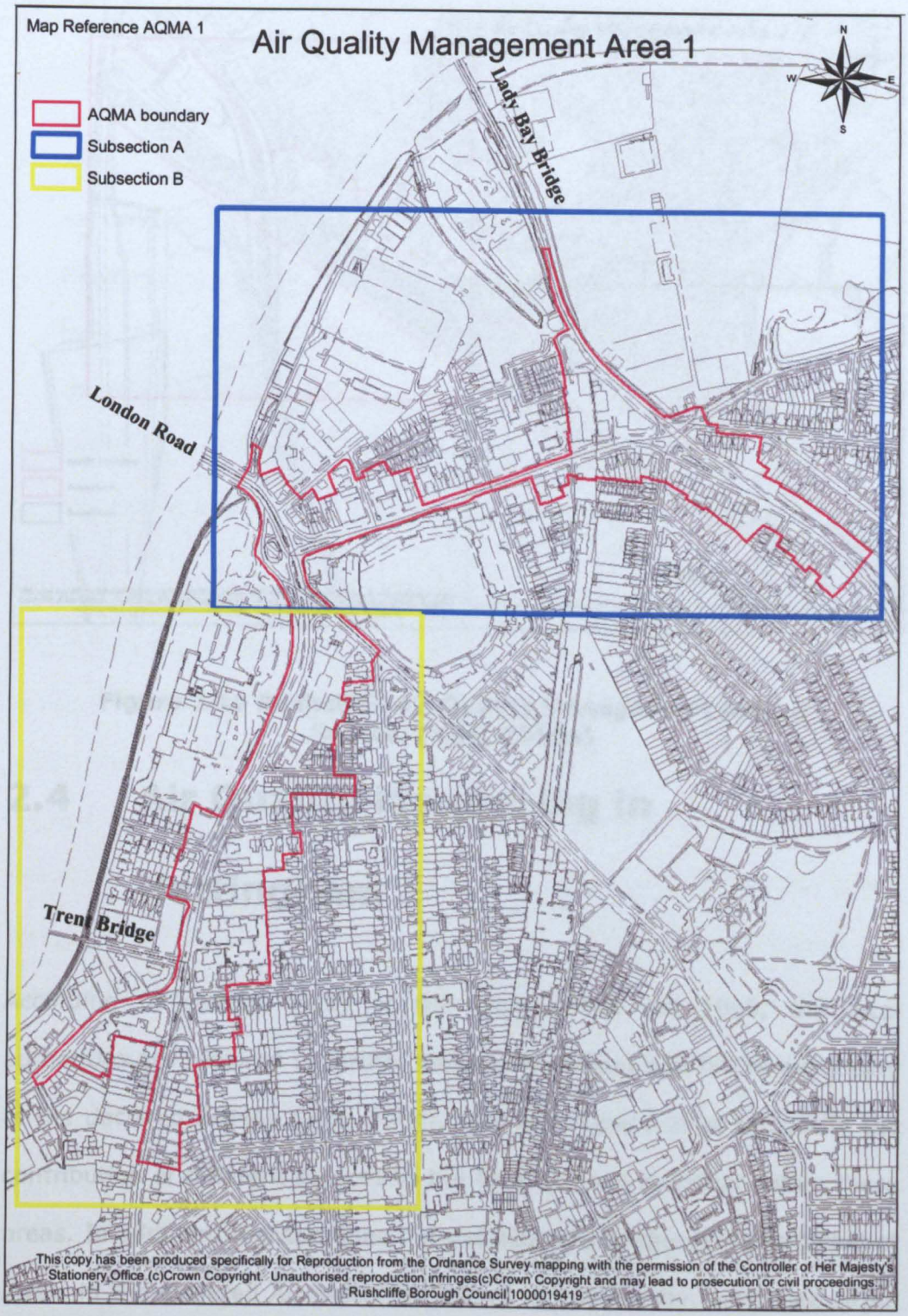

Figure 2.9 Rushcliffe Air Quality Management Area 1
Source: (RBC, 2010a)

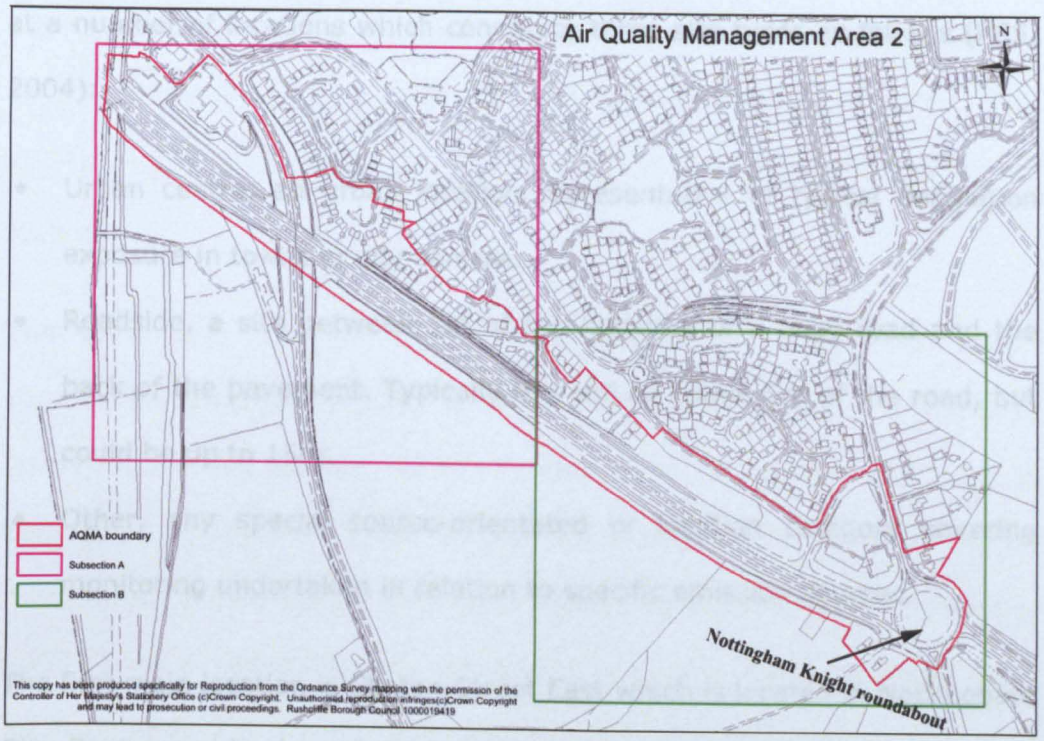

Figure 2.10 Rushcliffe Air Quality Management Area 2
Source: (RBC, 2010a)

2.4 Air Quality Monitoring in Nottingham

According to section 84(1) of the Environment Act 1995, the local authorities are required to further assess the current and future air quality in the declared AQMAs (PCS, 2004). This assessment aims to specify the contribution of different sources to the level of each pollutant within these areas. In addition, it determines the exceedances of the different pollutant levels in the declared AQMAs (PCS, 2004). Consequently, a focused AQAP can be prepared to meet the air quality objectives of each pollutant within these areas.

In order to assess the current and future air quality within AQMAs, it is necessary to undertake air quality monitoring within and around these areas. Nottingham City Council undertakes automatic air quality monitoring

at a number of locations which constitute three site types as follows (PCS, 2004):

- Urban centre, an urban location representative of typical population exposure in towns or city centres.
- Roadside, a site between 1m of the kerbside of a busy road and the back of the pavement. Typically this will be within 5m of the road, but could be up to 15m.
- Other, any special source-orientated or location category covering monitoring undertaken in relation to specific emission sources.

The first main location is Clinton Street East which is located in Nottingham City Centre and is classed as an 'Urban centre' site. The surrounding area comprises retail outlets and city centre business premises in an urban pedestrian area. The nearest road, the A6008, is a major through route approximately thirty metres from the site. The permanent Automatic Urban and Rural Network (AURN) monitoring station is located at this site and it comprises automatic monitoring equipment housed in a self-contained, air-conditioned fixed unit. Its manifold inlet is approximately three meters high and it has continuous automatic analysers that measure CO, NO, NO_2, PM_{10}, SO_2 and ozone (PCS, 2004). Figure 2.11 shows the site location of this automatic monitoring station.

The second main location is a suburban mixed industrial/commercial /residential location in the Queen's Medical Centre car park adjacent to the A52. It is twenty-five metres from the A52 ring road and approximately five metres from a minor service road and is classed as an 'Other' site. A mobile Air Quality Monitoring Station (AQMS) has been at this location since March 2002. It is a self-contained, air-conditioned station which has a sampling inlet approximately 2.5 metres high, and it has continuous

automatic analysers that measure CO, NO, NO_2, NO_x, PM_{10}, SO_2 and ozone. Temperature, wind speed and wind direction are also measured (PCS, 2004). Figure 2.11 shows the site location of this automatic monitoring station.

The third main location is Carter Gate which is a suburban mixed commercial/residential location in Nottingham City Centre near to the A60, Lower Parliament Street. It is classed as a 'Roadside' site and is approximately 10 metres from the A60 and approximately 2 metres from a minor road. A NO_X station has been located at this site since December 2003. It is a self-contained, air-conditioned unit with a sampling inlet approximately 2.5 metres high. NO, NO_2 and NO_x are measured using a continuous automatic analyser (PCS, 2004). Figure 2.11 shows the site location of this automatic monitoring station.

The fourth main location is at Lace Street which is a suburban mixed commercial/residential location in the Dunkirk area adjacent to the A6005 Beeston Road (a busy road traffic route). It is classed as a 'Roadside' site and is approximately 4 metres from Beeston Road and approximately 1 metre from a minor road. A NO_x station has been located at this site since March 2007. It is a self-contained, air-conditioned unit with a sampling inlet approximately 1.5 metres high. NO, NO_2 and NO_x are measured using a continuous automatic analyser (PCS, 2010). Figure 2.11 shows the site location of this automatic monitoring station.

The fifth main location is at the Nottingham City Hospital, Edwards Lane which is a suburban residential area of the City and is classed as an 'Other' site. The SO_2 Station, located at this site since March 2003, is approximately 100 metres from the coal-fired boiler plant in an area where modelling predicts the greatest ground level concentrations will occur. The

sampling inlet for this self-contained, air-conditioned unit is approximately 1.5 metres high and the continuous automatic analyser measures SO_2 (PCS, 2004).

There are many other locations which are equipped with NO_2 diffusion tubes to monitor annual mean NO_2 concentrations at these locations. Nottingham City Council has also commenced co-location of diffusion tubes with the AURN, AQMS and Carter Gate automatic analysers to enable bias correction to be determined (PCS, 2004). Figure 2.11 shows the site locations of NO_2 diffusion tubes in the City of Nottingham.

Figure 2.11 Monitoring Sites in the City of Nottingham

2.5 Local Transport Plans for Greater Nottingham

As mentioned before, one of the major contributors to the degradation of the air quality within Greater Nottingham is the traffic congestion (NCC and

NCC, 2006). The main reason for the traffic congestion is the predominance of the private car and particularly for work journeys as shown in Table 2.2. Consequently, the first local transport plan (LTP1), as well as the second local transport plan (LTP2), for Greater Nottingham were produced in order to encourage the modal shift from the private car to the other sustainable transport modes (NCC and NCC, 2006), thus reducing the traffic volumes and hence the emission rates in the transport-related AQMAs. Therefore, the measures of the local transport plans reflect those of the AQAPs targeted to help alleviate the traffic congestion and improve the air quality in the transport-related AQMAs (PCS, 2003).

Table 2.2 Mode of Travel to Work
Source: (NCC and NCC, 2006)

Work Place	Work at home	Metro/tram	Train	Bus	Motor cycle	Car as driver	Car as passenger	Taxi or minicab	Bicycle	On foot	Other
City Centre	0.3	0.1	4.2	36.8	0.4	42.2	5.7	0.9	2.1	7.1	0.2
Nottingham City	3.9	0.1	1.6	20.3	1.0	54.4	6.1	0.4	3.1	8.9	0.2
Greater Nottingham	7.6	0.0	1.2	15.1	1.0	55.3	6.1	0.4	3.2	9.9	0.2
Nottingham TTWA	7.7	0.0	1.1	13.9	1.1	55.5	6.2	0.4	3.4	10.4	0.3

* all figures are in %
* TTWA stands for Travel to Work Area

The LTP1 for Greater Nottingham was produced in July 2000 and expired at the end of March 2006 (NCC and NCC, 2006). The main objectives of LTP1 were to relieve the city centre, as well as the district centres, from cars to avoid congestion, and therefore the air pollution. In addition, it aimed to increase their accessibility by the public transport, cycles and foot. This was supposed to enhance the economic activity and encourage the development in these centres (NCC and NCC, 2006).

The main outcomes of the LTP1 were improving the quality and reliability of bus services as well as implementing the Nottingham Express Transit (NET) Line One. In addition, they included providing park and ride sites and introducing travel plans (NCC and NCC, 2006). All these outcomes offered, and may continue to offer, many opportunities to tackle the traffic congestion within Greater Nottingham as follows (NCC and NCC, 2006):

- through the adoption of land use planning policies over the last 30 years. This resulted in avoiding the dispersal of the land use activities and retaining the compact city form. This helped to maintain a development form for Greater Nottingham suitable for a balance of different transport modes;
- through reducing the need for travel by the planned growth of the conurbation and particularly the further expansion of the city centre. This is helped by locating new housing close to job opportunities;
- through increasing the viability of public transport by upgrading the existing transport network such as the provision of NET Line One. This is proving to be a highly popular alternative to the car, and hence is contributing to reducing congestion within the Line One corridor;
- through the provision of the Park and Ride sites that are associated with the NET system, bus, and the local rail stations. These sites are targeted to encourage the modal shift from the private car to the associated public transport modes, thus alleviating the congested transport links between these sites and the centres of high attraction;
- through the provision of high frequency bus services along most main routes. The majority are of high quality following heavy investment in the vehicle fleet over the last ten years by the operators;
- through the accessibility planning process which highlights and addresses deficiencies in public transport, walking and cycling service

provision, thus providing greater opportunity for the use of alternatives to the car;

- through motivating the utilisation of the heavy rail network;
- through the introduction of the Clear Zone which has already led to a reduction of traffic movements within the Central Core area. Completion of the Turning Point North scheme has reduced further non-essential cross-city centre vehicle movements;
- through the application of maximum parking standards and parking pricing policies that have been designed to encourage short stay shoppers over long stay commuters, thus reducing the number of private car journeys to workplaces and benefiting the local economy;
- through encouraging people to walk and cycle more, and particularly for journeys to work;
- through changing the travel behaviour by working with employers and schools to produce travel plans. These plans are targeted to reduce car commuting and to introduce smarter travel choices;
- through the awareness campaigns such as the 'Big Wheel' campaign. These campaigns are targeted to supply information to encourage people to shift from the private car to the more sustainable public transport modes;
- through the nomination of traffic managers, who have a duty to oversee the efficient operation of the highway network in terms of the attainment of the local transport plan's objectives; and
- through the Transport Innovation Fund announced by the Government. This potentially presents a new source of funding to tackle congestion linked with the introduction of traffic restraint.

The LTP2 for Greater Nottingham is the second to be produced jointly between Nottingham City Council and Nottinghamshire County Council

(NCC and NCC, 2006). It covers the five-year period from April 2006 to March 2011 and replaced the LTP1. The main function of the plan is to set out the local transport strategy and priority areas for investment over the plan period. The plan area includes the city of Nottingham, the boroughs of Broxtowe, Gedling, Rushcliffe and the Hucknall part of Ashfield (NCC and NCC, 2006).

The main objectives of LTP2 are tackling the traffic congestion and providing better air quality. In addition, they include improving accessibility, improving road safety, supporting regeneration and neighbourhood renewal, enhancing the quality of life and undertaking more cost efficient and effective maintenance of existing transport assets (NCC and NCC, 2006). Indeed, these other objectives are central to promoting the modal shift from the private car to the other transport modes such as public transport, walking and cycling. Therefore, they are heavily contributing to tackling congestion, and consequently to improving the air quality as well throughout the plan area (NCC and NCC, 2006).

The prospective outcomes of LTP2 are the development of transport and land use planning through reducing the transport network congestion and enhancing safety. In addition, these outcomes include making the transport network accessible to the development areas (regeneration areas). This will help attract investors to invest more within these areas, and hence help develop them and increase the job opportunities available there. Therefore, the traffic congestion is reduced by reducing the need to travel between these areas and the other centres of attraction (NCC and NCC, 2006).

The measures of LTP2 can contribute to improving the air quality by reducing the traffic emission levels within and around the transport-related

AQMAs. That can be accomplished through undertaking the following measures (NCC and NCC, 2006):

- reducing the need to travel through coordinated land use and transport planning. This can be attained by locating the major employment sites as well as the major services and shopping sites near to the residential areas. This can be attained through the creation of attractive and accessible district centres, providing a range of good quality services, which will promote sustainable communities and will help reduce transport demand into the city centre;
- promotion of cleaner alternatives to the car such as walking, cycling and public transport. That can be achieved through the adoption of Bus Strategy interventions to increase coverage and improve access to public transport services, as well as through the development of walking and cycling networks and undertaking Rights of Way Improvement Plans;
- more implementation of school and workplace travel plans to encourage increased modal shift from the private car to the other sustainable modes of transport while commuting to schools and workplaces;
- education and awareness raising measures including the Big Wheel Campaign and the Smarter Travel Choices programme. These measures support the take up of cleaner alternatives to the car;
- local authority enforcement of Clear Zone and other traffic restricted areas such as the designation of the city's central core area as a Clear Zone. This helps to encourage the take up of electrically powered and low emission local delivery vehicles, buses and taxis within these areas;

- promote procurement and use of cleaner vehicles through encouraging the take up of new vehicles which are generally much cleaner than the vehicles they replace. In addition, the Councils are promoting the preference for cleaner vehicles wherever possible in the case of pool cars and fleet vehicles. This is accomplished through the TransAct local grants scheme for Travel Plans and Travel Plans advice to employers;
- enforcing emission standards in order to ensure reducing emissions from road traffic. This can be attained through a combination of making vehicles more fuel efficient, development of new fuel (alternative fuel technology), and reducing traffic congestion to reduce the overall traffic volumes; and
- undertaking a Strategic Environmental Assessment for plans and programmes. This is a process for appraising the environmental impacts of plans and programmes including LTP2. The resulting environmental assessment report must be taken into consideration before a plan is approved.

Table 2.3 and Table 2.4 summarise the potential transport schemes which could contribute to tackling the identified air quality problems within the Nottingham city boundary. However, as the Broxtowe and Rushcliffe AQMAs have only very recently been declared (NCC and NCC, 2006), the identification of potential remedial schemes has not yet taken place.

Table 2.3 Nottingham City Centre AQMA Summary of Potential Schemes
Source: (NCC and NCC, 2006)

Timescale: Long = 5-10 years, Medium = 2 to 5 years, Short = Less than 5 years Cost: ££££ > £1 million, £££ = £500k - £1 million, ££ = £100k - £500k, £ = < £100k Air Quality Impact: High = >2 µgm-3 , Medium = 1 – 2 µgm-3 , Low = < 1 µgm-3 Rank: 1 = highest							
Scheme	Description	Lead Organisation	Air Quality Impact	Timescale	Cost	Non Air Quality Impact	Rank

A60 two-way traffic route	Huntingdon St/ Lower Parliament St to become strategic two-way route	City Council	High	Medium	££££	Development of North - South legible strategic traffic route. Allows central core area to expand eastwards	1
Two-way bus priority route	Cranbrook St/ Bellar Gate bus priority route and local access.	City Council	Medium	Medium	£££	Supports improved public transport accessibility and reliability	2
Primary Pedestrian Routes	Key junctions reconfigured to increase pedestrian priority and quality of routes upgraded.	City Council	Low	Short / Medium	££	Promotes walking, health and improved safety. Helps establish a framework for development	4=
Cycle links	Junction facilities and routes through redevelopment areas	City Council/ developers	Low	Medium	££	Promotes cycling, health and improved safety	4=
Travel Plans	Travel Plans required for major development proposals	Developers	Low	Short / Medium	£	Encourages modal change	4=
Station Masterplan	Rail capacity improvements and transport interchange	Rail industry partners/ City/ County Councils	Low	Medium/ Long	££££	Encourages modal change, will reduce congestion and support economic development	4=
Park and Ride	New site at Gamston	County Council	Low	Short	££££	Reduces congestion through less vehicle movements to the City Centre	4=

NET Phase 2	Network extensions to Clifton and Chilwell via Beeston	NET promoters	Low	Medium	££££	Encourages modal change, will reduce congestion & support economic development	4=
NET Future Phases	Other network extensions including Gedling/ West Bridgford	NET promoters	Low	Long	££££	Encourages modal change, will reduce congestion and support economic development	4=
A52 Ring Road upgrading	Upgrading of Ring Road Radcliffe to Clifton Bridge as recommended in the A52 MMS	Highways Agency	Medium	Long	££££	Reduced congestion by increasing capacity of alternative cross- city route around the south of the conurbation	3
New River Crossing	New Trent road crossing at Radcliffe	County Council	Medium	Long	££££	Reduced congestion through provision of an alternative route for cross-city traffic movements to the east of the conurbation	5

Table 2.4 Ring Road (QMC) AQMA Summary of Potential Schemes Source: (NCC and NCC, 2006)

Timescale: Long = 5-10 years, Medium = 2 to 5 years, Short = Less than 5 years Cost: ££££ > £1 million, £££ = £500k - £1 million, ££ = £100k - £500k, £ = < £100k Air Quality Impact: High = >2 µgm-3 , Medium = 1 – 2 µgm-3 , Low = < 1 µgm-3 Rank: 1 = highest							
Scheme	Description	Lead Organisation	Air Quality Impact	Timescale	Cost	Non Air Quality Impact	Rank

NET Phase 2	Network extensions to Clifton and Chilwell via Beeston (Including Park and Ride)	NET promoters	Mediu m	Medium	£££ £	Encourages modal change, will reduce congestion and support economic development	1
Ring Road Major	Junction capacity improvements, bus stop/small scale interchange facilities, cycle and footway upgrading, parking provision for residents	City Council	Mediu m	Medium	£££ £	Will reduce congestion, encourage modal change and improve safety	2=
Medi-link Ring Road service	High frequency Ring Road orbital bus service	City Council/ bus operators / Hospitals	Mediu m	Medium	£££	Improves accessibility and encourages modal change.	2=
QMC interchange	Development of bus interchange and in the future tram within hospital site	City Council/ NHS Trust	Low	Medium / Long	£££	Supports public transport integration	2=
Bus priority	Introduction of bus lanes through road space reallocation and other bus priority measures on A6200/A52 and A6005 corridors	City Council/ County Council / Highways Agency	Low	Medium	££	Will support modal change but may have adverse congestion impacts	4
Cycle links	Cycle network development	City Council	Low	Medium	££	Promotes cycling, health and improved safety	3=
Travel Plans	Updating of hospital and University plans	NHS trust/ University	Low	Short	£	Encourages modal change	3=

2.6 Major Transport Schemes

Transport schemes costing more than £5 million are defined as major schemes (NCC and NCC, 2006). There are six major transport schemes in

Greater Nottingham which were proposed to be taken forward during the LTP2 plan period. The main focus of these transport schemes is to deliver the objectives of LTP2 (NCC and NCC, 2006).

2.6.1 Hucknall Town Centre Improvement Scheme

This is an integrated package of proposals for Hucknall Town Centre including pedestrianisation, bus priority enforcement and cycle accessibility improvements. In addition, they include the provision of greater integration and improved interchange between the bus service and tram/rail services (NCC and NCC, 2006).

The proposals are being finalised but are likely to include the construction of a new section of road. This road will remove most of the traffic from the town centre and provide the opportunity to pedestrianise the High Street (NCC and NCC, 2006). A network of new and improved pedestrian and cycle facilities is to be incorporated into the scheme as well. The scheme measures will help to improve the retail and business environment and will cater for the additional travel demand within the town (NCC and NCC, 2006).

The scheme objectives should help to reduce congestion, and thus to improve air quality as follows (NCC and NCC, 2006):

- by significantly improving the environment in Hucknall town centre by the removal of the through traffic (approximately 15,000 vehicles daily);
- by improving cycling and walking facilities and networks such as routes between the tram/rail station and the town centre;

- by making cycling, walking and public transport journeys safer and more attractive;
- by improving bus punctuality and reliability, thereby enhancing the status of public transport; and
- by improving the interchanges between bus and rail/tram.

2.6.2 Ring Road Major Scheme

The ring road is a principal orbital road by which through traffic can avoid Nottingham city centre. It connects some of the most important employers and trip generators together. In addition, it constitutes the principal route for the heavy good vehicles, not to mention local pedestrians and cycle movements (NCC and NCC, 2006). The scheme is a package of proposals contributing to addressing a number of issues and problems which have been identified through consultation with different groups. These groups represent local businesses, public transport and freight operators, residents and cyclists (NCC and NCC, 2006). The identified key issues affecting the transport viability of the Ring Road are as follows (NCC and NCC, 2006):

- congestion and delay (both on the Ring Road and intersecting radial routes) affecting all road users including public transport;
- unattractiveness as a cross-city through route (incomplete in the north east) making it quicker to drive through the City Centre;
- inadequate, infrequent and unreliable orbital bus services;
- high accident figures;
- community severance;
- intimidating environment for pedestrians and cyclists;
- Air Quality Management Area near QMC/Dunkirk;
- inadequate interchange with NET Line One and radial bus services; and
- pressure on parking provision at key employment sites.

Consequently, the above mentioned key issues were analysed and the following scheme elements were proposed (NCC and NCC, 2006):

- junction improvements at a number of locations to provide overall capacity increases for orbital movements for all road-users. This will also enable better priority for radial bus movements, attract cross-city trips from City Centre routes and improve reliability and journey times for all users;
- securing a high frequency and high quality orbital bus service operating at a minimum 10 minute frequency serving the key destinations along the Ring Road;
- improved opportunities for interchange with radial bus services and with NET Line One and NET Phase 2 (see Section 2.6.5);
- real-time passenger information, and
- improved pedestrian/cyclist environment including upgraded street lighting, side road entry treatments and better enforcement of parking on the cycle tracks.

The scheme elements should help to reduce congestion, and thus to improve air quality as follows (NCC and NCC, 2006):

- it will reduce congestion at critical junctions on this important orbital strategic route;
- it supports complementary strategies in the Plan that encourage modal change for journeys to the City Centre;
- it will allow easier interchange with NET and with radial bus services, reducing the need for users to go into the City Centre for some journeys by car;
- supporting increased public transport use and reducing congestion will contribute to improving air quality; and

- improvements to pedestrian and cycle facilities will increase the attractiveness of these modes.

2.6.3 Turning Point North

The (now completed) Turning Point North transport scheme involved creating better connections for pedestrians and public transport users. This removed general traffic in the area around the Victoria Centre (NCC and NCC, 2006).

The scheme involved the alteration of the highway network to the Milton Street and Parliament Street area around the Victoria Shopping Centre. So it is only available for essential traffic such as the emergency services, buses, taxis, cyclists, and deliveries. General traffic benefits from using a new through-route across Shakespeare Street, South Sherwood Street (eastbound only), North Church Street (westbound only) and Upper Parliament Street (NCC and NCC, 2006). Figure 2.12 exhibits access changes to the Turning Point North zone from 2006.

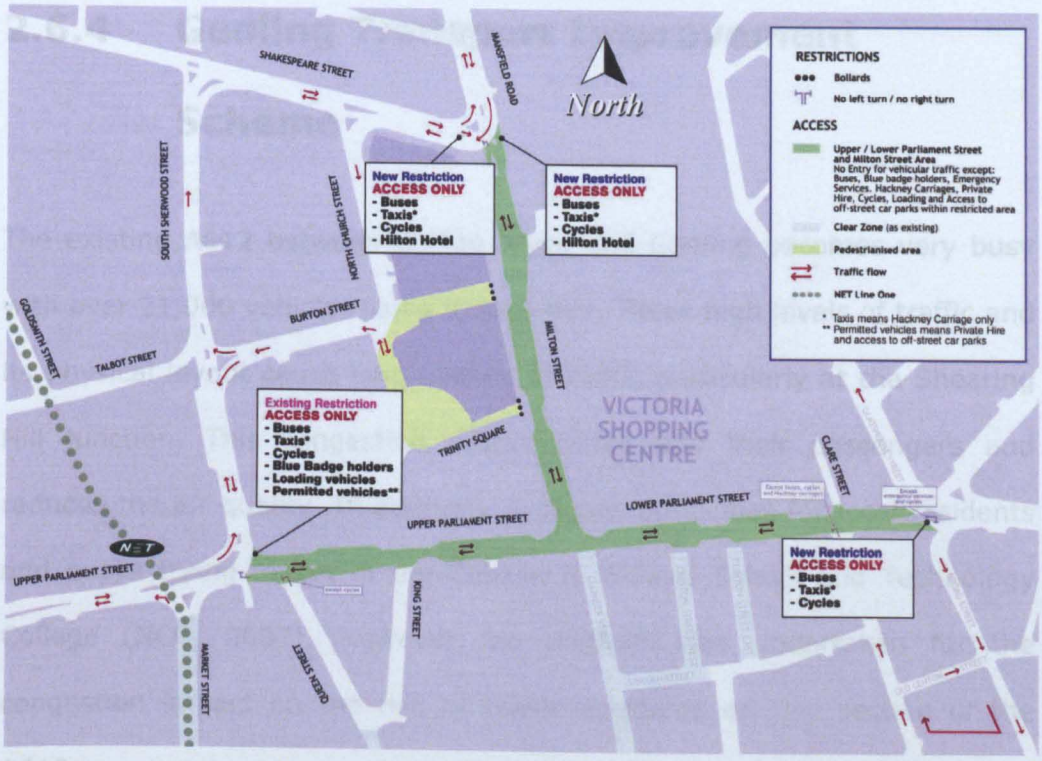

Figure 2.12 Access Changes to the Turning Point North zone from 2006, Source: http://www.thebigwheel.org.uk/turningpoint/ on 13th Feb. 2007

The scheme measures improved the facilities available to both pedestrians and bus users and thereby, encouraged the modal shift from the private car as follows (NCC and NCC, 2006):

- pedestrians: through introducing new and wider pavements and better, safer crossing points. In addition, through lessening traffic in some areas, reducing noise, fumes and safety concerns;
- bus users: through introducing more convenient access to and changes between bus services, which have been relocated to the Upper Parliament Street and Milton Street areas. In addition, through introducing greater bus priority in some areas including parts of Parliament Street, Milton Street, South Sherwood Street and Mansfield Road.

2.6.4 Gedling Transport Improvement Scheme

The existing A612 between Burton Joyce and Gedling becomes very busy with over 21,000 vehicles using it each day. These high levels of traffic and its physical layout cause long queues of traffic particularly at the Shearing Hill junction. This congestion delays buses and their passengers and reduces the air quality. In addition, it causes difficulties for local residents and pupils trying to get to the Carlton le Willows School and Technology College (NCC, 2007). However, no analysis was undertaken for the congestion impact on the risk of traffic accidents on this section of the A612.

The A612 Gedling Transport Improvement Scheme is considered one of the major transport schemes to provide priority for public transport, cyclists and pedestrians (NCC and NCC, 2006). Buses are no longer held up in the congestion on the A612 between Burton Joyce and Gedling. This means that journeys by bus are now faster, more reliable and more attractive to potential users as a result (NCC, 2007).

The scheme involved building a 2km section of new road and cycle track between the A612 Colwick Loop Road at Victoria Retail Park and the A612 Burton Road near Whitworth Drive (NCC, 2007). The new road crossed the Stoke Bardolph Sewage Treatment Works. In addition, it required the construction of several new structures including a bridge over the Nottingham to Lincoln Railway Line, as shown in Figure 2.13.

As part of the scheme, 'bus plugs' were introduced on Burton Road and Stoke Lane (NCC, 2007). Only buses and emergency service vehicles are allowed through the 'bus plugs', which are controlled by traffic lights.

However, it was not explained how the traffic lights operate to allow only buses and emergency service vehicles through the 'plugs'. Pedestrians, cyclists and horse riders are unaffected by the 'plugs'.

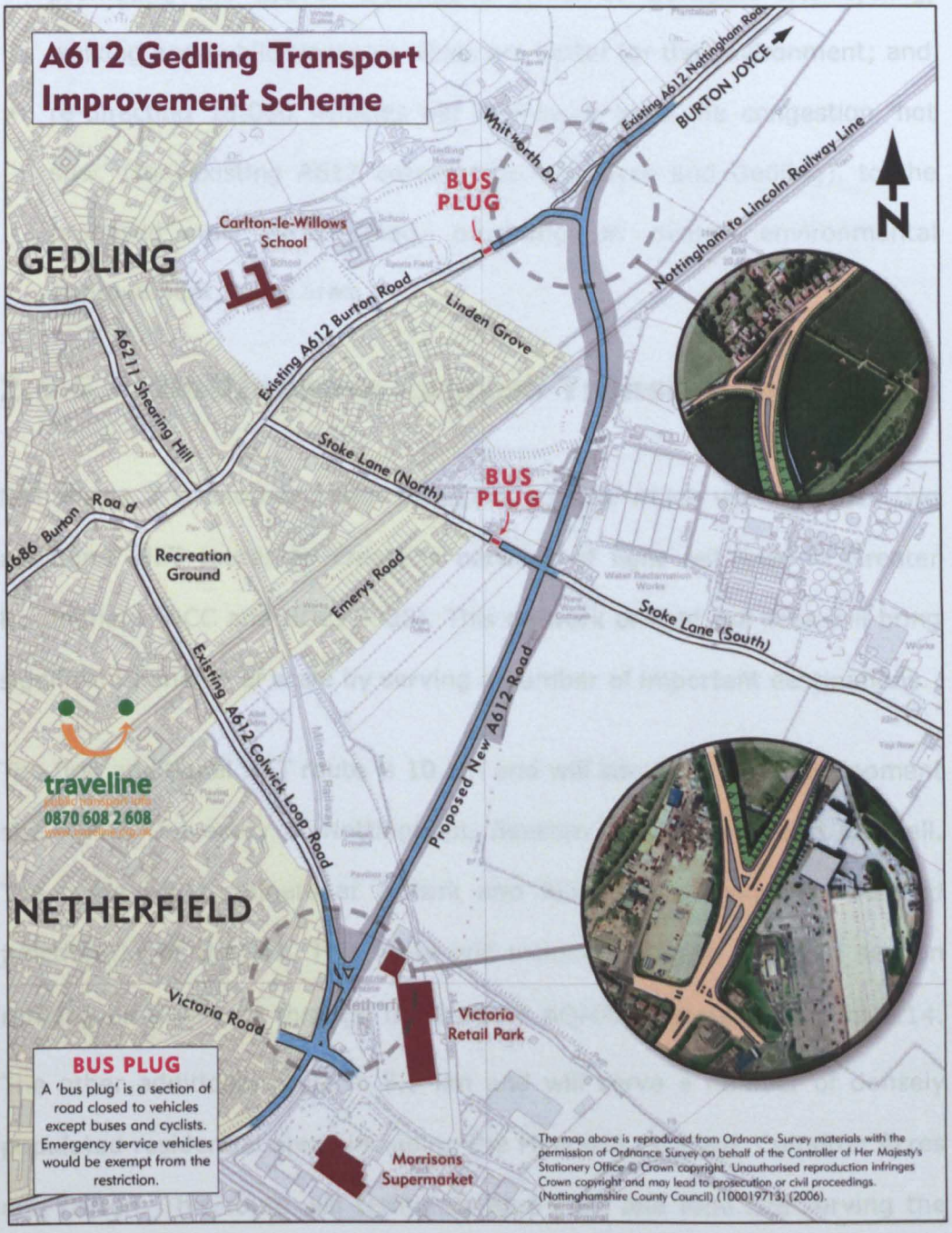

Figure 2.13 A612 Gedling Transport Improvement Scheme Source: (NCC, 2007)

The scheme measures help to reduce congestion, and thus to improve air quality as follows (NCC, 2007):

- providing priority for buses along the sections of the bypassed A612 and Stoke Lane. Therefore, journeys by bus are improved by up to 10 minutes for each inbound trip to the City in the morning peak hours;
- promoting the use of alternative forms of transport like cycling, walking and public transport which are better for the environment; and
- re-directing 18,000 vehicles per day away from the congestion 'hot spot' (the existing A612 between Burton Joyce and Gedling), to the proposed new A612 Road, providing an overall environmental improvement in the area.

2.6.5 Nottingham Express Transit Phase 2

NET Phase 2 is another major transport scheme which will introduce two additional NET routes to create a network of light rail lines in Greater Nottingham (NCC and NCC, 2006). This network of light rail lines will bring significant benefits of scale by serving a number of important destinations.

The first additional NET route is 10 km and will serve the ng2 development site, QMC, University of Nottingham, Beeston town centre, and Chilwell. The route will terminate at a Park and Ride site serving the A52 and junction 25 of the M1. This route will include a largely elevated section running on a viaduct through the Dunkirk AQMA as shown in Figure 2.14. The other additional route is 7.5 km and will serve a number of densely populated residential areas including the Meadows, Wilford, Compton Acres and Clifton. This route will terminate at a Park and Ride site serving the A453 and junction 24 of the M1 (NCC and NCC, 2006). Figure 2.15 shows the proposed NET Phase 2 routes as well as the existing Line One.

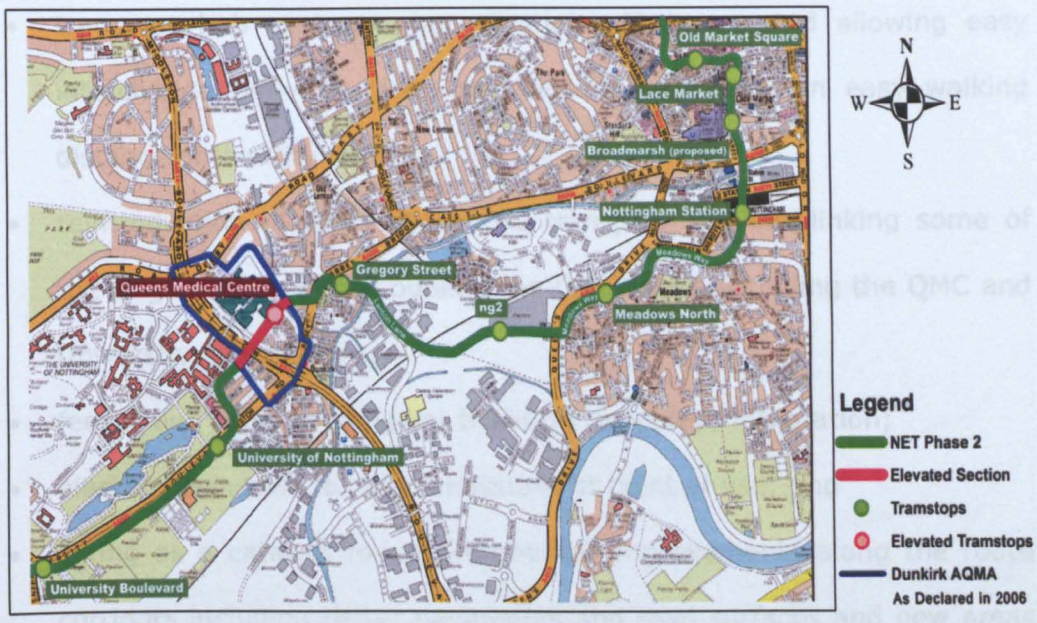

Figure 2.14 NET Phase 2 running Through the Dunkirk AQMA
Source: http://www.netphasetwo.com/
Accessed on 29/05/2010

The combined effects of NET Line One and the additional Phase 2 lines should help to reduce congestion, and thus to improve air quality as follows (NCC and NCC, 2006):

- up to 4 million car journeys to be taken off the roads;
- provision of over 5,500 Park and Ride spaces;
- segregated track sections and junction priority to ensure fast and reliable operation;
- providing improved accessibility to employment, education and other facilities, including for those living in areas of disadvantage both within the existing Line One corridor and new areas served by the Phase 2 routes;
- provision of high quality infrastructure serving busy transport corridors, raising the quality of local public transport to meet the expectations of modern passengers;

- transport hub at Nottingham Station will be created allowing easy interchange between tram, rail, bus and taxis within easy walking distance of the City Centre;
- reintroduction of cross-city public transport services linking some of the largest destinations outside the City Centre including the QMC and University campuses;
- feeder bus services and joint ticketing to achieve integration;
- electric propulsion for zero emissions at point of use; and
- acting as a catalyst for environmental improvements along the route corridors including better pavements and road surfaces and new areas of public space.

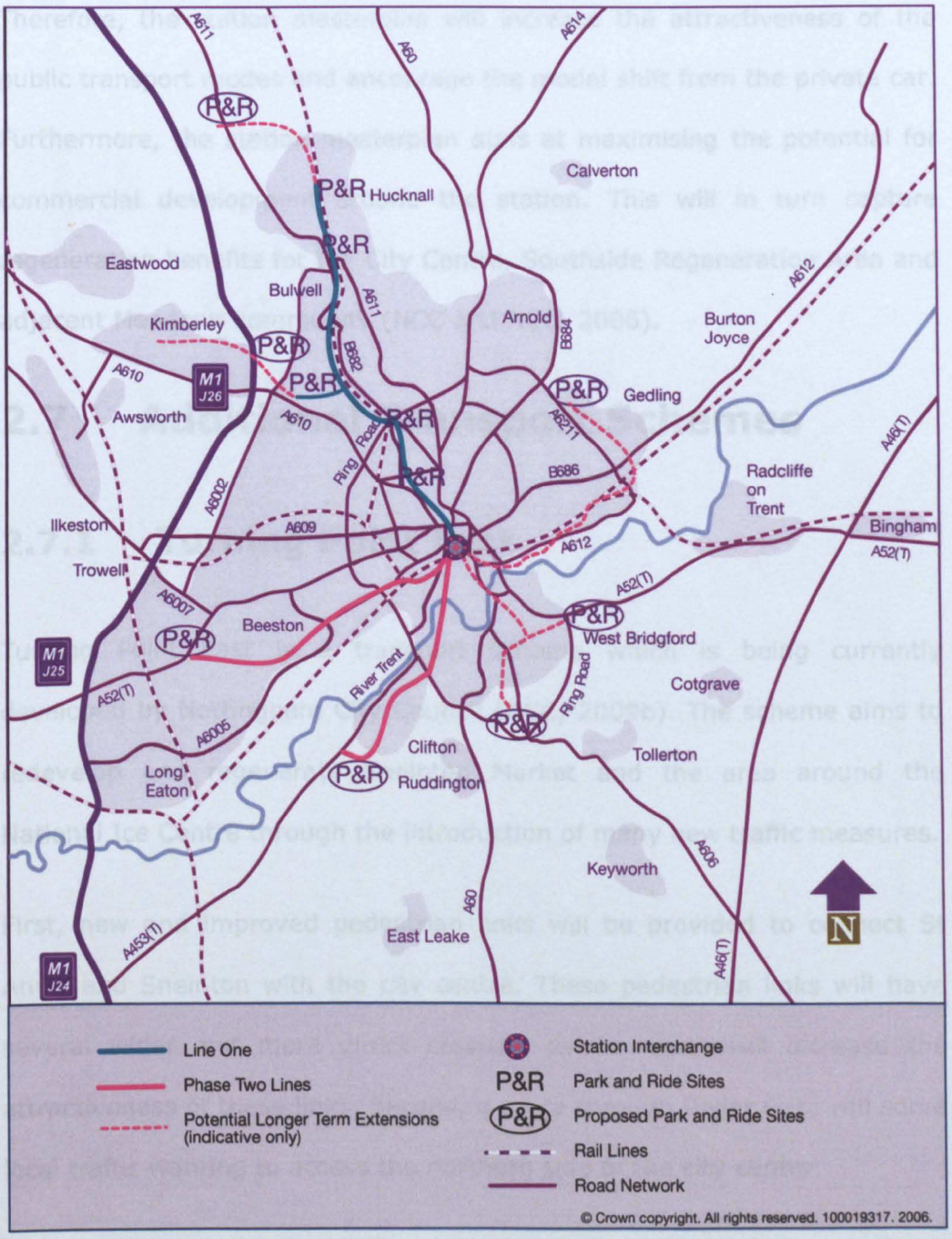

Figure 2.15 Nottingham Express Transit Network Proposals
Source: (NCC and NCC, 2006)

2.6.6 Nottingham Station Masterplan

The main objectives of the Station Masterplan are to improve and increase the passenger capacity, the level of service and customer satisfaction. In addition, these objectives include improving the integration of the rail services with tram and other public transport modes (NCC and NCC, 2006).

Therefore, the station masterplan will increase the attractiveness of the public transport modes and encourage the modal shift from the private car. Furthermore, the station masterplan aims at maximising the potential for commercial development around the station. This will in turn capture regeneration benefits for the City Centre, Southside Regeneration Area and adjacent Meadows community (NCC and NCC, 2006).

2.7 Additional Transport Schemes

2.7.1 Turning Point East

Turning Point East is a transport scheme which is being currently developed by Nottingham City Council (NCC, 2009b). The scheme aims to redevelop and regenerate Sneinton Market and the area around the National Ice Centre through the introduction of many new traffic measures.

First, new and improved pedestrian links will be provided to connect St Ann's and Sneinton with the city centre. These pedestrian links will have several wider and more direct crossing points which will increase the attractiveness of these links. Second, a route through Bellar Gate will serve local traffic wanting to access the northern side of the city centre.

The route through Bellar Gate will be provided with a new contraflow bus lane to improve the public transport links to the National Ice Centre, Eastside Island Site and Nottingham Station. Third, the plans of Turning Point East will convert the one-way Huntingdon Street and Lower Parliament Street to a two-way route for traffic heading north and south through the city. Figure 2.16 exhibits the layout of Turning Point East.

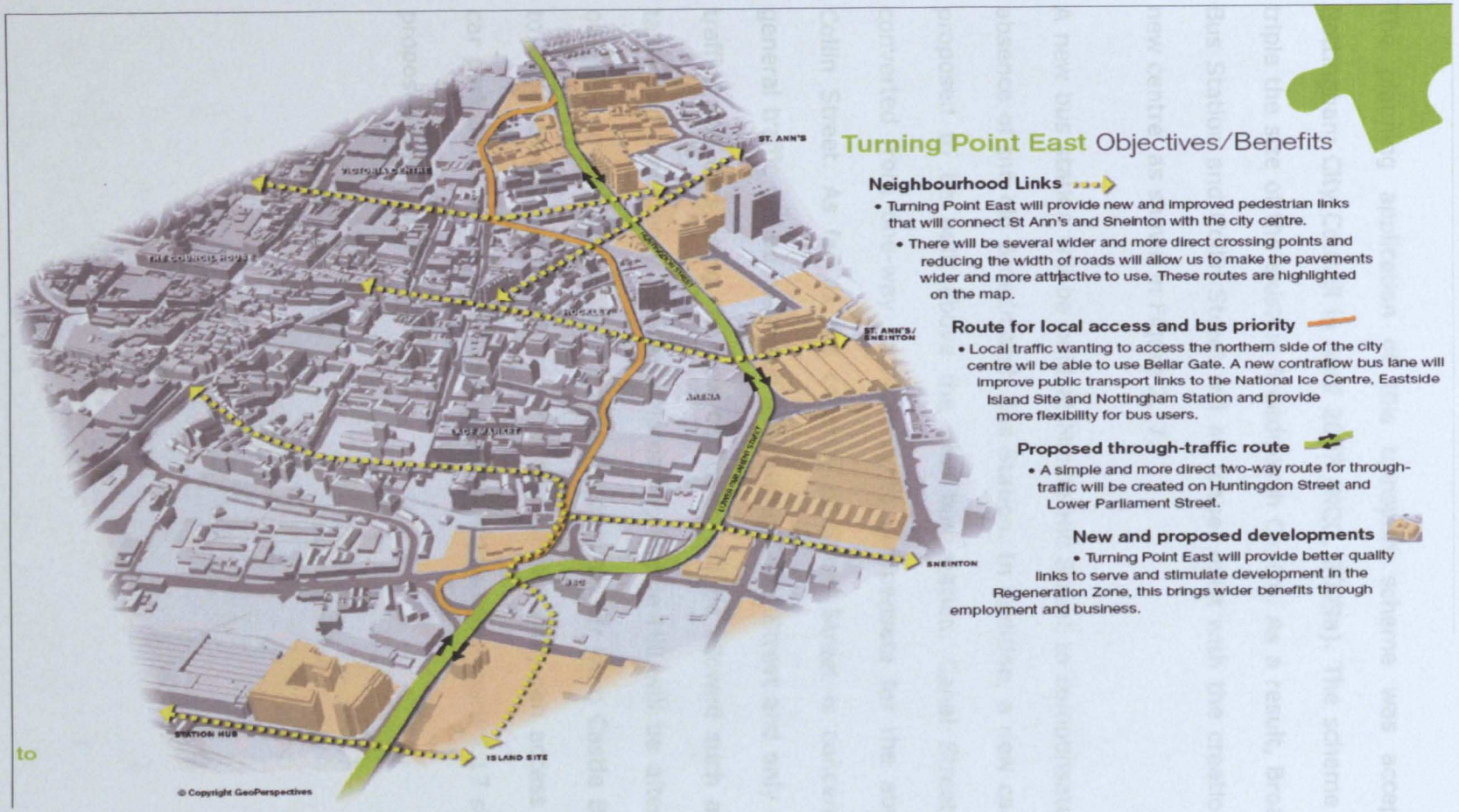

Figure 2.16 Turning Point East
Source: (NCC, 2009b)

2.7.2 Broadmarsh Shopping Centre Extension

The planning application of this transport scheme was accepted by Nottingham City Council in April 2007 (NCC, 2009a). The scheme aims to triple the size of the existing Broadmarsh Centre. As a result, Broadmarsh Bus Station and Collin Street will no longer exist with the creation of the new centre, as shown in Figure 2.17.

A new bus station will be built at Middle Hill Street to compensate for the absence of the old Broadmarsh Bus Station. In addition, a new car park is proposed to be built above the new bus station. Canal Street will be converted from one-way to two-way to compensate for the absence of Collin Street. As far as the capacity of Canal Street is concerned, the general traffic will be restricted from using Canal Street and only essential traffic, plus cars using the new car park, will be allowed such as buses, taxis and emergency vehicles. Moreover, Middle Hill will be altered from one-way to two-way so that people heading by car from Castle Boulevard to Canal Street, which will be converted to two-way, can access the new car park and use the new bus station at Middle Hill. Figure 2.17 shows the proposed layout of this scheme.

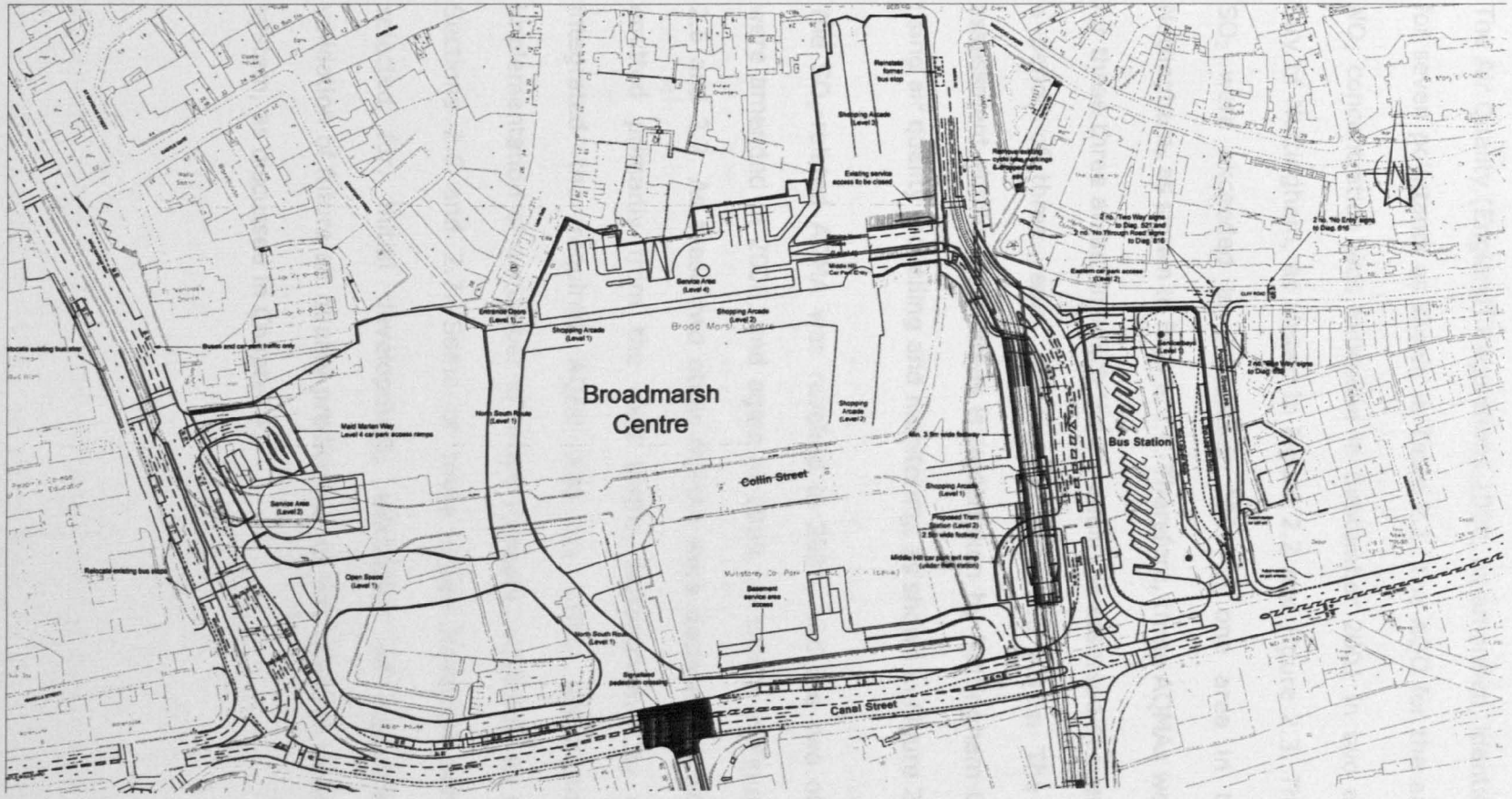

Figure 2.17 Proposed Layout of Broadmarsh Shopping Centre Extension Scheme
Source: (NCC, 2009a)

2.8 Summary

The Air Quality (England) Regulations 2000, as amended, identify the AQOs for seven pollutants as shown in Table 2.1. The AQO for the annual mean NO_2 concentration was exceeded in September 2001 in two areas in the City of Nottingham, as shown in Figure 2.2 and Figure 2.3. The AQOs for SO_2 were exceeded in September 2001 in one area in the City of Nottingham, as shown in Figure 2.1. Therefore, three AQMAs were declared for these three areas, in which the air quality is assessed sequentially, over a period of three years, against the exceeded AQOs. The air quality assessment within these areas is undertaken by Nottingham City council, using air quality modelling and monitoring, as shown in Figure 2.11.

The SO_2-related AQMA was revoked in 2006, and the two other AQMAs were amended in 2008, and again in 2009, as shown in Figures 2.4, 2.5 2.6 and 2.7. As these two other AQMAs were declared for NO_2, which is emitted primarily from the road traffic, Nottingham City Council has integrated the required AQAP into its LTP2, which involves the implementation of a number of urban transport schemes, as explained in Sections 2.6 and 2.7. Some of these urban transport schemes were selected for, initial development, evaluation of transferability, and validation of future air quality predictions, of this research decision support system, as discussed in Chapter 4.

Chapter 3

Air Pollution Dispersion Modelling and Visualisation

3.1 Introduction

This chapter provides a background about different types of air pollution dispersion modelling and compares them in order to select the suitable type for this research. The chapter then continues to compare different models within the selected type of air pollution dispersion modelling, which leads in Section 6.3 to the selection of the suitable model for this research. The chapter also reviews the factors affecting the validation of air pollution dispersion models and identifies the limitations of recent validation and verification strategies.

This chapter gives a brief background about the history of virtual reality modelling techniques along with their recent applications. The chapter also reviews the current visualisation strategies of air pollution dispersion data and addresses limitations of, and challenges identified by, these strategies.

3.2 Review of Air Pollution Modelling Options

Modelling is a powerful technique that can be used to assess the air quality against the mandatory AQOs. In addition, it can be used to assess the effectiveness of the proposed AQAPs in improving the air quality within the declared AQMAs. Furthermore, this technique can be used as a tool to

undertake a strategic air quality assessment for a wide range of action plans and programmes, including LTPs. In this process, local air quality impacts of the plan's measures are all considered and appraised and the resulting air quality assessment report can be taken into consideration before the plan is approved (NCC and NCC, 2006).

Traffic is considered today the main cause of pollution due to the international success in controlling the pollution from other sources, such as domestic heating and industrial sources, in the past decades (Bell, 2006;Hochadel et al., 2006). There are many sophisticated techniques to model the air pollution which have been developed in recent years. These include CALINE (Benson, 1992), CAR (Eerens et al., 1993), ADMS (CERC, 2006a), Operational Street Pollution Model (OSPM) (Berkowicz et al., 1994) and American Environmental Regulatory Model (AERMOD) (USEPA, 1998). On the other hand, there are some other simpler techniques which can be used to predict the long term pollutant concentrations by using existing or readily obtainable data (Briggs et al., 2000). An example of these techniques is the Land Use Regression Modelling (LURM) which associates the long term pollutant concentration to a small number of readily measurable predictor variables (Briggs et al., 2000).

3.2.1 Land Use Regression Modelling

Briggs et al. (2000) developed a regression model for assessing the relationship between traffic-related air pollution and health at the small area scale. In this study, the pollutant concentration of interest was the annual mean concentration of NO_2, and the three key variables used as predictors in the regression model were traffic volume in the 300m buffer zone around each site of interest, land cover in the 300m buffer zone, and surface altitude at the site of interest.

In order to develop and calibrate the regression model, monitoring work was undertaken for the annual mean NO_2 concentrations at approximately 80 sites. The traffic volume in the 300m buffer zone was calculated by multiplying the vehicle numbers during an 18-hour day by the travelled road length for each 20m wide ring buffer zone around the monitoring site. For each of the 15 20m wide ring buffer zones, from 0-20 to 280-300m from the monitoring site, data about vehicle numbers was obtained from traffic counts operated by local authorities and data about travelled road lengths were digitised from 1:10,000 aerial photographs. Land cover in the 300m buffer zone was computed by land cover class (high-density housing and industry) for the same buffer zones through the interpretation of 1:10,000 aerial photographs. The surface altitude at the site was determined from a digital terrain model. Regression analysis was then used to identify the 'best fit' weighted combination of buffer zones for traffic volume and land cover classes to be entered, together with the altitude, into the regression model with the NO_2 data for the 80 sites as follows:

$$C = 38.52 + 0.003705 \times Traff + 0.232\ Land - 5.673 \log_{10}(Alt),$$

where C = annual NO_2 concentration at 2 m above ground level, and Traff = weighted traffic volume factor for the 300-m buffer zone around the site, computed as:

$$Traff = 15 \times Tvol_{0\text{-}40} + Tvol_{40\text{-}300},$$

where $Tvol_{0\text{-}40}$ = vehicle kilometres travelled in the 40m buffer zone around the site (thousand vkt, during an 18-h day); $Tvol_{40\text{-}300}$ = vehicle kilometres travelled in the 40-300m buffer zone around the site

(thousand vkt, during an 18-h day); and $Land_{0\text{-}300}$ = the area of land surface under industrial and high-density residential land in the 0-300m buffer zone around the site (ha), computed as:

$$Land = 8 \times HDH_{0\text{-}300} + Ind_{0\text{-}300},$$

where $HDH_{0\text{-}300}$ = area of high-density housing within the 300m buffer zone of the site (ha); $Ind_{0\text{-}300}$ = area of industrial land within the 300m buffer zone around the site (ha); and Alt = altitude of the site (metres).

Another study employed the regression modelling technique to associate the annual mean NO_2 concentrations with the traffic-based variables. This study was conducted at the westerly end of the Ruhr-area in North-Rhine Westphalia, Germany (Hochadel et al., 2006). The study was undertaken in an area which comprised urban industrial cities and large adjacent rural areas. The study involved the computation of a diversity of traffic related predictors in order to test their correlation significance. The fit of linear regression models was judged by the percentage of explained variation (R^2). The traffic related predictors entered into the model were determined by the increase in R^2 attained by the additional inclusion of the respective predictor when the previous predictors are already entered into the model. For the Wesel region of the study area, some traffic based variables significantly correlated to the annual mean NO_2 concentrations, which gave the best model fit and the highest value of R^2, were found to be the daily traffic of heavy vehicles in the 250m buffer zone around each site, daily traffic of total vehicles in the 250-1000m buffer zone, maximum traffic intensity of total vehicles in the 50m buffer zone, distance to the nearest major road, and distance to the nearest highway (motorway or Federal road).

In order to develop the linear regression model of the Wesel region, which was not validated due to the lack of independent monitoring sites, monitoring work was undertaken for the annual mean NO_2 concentrations at 30 sites. The coordinates of these measurement sites were determined by GPS and the main road network in the study region was available in the form of a geographical database. The average daily traffic counts from the year 2000 were available and classified according to several vehicle types. ArcView version 8.3 was used for the data management. Traffic data were determined by creating circular buffers with radii 50, 100, 250, 500, and 1000m around the coordinates of the NO_2 monitoring sites used to develop the regression model. The daily traffic of heavy vehicles in the 250m buffer zone was calculated by multiplying the average number of heavy vehicles per day by the street length and summing up for all segments in the 0-50, 50-100, and 100-250m buffer zones. The daily traffic of total vehicles in the 250-1000m buffer zone was calculated by multiplying the 2000 annual average number of total vehicles per day by the street length and summing up for all segments in the 250-500 and 500-1000m buffer zones. The maximum traffic intensity of total vehicles in the 50m buffer zone was calculated by determining the highest number of total vehicles per day on a segment (over the year 2000) and summing up for all segments in the 0-50m buffer zone (vehicles per day). The distance to the nearest highway was determined as the distance of the midpoints of a 20m raster.

The daily traffic of heavy vehicles, daily traffic of total vehicles, maximum traffic intensity of total vehicles and distance to the nearest highway were brought together with the annual average concentrations of NO_2 at the monitoring sites, to derive a powerful linear regression model for the prediction of NO_2 annual concentrations. By use of predictors for the annual NO_2 concentrations, the model could attain an acceptable percentage of

variation within the Wesel region (R^2=0.81). However, no consideration was given in this regression model for the meteorological conditions prevailing in the Wesel region.

Despite the advantages of using readily obtainable data and requiring low computational costs, regression air pollution models have many disadvantages. First of all, LURM is only suitable to predict the air pollution over small areas (Briggs, 2007). The reason is that data from monitoring sites should not be simply extrapolated to large surrounding areas that may have different characteristics to the areas used in the initial development of the regression model. Differences in street and building configurations and traffic composition may change the dispersion of air pollution from small areas to larger surrounding areas (Hoek et al., 2008;Vienneau et al., 2010). To predict the air pollution over a large area, a dense and widely distributed network of monitoring stations is required which is not readily available due to the high monitoring cost.

Secondly, regression models can only predict the static air pollution such as the long term averages of air pollution concentrations. Therefore, regression models are not suitable to study the dynamic air pollution dispersion which requires the prediction of short-term averages of air pollution concentrations. The inability of LURM to model short-term air pollution concentrations makes LURM unsuitable to assess the air quality against the hourly concentration-based AQOs, such as the number of exceedances and percentiles.

3.2.2 GIS-based Moving Window Approach

Vienneau et al. (2009) developed a GIS-based moving window approach to model annual average concentrations of NO_2 across a large continental

area at 1km resolution. A 1km × 1km emissions grid was constructed and stored in GIS to cover the entire study area. Data on emissions was obtained from pre-existing emission inventories. Some of these inventories were inconsistent from one country to another in terms of the way in which local estimates were made. Hence, these inconsistent emission inventories were disaggregated by using GIS to a 1km grid. Then, a purpose-designed inventory was derived from these disaggregated inventories to provide the data required for the emissions grid which comprised industrial and traffic emissions of NO_x.

The GIS-based moving window approach involved passing a window, cell by cell, across the emissions grid to compute an emission intensity index at the central (target) cell within the moving window. Figure 3.1 gives an example for the moving window approach. The emission intensity index was the distance-weighted sum of emissions in cells which surround the target cell and are covered by the moving window. The distance weights of these surrounding cells were calculated by a predefined distance-decay function ($1/d^2$). Then, regression analysis was used to derive a calibration function to convert the calculated emission intensity index, at the target cell of the moving window, into a concentration of NO_2. 714 NO_2 monitoring sites were used to perform the regression analysis and compute the calibration function. 228 sites were reserved as an independent set of monitoring sites to validate the results of this approach. The results of applying the moving window approach to this validation set of independent monitoring sites gave $R^2 = 0.61$ and RMSE = ± 6.59 $\mu g/m^3$.

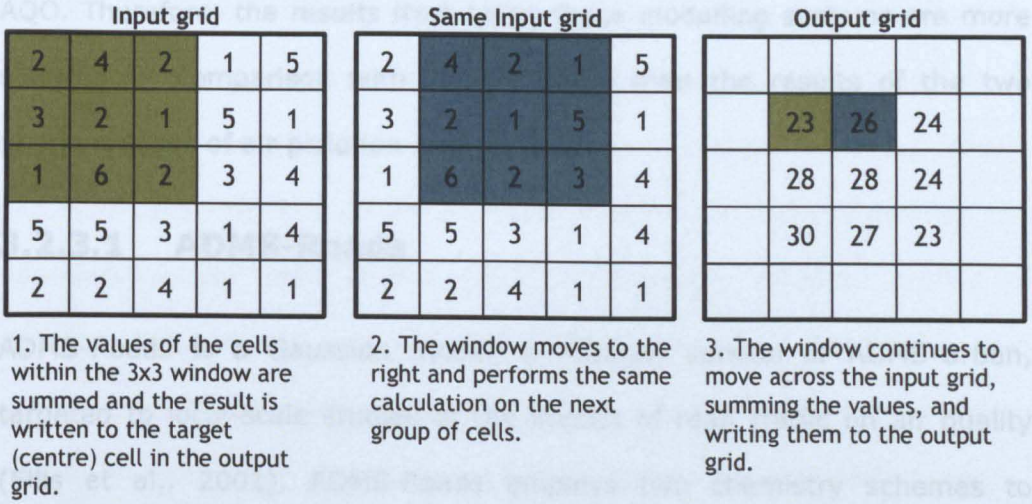

Figure 3.1 Moving Window Example

The developed moving window approach was similar to the LURM in terms of the need for low computational costs. However, this approach is better than the LURM in terms of its applicability to large continental areas. In addition, this approach explicitly depended on emissions which may enable this approach to predict the future air quality in response to future emission scenarios. However, the applicability of this approach is restricted by the need for a large number of monitoring sites to compute the calibration function and to validate the results of this approach. Moreover, as this approach did not use input data for hourly meteorological conditions, this approach can only model long-term, but not short-term, air pollution dispersion. Furthermore, with this approach, the air pollution could not be modelled at many different heights above the ground surface.

3.2.3 Sophisticated Dispersion Modelling

ADMS-Roads, CALINE4 and UK DMRB are the three common sophisticated modelling systems used to assess the impact of road traffic on air quality (Ellis et al., 2001). These systems are capable of not only predicting long-term pollution concentrations, but also estimating short-term concentrations, percentiles and the number of exceedances of a specific

AQO. Therefore, the results from using these modelling systems are more suitable for comparison with various AQOs than the results of the two previous types of air pollution modelling.

3.2.3.1 ADMS-Roads

ADMS-Roads is a Gaussian model, a reduced version of ADMS-Urban, targeted to local-scale studies of the impact of road traffic on air quality (Ellis et al., 2001). ADMS-Roads employs two chemistry schemes to basically simulate the chemical reactions between the road traffic emissions of NO and Ozone in the atmosphere as a secondary source adding to the levels of NO_2. Therefore, the chemistry schemes in ADMS-Roads improve the accuracy of the prediction of NO_2 concentration levels.

ADMS-Roads differs significantly from other models in that it applies up-to-date physics using parameterisations of the boundary layer structure based on the Monin-Obukhov length and the boundary layer height (CERC, 2006a). The Monin-Obukhov length provides a measure of the stability of the atmosphere, whereas many other models use the less precise Pasquill-Gifford stability parameter to characterise the boundary layer. In addition, ADMS-Roads has a non-Gaussian vertical profile of concentration in convective conditions which gives a better performance in validation tests (CERC, 2006a). All of these enable ADMS-Roads to model realistically the air pollution at any height from 0 – 3000metres above the ground surface. However, ADMS-Roads has high computational costs with runtimes of hours to days (Barrett and Britter, 2008, 2009).

3.2.3.2 CALINE4

CALINE4 was developed by the California Department of Transport and the US Federal Highways Agency. CALINE4 is a Gaussian model designed to

simulate junctions, parking lots, street canyons, bridges and underpasses. CALINE4 employs the discrete parcel model to account for the chemical reactions between NO and Ozone to produce NO_2 (Ellis et al., 2001). CALINE4 uses the Pasquill-Gifford stability parameter to characterise the boundary layer, and always uses a Gaussian vertical profile of concentration, even in convective conditions. Therefore, CALINE4 is less precise than ADMS-Roads in modelling the vertical air pollution dispersion above the ground surface and has long runtimes as is with ADMS-Roads.

CALINE4 has the drawback of not modelling the dispersion of the air pollution emissions of stationary sources which can be modelled in ADMS-Roads (Namdeo and Colls, 1996). This makes ADMS-Roads more suitable than CALINE4 for modelling the air quality in urban areas.

3.2.3.3 DMRB Screening Model

DMRB is a screening model developed by the UK Department of Transport. This model is based on a number of tables and algorithms which empirically relate the traffic flow, traffic speed, road type and traffic composition to the air pollution concentrations near roads. However, the DMRB screening model can only predict the annual mean and 24-hour mean concentrations, thus excluding the short-term (1-hour) mean concentrations.

3.2.3.1 Comparison of the Performance of CALINE4 and ADMS-Roads against the Same Data Set

Ellis et al. (2001) used the Caltrans highway 99 experiment to compare the validation results of CALINE4 to those of ADMS-Roads. Highway 99 is a dual carriageway located in California. Each carriageway is 7.3m wide and there is a 14m wide central reservation between the carriageways. A total

number of 10 monitors were used to monitor the tracer chemical Sulfur hexafluoride (SF6) during December 1981 to March 1982. The estimated concentrations were compared to the monitored ones for both CALINE4 and ADMS-Roads.

On one hand, the correlation coefficient (r) between the calculated and monitored concentrations for CALINE4 was found to be 0.51. On the other hand, the correlation coefficient between the calculated concentrations and the same monitored concentrations for ADMS-Roads was found to be 0.84. In addition, the slope of the regression best fit line in the case of ADMS-Roads was closer to 1.0, and its intercept was closer to zero, than these two values were in the case of CALINE4. This implies that the results of ADMS-Roads can fit better the monitored concentrations than the results of CALINE4 can do. Consequently, it can be concluded that ADMS-Roads is more accurate than CALINE4 in the modelling of the air pollution dispersion (Ellis et al., 2001).

3.2.3.2 Comparison between DMRB and ADMS-Roads

Ellis et al. (2001) modelled the air pollution dispersion due to a made up scenario of a simplified road segment of variable width and orientation, in order to compare ADMS-Roads and DMRB with regard to these two important parameters. The road orientation is important in relation to the dispersion pattern of pollution away from the road according to the prevailing wind direction. In addition, the narrower the road, the lower the air mixing of emissions along the road, and hence the higher will be the concentrations at a certain distance away from the road centreline.

The concentrations estimated by ADMS-Roads illustrated the effect of both the road orientation and width, on the pollution dispersion away from the road. Conversely, the concentrations calculated by DMRB were independent

of both the orientation and width of the road, since DMRB takes no account of both meteorological conditions and road width. Therefore, ADMS-Roads was found to be more precise than the DMRB model in the simulation of the air pollution dispersion away from the road.

3.3 Review of Factors Affecting Air Pollution Dispersion Modelling

This section reviews the most important factors that can affect the accuracy, and hence reliability, of air quality predictions made using sophisticated air pollution dispersion models.

3.3.1 Background Concentrations

One of the most important sorts of input data required for sophisticated air pollution dispersion models is the background pollution concentrations (Venegas and Mazzeo, 2006). The background concentrations in a model application area are those relevant to all emission sources not included in the model. These emission sources are usually located remote from, and upwind of, the model application area, and thus they are not considered explicitly whilst specifying the emission sources for the model (PCS, 2004). However, the emissions from local sources, not considered explicitly in the model, should also be included in the background concentrations. Therefore, the background concentrations may differ for various modelling of a single model application area as, for each modelling exercise, the local background sources are all the local emission sources minus those local sources explicitly considered for that particular modelling exercise.

In sophisticated air pollution models, the background concentrations are usually added to the modelled concentrations due to the explicitly

considered local emission sources, in order to compute the overall air pollution concentrations, which are compared to the national AQOs, throughout the model application area. Through the application of chemistry schemes, these models use the background concentrations of ozone to estimate the secondary concentrations of NO_2 from NO_x emissions (CERC, 2003), as explained in Section 3.3.2.

The non-local background concentrations can be obtained directly from monitoring stations remote from the model application area. This is to ensure that the measured concentrations are not affected by the local emission sources located inside the model application area (PCS, 2004). Therefore, for an urban model application area in which all the local sources of pollution are explicitly considered, which is usually hard to achieve due to the lack of data, then background concentrations from a rural monitoring station located outside (and ideally upwind of) the model application area should be used, to avoid the double-counting issues (CERC, 2006a).

For a model application area within a city, the background concentrations can also be estimated by using urban atmospheric dispersion models (AEA, 2009;Venegas and Mazzeo, 2006). These models estimate the annual mean urban background pollution concentrations throughout the entire modelled city area with low spatial resolution. However, the use of an annual mean background concentration is far from ideal for modelling anything other than an annual mean of a non-reactive pollutant, e.g. NO_X or PM_{10} but not NO_2 or ozone (CERC, 2009).

3.3.2 Modelling Atmospheric Chemical Reactions

Modelling of chemical reactions is crucial when predicting the critical pollutants such as NO_x (Laxen and Wilson, 2002). NO_x is emitted primarily from the road traffic and is composed of mainly NO and NO_2. After emission, the majority of NO reacts with the background ozone in the ambient air and converts NO to NO_2. Therefore, the proportion of primary NO_2 in the emitted NO_x concentrations is often smaller than that in the background NO_x concentrations (Laxen and Wilson, 2002). However, the widespread of diesel vehicles has increased the primary NO_2 proportion in traffic-emitted NO_x concentrations (Carslaw et al., 2007). As these vehicles are fitted with catalytic diesel particulate filters, these filters oxidise NO to NO_2, increasing primary NO_2 in NO_x emissions, and use the NO_2 as an oxidant to burn the filtered particles.

There are many modules within the air pollution dispersion modelling packages to model the oxidation of NO to NO_2. These modules help to derive the NO_2 concentrations out of the NO_x concentrations estimated by the air pollution dispersion models. Then, the air pollution dispersion model adds the derived NO_2 concentrations to the background NO_2 concentrations to estimate the total concentrations of NO_2 (Laxen and Wilson, 2002). The total concentrations of NO_2 are then compared to the monitored NO_2 concentrations to validate the air pollution dispersion model.

Hirtl and Baumann-Stanzer (2007) used data sets from street canyons in Stockholm, Berlin and London to evaluate the performance of ADMS-Roads when using the Derwent and Middleton chemical reaction approach. This approach calculates the output NO_2 concentrations from NO_x concentrations based on an empirical formula. It was found in the three presented cases

that ADMS-Roads tended to underestimate NO_x concentrations. Meanwhile, the Derwent and Middleton approach was found to overestimate the concentrations of NO_2 resulting from the estimated those of NO_x. Therefore, using the Derwent and Middleton approach balanced out the underestimation of NO_X concentrations and improved the comparison between the calculated NO_2 concentrations and the monitored NO_2 concentrations at the three sites. It was concluded also that in case of availability of the background concentrations of NO_x and O_3, the Chemical Reaction Scheme, another chemical reactions modelling approach, would be more successful with ADMS-Roads. This is because the Chemical Reaction Scheme accounts for more detailed modelling of the atmospheric chemical reactions (Hirtl and Baumann-Stanzer, 2007).

3.4 Validation and Verification of Air Pollution Dispersion Models

Hanna et al. (1991; 1993) recommended a number of statistics to compare the monitored air pollution concentrations and the model predictions. These statistics have been adopted as a common model evaluation framework for the European Initiative on "Harmonization within Atmospheric Dispersion Modelling for Regulatory Purposes" (Olesen, 2001). They comprise:

a. the fractional bias (FB) showing the tendency of the model to over predict or under predict;
b. the normalized mean square error (NMSE) showing the overall accuracy of the model;
c. the geometric mean bias (MG) showing the mean relative bias and indicating systematic errors;

d. the geometric variance (VG) showing the mean relative scatter and reflecting both systematic and random errors;
e. the Pearson correlation coefficient (R) describing the degree of association between observed concentrations and model results; and
f. the fraction of predictions within a factor of two of observations (FAC2).

These statistics are defined as follows:

$$FB = \frac{\overline{C_O} - \overline{C_P}}{0.5\,(\overline{C_O} - \overline{C_P})} \quad \textbf{(3.1)}$$

$$NMSE = \frac{\overline{(C_O - C_P)^2}}{\overline{C_O C_P}} \quad \textbf{(3.2)}$$

$$MG = \exp(\overline{lnC_O} - \overline{lnC_P}) \quad \textbf{(3.3)}$$

$$VG = \exp\left[\overline{(lnC_O - lnC_P)^2}\right] \quad \textbf{(3.4)}$$

$$R = \frac{\overline{(C_O - \overline{C_O})(C_P - \overline{C_P})}}{\sigma_{C_O}\sigma_{C_P}} \quad \textbf{(3.5)}$$

$$FAC2 = fraction\ of\ data\ that\ satisfy\ 0.5 \leq \frac{C_P}{C_O} \leq 2.0, \quad \textbf{(3.6)}$$

where C_p are model predictions; C_o are observations; over bar ($\overline{C}$) is the average over the dataset; and σ_C is the standard deviation over the dataset.

Recent studies used some or all of the above statistics to characterise the error between monitored concentrations and the model predictions (Cai and Xie, 2010;Ginnebaugh et al., 2010;Majumdar et al., 2009;Parra et al., 2010;Jain and Khare, 2010). The selection of only some of the above statistics was not justified in these recent studies. In addition, no

investigation of the identified error, between the calculated and monitored concentrations, was conducted so that this error can be minimised.

Nottingham City Council compared the monitored annual mean NO_2 concentrations at three continuous automatic monitoring stations to the modelled concentrations obtained using ADMS-Urban. The model overestimated the annual mean of monitored concentrations at the three sites (PCS, 2008). Therefore, the model results were multiplied by an adjustment factor, the average ratio of monitored to modelled annual mean concentrations at the three monitoring sites, to correct the annual mean results of the model. This might help to improve the long-term results; however it did not improve the short-term results of the model.

Namdeo et al. (2002) used the hourly predictions of ADMS-Urban and the hourly observations for the first half of 1993 to derive a multiplicative adjustment factor. The factor was applied to the air quality predictions for the second half of 1993 and the corrected predictions were compared to the corresponding observations. This approach improved the long-term results over the second half of 1993; however it did not show how much improvement was achieved on the short-term level. In addition, it is recommended to avoid the application of such an adjustment factor to the model results (CERC, 2009). Instead, the model set-up should be adjusted until the modelled results fit the monitored concentrations.

DEFRA (2009) states that the NO_x (not NO_2) concentrations should be verified and adjusted if NO_2 results of the model disagree with the monitored concentrations. This is to avoid smoothing the model performance, since the annual mean NO_2:NO_x relationship is relatively flat around the 40 $\mu g/m^3$ objective. Therefore, large changes in NO_x around the region of this objective may result in only small changes in predicted NO_2

levels. It also comments that "The adjustment of NO_x is often carried out on the component derived from local Road Traffic Emissions – the Road Contribution". This is because the source contribution is often small compared with the background contribution, and hence the verification of the source contribution can help to adequately assess the model performance. Therefore, Nottingham City Council used this approach to verify the annual mean NO_2 results of ADMS-Urban (PCS, 2010).

ADMS-Urban was used to predict the annual mean road contribution NO_X concentrations. At each monitoring site, the annual mean background NO_X was obtained from the national background maps and subtracted from the monitored total NO_X. This resulted in the monitored annual mean road contribution NO_X which was compared to the results of ADMS-Urban at each monitoring site to derive an average adjustment factor. The modelled ADMS-Urban results were multiplied by this factor and the adjusted results of NO_X were used, along with the background NO_2 concentrations, to derive the adjusted modelled total annual mean NO_2 concentrations by using the LAQM Tools – NO_X to NO_2 spreadsheet. Figure 3.2 shows the monitored total NO_2 versus adjusted modelled total NO_2 annual mean concentrations.

As shown in the figure below, this approach did not eliminate the error between the modelled and monitored annual mean NO_2 concentrations. This is probably because this approach adjusted the more reliable road component of the modelled NO_X, using measured traffic flow, traffic speed and hourly sequential meteorological data, by subtracting a less reliable figure, the background concentration estimated from the national background maps. In addition, the simple NO_X to NO_2 spreadsheet is usually imprecise and using a chemistry scheme to model the atmospheric chemical transformation of NO to NO_2 is more preferable (CERC, 2009). Moreover, this verification approach is only suitable for the modelled

annual mean concentrations and does not apply to the short-term hourly concentrations (CERC, 2009).

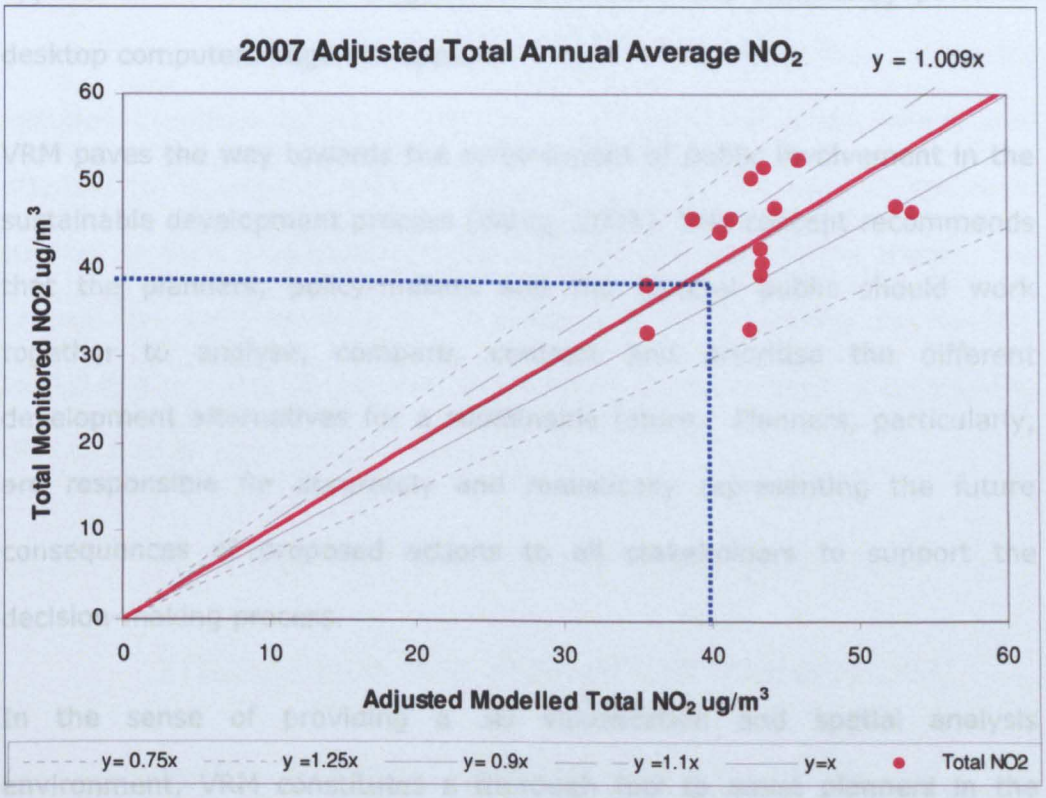

Figure 3.2 Verification Results of Annual Mean NO_2 Concentrations Source: (PCS, 2010)

3.5 Review of Virtual Reality Modelling

Virtual Reality Modelling (VRM) is the process of simulating real world objects into an immersive 3D digital environment (Beng, 2002). VRM allows for real time interaction with the simulated real world objects including flying around, jumping from one position to another and going back to previously viewed points. The main idea of VRM is the provision of a window through which one looks into a virtual world.

Initially, the development of VRM was restricted to highly specialised research communities associated with governmental organisations such as the military and large corporations. The main focus of the military application of VRM was to simulate the aircraft environment, in order to

reduce the risk exposure for inexperienced pilots by providing them with a safe and economic training environment. Only in the early 1990s, did the application of VRM start to grow as affordable and sufficiently powerful desktop computers began to appear.

VRM paves the way towards the achievement of public involvement in the sustainable development process (Wang, 2005). This concept recommends that the planners, policy-makers and the general public should work together to analyse, compare, contrast and prioritise the different development alternatives for a sustainable future. Planners, particularly, are responsible for accurately and realistically representing the future consequences of proposed actions to all stakeholders to support the decision-making process.

In the sense of providing a 3D visualisation and spatial analysis environment, VRM constitutes a thorough tool to assist planners in the development and analysis of different options for physical development. In addition, VRM better illustrates the implications of different planning alternatives for decision-makers than do other 2D visualisation methods. Furthermore, VRM helps demonstrate to the public the benefits of the planning decisions that have been taken. This in turn improves the decision-making process and encourages citizen participation through graphical presentations that are familiar and easy to understand.

The Virtual London project is an example of the representation of the urban environment in a virtual world. The Virtual London project primarily aims to realise a central initiative of the Greater London Authority known as e-Democracy (Evans et al., 2007). The goal of this initiative is to commission VRM to increase the citizen participation in democratic processes. The created virtual model was used to represent the virtual impacts of a

number of proposed scenarios. One of them was to highlight particular buildings, for instance, those buildings that are less than 10 years old. Another scenario was to show the administrative boundaries of each local government within the virtual city model. In addition, these scenarios included the visualisation of the vitality of particular areas, which was attained by visualising, using a range of colours, the relative economic success of each area alongside the physical geometry of the model. The project also explored some other points such as visualising the flooding extent due to a rise of sea level of 5 metres, in the context of considering the adverse effects of global warming.

3.6 Review of Recent Attempts to Integrate Air Pollution Modelling with Virtual Reality

Wang (2005) integrated the US Environmental Protection Agency's CAL3QHC air pollution model with GIS to prepare the model input data and present the results in a geographic context. Street segments and buildings were integrated with simulation results to give georeferenced 3D presentations, although the street canyon effect of buildings on air pollution dispersion was not taken into consideration in the air pollution model. Highway link-based traffic monitoring data for 2001, and 2020 travel demand simulation data, for the study area were provided for this research. Also provided were design capacity, speed at design capacity, and the number of lanes, for each link in the study area. The Bureau of Public Roads (BPR) model was used to predict current and future link-based travel speed. The BPR model is a standard curve that was developed

by fitting a polynomial equation to freeway speed-flow curves. As described by Dowling (1997), the standard BPR equation is expressed as:

$$S_e = \frac{S_f}{1 + a(V/c)^b},$$

where S_e is the predicted mean speed (length/time); S_f is the free-flow speed (length/time); V is the volume (vehicles/time); c is the practical capacity (vehicles/time); a = 0.15; b = 4 (constant, from Dowling, 1997). Both free-flow speed and practical capacity are derived from design capacity. The practical capacity is 80% of the design capacity. The free-flow speed is defined as 1.15 times the speed at practical capacity.

The CAL3QHC model was used to predict current and future CO concentrations. The air pollution model accounted only for the traffic-induced emissions with no account given to either industrial emissions or the background concentrations. This would cause a discrepancy between the calculated and real CO concentrations. The height of output receptors was fixed at 1.8 metres above the ground surface with no chance to change it. CAL3QHC did not have the option to change the spacing between adjacent output receptor points according to the pollution gradient. This may mask the rapidly changing CO concentrations' gradient particularly close to the modelled roads. Moreover, the air pollution model was not validated against any measured CO concentrations.

The 3D visualisation of CO was attained by using the calculated CO concentration instead of the Z coordinate at every output receptor point. Then, a 3D planar surface was interpolated between these receptor points to replace the terrain surface. However, taking off the terrain surface affects the degree of realism of the virtual scene. Furthermore, the floating CO surface created the illusion of having such CO concentrations at

disparate heights whereas, in fact, all the displayed CO concentrations were at 1.8 metres above the ground surface. Figure 3.3 shows the 3D virtual scenes of 2000 and 2020 CO concentrations.

Figure 3.3 implies that 2020 CO concentration levels are much higher than 2000 CO concentration levels, which is probably not true because the research team used the same traffic emissions' rate per vehicle for present and future CO level predictions. Hence, the total traffic emissions of CO increased in the future with the predicted future traffic growth. However, it is well known that the tighter emission standards in the future will result in cleaner vehicles which will significantly decrease the future traffic emissions' rate per vehicle. The reduced future traffic emission rate decreases the future traffic-induced air pollution concentrations which offsets the increase in the calculated air pollution concentrations due to the future traffic growth.

In addition to the reduction in the future traffic emissions' rate per vehicle, there is another significant pollution source which is the background concentrations, which were not accounted for in this study. The future background concentrations are always assumed to be much less than the current background concentrations due to cleaner vehicle and fuel technologies in the future. Therefore, the case is always that the lower future background concentrations and traffic emissions' rate per vehicle will be more significant than the higher future traffic volumes, which usually results in lower predicted total future pollution concentrations. Furthermore, the 2000 meteorological data were used for the prediction of the 2021 CO levels. Therefore, the actual 2021 air pollution dispersion may be completely different to the predicted dispersion, due to the potential differences between 2000 and 2021 meteorological conditions. This shows

the unreliability of the future air quality predictions which are depicted in Figure 3.3.

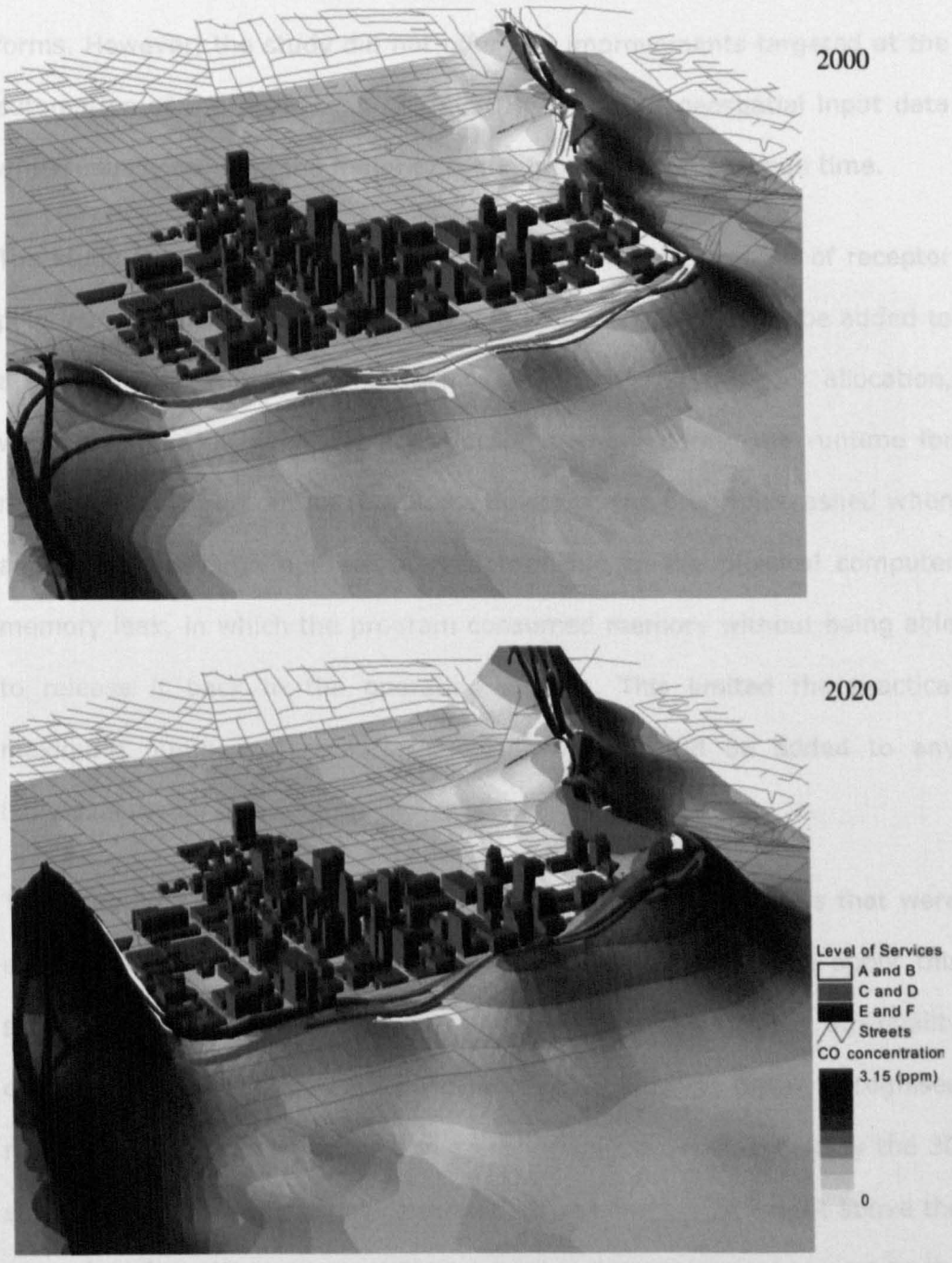

Figure 3.3 3D CO concentration Surfaces of 2000 and 2020
Source: (Wang, 2005)

Wang et al. (2008) further developed CAL3QHC to avoid the manual preparation of CAL3QHC input data which requires a massive amount of time and labour. They also aimed to remove the model limitations which

were 60 receptors and 120 roadway links. The study facilitated the preparation of basic air pollution input data such as receptor height, wind direction and the modelled pollutant type by using bespoke data entry forms. However, the study did not offer any improvements targeted at the automation of the processing of CAL3QHC traffic or geospatial input data which usually requires the majority of the input data preparation time.

The study theoretically removed the limitations to the number of receptor points and roadway links so that up to 50,000 receptors could be added to a single model run by using the dynamic computer memory allocation, which provided an expandable computer memory during the runtime for modelled roads and output receptors. However, the program crashed when adding such a large number of receptors due to the physical computer memory leak, in which the program consumed memory without being able to release it back to the operating system. This limited the practical maximum number of receptors to 100 which could be added to any individual model run.

The integrated system finally helped to just recognise roadways that were experiencing high levels of CO. However, the study did not apply this system to generate alternative traffic scenarios to mitigate air quality degradation in the highly polluted areas around these recognised roadways. Because the integrated system only managed to display the 3D surface of CO concentrations calculated at just one single height above the ground surface, Wang et al. (2008) did not include any improvement to the 3D representation of CO concentrations, although they did identify the true 3D visualisation of air pollution as a future challenge.

In late 2008, the UCL Centre for Advanced Spatial Analysis (CASA) collaborated with the Environmental Research Group (ERG) in King's

College London to create an interactive 3D air pollution map (CASA and ERG, 2008). The 3D virtual scenes of 63 sq km (9km x 7km) of central London were produced by CASA, and ERG provided the air pollution predictions of NO_2, NO_X and PM_{10} which were fused in these 3D virtual scenes to build the 3D air pollution map as shown in Figure 3.4 and Figure 3.5.

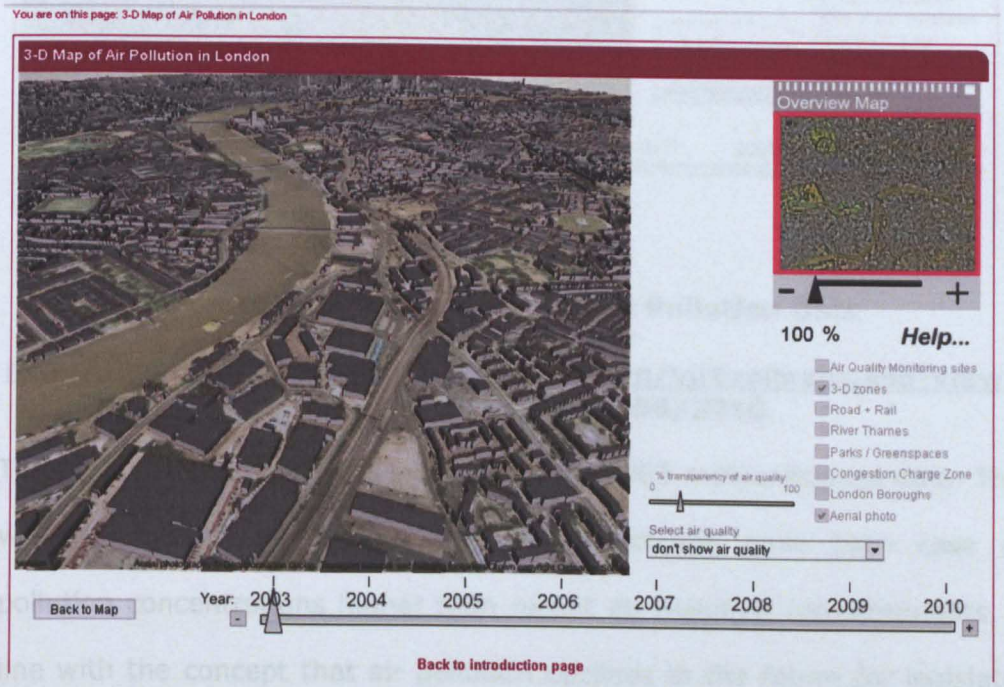

Figure 3.4 3D Map without the Air Pollution Data
Source:
http://www.londonair.org.uk/london/asp/virtualmaps.asp?view=maps - Accessed on 08/06/2010

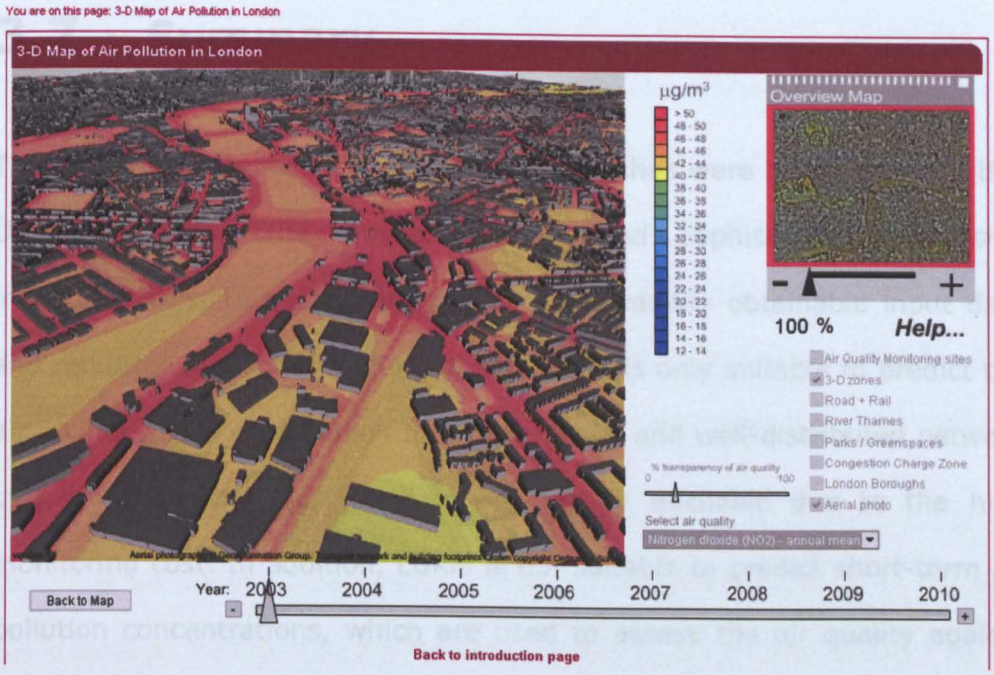

Figure 3.5 3D Map with the Air Pollution Data
Source:
http://www.londonair.org.uk/london/asp/virtualmaps.asp?view=maps - Accessed on 08/06/2010

The air pollution predictions were based on 2003 meteorological data. That was a precautionary approach which realistically gave base case air pollution concentrations higher than recent air pollution measurements, in line with the concept that air pollution declines in the future for legislated emissions. However, this obviously means that the base case scenario (2003) of the air pollution model was not validated against 2003 air pollution measurements, which is likely to reduce the reliability of future air quality predictions of this air pollution model.

The colour scheme of air pollution contour bands in Figure 3.5 comprised twenty colours. This large number of colours has the potential to distract rather than impress the observer. Moreover, this 3D air pollution map displayed only the ground-level air pollution concentrations, thus excluding the air pollution at other levels above the ground surface. Therefore, this 3D air pollution map does not overcome the challenge identified above by Wang et al. (2008).

3.7 Summary

Three different air pollution modelling approaches were investigated in this chapter: LURM, GIS moving window and sophisticated dispersion modelling. Despite the advantages of using readily obtainable input data and requiring low computational costs, LURM is only suitable to predict the air pollution over small areas that have dense and well-distributed network of monitoring stations, which is not readily available due to the high monitoring cost. In addition, LURM is not suitable to predict short-term air pollution concentrations, which are used to assess the air quality against the hourly concentration-based AQOs, since it does not use input data for short-term meteorological conditions.

The GIS moving window approach is similar to the LURM in terms of the need for low computational costs. However, this approach is better than the LURM in terms of its applicability to large continental areas. However, the applicability of this approach is restricted by the need for a large number of monitoring sites, and it can only model long-term, but not short-term, air pollution dispersion, since it does not use input data for hourly meteorological conditions. Furthermore, with this approach, the air pollution could not be modelled at many different heights above the ground surface.

Sophisticated air pollution models are capable of not only predicting long-term pollution concentrations, but also estimating short-term concentrations, percentiles and the number of exceedances of a specific AQO, although they require high computational costs with runtimes of hours to days. Therefore, the results from using these models are more suitable for comparison with various AQOs than the results of the two previous types of air pollution modelling. In terms of model validation,

ADMS-Roads was found more accurate that CALINE4 in modelling air pollution dispersion horizontally and vertically above the ground surface. In addition, ADMS-Roads can model the dispersion of the air pollution emissions of stationary sources which cannot be modelled in CALINE4. In terms of model sensitivity to the road width and orientation, ADMS-Roads was found much more sensitive than the DMRB screening model, since DMRB takes no account of both meteorological conditions and road width.

Some recent attempts were undertaken to give a 3D representation of modelled air pollution dispersion. These attempts were only able to show the output air pollution at a single height above the ground surface in a 3D context, and identified the true 3D visualisation of air pollution as a future challenge. Some of these attempts displayed the modelled air pollution as a floating surface, creating the illusion of having such output air pollution at many disparate heights above the ground surface. The other attempts displayed the air pollution using 20 colours, which has the potential to distract rather than impress the observer.

Chapter 4

Selection of Urban Transport Schemes for This Research Project

4.1 Introduction

The aim of this chapter is to discuss and justify the selection of the transport schemes which are considered in this research project. This is achieved by the investigation of two objectives.

Firstly, criteria were identified to select the transport schemes that are and will be implemented in Greater Nottingham. Data availability from Nottingham City Council was the reason for deciding to limit the selection of transport schemes to only those of Greater Nottingham.

Secondly, these selection criteria were applied to Greater Nottingham's transport schemes to split them into three categories.

The first category consisted of transport schemes that could be used in the *initial development* of this research decision-support system. The second category comprised transport schemes which could be used to *investigate the transferability* of the decision-support system. The third category included transport schemes which could be used to *assess the accuracy of future air quality predictions* using this decision-support system.

4.2 Selection criteria for Transport Schemes

As far as the transport-induced air pollution is concerned, the first criterion of selection was the involvement of the transport scheme with a transport-related AQMA, which has air quality problems due to the road traffic. AQMAs usually have intensive air quality monitoring within, and around, them. That in turn would ensure the availability of monitoring data required to calibrate and validate the air pollution dispersion model in these areas.

The second criterion was the availability of geometric, geographic and spatial data required to extract the georeferenced Digital Terrain Model (DTM), raster layer and other features covering the areas affected by the implementation of the identified transport schemes. This data was required to build the 3D city model, part of the 3D air pollution dispersion interface. The raster image layer of the study area would constitute the geographic interface of the air pollution model. This geographic interface was required to specify the location and spatial extent of the air pollution sources located in the area affected by the implementation of these identified transport schemes.

The third criterion was the availability of traffic data, such as the flow and the speed, required to run the air pollution model. This traffic data includes flows/counts/speeds for the current principal roads and the prospective after the implementation of these identified transport schemes. The fourth criterion was the availability of emission data for industrial air pollution sources located in the area which would probably be affected by the implementation of the identified transport schemes.

The fifth criterion was the availability of pre- and post-implementation monitoring and modelling data for the identified transport schemes that has already been implemented. This would offer the opportunity to validate further the air pollution dispersion model. This further validation could be accomplished by comparing the predicted air pollution concentrations to the concentrations monitored after the actual implementation of these transport schemes.

Table 4.1 lists the potential transport schemes in Greater Nottingham and the suitability of each transport scheme for the five criteria identified above. Data availability in this table was compiled after communicating with the Pollution Control and Envirocrime Section and the Transportation Team in Nottingham City Council.

Table 4.1 Coincidence between the Transport Schemes and the Selection Criteria

Transport Scheme	Coincide with AQMA	Spatial data	Traffic data	Emission data	Scheme complete
NET Phase 2	√	√	√	√ (Dunkirk AQMA)	
Ring Road Major	√	√	√	√ (Dunkirk AQMA)	
Turning Point North	√	√	√	√	√
Hucknall Town Centre Improvement					
Gedling Transport Improvement					√
Station Master Plan	√				
Turning Point East	√	√	√	√	
Broadmarsh Shopping Centre Extension	√	√	√	√	

4.3 Selection and Categorisation of Transport Schemes

The NET Phase 2 and Ring Road Major schemes were the first two transport schemes to meet 4 out of 5 of the selection criteria shown in Table 4.1, in both cases focusing on the sections coincident with the Dunkirk AQMA. The availability of data for these two proposed transport schemes was confirmed for this research project. Hence, these two transport schemes were selected for the initial development of this research DSS.

The Ring Road Major and NET Phase 2 schemes were presumed to directly affect the air quality in the Dunkirk AQMA (NCC and NCC, 2006). Furthermore, the early communications with Nottingham City Council revealed the potential of gathering 2006 traffic data for the Dunkirk AQMA. The spatial data coverage needed to build and develop the 3D city model of the Dunkirk AQMA, was found to be available also. Therefore, initially the air quality impacts of the implementation of both the Ring Road Major and NET Phase 2 schemes in the Dunkirk AQMA were selected as two transport case studies for the initial development of this research DSS.

However, further investigations regarding the Ring Road Major scheme revealed that this scheme was mainly concerned with junction improvements. These junction improvements involved acquiring land to widen one or more of the junction approaches. This would provide the opportunity to add additional right-turn and/or left-turn lanes to the junction layout. However, ADMS-Roads, the air pollution modelling package used in this research project, ignores the end effects of road links such as junctions.

The nearest junction to the Dunkirk AQMA to be improved within the framework of the Ring Road Major scheme was Crown Island. This junction is some distance away from the Dunkirk AQMA, and hence the air quality benefits of improving the junction would probably be minimal, or even negligible, in the Dunkirk AQMA. Therefore, it was concluded that the Ring Road Major scheme was not suitable for use in this research project. Consequently, the NET Phase 2 scheme, focusing on the elevated section to run through the Dunkirk AQMA (see Figure 2.14 in Section 2.6.5), was the key case study selected for the initial development of the DSS.

Data required to model the air quality impacts of the Turning Point East and Broadmarsh Shopping Centre Extension schemes was obtained after the initial development of the DSS. These two transport schemes coincided with parts of the Nottingham City Centre AQMA. The data required for the building of the 3D city model of the City Centre AQMA was also later found to be available for this research project. These two transport schemes were similar to NET Phase 2 in terms of being proposed at the time of undertaking this research. Therefore, the Turning Point East and Broadmarsh Shopping Centre Extension schemes were selected to investigate the transferability of this research DSS to a wide range of transport schemes, as justified in Chapter 9.

The Turning Point North scheme was completed, and in operation, at the time of undertaking this research project. This transport scheme was the only completed scheme (see Table 4.1) for which data was available for this research project. Furthermore, the Turning Point North scheme coincided with parts of the City Centre AQMA with the permanent AURN air quality monitoring station nearby in Clinton Street East. So the Turning Point North scheme was selected to assess the accuracy of future air

quality predictions made using this research DSS, as discussed later in Chapter 10.

4.4 Summary

This chapter introduced five criteria to select the Greater Nottingham transport schemes for consideration in this research project. Four schemes were chosen.

Firstly, NET Phase 2 was selected to investigate its air quality impacts in the Dunkirk AQMA for the purpose of the initial development of this research DSS. Secondly, the Turning Point East and Broadmarsh Shopping Centre Extension schemes were selected to investigate their air quality impacts in the Nottingham City Centre AQMA, with regard to the wider application of the DSS to other transport schemes. Thirdly, the Turning Point North scheme was selected to investigate its air quality impacts in the Nottingham City Centre AQMA for the purpose of testing the accuracy of future air quality predictions made using this research DSS.

Chapter 5

Traffic Data Processing and Forecasting Relating to NET Phase 2 Implementation in the Dunkirk AQMA

5.1 Introduction

The aim of this chapter is to present the processing and forecasting of present and future traffic data required for the initial development of the research decision-support system. The aim of this chapter was achieved by the investigation of five objectives:

1. selection of the principal roads, with a significant air quality impact, in the Dunkirk AQMA were selected for consideration in the air pollution model of the research decision-support system;
2. definition of the acceptable forms of different traffic data items required for input into this air pollution model;
3. understanding the traffic data as initially obtained from Nottingham City Council;
4. development of the strategy for processing this initial traffic data into the correct form for input into the air pollution model;
5. forecasting of future traffic data for the principal roads in the Dunkirk AQMA after the implementation of NET Phase 2.

5.2 Selected Principal Roads in Dunkirk AQMA

Discussions with the Pollution Control Section in Nottingham City Council were undertaken to identify the principal roads to be considered in the air pollution model of the Dunkirk AQMA. These consultations resulted in Derby Road, Clifton Boulevard, Abbey Street and Beeston Road being identified as the main roads to be considered in the air pollution model. The Pollution Control Section advised that the consideration of other minor roads in the Dunkirk AQMA would have little impact on the air quality, and also the traffic data of these minor roads were not available in the city council. Figure 5.1 displays the roads considered in the air pollution model of the Dunkirk AQMA.

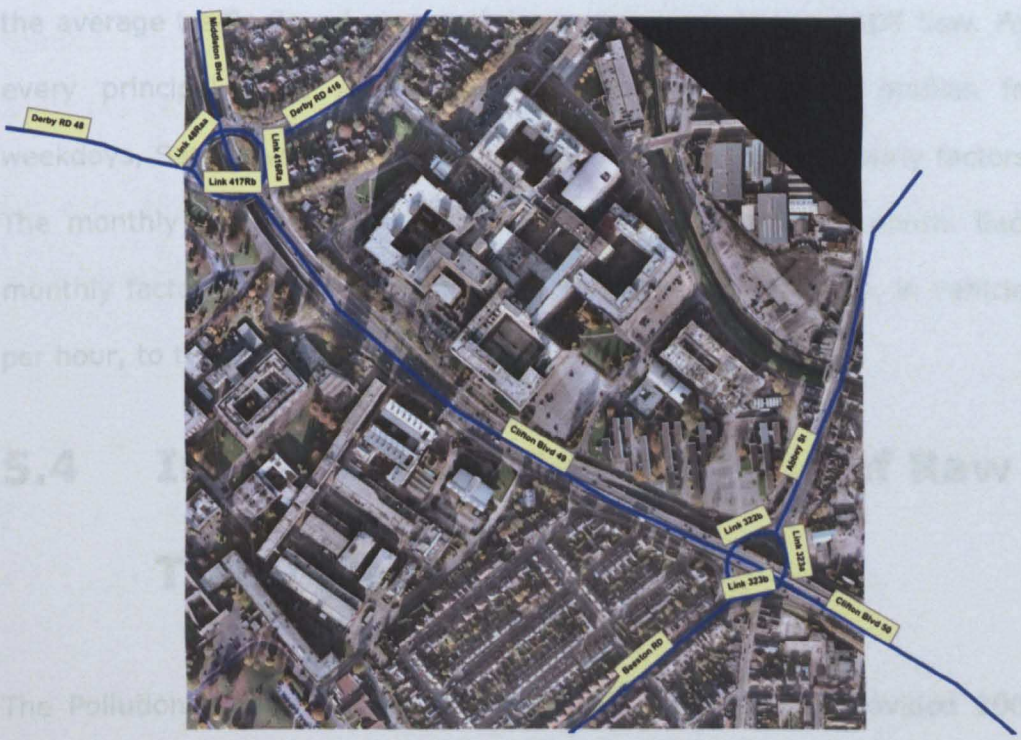

Figure 5.1 Principal Roads for Air Pollution Model of Dunkirk AQMA

5.3 Accepted Forms of Traffic Input Data

ADMS-Roads accepts the traffic input data of every road split into two categories, Light Duty Vehicles (LDV) and Heavy Duty Vehicles (HDV). The LDV category comprises vehicles with a gross vehicle weight less than or equal to 3.5 tonnes (DMRB, 2007). The HDV category comprises vehicles with a gross vehicle weight greater than 3.5 tonnes. For every road and each vehicle category, ADMS-Roads requires the traffic speed and the Annual Average Daily Traffic (AADT) flow in vehicles per hour.

For every principal road, ADMS-Roads optionally requires the hourly and monthly traffic profiles. The hourly traffic profile for a given day of the week is a set of 24 factors, one per hour. Each hourly factor is the ratio of the average traffic flow during each hour of the day to the AADT flow. For every principal road, ADMS-Roads accepts hourly traffic profiles for weekdays, Saturdays and Sundays, relating therefore to 72 hourly factors. The monthly traffic profile is a set of 12 factors, one per month. Each monthly factor is the ratio of the monthly average traffic flow, in vehicles per hour, to the AADT flow.

5.4 Initial Form and Processing of Raw Traffic Data

The Pollution Control Section in Nottingham City Council provided 2006 traffic speed data for the main roads selected for consideration in the air pollution model of the Dunkirk AQMA. They also provided the percentages required to split the traffic flow data for every principal road considered in

the Dunkirk AQMA air pollution model into three traffic categories: Heavy Goods Vehicles (HGV), Light Goods Vehicles (LGV) and Public Service Vehicles (PSV). LGV category was confirmed equivalent to LDV; HGV plus PSV categories were confirmed equivalent to HDV.

The Traffic Control Centre in Nottingham City Council provided the 2006 data that is collected automatically by detectors embedded in the two directions of each principal road considered in the Dunkirk AQMA air pollution model. The data supplied by the Traffic Control Centre was in the form of the traffic count every five minutes for every requested road for all of the year 2006. This produced a very large dataset which could not be processed manually. Visual Basic for Applications (VBA) was used in Microsoft Excel to automate the processing of the raw traffic flow data to obtain the AADT flow, the hourly and the monthly traffic profile for every principal road considered in the Dunkirk AQMA air pollution model. The VBA computer program automated the processing of the raw traffic flow data by using the following mathematics:

For each day, the five-minute flow data was automatically aggregated to yield hourly flow data.

Let f_{ijk} = the total traffic flow in both directions in hour i of day j of month k, and let N_k = the number of days in month k, such that i = 0,...,23, j = 1,..., N_k (where N_k = 28, 29, 30 or 31 as appropriate), and k = 1,...,12.

Therefore

$$\text{AADT (vehicles/hour)} = \frac{\sum_{k=1}^{12}\sum_{j=1}^{N_k}\sum_{i=0}^{23} f_{ijk}}{[\sum_{k=1}^{12} N_k] \times 24}, \qquad \textbf{(5.1)}$$

$$\text{Monthly Average}_k\text{(vehicles/hour)} = \frac{\sum_{j=1}^{N_k}\sum_{i=0}^{23} f_{ijk}}{N_k \times 24}, \quad \forall k, k = 1, \dots, 12, \qquad \textbf{(5.2)}$$

$$\text{Monthly Factor}_k = \frac{\text{Monthly Average}_k}{\text{AADT}}, \quad \forall k, k = 1, \dots, 12. \qquad \textbf{(5.3)}$$

Let p_k , q_k and r_k = the number of weekdays, Saturdays and Sundays, respectively, in month k, such that $p_k + q_k + r_k = N_k$ $\forall k, k = 1, \dots, 12$.

Therefore, the Hourly Average_i(vehicles/hour):

$$\text{for weekdays (if j denotes weekdays)} = \frac{\sum_{k=1}^{12}\sum_{j=1}^{p_k} f_{ijk}}{\sum_{k=1}^{12} p_k} \forall i, i = 0, \dots, 23, \qquad \textbf{(5.4)}$$

$$\text{for Saturdays (if j denotes Saturdays)} = \frac{\sum_{k=1}^{12}\sum_{j=1}^{q_k} f_{ijk}}{\sum_{k=1}^{12} q_k} \forall i, i = 0, \dots, 23, \qquad \textbf{(5.5)}$$

$$\text{for Sundays (if j denotes Sundays)} = \frac{\sum_{k=1}^{12}\sum_{j=1}^{r_k} f_{ijk}}{\sum_{k=1}^{12} r_k} \forall i, i = 0, \dots, 23. \qquad \textbf{(5.6)}$$

Hence there are 3 × 24 = 72 different day-related hourly average traffic flows so, correspondingly, there are 72 hourly factors, such that:

$$\text{Hourly Factor}_i = \frac{\text{Hourly Average}_i}{\text{AADT}} \quad \forall i, i = 0, \dots, 23. \qquad \textbf{(5.7)}$$

Therefore, the full traffic flow data processing output for each principal road was:

- 24 hourly factors for weekdays, in order, from hour 0 to hour 23.
- 24 hourly factors for Saturdays, in order, from hour 0 to hour 23.
- 24 hourly factors for Sundays, in order, from hour 0 to hour 23.
- 12 monthly factors for the 12 months, in order, from January to December.

A number of challenges in terms of lack of data from some detectors for some time periods during the year 2006 needed to be overcome. If the corresponding traffic data was available for another year, then that was used, factored using traffic data from the nearest detectors, for that other year and 2006. If the corresponding traffic data from another year was not available, then 2006 traffic data from the nearest available detectors was used.

For the Clifton Boulevard detectors, traffic data was only available for 2005. Traffic data from the nearest detectors to the Clifton Boulevard detectors was collected in both 2005 and 2006. This data was processed to provide multiplicative factors to shift the 2005 five-minute traffic counts of Clifton Boulevard to 2006. Steps were taken in the VBA code to avoid division by zero in the calculation of these shift factors. Figure 5.2 to Figure 5.9 depict the VBA computer program output monthly and hourly traffic profiles for the principal roads considered in the Dunkirk AQMA air pollution model.

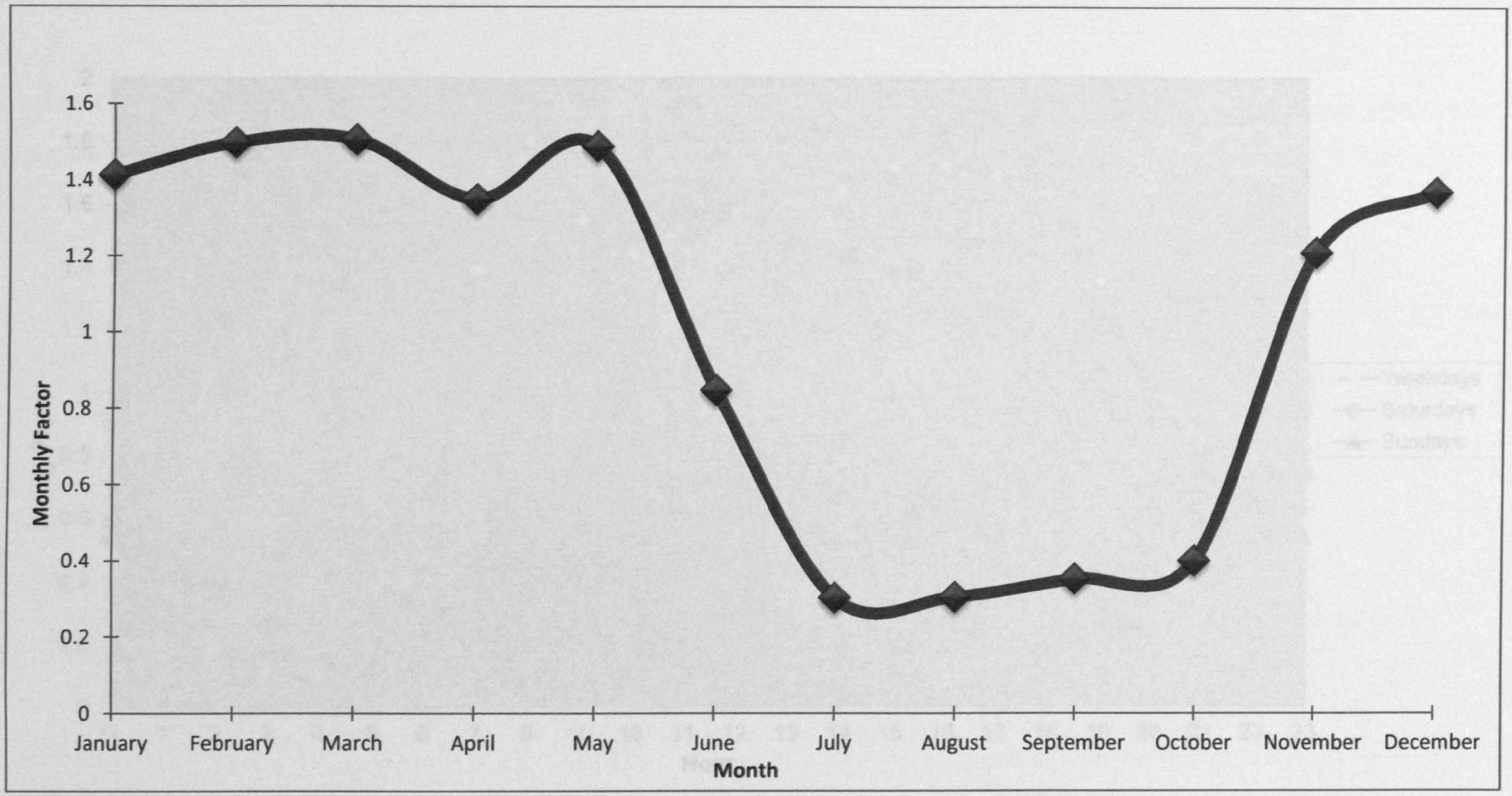

Figure 5.2 Derby Road 2006 Monthly Traffic Flow Profile

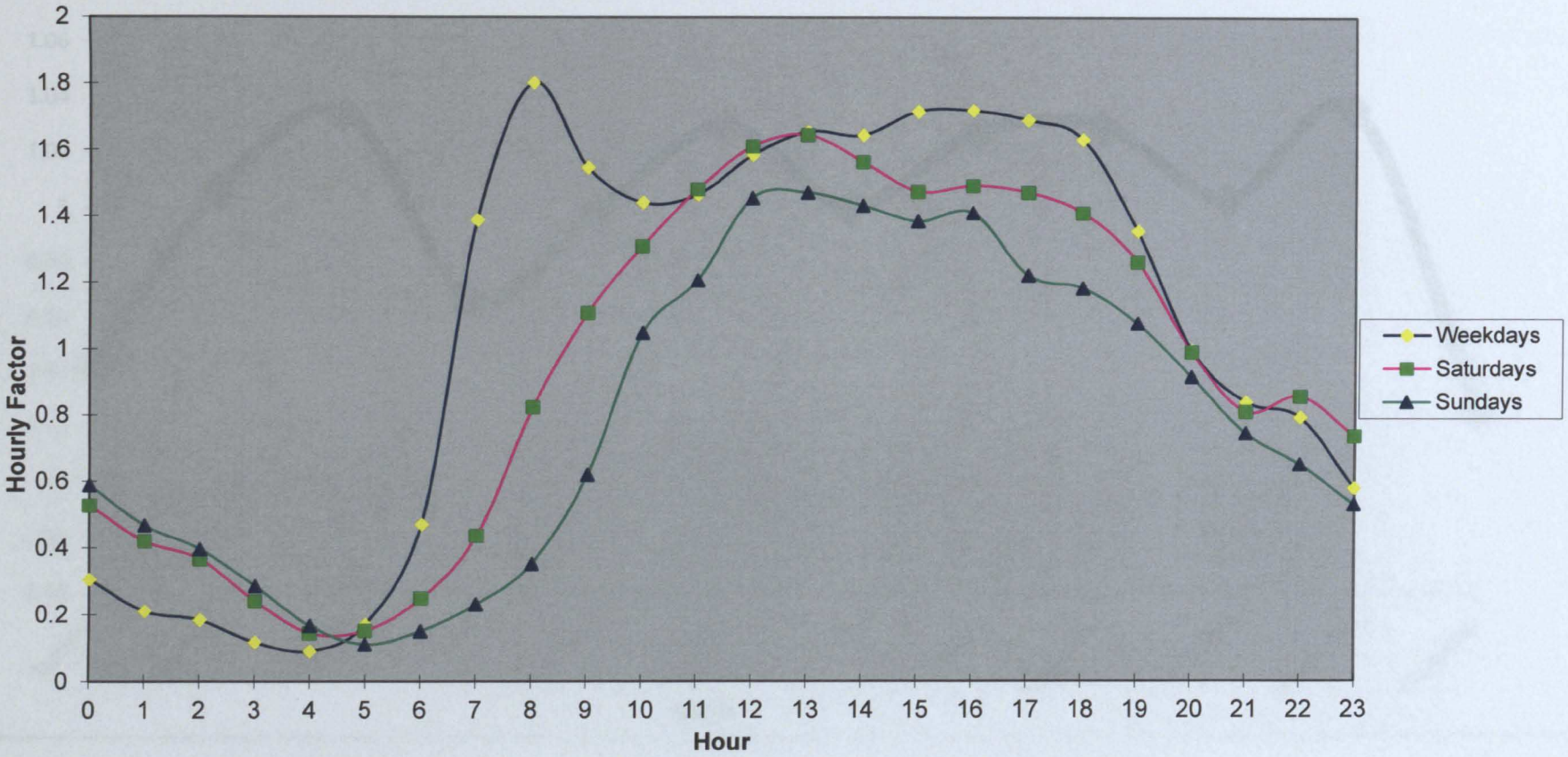

Figure 5.3 Derby Road 2006 Hourly Traffic Flow Profiles for Weekdays, Saturdays and Sundays

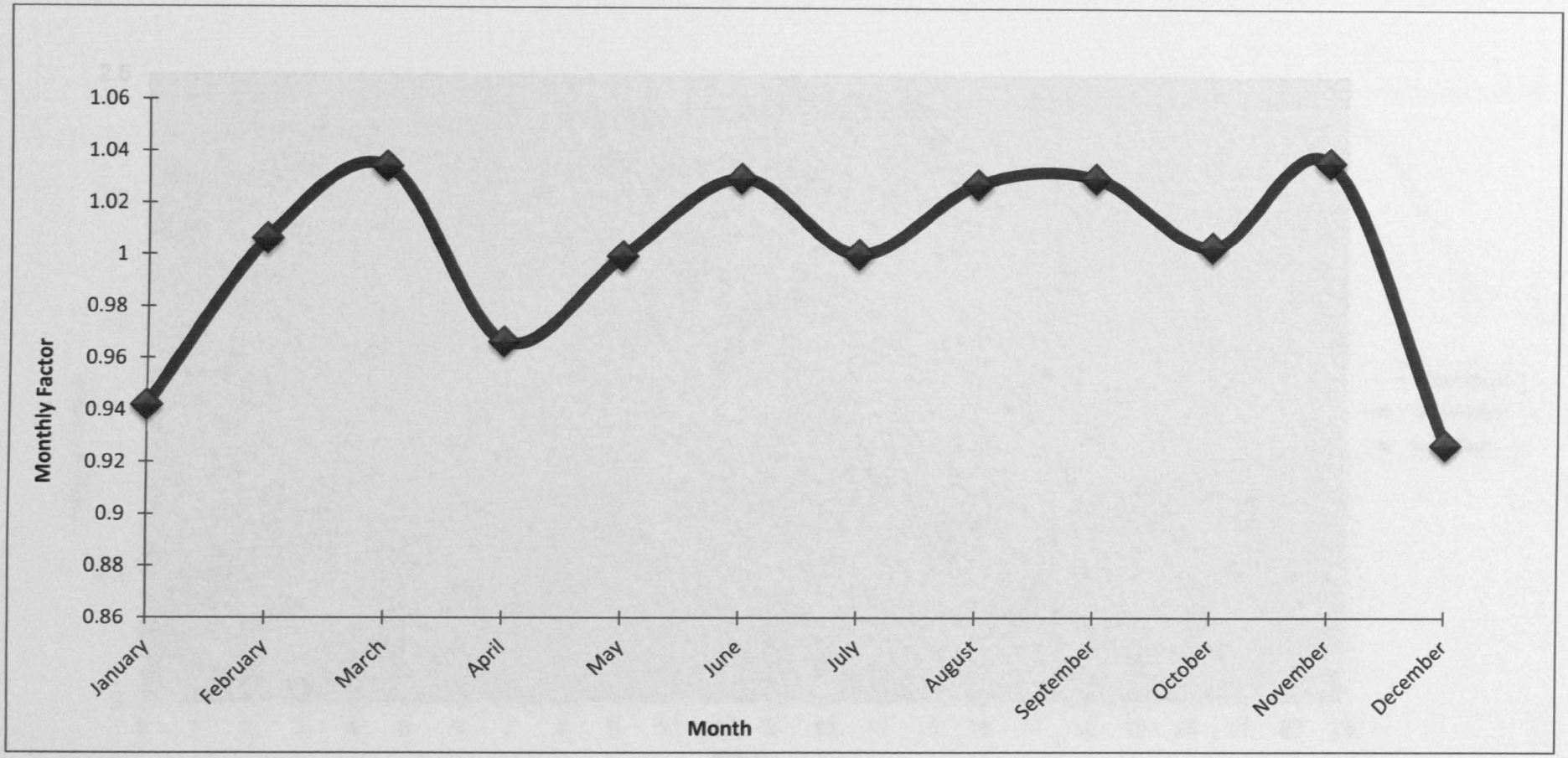

Figure 5.4 Clifton Boulevard 2006 Monthly Traffic Flow Profile

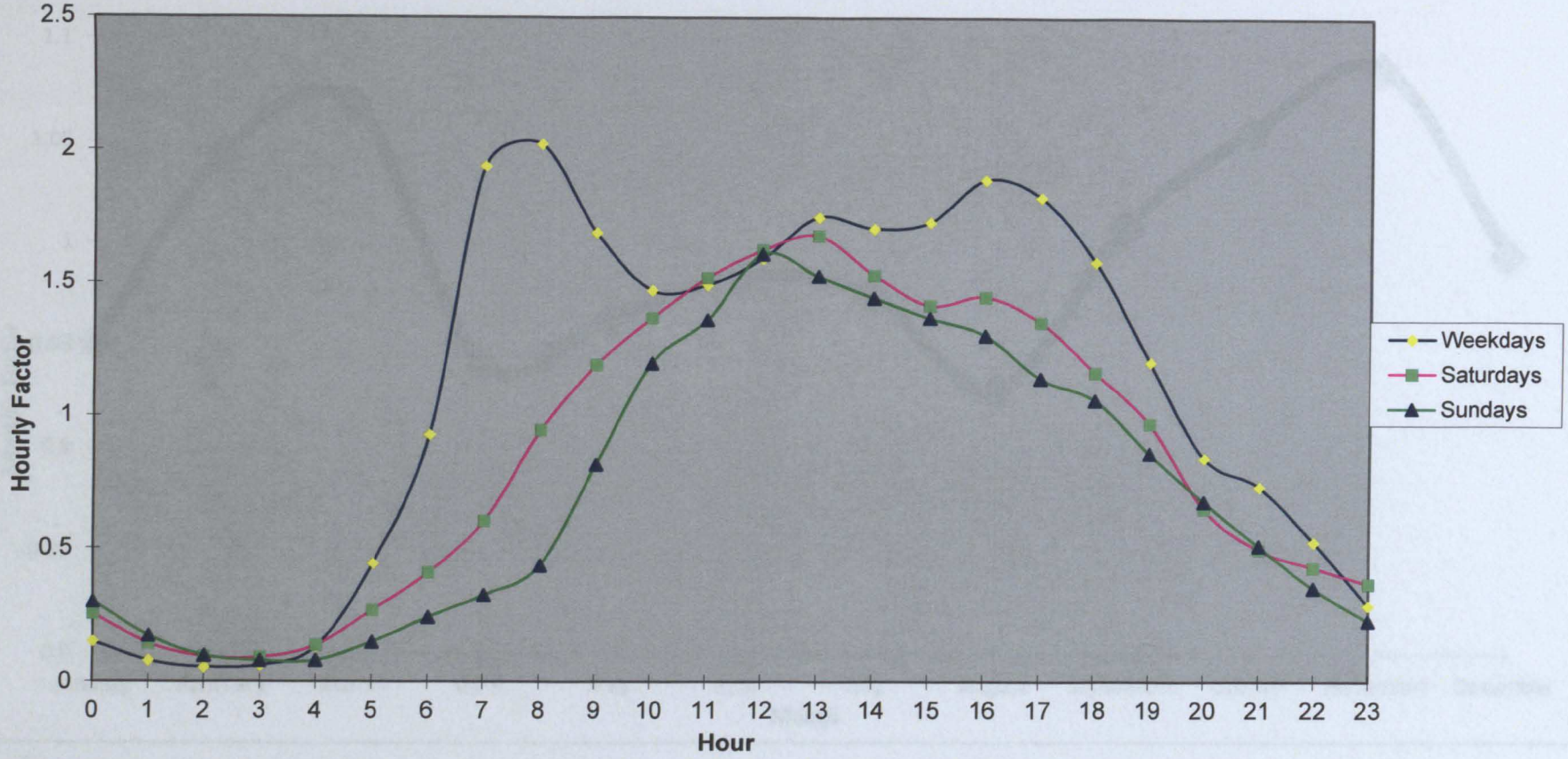

Figure 5.5 Clifton Boulevard 2006 Hourly Traffic Flow Profiles for Weekdays, Saturdays and Sundays

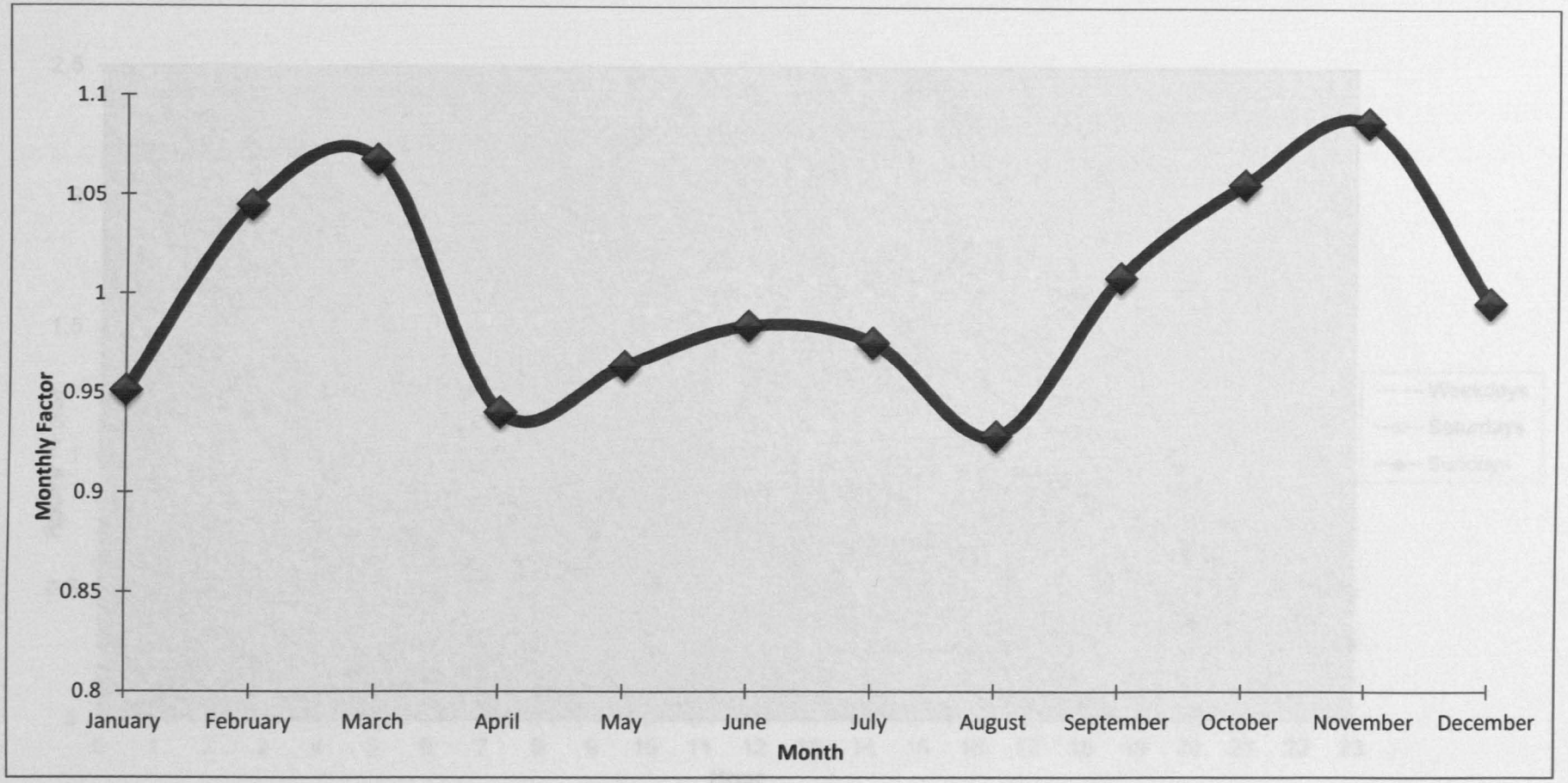

Figure 5.6 Abbey Street 2006 Monthly Traffic Flow Profile

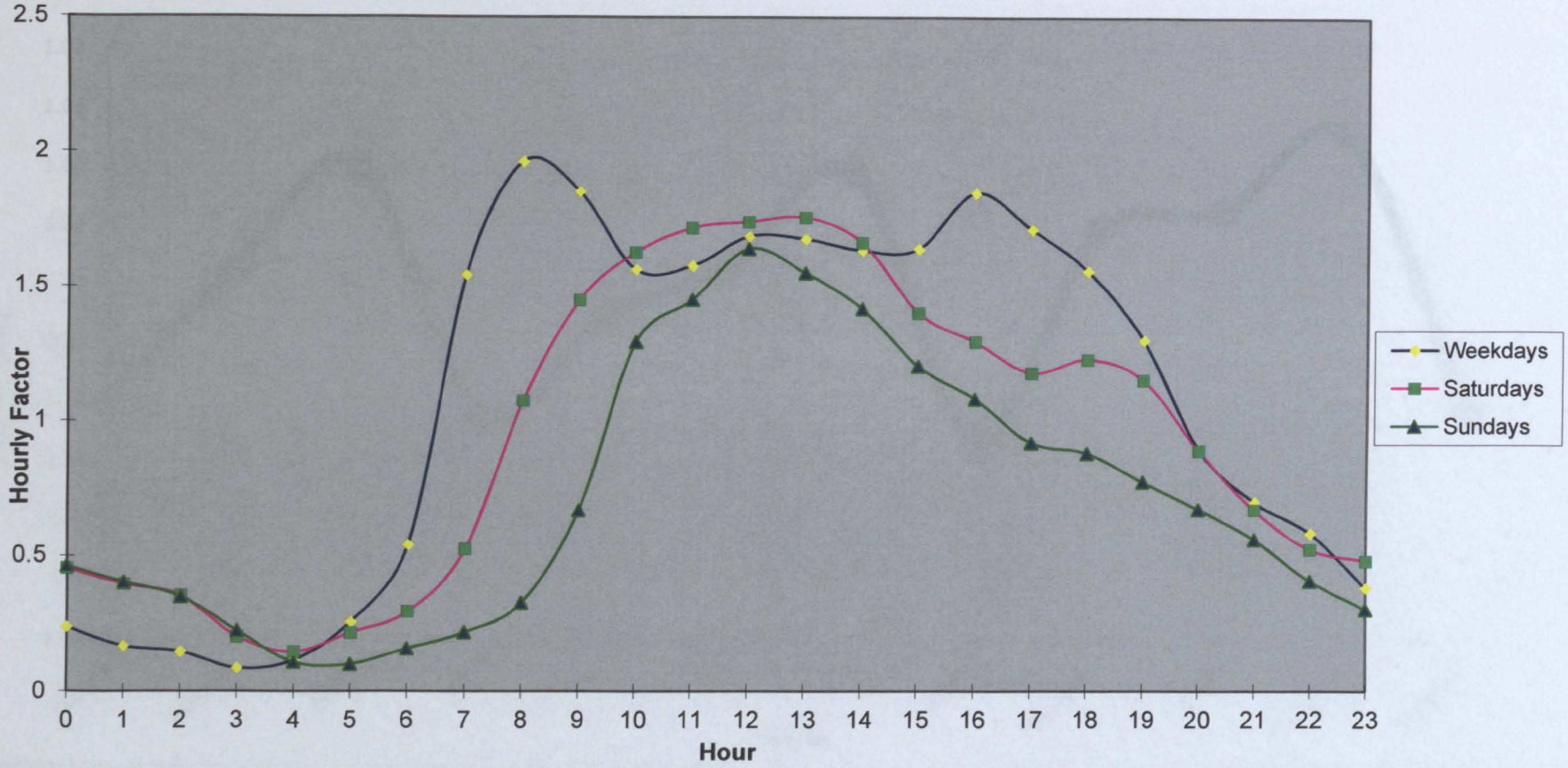

Figure 5.7 Abbey Street 2006 Hourly Traffic Flow Profiles for Weekdays, Saturdays and Sundays

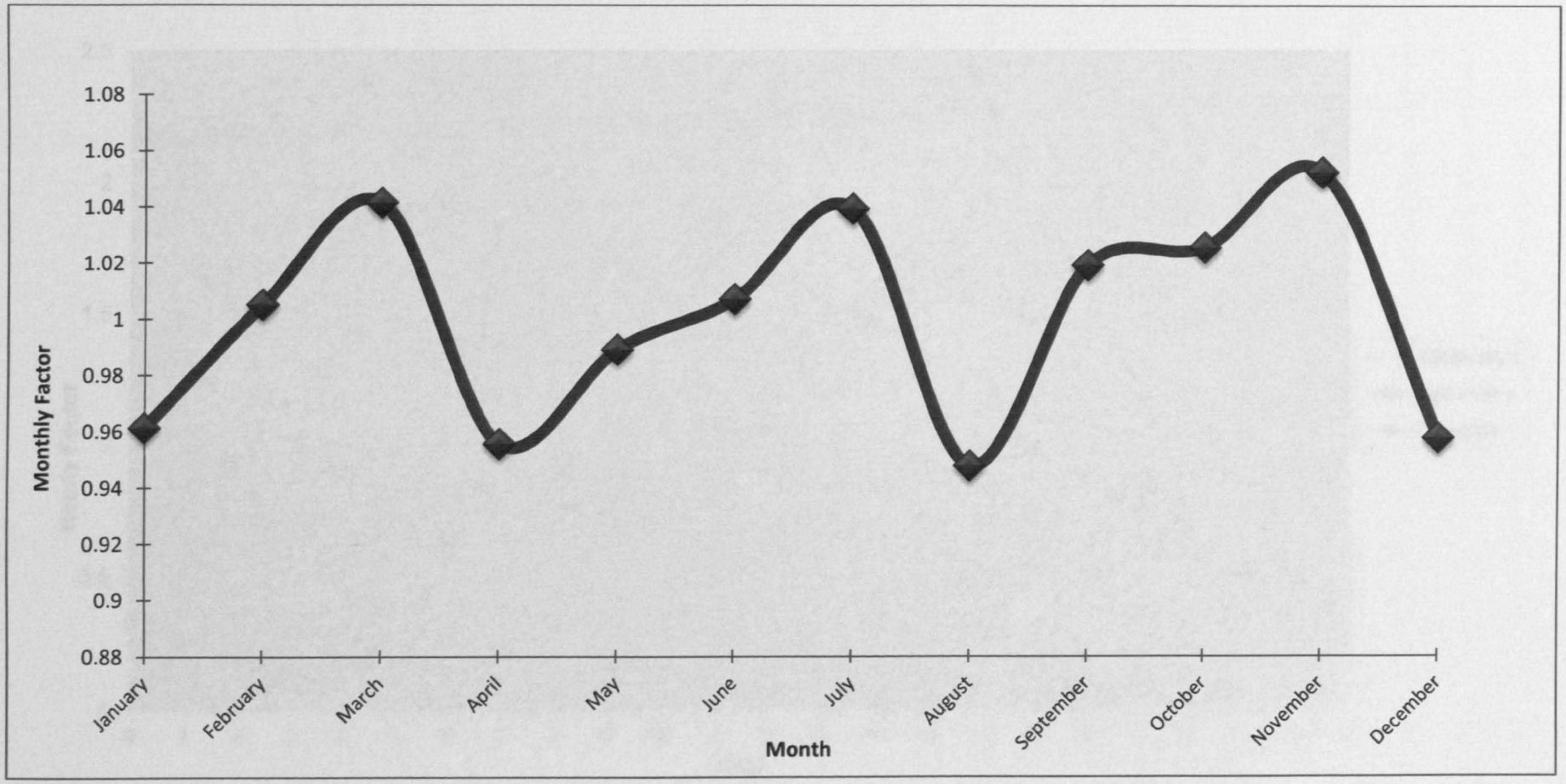

Figure 5.8 Beeston Road 2006 Monthly Traffic Flow Profile

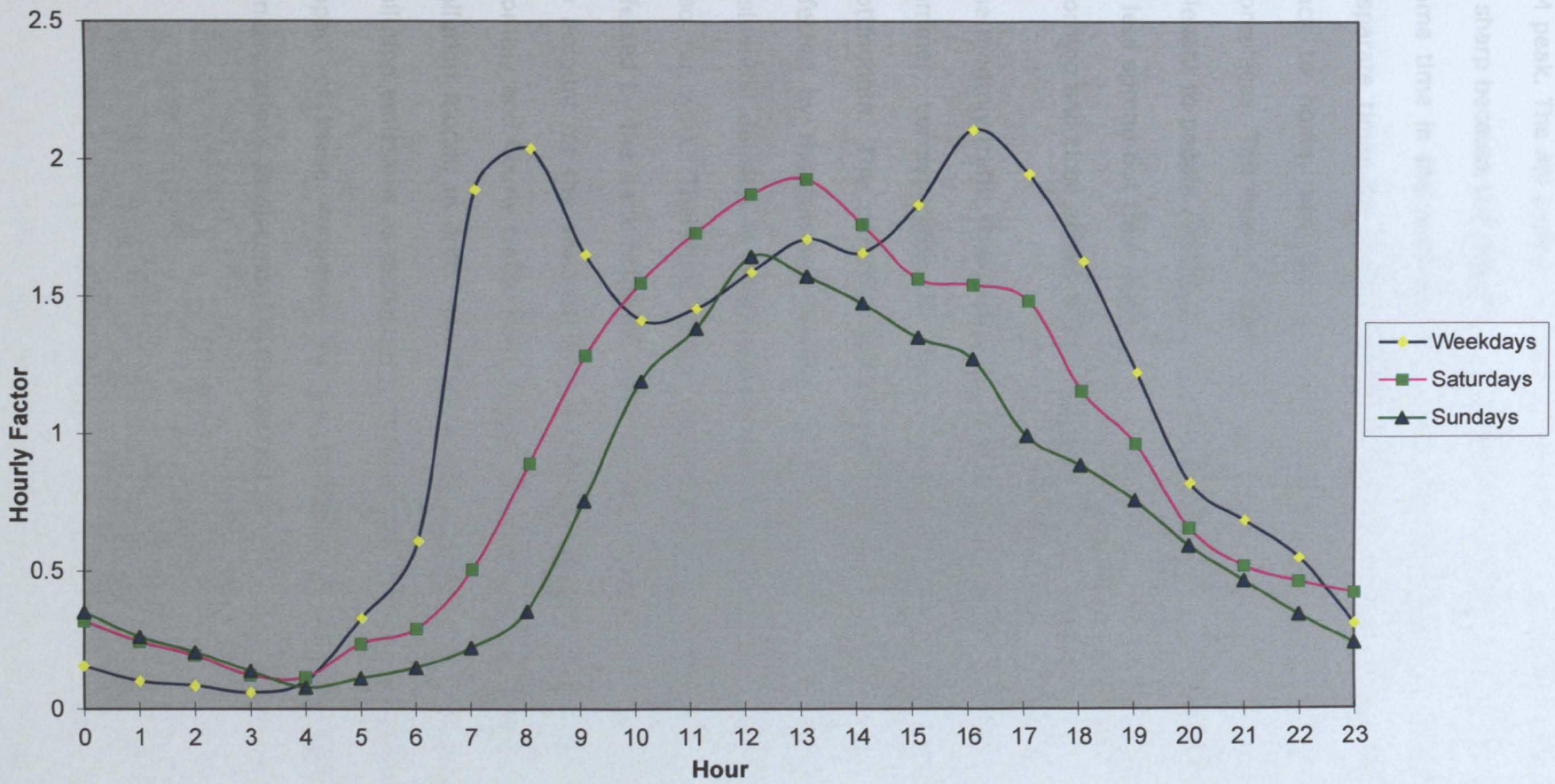

Figure 5.9 Beeston Road 2006 Hourly Traffic Flow Profiles for Weekdays, Saturdays and Sundays

The hourly traffic flow profiles of weekdays have two peaks, AM peak and PM peak. The AM peak is relevant to travelling to workplace, and this peak is sharp because the majority of workplaces, as well as schools, start at the same time in the morning. The PM peak is more spread out due to the disparate times for which employees can leave the workplace travelling back to home, and also because schools tend to finish earlier than workplaces. The hourly traffic flow profiles of weekends have one peak, relevant to people commuting to shops for shopping. The peak in Sundays is less spread out than that in Saturdays, because shops open later in the morning and close earlier in the afternoon.

The monthly traffic flow profile of Derby Road exhibits lower traffic flows in summer, corresponding to the summer holiday in the University of Nottingham. The monthly traffic flow profiles of other roads are less affected by the summer holiday, as they are located in areas of high residential density, in which people not only commute for education but also for work. Therefore, these monthly traffic flow profiles are more affected by the bank holidays, such as the Christmas and Easter holidays. To account for the seasonal and hourly variations in the AADT flow, the monthly and hourly traffic flow profiles were used as input data to the air pollution model, in order to reflect these variations in estimating the air pollution emissions as discussed in Section 6.3, and also to investigate the impact of these variations on the accuracy of modelled air pollution concentrations as discussed in Section 6.4.3.

5.5 Future Traffic Scenarios Relating to NET Phase 2 Implementation

Forecast traffic flows were provided by Consultant MVA who produced a wide-area SATURN (Simulation and Assignment of Traffic to Urban Road Networks) model. SATURN (Van Vliet, 1982) was developed at the Institute of Transport Studies, University of Leeds and is used in 30 countries, including application by 80 UK Local Authorities. SATURN is a tactical transport model that estimates the traffic volume on each link of a road network assuming a fixed trip matrix. This type of model is distinguished from assignment models used to model strategic transport by its very detailed representation of the road network and the modelling of turning movements at junctions.

The SATURN model provided by Consultant MVA reflected network changes, strategic developments and capacity constraints which might limit traffic growth. In addition to NET Phase 2, changes in travel demand as a result of known committed development proposals were also included in the SATURN model such as re-development of the NG2 site and the proposed Tesco store in Beeston. Therefore, the SATURN model was used to output the traffic flow changes for two main traffic scenarios:

- "Do-Minimum" – which takes account of traffic flow changes to 2021 (including changes arising from adjacent committed developments); and
- "Do-Something" – which takes into account the Do-Minimum traffic flow changes plus further changes arising from the introduction of NET Phase 2 and layout changes required to accommodate this transport scheme.

5.6 Forecast Future Travel Demand for NET Phase 2 Traffic Scenarios

For both traffic scenarios discussed in Section 5.5, the future traffic data required for the air pollution model was the traffic flow and speed over the road network in the Dunkirk AQMA. After contacting the team in the NET Project Office in Nottingham City Council, it was found that the majority of available transport studies, based on the SATURN modelling described in Section 5.5, focused on assessing traffic impacts on the capacity of junctions along NET routes. LINSIG was used to predict the capacity performance of 'stand alone' signalised junctions, and TRANSYT was used for signalised junctions which are linked. PICADY (for major – minor priority junctions) and ARCADY (for roundabout junctions) were used to estimate capacity at non-signalised junctions. However, the explicit impact of NET Phase 2 on future traffic flow, congestion and speed along roads was not available for this research project.

Discussions with the Environment Section in the Estate Office of the University of Nottingham identified a document to give the explicit impact of NET Phase 2 on future traffic flows (Carter, 2007). This document contained the forecast for future travel demand by public transport in persons per hour for various Nottingham areas for both traffic scenarios being considered, as given in Table 5.1 and Table 5.2. In addition, this document contained the forecast for future travel demand by car, in vehicles per hour, for various Nottingham areas for both traffic scenarios, as shown in Table 5.3 and Table 5.4.

Table 5.1 Modelled Public Transport Travel Demand – AM Peak
Source: (Carter, 2007)

AM Peak Hour	Public Transport Demand – Persons		Growth 2006-2021 %	Impact of NET on growth %
Area	2006	2021		
Greater Nottingham				
without NET Phase Two	26800	29210	9.0	
with NET Phase Two		30320	13.1	46
Nottingham City Area				
without NET Phase Two	21740	23990	10.4	
with NET Phase Two		25030	15.1	46
Central Area				
without NET Phase Two	16580	18570	12.0	
with NET Phase Two		19290	16.4	37

Table 5.2 Modelled Public Transport Travel Demand – Inter Peak
Source: (Carter, 2007)

Inter Peak Hour	Public Transport Demand – Persons		Growth 2006-2021 %	Impact of NET on growth %
Area	2006	2021		
Greater Nottingham				
without NET Phase Two	18430	19860	7.8	
with NET Phase Two		20540	11.4	47
Nottingham City Area				
without NET Phase Two	14470	15710	8.6	
with NET Phase Two		16310	12.8	48
Central Area				
without NET Phase Two	10360	11380	9.9	
with NET Phase Two		11730	13.3	34

Table 5.3 Modelled Travel Demand of Car Vehicles, 2006 and 2021 – AM Peak
Source: (Carter, 2007)

AM Peak Hour	Travel Demand - Car Vehicles		Growth 2006-2021 %	Impact of NET on growth %
Area	2006	2021		
Greater Nottingham excluding P&R users				
without NET Phase Two	72470	84830	17.0	
with NET Phase Two		83960	15.8	-7.00
Nottingham City Area excluding P&R users				
without NET Phase Two	37850	43910	16.0	
with NET Phase Two		43140	14.0	-13
Central Area excluding P&R users				
without NET Phase Two	9730	11120	14.3	
with NET Phase Two		10630	9.3	-35
Park and Ride Users				
without NET Phase Two	870	1170	34.5	
with NET Phase Two		1580	82.1	138

Table 5.4 Modelled Travel Demand of Car Vehicles, 2006 and 2021 – Inter Peak
Source: (Carter, 2007)

Inter Peak Hour	Travel Demand – Car Vehicles		Growth 2006-2021 %	Impact of NET on growth %
Area	2006	2021		
Greater Nottingham excluding P&R users				
without NET Phase Two	48840	58520	19.8	
with NET Phase Two		58130	19.0	-4.10
Nottingham City Area excluding P&R users				
without NET Phase Two	26050	29420	12.9	
with NET Phase Two		29060	11.6	-11
Central Area excluding P&R users				
without NET Phase Two	5080	5250	3.4	
with NET Phase Two		5070	-0.2	-104
Park and Ride Users				
without NET Phase Two	610	750	23.5	
with NET Phase Two		1010	65.8	180

Carter (2007) only contained the forecast for future travel demand by light and other goods vehicles for the wider area of Greater Nottingham, which comprises Nottingham City area and the surrounding districts of Gedling, Rushcliffe and Broxtowe, as shown in Table 5.5. It also gave the forecast for future NET Phase 2 patronage as shown in Table 5.6. The future travel demand forecasts for NET Phase 2 in Carter (2007) were based on local planning data projections to 2021. Therefore, all other input data to the air pollution model, such as the background concentrations and the emission year, were also projected to 2021 as shown later in Section 8.2.

Table 5.5 Modelled Do-Minimum Travel Demand for Greater Nottingham, including Park and Ride
Source: (Carter, 2007)

Time Period/Year	Travel Demand				
	PT person	Car vehicle	Light Goods	Other Goods	All highway
AM peak hour					
2006 do minimum	26800	73340	10030	6850	90220
2021 do minimum	29210	85990	13950	7820	107760
Interpeak hour					
2006 do minimum	18430	49450	10540	10360	70340
2021 do minimum	19860	59270	14660	11810	85630
Growth AM peak					
2006-2021 %	9.0	17.3	39.1	14.0	19.4
Growth Interpeak					
2006-2021 %	7.8	19.9	39.1	14.0	21.7

Table 5.6 NET Phase 2 – Summary Patronage Forecasts
Source: (Carter, 2007)

NET Phase 2 Demand updated for 2013 opening			
	2013 opening year	2016 1st full year	2021
Annual Patronage (millions)			
peak periods	3.8	5.5	6
off-peak periods	5.2	7.4	7.9
total	9.1	13	13.9
Of which:			
ex public transport %	64	61	60
mode/distribution shift %	18	21	21
park and ride %	13	14	14
trip generation %	5	5	5

5.7 Production of Future Traffic Data

The traffic data available in Carter (2007) was split into four main categories, public transport people, car vehicles, light goods vehicles and other goods vehicles. However, the 2006 traffic flow data in the form of the

traffic count every five minutes provided by Nottingham City Council was split into three main categories HGV, LGV and PSV, as stated in Section 5.4. Translating the 2006 traffic categories to 2021 necessitated contacting Nottingham City Council again to inquire about the precise meaning of these three categories in order to translate the above-mentioned four categories into these three categories.

Nottingham City Council confirmed that HGV stands for lorries, LGV stands for cars and PSV stands for buses. Consequently, the LGV category was considered to correspond to the car vehicles category. Light goods and other goods vehicle categories in Carter (2007) were aggregated together to correspond to the HGV category of the 2006 traffic flow data. Public transport categories in 2006 and 2021 without NET Phase 2 in Carter (2007) were considered to correspond to the PSV category of the 2006 traffic flow data. However, the public transport category in 2021 with NET Phase 2 in Carter (2007) was split into two categories, PSV (buses) and NET Phase 2 (trams).

As stated in Section 5.3, for every principal road considered in the Dunkirk AQMA air pollution model, the 2006 traffic flow input data needed to be split into two categories, LDV and HDV. For each of these principal roads, the 2006 traffic flow data obtained from Nottingham City Council was aggregated together to give the total 2006 traffic flow. The percentages of LGV, PSV and HGV, obtained from Nottingham City Council, were used to split the total 2006 traffic flow into the car vehicles, public transport and goods vehicles categories respectively. Then, the traffic growth factors, the average of both peak hour and inter-peak hour factors, derived from Carter (2007), were used to project each category from 2006 to 2021 for the Do-Minimum scenario.

The traffic growth factors used, obtained from Carter (2007), were those derived from the Nottingham City Area data as this area is more representative of the Dunkirk AQMA than are the other Nottingham areas used in Carter (2007). A spreadsheet was designed to contain the categorised 2006 traffic flow data for each principal road in the Dunkirk AQMA air pollution model. Therefore, the projection of the categorised traffic flow data for each road from 2006 to 2021 for both traffic scenarios being considered could be automated. Then, the projected categorised 2021 traffic flows were split into LDV and HDV, as required by the air pollution model. As stated in Section 5.4, LGV=LDV and HGV+PSV=HDV.

For car vehicles in the Do-Minimum scenario:

$$2021\ \text{count} = \left(1 + \frac{16 + 12.9}{200}\right) \times 2006\ \text{count}, \qquad \textbf{(5.8)}$$

where 16 and 12.9 are the growth percentages for both peak hour and inter-peak hour from Table 5.3 and Table 5.4 respectively.

For buses in the Do-Minimum scenario:

$$2021\ \text{count} = \left(1 + \frac{10.4 + 8.6}{200}\right) \times 2006\ \text{count}, \qquad \textbf{(5.9)}$$

where 10.4 and 8.6 are the growth percentages for both peak hour and inter-peak hour from Table 5.1 and Table 5.2 respectively.

For goods vehicles in the Do-Minimum scenario:

$$2021\ \text{count} = \left(1 + \frac{29 + 26.65}{200}\right) \times 2006\ \text{count}, \qquad \textbf{(5.10)}$$

where 29 and 26.65 are the growth percentages for both peak hour and inter-peak hour respectively. These figures were calculated by summing up the figures for light goods and other goods from Table 5.5 to obtain figures

for total goods. Then, the growth percentages corresponding to total goods were calculated for both peak and inter-peak hours.

For the Do-Something scenario, the growth rate of goods vehicles was assumed to be the same as that in the Do-Minimum scenario. This was obviously because the introduction of NET Phase 2 is only supposed to increase the public transport demand and to encourage modal shift from car to public transport, and hence to reduce the car vehicles demand. Therefore, as NET is for transporting passengers not goods, the impact of the introduction of NET Phase 2 on the goods vehicles demand may be presumed to be so small as to be negligible. That was probably the reason that Carter (2007) did not include growth factors for the goods vehicles demand for the Do-Something scenario.

For the impact of the introduction of NET Phase 2 on 2021 car vehicles demand, the growth factors for peak hour and inter-peak hour were taken from Table 5.3 and Table 5.4 respectively. Obviously, the introduction of NET Phase 2 would result in lower growth rates of car vehicles demand, because of the anticipated modal shift from the private car to public transport after the implementation of NET Phase 2.

Consequently, the introduction of NET Phase 2 would result in higher growth rates of the public transport demand than those in the Do-Minimum scenario. However, the challenge was to split the 2021 public transport demand with NET Phase 2 into bus demand and tram demand. The 2021 bus demand with NET Phase 2 would be input to the air pollution model to predict the 2021 air quality in the Dunkirk AQMA. The 2021 tram demand would not be entered into the air pollution model as a tram is an electrical vehicle with zero pollution emissions.

Firstly, the 2021 annual public transport demand with NET Phase 2 was determined from the average of the peak and inter-peak 2021 hourly demands listed in Table 5.1 and Table 5.2. Then, the 2021 annual public transport demand with NET Phase 2 minus the 2021 annual demand of NET Phase 2 (from Table 5.6) yielded the 2021 annual bus demand with NET Phase 2. Then, the average 2021 hourly bus demand was derived from the 2021 annual bus demand. The average of the 2006 peak and inter-peak hourly bus demands, listed in Table 5.1 and Table 5.2, was derived. Then, the 15-year growth factor of the average hourly bus demand from 2006 to 2021 was calculated as the ratio of the average 2021 hourly bus demand to the average 2006 hourly bus demand.

This procedure was performed twice, once with public transport hourly demands for Greater Nottingham, and again with public transport hourly demands for the Nottingham City Area, as given in Table 5.1 and Table 5.2. That was because it was not clear enough whether the 2021 annual demand of NET Phase 2, from Table 5.6, was for all of the SATURN model area, Greater Nottingham, or was just for the Nottingham City Area. In both cases, the 15-year growth factor of the average hourly bus demand from 2006 to 2021 was found to be 5.4%.

For car vehicles in the Do-Something scenario:

$$2021\ \text{count} = \left(1 + \frac{14 + 11.6}{200}\right) \times 2006\ \text{count}, \qquad \textbf{(5.11)}$$

where 14 and 11.6 are the growth percentages for both peak hour and inter-peak hour from Table 5.3 and Table 5.4 respectively.

For buses in the Do-Something scenario:

$$2021\ \text{count} = \left(1 + \frac{5.4}{100}\right) \times 2006\ \text{count}, \qquad \textbf{(5.12)}$$

where 5.4 is the 15-year growth percentage of the average hourly bus demand from 2006 to 2021 with the introduction of NET Phase 2.

5.8 Future Traffic Speed Data Estimation

The future traffic speed had to be estimated because the air pollution model required the future traffic speed for both LDV and HDV traffic categories for every principal road considered in the Dunkirk AQMA air pollution model for both 2021 scenarios being considered. With no 2021 traffic speed data available, it was decided to estimate the future traffic speed with reference to the future traffic flow by using the fundamental traffic flow theory (Abdulhai and Katten, 2004):

$$\text{Traffic Flow} = \text{Traffic Density} \times \text{Space Mean Speed} \qquad \textbf{(5.13)}$$

Figure 5.10 is the graphical representation of Equation (5.13) as a relationship between the traffic flow and speed. It was assumed that the 2006 road network in Nottingham was normally not congested, so traffic flow levels were generally well below capacity. Hence 2021 traffic density, corresponding to a higher travel demand as predicted using the SATURN model in Table 5.5, will become greater than the 2006 traffic density due to the anticipated future rise in car ownership in Nottingham (NCC and NCC, 2009). Therefore, as a result of the increase in travel demand, and hence traffic density, from 2006 to 2021, it was expected that 2021 traffic speeds will be lower than 2006 traffic speeds for both peak and inter-peak

periods, reflecting the increase in traffic flows expected on the road network (Carter, 2007). Consequently, the transition from 2006 to 2021 traffic conditions was assumed to follow the top part of Figure 5.10. In addition, the future changes in junction design were anticipated to give the tram a high priority at junctions, reducing the priority for other modes of transport. This further supports the hypothesis of having lower 2021 traffic speed in Nottingham than in 2006. Using present and future traffic flows, the future traffic speed was estimated from the present traffic speed as follows:

$$\text{2021 Traffic Speed} = \text{2006 Traffic Speed} \times \frac{\text{2006 Traffic Flow}}{\text{2021 Traffic Flow}} \qquad \textbf{(5.14)}$$

Equation (5.14) was applied to estimate 2021 traffic speed data from 2006 traffic speed data for both the LDV and HDV traffic categories of the 2021 traffic flow for every principal road considered in the Dunkirk AQMA air pollution model. The estimation of 2021 traffic speed data was undertaken for the two traffic scenarios of NET Phase 2, the Do-Minimum and Do-Something scenarios.

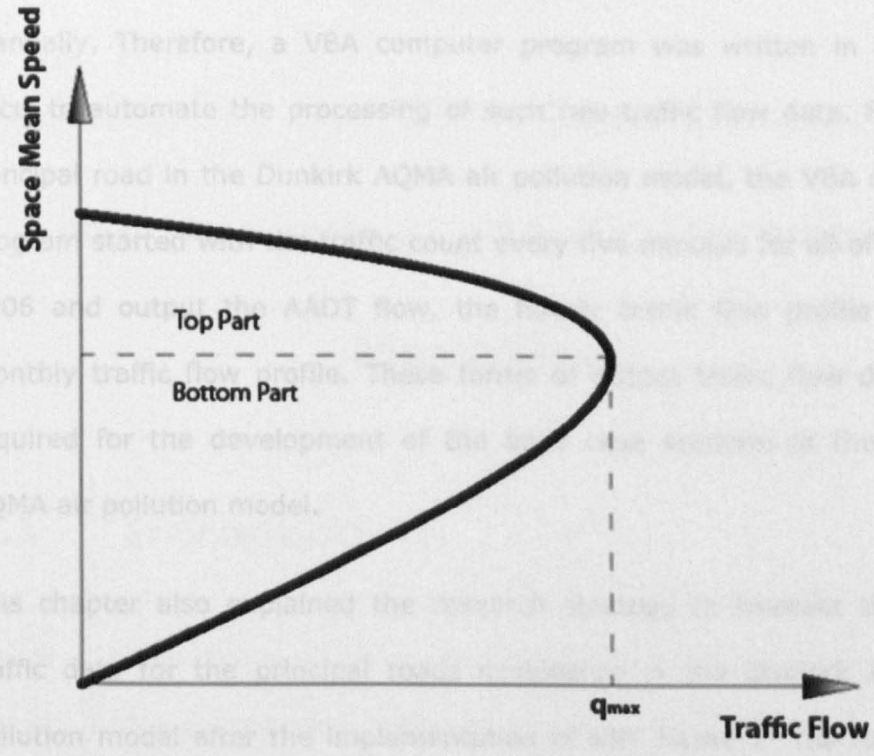

Figure 5.10 Flow versus Speed of Traffic Flow Theory (Abdulhai and Katten, 2004)

5.9 Summary

This chapter presented the processing of 2006 traffic data required to build the base case scenario of the Dunkirk AQMA air pollution model for the initial development of this research decision-support system. This started with the selection of Derby Road, Clifton Boulevard, Abbey Street and Beeston Road for consideration in the Dunkirk AQMA air pollution model. The traffic data for these principal roads required for input into the air pollution model were the traffic speed, the AADT flow split into the LDV and HDV categories and optionally the hourly and monthly traffic flow profiles.

Nottingham City Council provided the traffic speed data for the principal roads selected for consideration in the Dunkirk AQMA air pollution model. The raw traffic flow data for these roads provided by Nottingham City Council was in the form of the traffic count every five minutes for the whole

of the year 2006, but the very large dataset could not be processed manually. Therefore, a VBA computer program was written in Microsoft Excel to automate the processing of such raw traffic flow data. For every principal road in the Dunkirk AQMA air pollution model, the VBA computer program started with the traffic count every five minutes for all of the year 2006 and output the AADT flow, the hourly traffic flow profile and the monthly traffic flow profile. These forms of output traffic flow data were required for the development of the base case scenario of the Dunkirk AQMA air pollution model.

This chapter also explained the research strategy to forecast the future traffic data for the principal roads considered in the Dunkirk AQMA air pollution model after the implementation of NET Phase 2. The forecasting of future traffic flows utilised results from SATURN traffic modelling of Greater Nottingham undertaken by the MVA consultancy. The results of this traffic modelling were given in Carter (2007) in the form of traffic growth factors from 2006 to 2021 for the Do-Minimum and Do-Something NET Phase 2 traffic scenarios.

For every principal road in the Dunkirk AQMA air pollution model, the traffic growth factors from Carter (2007) were used to project the 2006 AADT flow to 2021 in the Do-Minimum and Do-Something scenarios. The fundamental traffic flow theory was considered in order to justify the estimation of the 2021 traffic speed data from the 2006 traffic speed data using the ratio of the 2006 traffic flow to the 2021 traffic flow for the two scenarios considered. The 2021 traffic flow and speed data were required for the development of the Do-Minimum and Do-Something air quality scenarios of the Dunkirk AQMA air pollution model.

Chapter 6

Developing the Base Case Scenario of the Dunkirk AQMA Air Pollution Modelling

6.1 Introduction

The aim of this chapter is to develop the 2006 base case scenario of the Dunkirk AQMA air pollution model as a part of the initial development of the research decision-support system. The base case scenario model simulates the air quality of a past or present year for which the air quality monitoring data is available. The monitoring data is used to validate the results of the base case scenario model. This should improve the reliability of the air quality modelling of future scenarios based on the base case scenario.

The 2006 base case scenario of the Dunkirk AQMA air pollution model is designed to achieve two important criteria. The first criterion is obtaining reliable predictions of air pollution dispersion in the Dunkirk AQMA. The second criterion is facilitating the 3D visualisation of the output air pollution concentrations in the Dunkirk 3D city model. The aim of this chapter is attained by the investigation of four objectives:

1. The selection of air pollutants for consideration in the base case scenario.
2. The description of the set-up of the base case scenario. This comprises the selection of the air pollution modelling package that can most

effectively achieve the aim of this research project. This also includes the description of various input data and simulation options of the air pollution modelling package, in which the base case scenario was set-up.

3. The demonstration of different techniques and strategies adopted in the research project to calibrate and validate the base case scenario model.
4. The explanation of the design of the base case scenario output grid of receptors for the 3D visualisation of the output air pollution concentrations at and above the ground surface in the Dunkirk 3D city model.

6.2 Air Pollutants of Base Case Scenario Modelling

Nitrogen dioxide (NO_2) was selected as the output air pollutant for all of the air quality modelling in this research project. The first reason for selecting NO_2 was that the air pollutant of concern in the Dunkirk AQMA was NO_2. Therefore, the majority of available air pollution monitoring data, required to validate the base case scenario model in and around the Dunkirk AQMA, was NO_2 data. The second reason for selecting NO_2 was that NO_2 is emitted primarily by the road traffic. Therefore, some modal shift from the private car to NET Phase 2 is anticipated to reduce the high NO_2 levels in the Dunkirk AQMA (NCC and NCC, 2006).

In reality, the chemical reactions of nitrogen oxides (NO_x) with Ozone (O_3) in the atmosphere affect NO_2 concentrations (CERC, 2006a). Hence, to simulate reality and obtain accurate predictions of NO_2 concentrations, the chemical reactions of NO_x were considered in the base case scenario

model. This necessitated selecting NO_x and O_3 in addition to NO_2 for consideration in the base case scenario model.

6.3 Set-up of Base Case Scenario Modelling

As mentioned before in sub-section 3.2.3, ADMS-Roads was found to estimate the air pollution due to the road traffic more precisely than other common sophisticated air pollution dispersion models (Ellis et al., 2001). ADMS-Roads gave relative to other models good estimates when compared with the monitored concentrations (Hirtl and Baumann-Stanzer, 2007). ADMS-Roads was capable of modelling long-term and short-term air pollution concentrations. This facilitated the output of the air pollution modelling results in many forms that are easily comparable to different AQOs (CERC, 2006a).

In addition to modelling the horizontal air pollution dispersion, ADMS-Roads is capable also of modelling precisely the vertical dispersion of air pollution. This enables ADMS-Roads to model the air pollution at many heights above the ground surface, which is required later for building the 3D air pollution dispersion interface, as described in Chapter 7. Therefore, ADMS-Roads was chosen as the software for all the air quality modelling in this research project.

Discussions with the Pollution Control Section in Nottingham City Council were undertaken to identify the set-up of the base case scenario in ADMS-Roads.

These consultations resulted in the following set-up:

- 2006 was selected as the base case year due to the availability of traffic and emissions factor input data required for running the air quality model and air pollution data for validating its results.
- Derby Road, Clifton Boulevard, Abbey Street and Beeston Road were selected as the main roads to be considered in the air pollution model base case scenario, as explained in Section 5.2. These roads were defined as non-canyon streets in the ADMS-Roads interface.
- The output 2006 AADT flow from the VBA computer program, discussed in Section 5.4, was used as the traffic input data for the base case scenario model. ADMS-Roads used the average traffic speed for the main roads to identify the traffic emissions factors (for average national vehicle fleet) factors according to the 2003 DMRB database, in order then, for each main road, to multiply the factor by the AADT flow to yield the traffic emission (per second) rate.
- The output 2006 hourly and monthly traffic profiles from the VBA computer program, discussed in Section 5.4, were compiled to a fac file. This file was imported into the base case scenario model to account for the seasonal and hourly changes in the traffic emissions. For each hour in a month, the traffic flow, used in the base case scenario to derive the traffic emissions, was the AADT flow × monthly factor × hourly factor.
- The Chemical Reaction Scheme was selected for the simulation of the atmospheric chemical reactions of NO_x as the required background concentrations of NO_x, NO_2 and O_3 were available from the Rochester monitoring station, as mentioned in a next bullet point.
- Surface roughness = 0.5, as recommended by the Pollution Control Section NCC for the study area, and consistent with that suggested by

the typical roughness lengths recommended for ADMS-Roads in Figure 6.1, latitude = 52° and minimum Monin-Obukhov length = 30.

- Three point sources all boilers were defined in the base case scenario: Boots, QMC main and Nottingham University. The emitted pollutant, from the three point sources, was NO_x as NO_2. As the chemical reactions option was selected, ADMS-Roads assumed that 10% of NO_x as NO_2 emissions was NO_2.
- The 2006 hourly sequential meteorological data measured by the Nottingham Watnall Weather Station was used for all air quality modelling scenarios. The meteorological data included 10 parameters: Station Number, Year, Day, Hour, Surface Temperature, Wind Speed, Wind Direction, Precipitation, Cloud Cover and Degree of Humidity. The wind speed was measured at a height of 10 metres above the ground surface and the wind sector size was 10°. Figure 6.2 shows the 2006 wind rose for the Watnall Weather Station. It was assumed that the weather conditions in the Watnall and Dunkirk areas of Nottingham were identical at all times.
- The 2006 hourly sequential concentrations, measured by the Rochester air quality monitoring station, were used as background levels in the base case scenario model. This is an AURN station sited at a rural site distant from urban air pollution, as shown in Figure 6.3, and hence DEFRA recommends using Rochester monitoring data as background levels for modelling urban air quality in the UK, in order to avoid double counting issues. The background concentrations comprised NO_x, NO_2, O_3, PM_{10} and SO_2 concentrations.
- The base case scenario model was configured to output the modelled 2006 hourly and annual mean NO_x, NO_2 and O_3 concentrations at the

site of the AQMS (described in Section 2.4) in the Dunkirk AQMA, for the model validation.

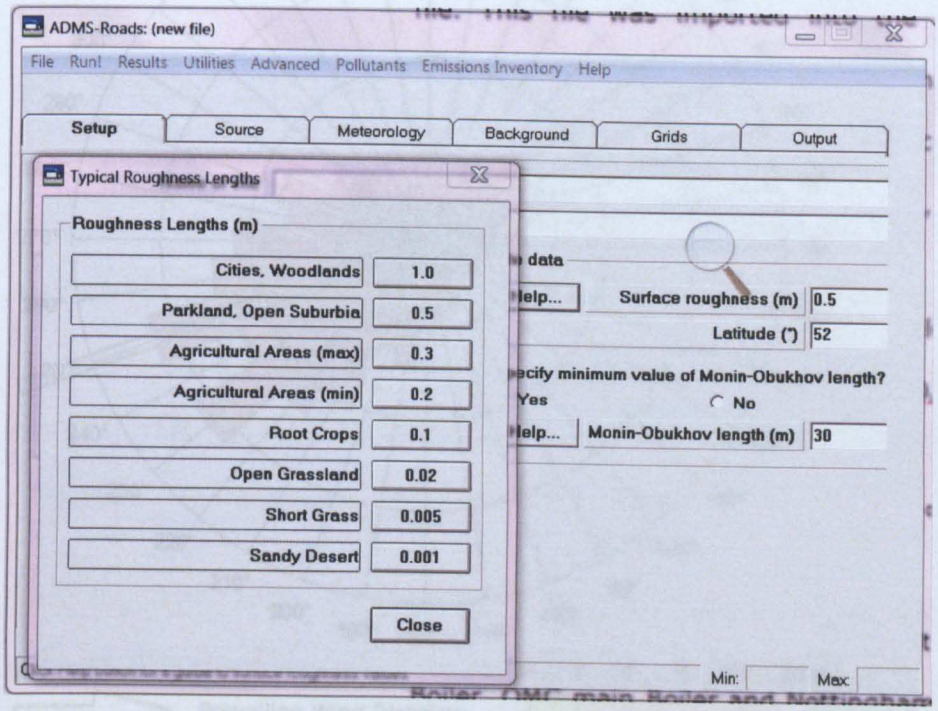

Figure 6.1 Typical Surface Roughness Lengths Recommended for ADMS-Roads

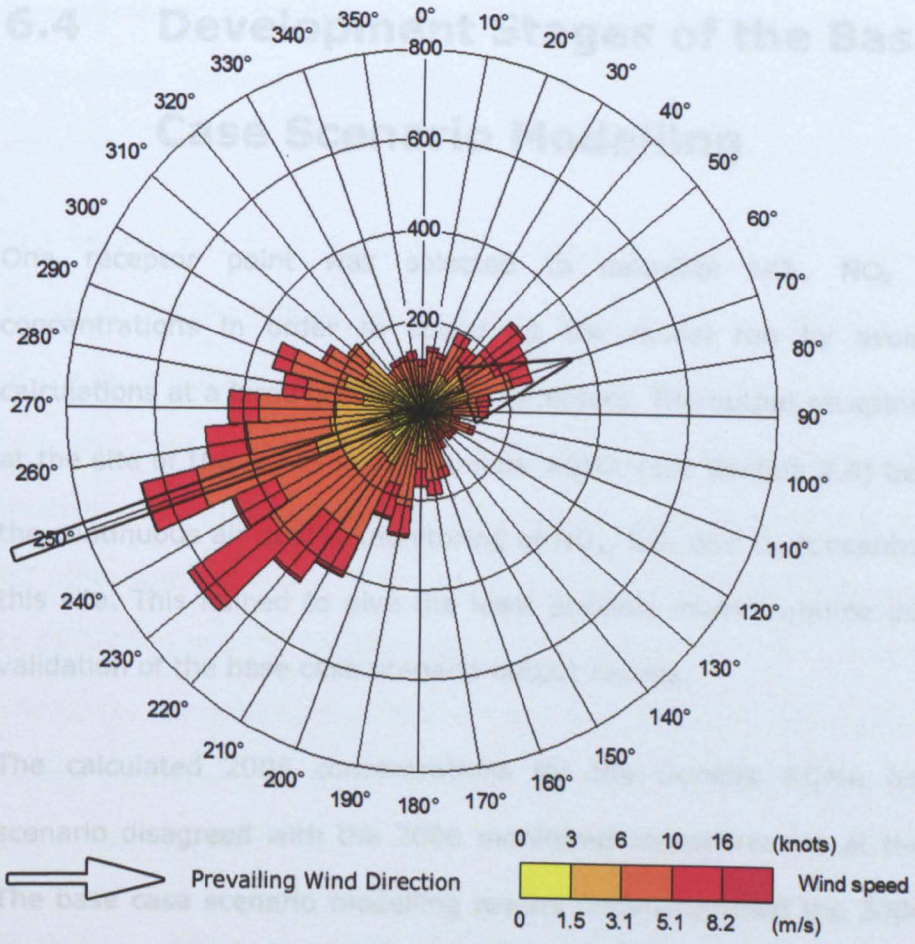

Figure 6.2 The Watnall Weather Station Wind Rose for 2006

Figure 6.3 Site Map for the Rochester Background Monitoring Station

6.4 Development Stages of the Base Case Scenario Modelling

One receptor point was selected to calculate NO_x, NO_2 and O_3 concentrations in order to speed up the model run by avoiding the calculations at a large grid of output receptors. The output receptor was set at the site of the AQMS in the Dunkirk AQMA (see Section 2.4) because of the continuous air quality monitoring of NO_x, NO_2 and O_3 concentrations at this site. This helped to give the least possible model runtime during the validation of the base case scenario output results.

The calculated 2006 concentrations for the Dunkirk AQMA base case scenario disagreed with the 2006 monitored concentrations at the AQMS. The base case scenario modelling results underestimated the 2006 annual means of monitored NO_x and NO_2 by 37.6% and 25.6% respectively, and overestimated the 2006 annual mean of monitored O_3 concentrations by 42.7% at the AQMS. This necessitated developing the design of the Dunkirk AQMA base case scenario model by performing two operations. The first operation was the calibration of the base case scenario model. The calibration of sophisticated air pollution dispersion models is a novel concept which is first introduced into the science of air pollution dispersion modelling by this research project.

The calibration of air pollution dispersion models was defined in this research project as the process of finding the true input data and simulation options of the base case scenario model, on the basis of given monitored air pollution concentrations in the area of the air pollution model application. Hence, the calibration of the Dunkirk AQMA base case scenario model aimed to minimise the difference between the calculated

concentrations of the base case scenario and the corresponding monitored air pollution concentrations at the AQMS by developing the set-up of this scenario.

The second operation used in this research project, for developing the design of the Dunkirk AQMA base case scenario model, was the validation of the air pollution model after each stage of calibration. The validation of the base case scenario model is defined, in this research project, as the process of determining the degree of agreement between the output air pollution concentrations of the base case scenario model after each stage of calibration and the corresponding monitored air pollution concentrations. Therefore, the validation is used for the assessment of the quality of each calibration stage, and hence for deciding the final development stage of the calibration process.

6.4.1 Macro-calibration and Validation of the Base Case Scenario Modelling

The term macro-calibration in this research project refers to developing the design of the base case scenario model so that the calculated concentrations agree with the corresponding monitored concentrations on the annual mean level. Macro-calibration was the initial stage of the calibration process of the Dunkirk AQMA base case scenario model. The macro-validation was undertaken by the direct comparison between the calculated and monitored annual means of NO_x, NO_2 and O_3 at the AQMS.

One scenario used to macro-calibrate the Dunkirk AQMA base case scenario model was by increasing the primary NO_2 emissions from traffic. The average primary NO_2 fraction (f-NO_2) from traffic emissions, in the UK except London, was projected to increase from 11% to 18% between 2002

and 2010 (AQEG, 2007). However, ADMS-Roads by default assumed that f-NO_2 in NO_x as NO_2 traffic emissions was 10%. Therefore, a value of f-NO_2 for all roads in the base case scenario model was computed by linear interpolation as 14.5% for the year 2006. This increased the calculated output NO_2 concentrations, however the base case scenario model underestimated the annual means of monitored NO_x and NO_2 concentrations at the AQMS by 37.6% (unchanged) and 23.8% respectively. Therefore, increasing f-NO_2 from the traffic emissions from 10% to 14.5% was not effective for the macro-calibration of the base case scenario model.

A group of sensitivity studies undertaken for ADMS-Urban indicated that the lower the surface roughness, the lower the active mixing of pollutants and hence, the greater the calculated concentrations (CERC, 2003). These studies also indicated that the lower the value of the minimum Monin-Obukhov Length, the lower the mixing rate and hence, the greater the calculated concentrations.

Therefore, the impact of these two factors, surface roughness and minimum Monin-Obukhov Length, on the calculated NO_2 concentrations by ADMS-Roads was investigated to macro-calibrate the base case scenario model. As far as increasing the value of the calculated NO_2 concentrations was concerned, the value of the surface roughness needed to decrease to less than 0.5, the initial value selected in the set-up of the base case scenario model. However, reducing the value of the surface roughness to less than 0.5 resulted in an unsuitable site definition for the Dunkirk AQMA in ADMS-Roads, as shown in Figure 6.1. Therefore, the value of surface roughness was retained at 0.5.

The impact of reducing the value of the minimum Monin-Obukhov Length from 30, the initial value selected in the set-up of the base case scenario model, to 10, the least possible value in ADMS-Roads, on the calculated NO_2 concentrations was also investigated. After the reduction in the value of minimum Monin-Obukhov Length, the base case scenario model underestimated the annual means of monitored NO_x and NO_2 concentrations at the AQMS by 33.3% and 22.4% respectively. Therefore, it was concluded that reducing the value of the minimum Monin-Obukhov Length from 30 to 10 metres was not effective for the macro-calibration of the base case scenario model.

Further communications with the Pollution Control Section in Nottingham City Council revealed that they use a grid air pollution source in ADMS-Urban to compensate for the difference between rural and urban background concentrations. Grid sources are used in ADMS-Urban to model residual, poorly-defined or diffused emissions in urban areas, such as the emissions from domestic heating sources and minor roads (CERC, 2006b). This enables ADMS-Urban to model emissions from sources that are not explicitly entered into the air pollution model. However, the capability to model emissions from such air pollution sources is only available in ADMS-Urban, not in ADMS-Roads. Therefore, it was decided to increase the rural background concentrations for the Dunkirk AQMA base case scenario in ADMS-Roads to account for the impact of the absent grid source.

A trial and error approach was adopted to macro-calibrate the base case scenario model by adjusting the background concentrations until there was a good agreement between the annual means of calculated and monitored 2006 NO_2 concentrations at the AQMS. This trial and error approach was the only way to estimate the hourly sequential urban background concentrations in the Dunkirk AQMA which were neither measurable nor

available in any national inventory. This involved a number of technical challenges to amend the hourly sequential rural background concentrations file, and to maintain the structure of the resultant urban background concentrations file so that it could be read by the air pollution model.

The main modelled pollutant in the Dunkirk AQMA base case scenario model was NO_2, the traffic-induced air pollutant for which the Dunkirk AQMA was declared. However, as mentioned in Section 6.2, the NO_2 concentrations calculated by ADMS-Roads are linked to the output NO_x and O_3 concentrations through chemical reactions, which take place in the atmosphere, as follows:

$$NO_{x\ \text{traffic + industrial}} = NO_{\text{traffic + industrial}} + NO_{2\ \text{primary (traffic + industrial)}}$$

$$NO_{\text{traffic + industrial}} + O_{3\ \text{background}} \xrightarrow{\text{chemical reactions}} NO_{2\ \text{Secondary (traffic + industrial)}} + O_2$$

$$NO_{2\ \text{total}} = NO_{2\ \text{primary (traffic + industrial)}} + NO_{2\ \text{Secondary (traffic + industrial)}} + NO_{2\ \text{background}}$$

Therefore, it was decided to macro-calibrate the Dunkirk AQMA base case scenario model not only for NO_2 but also for NO_x and O_3 concentrations. The base case scenario was initially created in ADMS-Roads version 2.2. The values in the 'Background' field of Table 6.1 were added to every hour of the 2006 NO_2, NO_x, and O_3 rural background concentrations to macro-calibrate the base case scenario model. However, adding these values to the original background concentrations file resulted in having many consecutive hours with a negative O_3 background concentration which raised an error and interrupted the model run.

This technical problem was overcome by replacing the negative, invalid, O_3 background concentrations with zero in the macro-calibrated background concentrations file. Another computer logic was applied to the macro-calibrated background concentrations file to preserve the fact that NO_x is

$NO + NO_2$. Hence, for every hour in the macro-calibrated background concentrations file, if $NO_2 > NO_x$, $NO_2 = NO_x$.

The macro-validation after each stage of the macro-calibration was undertaken by comparing the calculated concentrations and the target (monitored) concentrations in Table 6.1. The calculated concentrations were the 2006 annual mean NO_2, NO_x, and O_3 concentrations that were calculated at the AQMS by the air pollution model of the Dunkirk AQMA base case scenario.

The target concentrations were the 2006 annual means of the monitored NO_2, NO_x, and O_3 concentrations at the AQMS. Run 9 version 2.2 in Table 6.1 gave the least difference between the calculated and target concentrations. Therefore, at one stage, this run was considered as the final macro-calibration development stage of the Dunkirk AQMA base case scenario in ADMS-Roads version 2.2.

However, after the macro-calibration of the base case scenario in ADMS-Roads version 2.2, version 2.3 became available. Version 2.3 of ADMS-Roads introduced new features to improve the simulation of the air pollution dispersion. Therefore, it was decided to repeat the macro-calibration exercise of the base case scenario model by using ADMS-Roads version 2.3. Run 23 version 2.3 in Table 6.1 gave the least difference between the calculated and target concentrations. Therefore, the air pollution model of this run was selected as the final macro-calibrated version of the Dunkirk AQMA base case scenario model in this research project.

Table 6.1 Macro-calibration Development Stages of the Dunkirk AQMA Base Case Scenario Model

RUN 1 version 2.2	Background ($\mu g/m^3$)	Δ background ($\mu g/m^3$)	calculated concentrations ($\mu g/m^3$)	Δ calculated ($\mu g/m^3$)	Target concentrations ($\mu g/m^3$)
NO_2	0	0	26.51	0	35.29
NO_x	0	0	42.18	0	67.60
O_3	0	0			31.00
RUN 7 version 2.2	**Background**	**Δ background**	**calculated concentrations**	**Δ calculated**	**Target concentrations**
NO_2	+4.39	+4.39	32.24	+5.73	35.29
NO_x	+12.71	+12.71	54.89	+12.71	67.60
O_3	0	0			31.00
RUN 8 version 2.2	**Background**	**Δ background**	**calculated concentrations**	**Δ calculated**	**Target concentrations**
NO_2	+4.29	-0.10	35.33	+8.82	35.29
NO_x	+25.42	+12.71	67.60	+25.42	67.60
O_3	0	0	39.24		31.00
RUN 9 version 2.2	**Background**	**Δ background**	**calculated concentrations**	**Δ calculated**	**Target concentrations**
NO_2	+7.70	+3.41	35.38	+8.87	35.29
NO_x	+25.42	0	67.60	+25.42	67.60
O_3	-12.60	-12.60	30.96		31.00

Table 6.1 Macro-calibration Development Stages of the Dunkirk AQMA Base Case Scenario Model (continued)

RUN 1 version 2.3	Background ($\mu g/m^3$)	Δ background ($\mu g/m^3$)	calculated concentrations ($\mu g/m^3$)	Δ calculated ($\mu g/m^3$)	Target concentrations ($\mu g/m^3$)
NO_2	0	0	26.25	0	35.29
NO_x	0	0	42.19	0	67.60
O_3	0	0	44.23	0	31.00
RUN 9 version 2.3	**Background**	**Δ background**	**calculated concentrations**	**Δ calculated**	**Target concentrations**
NO_2	+7.70	+7.70	37.27	+11.03	35.29
NO_x	+25.42	+25.42	67.61	+25.42	67.60
O_3	-12.60	-12.60	28.99	-15.24	31.00
RUN 17 version 2.3	**Background**	**Δ background**	**calculated concentrations**	**Δ calculated**	**Target concentrations**
NO_2	+7.70	0	37.70	+11.46	35.29
NO_x	+25.42	0	67.61	+25.42	67.60
O_3	-10.60	+2.00	30.35	-13.88	31.00
RUN 18 version 2.3	**Background**	**Δ background**	**calculated concentrations**	**Δ calculated**	**Target concentrations**
NO_2	+5.25	-2.45	36.48	+10.23	35.29
NO_x	+25.42	0	67.61	+25.42	67.60
O_3	-9.60	+1.00	29.98	-14.24	31.00

Table 6.1 Macro-calibration Development Stages of the Dunkirk AQMA Base Case Scenario Model (continued)

RUN 19 version 2.3	Background ($\mu g/m^3$)	Δ background ($\mu g/m^3$)	calculated concentrations ($\mu g/m^3$)	Δ calculated ($\mu g/m^3$)	Target concentrations ($\mu g/m^3$)
NO_2	+2.85	-2.40	35.62	+9.37	35.29
NO_x	+25.42	0	67.60	+25.41	67.60
O_3	-7.60	+2.00	30.22	-14.01	31.00
RUN 20 version 2.3	**Background**	**Δ background**	**calculated concentrations**	**Δ calculated**	**Target concentrations**
NO_2	+1.85	-1.00	36.52	+10.27	35.29
NO_x	+25.42	0	67.60	+25.41	67.60
O_3	-2.10	+5.50	33.42	-10.81	31.00
RUN 21 version 2.3	**Background**	**Δ background**	**calculated concentrations**	**Δ calculated**	**Target concentrations**
NO_2	+1.85	0	35.87	+9.63	35.29
NO_x	+25.42	0	67.60	+25.41	67.60
O_3	-4.50	-2.40	31.80	-12.43	31.00
RUN 22 version 2.3	**Background**	**Δ background**	**calculated concentrations**	**Δ calculated**	**Target concentrations**
NO_2	+1.60	-0.25	35.48	+9.24	35.29
NO_x	+25.42	0	67.60	+25.41	67.60
O_3	-5.50	-1.00	31.00	-13.22	31.00

Table 6.1 Macro-calibration Development Stages of the Dunkirk AQMA Base Case Scenario Model (continued)

RUN 23 version 2.3	Background ($\mu g/m^3$)	Δ background ($\mu g/m^3$)	calculated concentrations ($\mu g/m^3$)	Δ calculated ($\mu g/m^3$)	Target concentrations ($\mu g/m^3$)
NO_2	+1.48	-0.12	35.45	+9.20	35.29
NO_x	+25.42	0	67.60	+25.41	67.60
O_3	-5.40	-0.90	31.01	-13.22	31.00
RUN 79 version 2.3	**Background**	**Δ background**	**calculated concentrations**	**Δ calculated**	**Target concentrations**
NO_2	+7.02	+5.54	36.89	+10.65	35.29
NO_x	+25.42	0	67.61	+25.42	67.60
O_3	-12.40	-7.00	28.86	-15.37	31.00
RUN 80 version 2.3	**Background**	**Δ background**	**calculated concentrations**	**Δ calculated**	**Target concentrations**
NO_2	+10.12	+3.10	38.73	+12.48	35.29
NO_x	+25.42	0	67.61	+25.42	67.60
O_3	-13.20	-0.80	29.46	-14.77	31.00
RUN 81 version 2.3	**Background**	**Δ background**	**calculated concentrations**	**Δ calculated**	**Target concentrations**
NO_2	+14.55	+4.43	41.64	+15.39	35.29
NO_x	+25.42	0	67.61	+25.42	67.60
O_3	-15.30	-2.10	29.18	-15.05	31.00
RUN 82 version 2.3	**Background**	**Δ background**	**calculated concentrations**	**Δ calculated**	**Target concentrations**
NO_2	+17.18	+2.63	43.56	+17.31	35.29
NO_x	+25.42	0	67.61	+25.42	67.60
O_3	-16.71	-1.41	28.69	-15.54	31.00

The results of run 23 version 2.3 in Table 6.1 were used to derive the following equations which could be used to evaluate directly the background concentration adjustment values, required to macro-calibrate a base case scenario model, without the trial and error approach:

$$\Delta NO_{2\,background} = \frac{(\overline{NO}_{2\,monitored} - \overline{NO}_{2\,uncalibrated})}{9.2} \times 1.48, \qquad \textbf{(6.1)}$$

where $\overline{NO}_{2\,monitored}$ is the annual mean of the monitored NO_2 concentrations and $\overline{NO}_{2\,uncalibrated}$ is the annual mean of the calculated NO_2 concentrations using the rural background concentrations.

$$\Delta NO_{x\,background} = \overline{NO}_{x\,monitored} - \overline{NO}_{x\,uncalibrated}, \qquad \textbf{(6.2)}$$

where $\overline{NO}_{x\,monitored}$ is the annual mean of the monitored NO_X concentrations and $\overline{NO}_{x\,uncalibrated}$ is the annual mean of the calculated NO_X concentrations using the rural background concentrations.

$$\Delta O_{3\,background} = \frac{(\overline{O}_{3\,monitored} - \overline{O}_{3\,uncalibrated})}{(-13.22)} \times (-5.40), \qquad \textbf{(6.3)}$$

where $\overline{O}_{3\,monitored}$ is the annual mean of the monitored O_3 concentrations and $\overline{O}_{3\,uncalibrated}$ is the annual mean of the calculated O_3 concentrations using the rural background concentrations.

6.4.2 Micro-calibration and Validation of the Base Case Scenario Modelling

The term micro-calibration in this research project refers to developing the design of the base case scenario model so that the calculated NO_2 concentrations agree with the corresponding monitored NO_2 concentrations on the hourly level. The micro-calibration follows the macro-calibration to give a base case scenario model which is valid not only on the annual mean

level but also on the hourly level. Therefore, the micro-calibration started off with the macro-calibrated version of the Dunkirk AQMA base case scenario model.

The design of the micro-calibrated version of the base case scenario model was the final development stage of the base case scenario model. This final development stage would act as the base for reliable air quality modelling of future scenarios, such as modelling the air quality after the implementation of NET Phase 2. The micro-validation was undertaken by comparing two one-dimensional arrays of 2006 calculated and monitored hourly NO_2 concentrations at the AQMS. Figure 6.4 illustrates the process of calibration and validation for the base case scenario model development.

The calculated 2006 hourly air pollution concentrations, after each stage of the micro-calibration, constituted a one-dimensional array that comprised 365×24=8760 records for each output air pollutant. To micro-validate the air pollution model after each stage of micro-calibration, the one-dimensional array of calculated 2006 hourly NO_2 concentrations was compared statistically to the corresponding one-dimensional array of monitored 2006 hourly NO_2 concentrations at the AQMS. The aim of the comparison was to find out if there was a statistically significant difference between the two arrays of NO_2 concentrations.

The statistical approach to compare the two arrays of calculated and monitored 2006 hourly NO_2 concentrations depended on the definition of these two arrays. If these two arrays were to be defined as two samples of two bigger populations, statistical tests would be the best approach to compare statistically the two bigger populations (Kanji, 2006). However, if these two arrays represented the two populations to compare, statistical

tests would not be suitable and descriptive statistics would be the convenient statistical approach to compare these two populations.

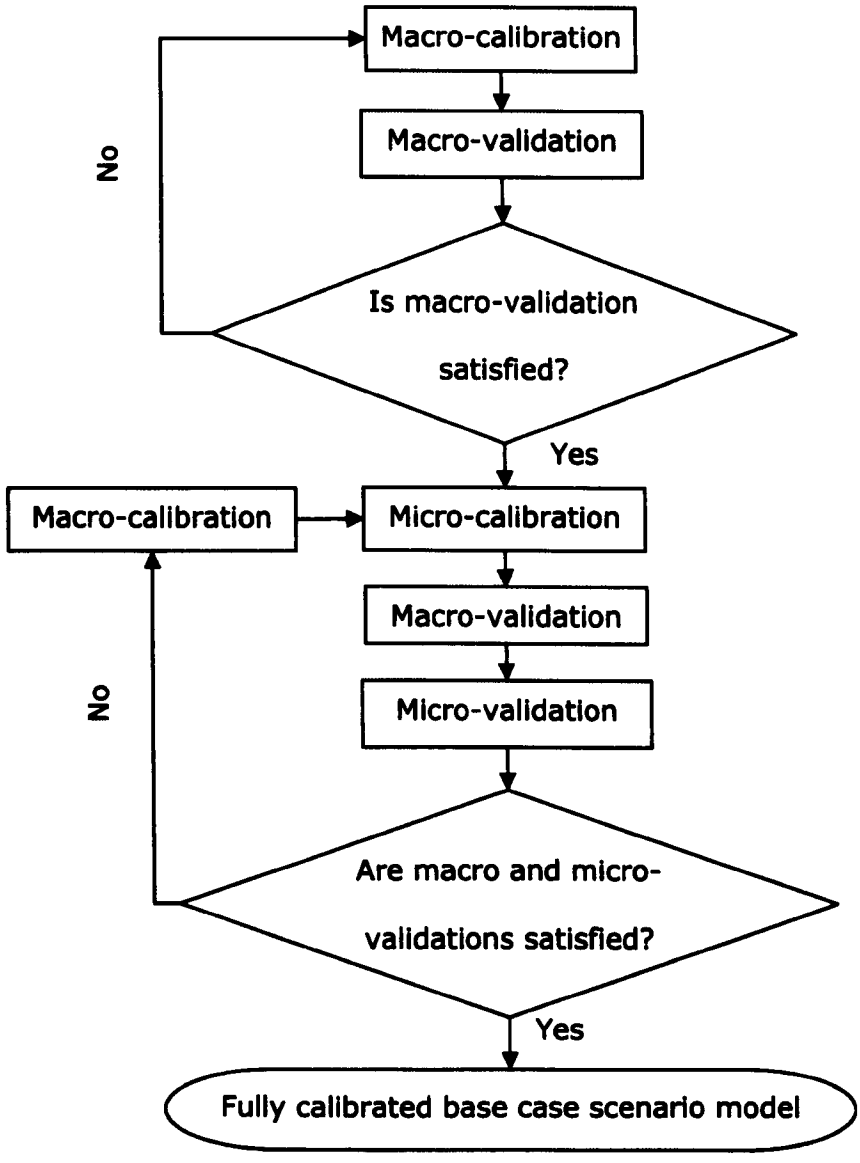

Figure 6.4 Calibration and Validation Process for Base Case Scenario Model Development

Therefore careful consideration was given to define correctly the two arrays of calculated and monitored 2006 hourly NO_2 concentrations at the AQMS, concluding that these two arrays should be defined as two populations, not as two samples. The reason was that these two arrays of concentrations did not comprise NO_2 concentrations from any year other than 2006. Therefore, a hypothesis that these two arrays are two samples of two bigger populations that may extend over many years of time was invalid.

Moreover, these two arrays did not include NO_2 concentrations averaged over any time other than an hour. Therefore, a hypothesis that these two arrays are two samples of two bigger populations that may comprise air pollution concentrations calculated or measured over a diversity of averaging times was invalid. Consequently, descriptive statistics were used to compare the two populations.

6.4.2.1 Micro-validation Descriptive Statistics

The mathematical model of the perfect relationship between the 2006 hourly calculated and monitored NO_2 concentrations at AQMS was $y_i = x_i$, where y_i and x_i were the calculated and monitored NO_2 concentrations for hour i at the AQMS respectively. The value of i ranged from 1 to 8760 which was the total number of hours in a year. The graphical representation of this perfect relationship was a straight line with a slope of 45° that passes through the origin.

As the perfect relationship was a linear relationship, the aim of using descriptive statistics, for the micro-validation of the base case scenario model, was the evaluation of the degree of linearity of the actual relationship between the 2006 hourly calculated and monitored NO_2 concentrations at the AQMS. The aim also included the evaluation of the drift of this actual relationship away from the perfect relationship on an hourly level.

Three descriptive statistics were used to compare the two populations of 2006 calculated and monitored hourly NO_2 concentrations at the AQMS on the micro, hourly, level. The first descriptive statistic was the correlation coefficient (r). r is a measure of the linear association between two variables (SPSS, 2008). Therefore, r was used in the micro-validation of the base case scenario model, to measure the degree of linearity of the

actual relationship between the 2006 hourly calculated and monitored NO_2 concentrations at the AQMS.

The 2006 hourly calculated and monitored NO_2 concentrations at the AQMS were characterised in SPSS as two scale, continuous, variables. Pearson's correlation coefficient is the suitable coefficient for the examination of the linear association between continuous variables (SPSS, 2008), and hence it was used to compare these two variables before the calibration, after the macro-calibration and after the micro-calibration. The theory was that the higher Pearson's correlation coefficient, the closer the actual relationship between calibrated and monitored concentrations to the perfect straightline relationship.

The second descriptive statistic, used in the micro-validation of the base case scenario model, was the Root Mean Square Error (RMSE). RMSE is a goodness of fit measure that measures the average difference between the estimated value of a quantity and its true value (SPSS, 2008). Therefore, RMSE was used in the micro-validation to compute the average of the differences between the hourly calculated and monitored NO_2 concentrations at the AQMS for all of the year 2006.

The RMSE was mainly used to examine the extent of the drift of the actual relationship away from the perfect relationship between 2006 hourly calculated and monitored NO_2 concentrations at the AQMS after each stage of micro-calibration. RMSE was calculated for the micro-validation of the Dunkirk AQMA base case scenario model as follows:

$$RMSE = \sqrt{\frac{\sum_{i=1}^{8275}(Calculated_i - Monitored_i)^2}{8275}}, \qquad \textbf{(6.4)}$$

where 8275 is the number of hours for which data existed for both calculated and monitored NO_2 concentrations. For some hours, the model could not calculate the hourly NO_2 concentration because of the lack of meteorological data for these hours. There were also some hours for which there were no monitored data. The hours with either no calculated, or no monitored, NO_2 concentrations were excluded from the year 2006. To speed up the calculation of the RMSE after each stage of the micro-calibration, a VBA computer program was written by the author in Microsoft Excel to automate the calculation of the RMSE.

The third descriptive statistic, used in the micro-validation of the base case scenario model, was the slope of the best fit line which was obtained by using the linear regression through the origin in SPSS. Linear regression through the origin was used because it was already known that the perfect relationship between hourly calculated and monitored concentrations was $y = x$ without a constant.

The linear regression analysis was undertaken for three cases, uncalibrated versus monitored, macro-calibrated versus monitored, and micro-calibrated versus monitored, concentrations. In all these three cases, the independent variable was the monitored concentrations. The comparison between the calculated and monitored hourly NO_2 concentrations at the AQMS was undertaken by the comparison between the slope of the best fit line through the origin and 1.0, the slope of the perfect relationship.

The slope of the regression best fit line through the origin was mainly used to examine the direction of the drift of the actual relationship away from the perfect relationship between the 2006 calculated and monitored hourly NO_2 concentrations at the AQMS after each stage of micro-calibration. Therefore, the slope of the best fit line through the origin was used for the

examination of whether the majority of the model's output results underestimated or overestimated the 2006 monitored NO_2 concentrations at the AQMS on the micro, hourly, level. The magnitude and sign of the difference between the slope of the best fit line through the origin and 1.0 indicated the tendency of the base case scenario output NO_2 concentrations to underestimate or overestimate the 2006 monitored NO_2 concentrations on the micro level.

The slope of the regression best fit line through the origin could also be used for the estimation of the difference between the calibrated and monitored NO_2 concentrations for the hours missing either the calculated or monitored NO_2 concentration in the original dataset. Moreover, the slope of the regression best fit line through the origin was used for the graphical representation of the linear approximation of the actual relationship between calibrated and monitored hourly NO_2 concentrations at the AQMS as shown in the next section.

6.4.2.2 Micro-calibration Development Stages

The base case scenario of the Dunkirk AQMA air pollution model was run with the uncalibrated rural background concentrations file to output the 2006 calculated hourly NO_2 concentrations at the AQMS. This was carried out for the identification of the initial discrepancy, before any calibration, between the 2006 calculated and monitored hourly NO_2 concentrations at the AQMS, as shown in Figure 6.5. Then, the base case scenario model was run with the macro-calibrated background concentrations file, corresponding to run 23 version 2.3 in Table 6.1, to output the 2006 calculated hourly NO_2 concentrations at the AQMS. This was for the micro-validation of the macro-calibrated base case scenario model as shown in Figure 6.6.

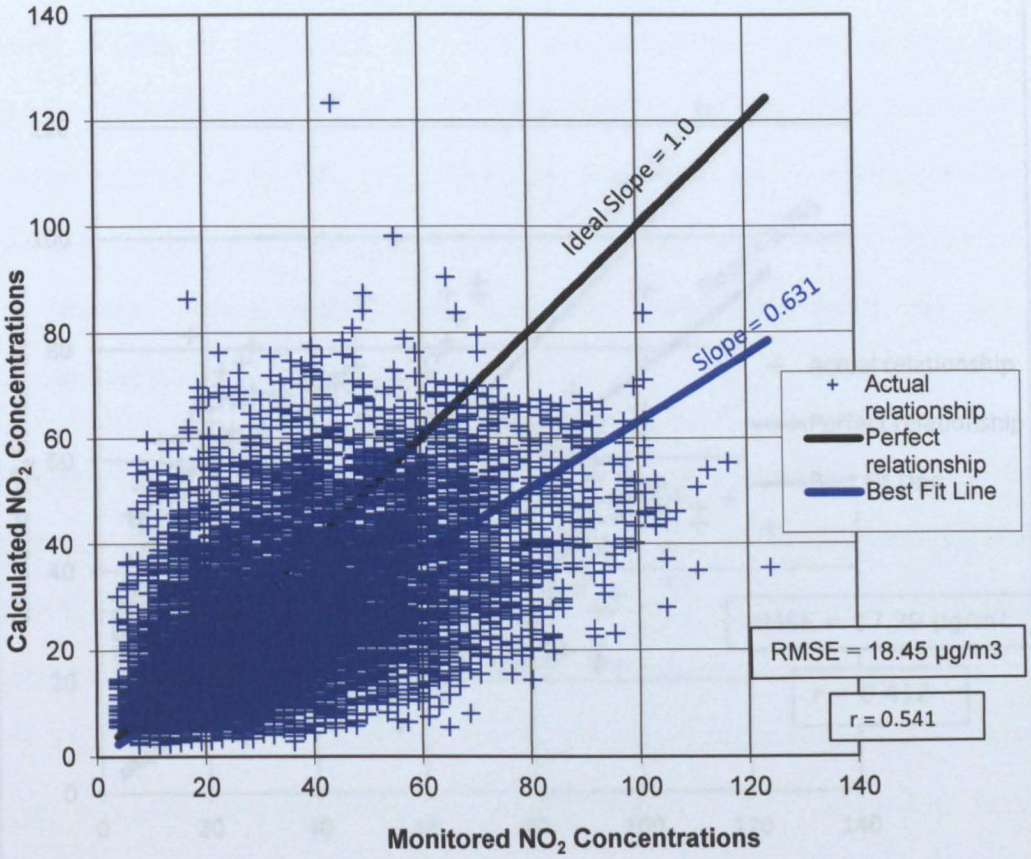

Figure 6.5 Scatter Diagram of Hourly NO_2 Concentrations at the AQMS before any Calibration

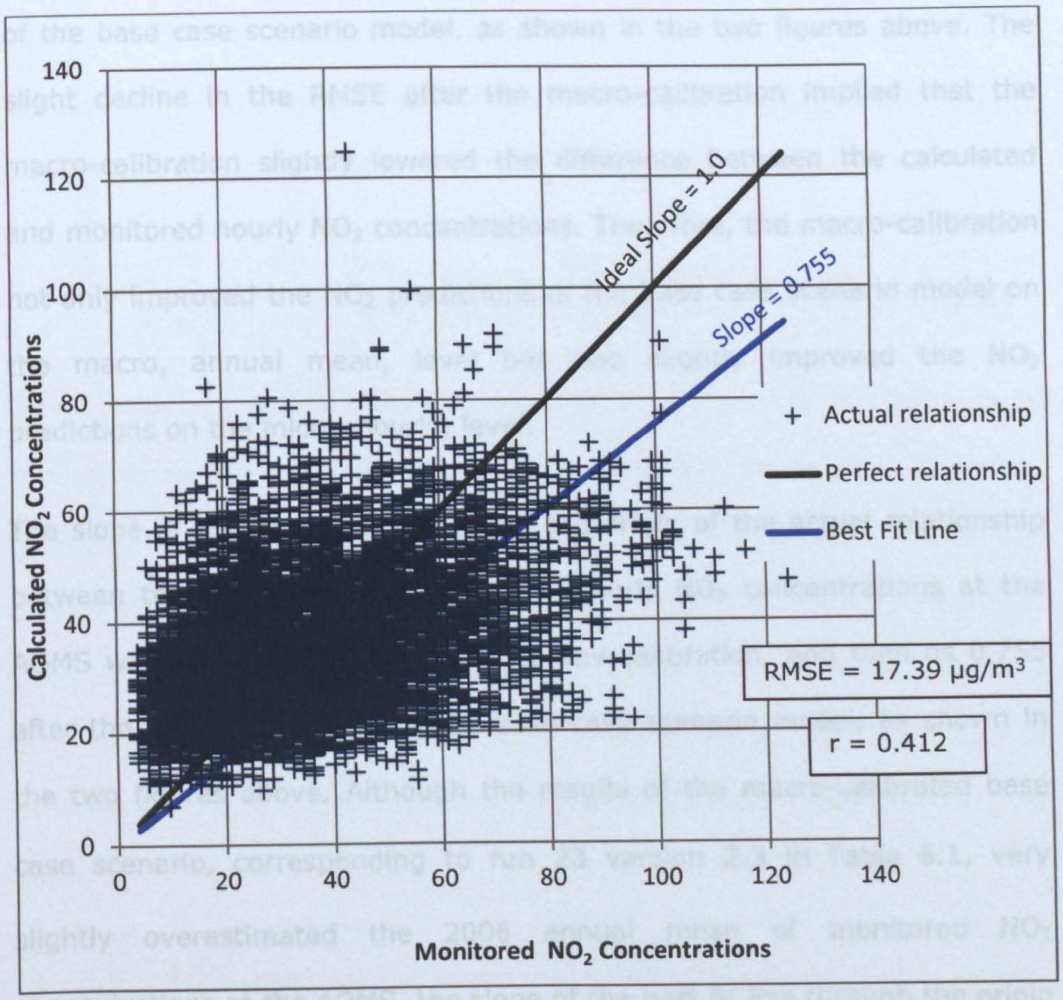

Figure 6.6 Scatter Diagram of Hourly NO_2 Concentrations at the AQMS after Macro-calibration

Pearson's correlation coefficients were calculated as 0.541 before any calibration, and then as 0.412 after the macro-calibration of the base case scenario model, as shown in the two figures above. The slight decline in Pearson's correlation coefficient after the macro-calibration implied that the macro-calibration slightly decreased the degree of linearity of the actual relationship between the calculated and monitored hourly NO_2 concentrations at the AQMS. Hence, the macro-calibration slightly increased the drift of the shape of this actual relationship away from the perfect straight-line relationship.

On the other hand, the values of the RMSE were calculated as 18.45 µg/m^3 before the calibration, and then as 17.39 µg/m^3 after the macro-calibration

of the base case scenario model, as shown in the two figures above. The slight decline in the RMSE after the macro-calibration implied that the macro-calibration slightly lowered the difference between the calculated and monitored hourly NO_2 concentrations. Therefore, the macro-calibration not only improved the NO_2 predictions of the base case scenario model on the macro, annual mean, level but also slightly improved the NO_2 predictions on the micro, hourly, level.

The slope of the best fit line through the origin of the actual relationship between the calculated and monitored hourly NO_2 concentrations at the AQMS was calculated as 0.631 before any calibration, and then as 0.755 after the macro-calibration of the base case scenario model, as shown in the two figures above. Although the results of the macro-calibrated base case scenario, corresponding to run 23 version 2.3 in Table 6.1, very slightly overestimated the 2006 annual mean of monitored NO_2 concentrations at the AQMS, the slope of the best fit line through the origin after the macro-calibration was less than 1.0.

This indicated that the macro-calibrated base case scenario model generally underestimated the monitored NO_2 concentrations at the AQMS on the micro, hourly, level. However, the slight increase in the slope of the best fit line after the macro-calibration implied that the macro-calibration slightly reduced the tendency of the base case scenario model to underestimate the monitored hourly NO_2 concentrations at the AQMS. This, together with the reduction in the RMSE after the macro-calibration, confirmed the slight improvement of the NO_2 predictions of the base case scenario model, after the macro-calibration, on the micro, hourly, level.

To improve further the NO_2 predictions of the base case scenario model on the micro level, the idea of micro-calibration was developed. This idea

depended on the modification of Equations (6.1), (6.2) and (6.3) in order to generate three one-dimensional arrays for $\Delta NO_{2\ background}$, $\Delta NO_{X\ background}$ and $\Delta O_{3\ background}$ as follows:

$$\Delta NO_{2\ background\ i} = \frac{(NO_{2\ monitored\ i} - NO_{2\ uncalibrated\ i})}{(NO_{2\ macro\ i} - NO_{2\ uncalibrated\ i})} \times 1.48, \qquad \textbf{(6.5)}$$

where $\Delta NO_{2\ background\ i}$ is the adjustment value for the rural NO_2 background concentration for the hour i. $NO_{2\ monitored\ i}$ is the monitored hourly NO_2 concentration for the hour i. $NO_{2\ uncalibrated\ i}$ is the calculated hourly NO_2 concentration for the hour i using the uncalibrated rural background concentrations. $NO_{2\ macro\ i}$ is the calculated hourly NO_2 concentration for the hour i using the macro-calibrated background concentrations. The value of i ranged from 1 to 8760, which was the total number of hours in the year 2006.

$$\Delta NO_{X\ background\ i} = NO_{x\ monitored\ i} - NO_{x\ uncalibrated\ i}, \qquad \textbf{(6.6)}$$

where $\Delta NO_{X\ background\ i}$ is the adjustment value for the rural NO_X background concentration for the hour i. $NO_{X\ monitored\ i}$ is the monitored hourly NO_X concentration for the hour i. $NO_{X\ uncalibrated\ i}$ is the calculated hourly NO_X concentration for the hour i using the uncalibrated rural background concentrations. The value of i ranged from 1 to 8760, which was the total number of hours in the year 2006.

$$\Delta O_{3\ background\ i} = \frac{(O_{3\ monitored\ i} - O_{3\ uncalibrated\ i})}{(O_{3\ macro\ i} - O_{3\ uncalibrated\ i})} \times (-5.4), \qquad \textbf{(6.7)}$$

where $\Delta O_{3\ background\ i}$ is the adjustment value for the rural O_3 background concentration for the hour i. $O_{3\ monitored\ i}$ is the monitored hourly O_3 concentration for the hour i. $O_{3\ uncalibrated\ i}$ is the calculated hourly O_3 concentration for the hour i using the uncalibrated rural background

concentrations. $O_{3\,macro\,i}$ is the calculated hourly O_3 concentration for the hour i using the macro-calibrated background concentrations. The value of i ranged from 1 to 8760, which was the total number of hours in the year 2006.

The three one-dimensional arrays of $\Delta\ NO_{2\ background}$, $\Delta\ NO_{X\ background}$ and $\Delta\ O_{3\ background}$, calculated by the above equations, were added to the arrays of the uncalibrated hourly sequential rural background concentrations of NO_2, NO_X and O_3, respectively. Hence the micro-calibrated background concentrations file was created based on the above three equations. However, running the Dunkirk AQMA base case scenario model with these micro-calibrated background concentrations resulted in the overestimation of the annual means of the monitored NO_2, NO_X and O_3 concentrations at the AQMS as shown in Table 6.2. In addition, using these micro-calibrated background concentrations increased the difference between the calculated and monitored hourly NO_2 concentrations on the micro, hourly, level. This was indicated by the large increase in the RMSE as shown in Table 6.2.

Table 6.2 Micro-calibration Development Stages of the Dunkirk AQMA Base Case Scenario Model

case description	receptor name	annual mean NO_x		annual mean NO_2		annual mean O_3		NO_2 RMSE before calibration	NO_2 RMSE after macro-calibration	NO_2 RMSE after micro-calibration
		calculated	monitored	calculated	monitored	calculated	monitored			
based on equations (6.5), (6.6) and (6.7).	AQMS	73.37	67.60	37.90	35.29	39.43	31.00	18.45	17.39	117.83
based on equations (6.8), (6.9), (6.10) and run 23.	AQMS	68.46	67.60	31.58	35.29	34.99	31.00	18.45	17.39	11.07
based on equations (6.8), (6.9), (6.10) and run 79.	AQMS	67.71	67.60	33.03	35.29	33.10	31.00	18.45	17.39	6.63
based on equations (6.8), (6.9), (6.10) and run 80.	AQMS	67.55	67.60	33.96	35.29	32.52	31.00	18.45	17.39	5.11
based on equations (6.8), (6.9), (6.10) and run 81.	AQMS	67.48	67.60	34.85	35.29	31.47	31.00	18.45	17.39	4.21
based on equations (6.8), (6.9), (6.10) and run 82.	AQMS	67.47	67.60	35.19	35.29	30.96	31.00	18.45	17.39	4.09
based on equations (6.8), (6.9), (6.10) and run 82 with no FAC file.	AQMS	68.65	67.60	35.51	35.29	30.74	31.00	18.45	17.39	5.71

A possible reason for the large increase in the RMSE after the micro-calibration based on Equations (6.5), (6.6) and (6.7) was the use of the macro-calibrated hourly concentrations in these equations. As discussed before with regard to Figure 6.6, the hourly calculated concentrations of the macro-calibrated base case scenario were not precise enough. The macro-calibrated base case scenario model of the Dunkirk AQMA was validated only on the macro, annual mean, level. Therefore, instead of using $NO_{2\,macro\,i}$ and $O_{3\,macro\,i}$, the macro-calibrated calculated hourly NO_2 and O_3 concentrations, it was decided to alter two of the three equations for the micro-calibration of the base case scenario model, using the macro-calibrated annual mean NO_2 and O_3 concentrations, so that:

$$\Delta NO_{2\,background\,i} = \frac{(NO_{2\,monitored\,i} - NO_{2\,uncalibrated\,i})}{(\overline{NO}_{2\,macro} - \overline{NO}_{2\,uncalibrated})} \times \Delta NO_{2\,macro\,background,} \quad \textbf{(6.8)}$$

where $\Delta NO_{2\,background\,i}$ is the adjustment value for the rural NO_2 background concentration for the hour i. $NO_{2\,monitored\,i}$ is the monitored hourly NO_2 concentration for the hour i. $NO_{2\,uncalibrated\,i}$ is the calculated hourly NO_2 concentration for the hour i using the uncalibrated rural background concentrations. The value of i ranged from 1 to 8760, which was the total number of hours in the year 2006. $\overline{NO}_{2\,macro}$ is the annual mean NO_2 concentration calculated using the macro-calibrated background concentrations. $\overline{NO}_{2\,uncalibrated}$ is the annual mean NO_2 concentration calculated using the uncalibrated rural background concentrations. $\Delta NO_{2\,macro\,background}$ is the macro-calibration adjustment value for the rural NO_2 background concentrations, as given in the column headed 'Background' in Table 6.1.

In respect of NO_X, Equation (6.6) was unchanged so that:

$$\Delta NO_{X\ background\ i} = NO_{x\ monitored\ i} - NO_{x\ uncalibrated\ i}, \quad \textbf{(6.9)}$$

where $\Delta NO_{X\ background\ i}$ is the adjustment value for the rural NO_X background concentration for the hour i. $NO_{X\ monitored\ i}$ is the monitored hourly NO_X concentration for the hour i. $NO_{X\ uncalibrated\ i}$ is the hourly NO_X concentration for the hour i calculated using the uncalibrated rural background concentrations. The value of i ranged from 1 to 8760, which was the total number of hours in the year 2006.

$$\Delta O_{3\ background\ i} = \frac{(O_{3\ monitored\ i} - O_{3\ uncalibrated\ i})}{(\overline{O}_{3\ macro} - \overline{O}_{3\ uncalibrated})} \times \Delta O_{3\ macro\ background}, \quad \textbf{(6.10)}$$

where $\Delta O_{3\ background\ i}$ is the adjustment value for the rural O_3 background concentration for the hour i. $O_{3\ monitored\ i}$ is the monitored hourly O_3 concentration for the hour i. $O_{3\ uncalibrated\ i}$ is the calculated hourly O_3 concentration for the hour i using the uncalibrated rural background concentrations. The value of i ranged from 1 to 8760, which was the total number of hours in the year 2006. $\overline{O}_{3\ macro}$ is the annual mean O_3 concentration calculated using the macro-calibrated background concentrations. $\overline{O}_{3\ uncalibrated}$ is the annual mean O_3 concentration calculated using the uncalibrated rural background concentrations. $\Delta O_{3\ macro\ background}$ is the macro-calibration adjustment value for the rural O_3 background concentrations, as given in the column headed 'Background' in Table 6.1.

A VBA computer program was written by the author in MS Excel in order to automate the generation of the three hourly sequential one-dimensional arrays for $\Delta NO_{2\ background}$, $\Delta NO_{X\ background}$ and $\Delta O_{3\ background}$ using the above three equations. For any hour in the year 2006, if either the calculated or monitored hourly concentration was missing, then the equation relevant to the type of missing concentration would not be usable. This was handled in the VBA computer program as follows: $\Delta NO_{2\ background\ i} = \Delta NO_{2\ macro\ background}$

for the hours of missing hourly NO_2 concentrations, $\Delta\ NO_{X\ background\ i} = \Delta\ NO_{X\ macro\ background}$ for the hours of missing hourly NO_X concentrations, and $\Delta\ O_{3\ background\ i} = \Delta\ O_{3\ macro\ background}$ for the hours of missing hourly O_3 concentrations.

The VBA computer program applied Equations (6.8), (6.9) and (6.10) along with the macro-calibration results of run 23 version 2.3 in Table 6.1 to generate the micro-calibrated background concentrations file. Running the Dunkirk AQMA base case scenario model with this background concentrations file significantly improved the RMSE, r and the slope of the best fit line through the origin as shown in Table 6.2 and Figure 6.7. This indicated a significant improvement for NO_2 hourly predictions by the base case scenario model when using this background concentrations file. However, the base case scenario model with this background concentrations file underestimated the annual mean of monitored NO_2 concentrations, and overestimated the annual mean of monitored O_3 concentrations, at the AQMS as shown in Table 6.2. Hence, using the trial and error macro-calibration approach, it was necessary to undertake additional runs of ADMS-Roads, beyond run 23 version 2.3, as shown in Table 6.1.

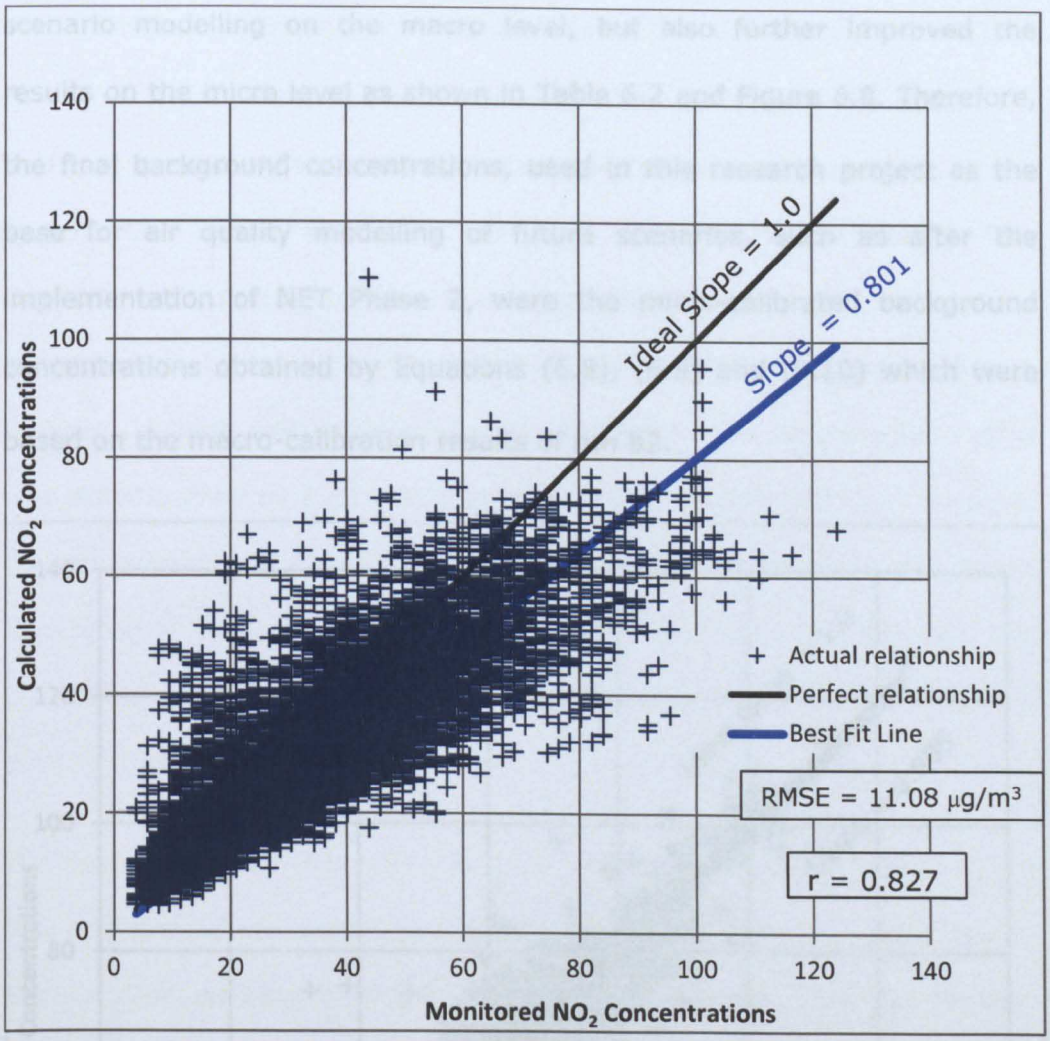

Figure 6.7 Scatter Diagram of Hourly NO_2 Concentrations at the AQMS after the Micro-calibration based on Run 23

The background concentrations of these additional macro-calibration runs were modified so that the annual mean of monitored NO_2 concentrations was deliberately overestimated, and the annual mean of monitored O_3 concentrations was deliberately underestimated, by these runs, numbered 79-82 in Table 6.1. Consequently, after the 'normal' micro-calibration underestimation of the annual mean of monitored NO_2 concentrations and the 'normal' micro-calibration overestimation of the annual mean of monitored O_3 concentrations, the micro-calibration runs based on the results of these additional macro-calibration runs gave a good estimate of the annual means of both the monitored NO_2 and O_3 concentrations at the AQMS. This not only improved the results of the micro-calibrated base case

scenario modelling on the macro level, but also further improved the results on the micro level as shown in Table 6.2 and Figure 6.8. Therefore, the final background concentrations, used in this research project as the base for air quality modelling of future scenarios, such as after the implementation of NET Phase 2, were the micro-calibrated background concentrations obtained by Equations (6.8), (6.9) and (6.10) which were based on the macro-calibration results of run 82.

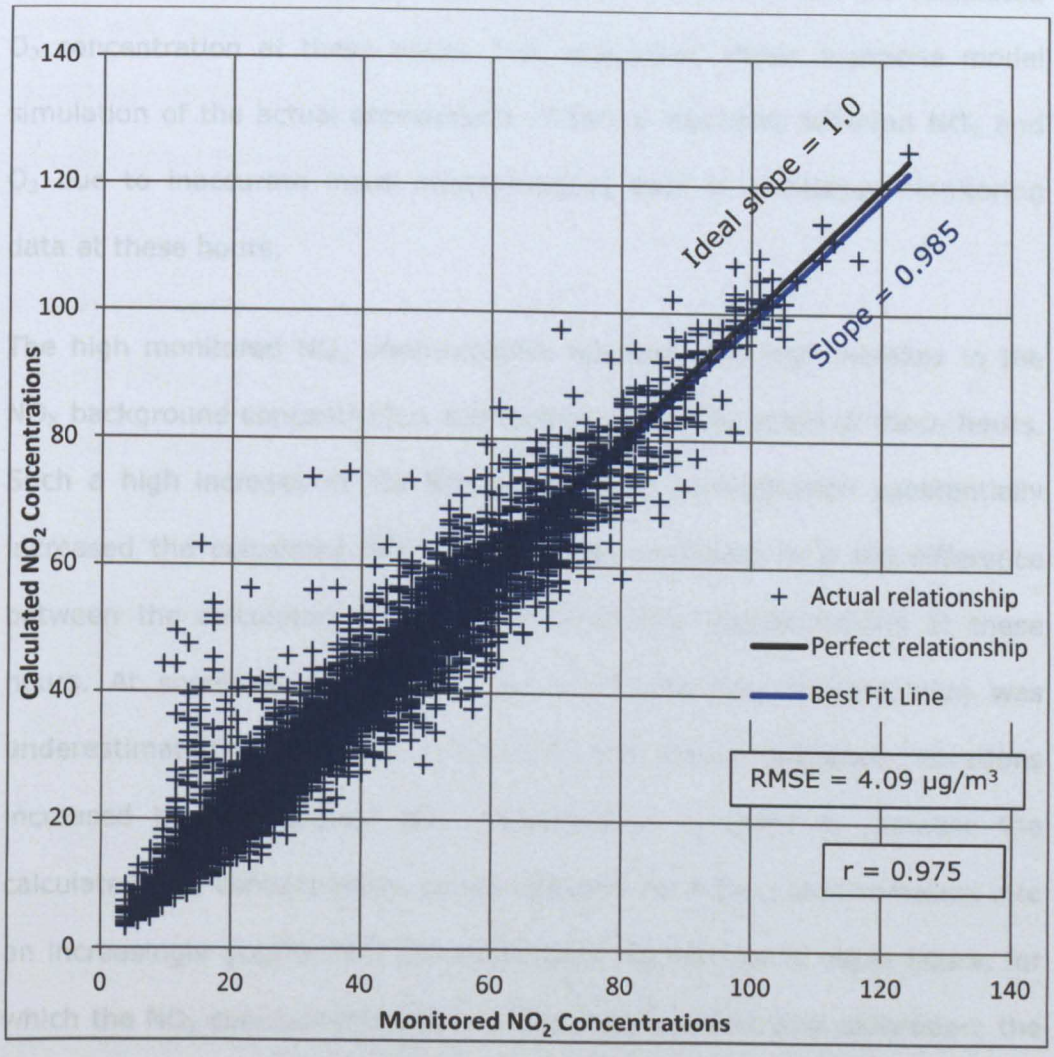

Figure 6.8 Scatter Diagram of Hourly NO_2 Concentrations at the AQMS after the Micro-calibration based on Run 82

The micro-calibration development, from run 23 to run 82, increased the error between the calculated and monitored NO_2 concentrations at a few hours, as implied by the comparison between the scatter in the

overestimated points on the lower left side of Figure 6.7 and Figure 6.8. A thorough investigation was undertaken in order to identify the reason for such unexpected behaviour of the micro-calibration process at these hours. A potential reason was the very high ratio of the monitored NO_X concentration to the monitored NO_2 concentrations, e.g. 7, which was accompanied by a high monitored O_3 concentration at these hours. However, a high calculated NO_X concentration by the air pollution model was accompanied by high calculated NO_2 concentration and low calculated O_3 concentration at these hours. This suggested either imprecise model simulation of the actual atmospheric chemical reactions between NO_X and O_3 due to inaccurate input meteorological data or imprecise monitoring data at these hours.

The high monitored NO_X concentration resulted in a high increase in the NO_X background concentration due to the micro-calibration at these hours. Such a high increase in the NO_X background concentration substantially increased the calculated NO_2 concentration, resulting in a big difference between the calculated and low monitored NO_2 concentrations at these hours. At some of these hours, for which the NO_2 concentration was underestimated before any calibration, the micro-calibration iterations increased the background NO_2 concentration in order to increase the calculated NO_2 concentration, which changed the NO_2 underestimation into an increasingly greater NO_2 overestimation. At the rest of these hours, for which the NO_2 concentration was overestimated before any calibration, the reduction in calculated NO_2 concentration due to the micro-calibration iterations was masked by the increase in calculated NO_2 concentration due to the high NO_X background concentration.

6.4.3 Impact of Traffic Profiles on the Validation of the Base Case Scenario Modelling

As mentioned in Section 6.3, the hourly and monthly traffic profiles were considered in the set-up of the base case scenario model by a special text file, a FAC file. The impact of the traffic profiles on the macro and micro levels was investigated by turning off this FAC file in the final micro-calibrated version of the Dunkirk AQMA base case scenario model, corresponding to run 82 in Table 6.2. The exclusion of the traffic profiles did not have a significant impact on the calculated annual mean NO_2, NO_X and O_3 concentrations as shown in Table 6.2. Therefore, it was concluded that the consideration of the traffic profiles in the base case scenario model was not important for the macro-validation.

On the other hand, the exclusion of the traffic profiles slightly worsened the hourly calculated NO_2 concentrations as shown in Figure 6.9. This was indicated by the higher RMSE, the lower r, and the slightly lower slope of the best fit line through the origin, without a FAC file in Figure 6.9 than the corresponding values with a FAC file in Figure 6.8. Therefore, it was concluded that the incorporation of the traffic profiles in the base case scenario model could further improve the micro-validation by reducing the RMSE between the calculated and monitored hourly NO_2 concentrations by 28.4%.

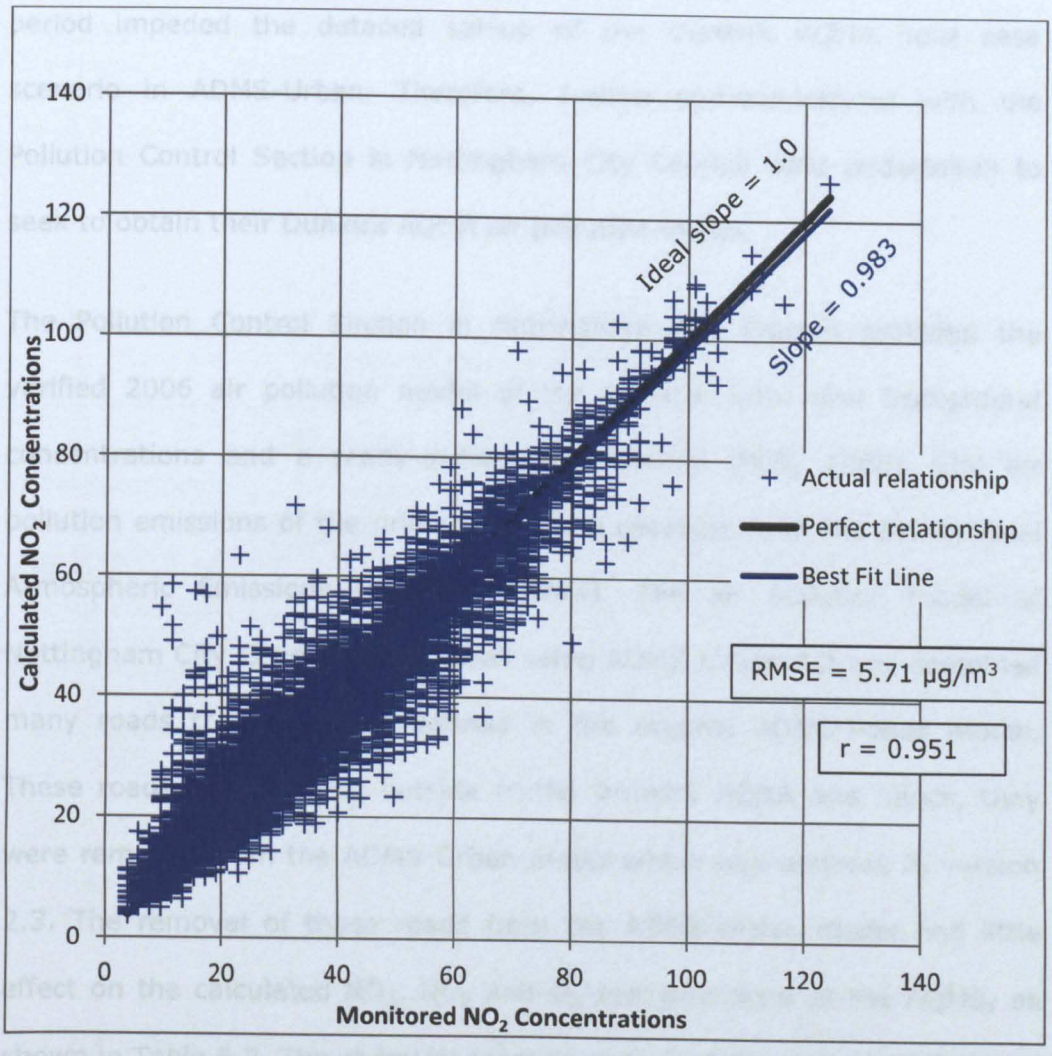

Figure 6.9 Scatter Diagram of Hourly NO_2 Concentrations at the AQMS after the Micro-calibration based on Run 82 without a FAC file

6.4.4 The Calibration of, versus the Use of Grid Sources in, the Base Case Scenario Modelling

As mentioned in Section 6.4.1, the option of grid air pollution sources was not available in ADMS-Roads. Therefore, many communications were undertaken with Cambridge Environmental Research Consultants (CERC), the company which developed the whole family of ADMS software, in order to obtain a trial version of ADMS-Urban. CERC provided a full version of ADMS-Urban version 2.3 with a trial license for a week. The short trial

period impeded the detailed set-up of the Dunkirk AQMA base case scenario in ADMS-Urban. Therefore, further communications with the Pollution Control Section in Nottingham City Council were undertaken to seek to obtain their Dunkirk AQMA air pollution model.

The Pollution Control Section in Nottingham City Council provided the verified 2006 air pollution model of the Dunkirk with rural background concentrations and a ready-defined grid source (PCS, 2008). The air pollution emissions of the grid source were obtained from the UK National Atmospheric Emissions Inventory (NAEI). The air pollution model of Nottingham City Council was created using ADMS-Urban 2.2 and contained many roads that were not defined in the original ADMS-Roads model. These roads were located outside of the Dunkirk AQMA and hence, they were removed from the ADMS-Urban model which was updated to version 2.3. The removal of these roads from the ADMS-Urban model had little effect on the calculated NO_2, NO_X and O_3 concentrations at the AQMS, as shown in Table 6.3. The chemical reaction setting of the initial ADMS-Urban model was the Chemical Reaction Scheme (CRS) with a trajectory model which was adjusted to CRS only, the ADMS-Roads chemical reaction setting. This was used to give a fair comparison between ADMS-Urban with a grid source and rural background concentrations and ADMS-Roads with calibrated background concentrations only.

The modified ADMS-Urban model with CRS was run to output the 2006 annual mean concentrations of NO_2, NO_X and O_3 at the AQMS as shown in Table 6.3. Comparing Table 6.2 with Table 6.3, the calculated annual mean NO_2, NO_X and O_3 concentrations from the ADMS-Roads model, with micro-calibrated background concentrations, were closer to the corresponding annual means of monitored concentrations than were the calculated annual means from the ADMS-Urban model, with a grid source and rural

background concentrations. This indicated that the ADMS-Roads model, with micro-calibrated background concentrations only, was more precise than the ADMS-Urban model, with a grid source and rural background concentrations, on the macro level.

Table 6.3 Monitored versus Calculated Annual Mean Concentrations at the AQMS by ADMS-Urban

Case description	NO_2 annual mean $\mu g/m^3$		NO_X annual mean $\mu g/m^3$		O_3 annual mean $\mu g/m^3$	
	calculated	monitored	calculated	monitored	calculated	monitored
ADMS-Urban with all road sources and CRS	37.79	35.29	69.34	67.6	35.04	31
ADMS-Urban with Dunkirk AQMA road sources and CRS	37.65	35.29	69.31	67.6	35.18	31
ADMS-Urban with Dunkirk AQMA road sources and CRS with trajectory model	37.77	35.29	69.31	67.6	35.07	31

The 2006 hourly NO_2 concentrations calculated by the ADMS-Urban model were compared to the 2006 hourly monitored NO_2 concentrations at the AQMS as shown in Figure 6.10. Hence, comparing Figure 6.10 with Figure 6.8, the results of the ADMS-Urban model, with a grid source and rural background concentrations, gave a much higher RMSE than did the results of the ADMS-Roads model, with micro-calibrated background concentrations only. In addition, the results of the ADMS-Urban model gave a much lower r, and a lower slope of the best fit line through the origin, than did the results of the ADMS-Roads model, with micro-calibrated background concentrations only. Therefore, the results of the ADMS-Roads model, with micro-calibrated background concentrations only, were much closer to the 2006 hourly NO_2 concentrations monitored by the AQMS than were the results of the ADMS-Urban model, with a grid source

and rural background concentrations. This indicated that the ADMS-Roads model, with micro-calibrated background concentrations only, was much more precise than the ADMS-Urban model, with a grid source and rural background concentrations, on the micro level.

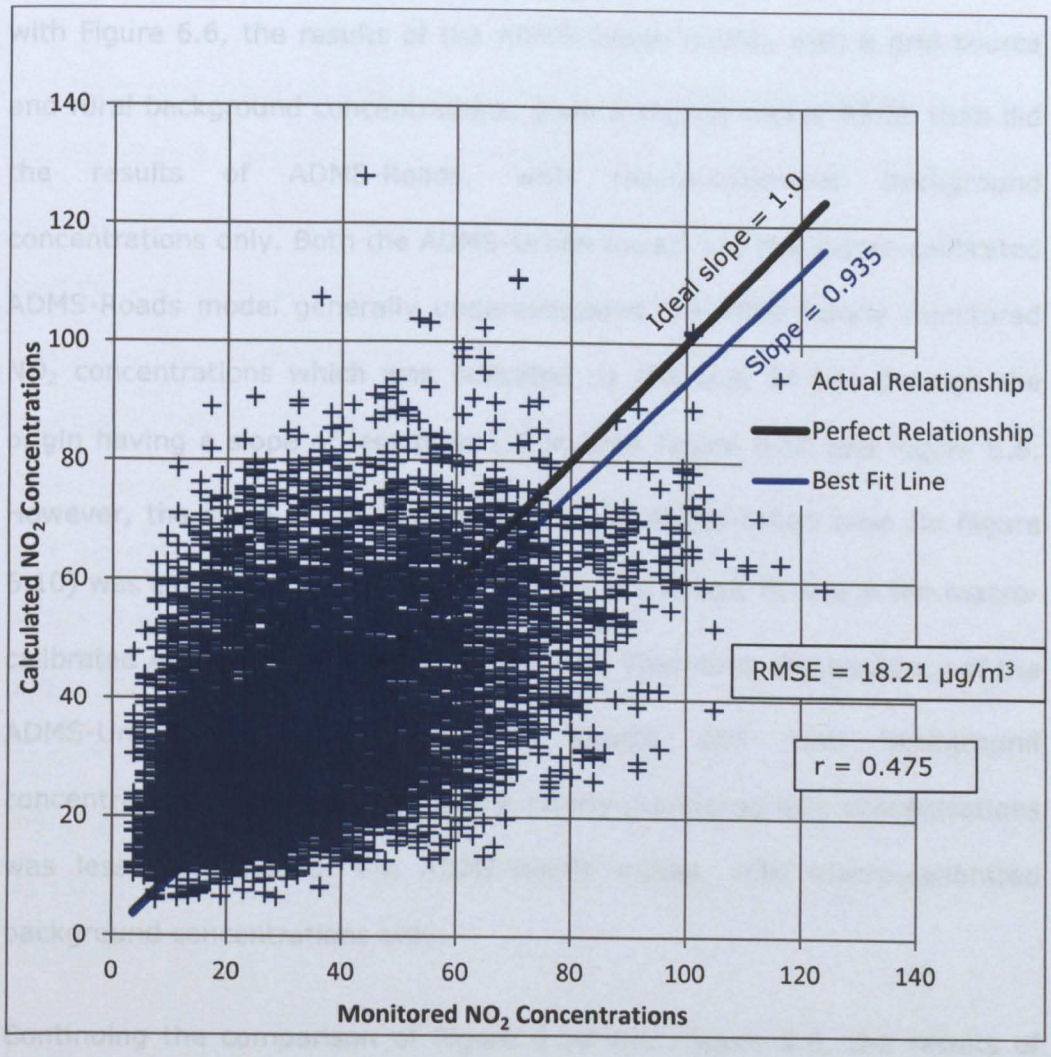

Figure 6.10 Scatter Diagram of Monitored versus Calculated Hourly NO_2 Concentrations at the AQMS by ADMS-Urban

Comparing Table 6.1 (run 23, version 2.3) with Table 6.3, the calculated annual mean NO_2, NO_X and O_3 concentrations from the ADMS-Roads model, with macro-calibrated background concentrations only, were closer to the corresponding annual means of monitored concentrations than were the calculated annual means from the ADMS-Urban model, with a grid source and rural background concentrations. This indicated that the ADMS-

Roads model, with macro-calibrated background concentrations only, was more precise than the ADMS-Urban model, with a grid source and rural background concentrations, on the macro level.

In respect of the 2006 hourly NO2 concentrations, comparing Figure 6.10 with Figure 6.6, the results of the ADMS-Urban model, with a grid source and rural background concentrations, gave a slightly higher RMSE than did the results of ADMS-Roads, with macro-calibrated background concentrations only. Both the ADMS-Urban model and the macro-calibrated ADMS-Roads model generally underestimated the 2006 hourly monitored NO_2 concentrations which was indicated by the best fit line through the origin having a slope of less than 1.0 in both Figure 6.10 and Figure 6.6. However, the slope of the best fit line in the ADMS-Urban case (in Figure 6.10) was closer to 1.0 than was the slope of the best fit line in the macro-calibrated ADMS-Roads case (in Figure 6.6). Therefore, the tendency of the ADMS-Urban model, with a grid source and rural background concentrations, to underestimate the hourly monitored NO_2 concentrations was less than that of the ADMS-Roads model, with macro-calibrated background concentrations only.

Continuing the comparison of Figure 6.10 with Figure 6.6, the results of ADMS-Urban, with a grid source and rural background concentrations, gave a slightly higher r than did the results of ADMS-Roads, with macro-calibrated background concentrations only. This implied that the ADMS-Urban model slightly increased the degree of linearity of the actual relationship between the calculated and monitored hourly NO_2 concentrations at the AQMS. Hence, the actual relationship between the calculated and monitored hourly NO_2 concentrations was slightly closer to the perfect straight line relationship in the case of the ADMS-Urban model

than it was in the case of the macro-calibrated ADMS-Roads model. The RMSE, r and the slope of the best fit line through the origin indicated that the ADMS-Roads model, with macro-calibrated background concentrations only, was almost as precise as the ADMS-Urban model, with a grid source and rural background concentrations, on the micro level.

The trajectory model of CRS is used along with a grid air pollution source in ADMS-Urban to adjust the background concentrations in the main model domain, the model application area, on the basis of the grid source emissions (CERC, 2006b). The trajectory model uses the grid source domain, which is usually larger than the main model domain. Then, the trajectory model increases the background concentrations within the nested main model domain, to take account of the emissions in the larger grid source domain. This converts the rural background concentrations within the model application area to urban background concentrations before ADMS-Urban actually starts its calculations of the air pollution concentrations. Therefore, it was decided to investigate the impact of running the modified ADMS-Urban model with the trajectory model of CRS on the annual mean and hourly calculated air pollution concentrations at the AQMS.

Running the ADMS-Urban model with only the roads of the Dunkirk AQMA and the trajectory model of CRS did not significantly change the calculated annual mean NO_2, NO_X and O_3 concentrations at the AQMS from the calculated annual means of these concentrations by using CRS only, as shown in Table 6.3. In addition, comparing Figure 6.11 with Figure 6.10, running the ADMS-Urban model with the trajectory model of CRS did not significantly change the RMSE, r or the slope of the best fit line through the origin of the actual relationship between the hourly calculated and monitored NO_2 concentrations at the AQMS. Therefore, it was concluded

that using the trajectory model of CRS for running ADMS-Urban did not provide any significant improvement to running ADMS-Urban with CRS only, on either the macro or the micro level. Therefore using the trajectory model of CRS did not change the results of comparing the ADMS-Urban model, with rural background concentrations and a grid source, to the ADMS-Roads model, with either macro or micro-calibrated background concentrations.

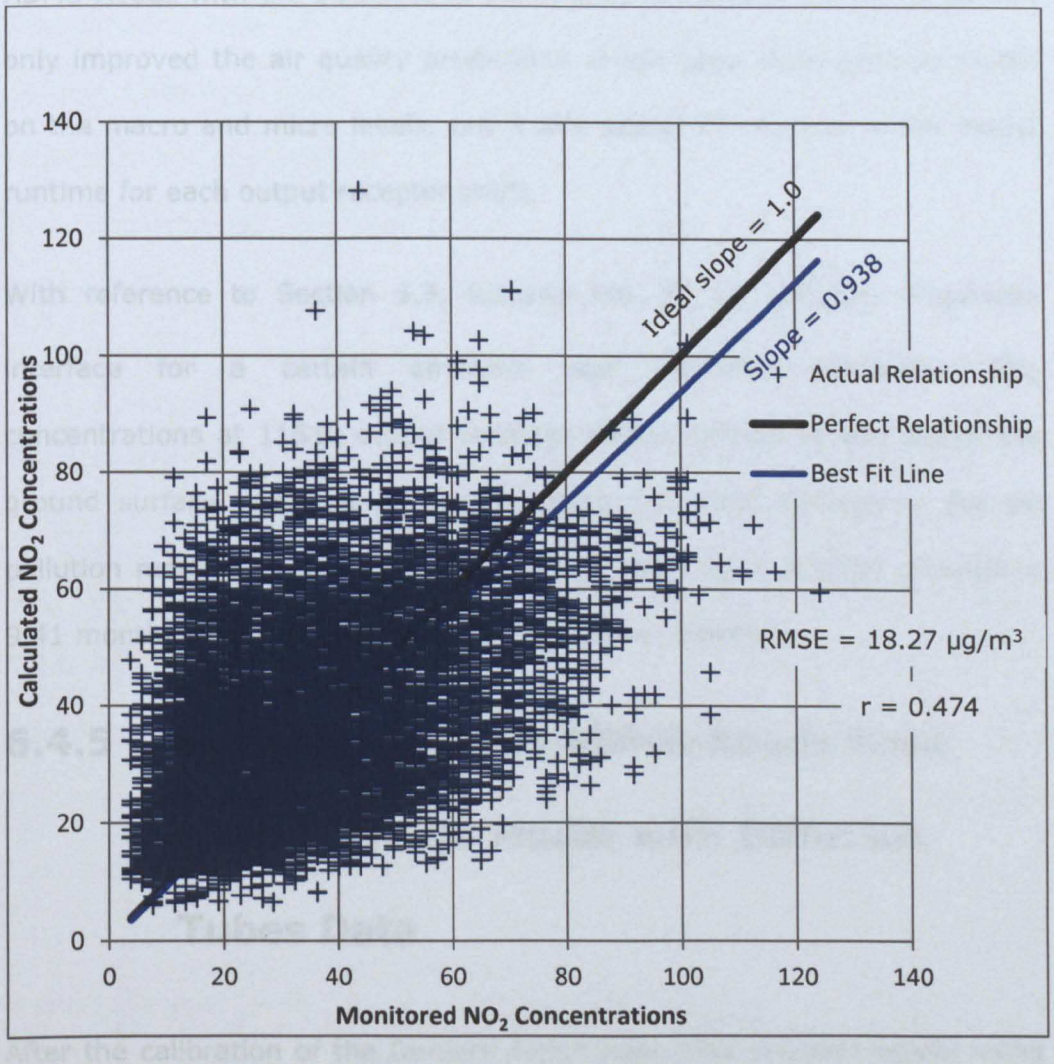

Figure 6.11 Scatter Diagram of Monitored versus Calculated Hourly NO_2 Concentrations at the AQMS by ADMS-Urban with the Trajectory Model of CRS

In terms of the model runtime, running ADMS-Urban with the road sources of the Dunkirk AQMA, a grid source, rural background concentrations and either the CRS or the trajectory model of CRS required 44 minutes to

calculate the annual mean and hourly concentrations of NO_2, NO_X and O_3 at a single output receptor point, the site of the AQMS. On the other hand, running ADMS-Roads with the same road sources of the Dunkirk AQMA, the CRS and either the macro-calibrated or micro-calibrated background concentrations required 9 minutes to calculate the annual mean and hourly concentrations of NO_2, NO_X and O_3 at the same output receptor point, the site of the AQMS. Therefore, compared to running ADMS-Urban, using ADMS-Roads with the background concentrations calibration technique not only improved the air quality predictions of the base case scenario model on the macro and micro levels, but it also saved 35 minutes of the model runtime for each output receptor point.

With reference to Section 6.5, building the 3D air pollution dispersion interface for a certain emission year required calculating NO_2 concentrations at 11610 output receptor points defined at and above the ground surface. With simple mathematics, the total savings in the air pollution model runtime could be $11610 \times (44 - 9) = 406350$ minutes $\approx$ 9.41 months for each 3D air pollution dispersion interface.

6.4.5 Calibration of the ADMS-Roads Base Case Scenario Model with Diffusion Tubes Data

After the calibration of the Dunkirk AQMA base case scenario model using the continuous monitoring data from the AQMS, further monitoring data from the diffusion tubes located in the Dunkirk AQMA in 2006 and 2007, was obtained from Nottingham City Council. Additionally, Nottingham City Council provided 2007-2008 data from the Lace Street continuous monitor described in Section 2.4, as this monitor only started monitoring the air

quality in 2007. Therefore, it was decided to attempt to macro-validate the results of the macro-calibrated base case scenario model by using the 2006 monitoring data of these diffusion tubes. Moreover, Nottingham City Council provided a sensible estimate for the 2006 annual mean NO_2 concentration at the location of the Lace Street continuous monitor by Beeston Road. This sensible estimate is based on ADMS predictions from a wide-area air pollution model created by the Pollution Control Section.

The diffusion tube at Clifton Boulevard Facade has only been at this location since April 2006. Therefore, this diffusion tube only captured NO_2 concentrations at this location for 9 months in 2006 rather than for one full year. Consequently, the monitored annual mean NO_2 concentration of this diffusion tube was proven unreliable, and hence the diffusion tube was excluded from the macro-validation list of diffusion tubes.

The Dunkirk AQMA base case scenario model was run with the macro-calibrated background concentrations to calculate the 2006 annual mean NO_2 concentration at seven output receptor points, as shown in Figure 6.12, defined at the geographical locations of the 2006 diffusion tubes, including the geographical location of the Lace Street continuous monitor. The calculated annual mean NO_2 concentration agreed with the diffusion tube monitored annual mean NO_2 concentration for two receptor points, but not for the five receptor points on Beeston Road. The base case scenario model with the macro-calibrated background concentrations generally underestimated the annual mean NO_2 concentration monitored by the diffusion tubes located on Beeston Road.

The Pollution Control Section in Nottingham City Council advised that diffusion tubes were not as accurate as real time continuous monitoring, however they could give a good indication of what was happening with the

air quality in the Dunkirk AQMA. Therefore, the 2006 monitoring data from the diffusion tubes could not be used directly for the validation of the base case scenario model. Instead, the calculated annual mean NO_2 concentration at the Lace Street continuous monitor was compared to the city council's estimated annual mean NO_2 concentration at the location of this continuous monitor by Beeston Road.

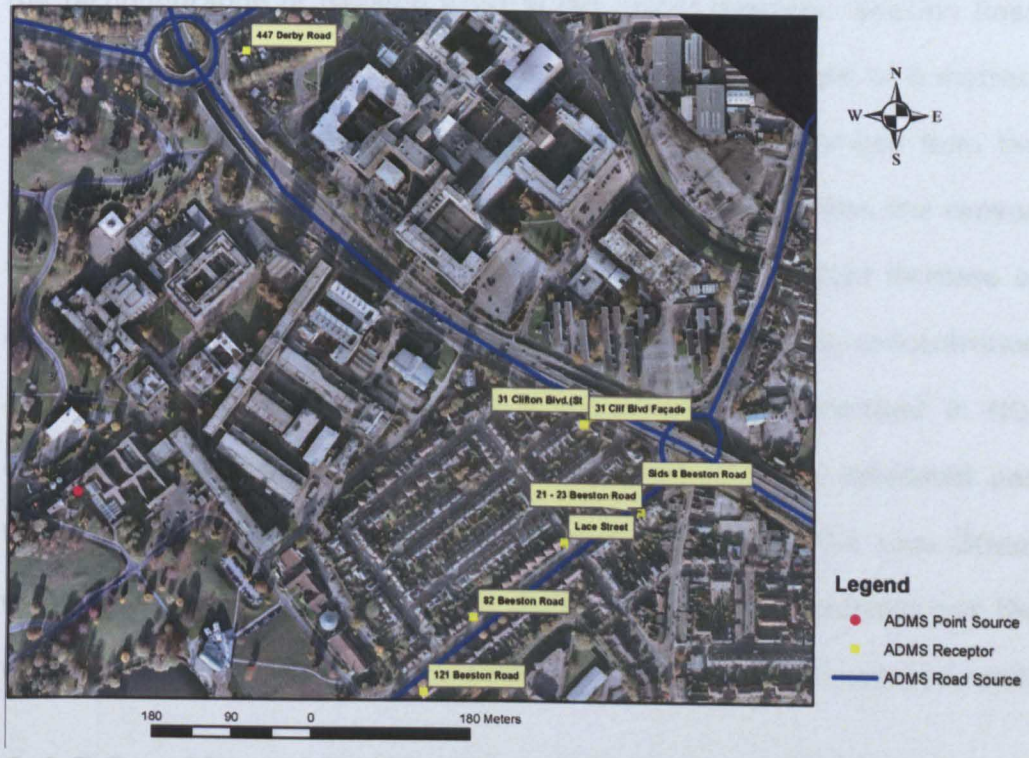

Figure 6.12 NO_2 Diffusion Tubes in the Dunkirk AQMA

The base case scenario model with the macro-calibrated background concentrations underestimated the city council's estimate of the annual mean NO_2 concentration at the Lace Street continuous monitor. Therefore, although not so reliable, the Beeston Road diffusion tubes appeared to provide supporting evidence that the base case scenario model with the macro-calibrated background concentrations underestimated the annual mean NO_2 concentration in this Beeston Road area. The Lace Street continuous monitor indicated that the magnitude of the underestimation was 8.87 $\mu g/m^3$. Consequently, three different approaches were tried in

order to improve this macro-validation at the Lace Street continuous monitor, as described below.

6.4.5.1 Beeston Road Reconfiguration Approach

One possible approach to increasing the calculated annual mean NO_2 concentration at the receptor points in the Beeston Road area was to try the reconfiguration of Beeston Road in the model interface. Beeston Road was reconfigured to be a street canyon with a canyon height of 6 metres. The width of Beeston Road in the model interface was changed from the actual carriageway width to the building edge to edge distance, the canyon width. However, this reconfiguration only resulted in a slight increase of approximately 0.63 $\mu g/m^3$ in the calculated annual mean NO_2 concentration at the receptor points located inside the canyon. The increase in NO_2 concentration was far from bridging the gap between the estimated and the calculated 2006 annual mean NO_2 concentration at the Lace Street continuous monitor. Therefore, this development was abandoned and the configuration of Beeston Road returned to being that of a non-canyon road.

6.4.5.2 Altered Traffic Flow and Speed Approach

The aim of this approach was to investigate the possibility of altering the traffic flow and/or speed for Beeston Road and/or Abbey Street, the two nearest principal roads to the Lace Street continuous monitor, in order to increase the calculated annual mean NO_2 concentration, so that it agreed with the city council's estimated annual mean NO_2 concentration at the Lace Street continuous monitor. Table 6.4 shows the results of this investigation with two traffic flow/speed scenarios highlighted in yellow, which achieved this aim.

Table 6.4 Calculated and Monitored Annual Mean NO_2 Concentrations at the AQMS and Lace Street for Various Traffic Flow and Speed Scenarios

Scenario	AQMS calculated annual mean NO_2	AQMS monitored annual mean NO_2	Lace Street calculated annual mean NO_2	Lace Street monitored annual mean NO_2
As it was, before any amendments	35.45	35.29	36.13	45
1.245 × Traffic Flow of Beeston RD, 322a and 323b	35.50	35.29	36.88	45
1.245 × Traffic Flow of Beeston RD, Abbey St, 322a, 322b, 323a and 323b	35.54	35.29	36.93	45
1.5 × Traffic Flow of Beeston RD, Abbey St, 322a, 322b, 323a and 323b	35.63	35.29	37.74	45
3.81 × Traffic Flow of Beeston RD, Abbey St, 322a, 322b, 323a and 323b	36.50	35.29	44.29	45
4.0 × Traffic Flow of Beeston RD, Abbey St, 322a, 322b, 323a and 323b	36.57	35.29	44.79	45
4.0 × Traffic Flow of Beeston RD, Abbey St, 322a, 322b, 323a and 323b & Traffic Speed of Beeston RD, Abbey St, 322a, 322b, 323a and 323b / 4.0	37.22	35.29	49.79	45
3.0 × Traffic Flow of Beeston RD, Abbey St, 322a, 322b, 323a and 323b & Traffic Speed of Beeston RD, Abbey St, 322a, 322b, 323a and 323b / 3.0	36.52	35.29	44.77	45
2.0 × Traffic Speed of Beeston RD, Abbey St, 322a, 322b, 323a and 323b	35.56	35.29	37.62	45
Traffic Speed of Beeston RD, Abbey St, 322a, 322b, 323a and 323b / 2.0	35.54	35.29	36.80	45
Traffic Speed of Beeston RD, Abbey St, 322a, 322b, 323a and 323b / 4.0	35.65	35.29	37.64	45

The first of the two highlighted scenarios in Table 6.4 increased hypothetically the traffic flows of Beeston Road, Abbey Street and the connecting roundabout links (322a, etc) by a factor of four, without altering the traffic speed, assuming enough available road capacity. The second of these two scenarios increased hypothetically the traffic flows of Beeston Road, Abbey Street and the connecting roundabout links by a factor of three, as well as decreasing the traffic speed of all these links by a factor of three, assuming enough available road capacity. Altering only the traffic speed was not enough to eliminate the difference between the calculated and estimated annual mean NO_2 concentrations at the Lace Street continuous monitor. The traffic speed could neither be multiplied by more than 2.0, nor divided by more than 4.0, owing to the speed limits of the built-in emission factors in ADMS-Roads.

Although the two highlighted scenarios in Table 6.4 satisfactorily decreased the difference between the calculated and monitored annual mean NO_2 concentrations at the Lace Street continuous monitor, they increased the difference between the calculated and monitored annual mean NO_2 concentrations at the AQMS. In addition, they added Abbey Street, and a wide area around Beeston Road and Abbey Street, to the already declared NO_2 Dunkirk AQMA as shown in Figure 6.13. This was confirmed as being incorrect by the Pollution Control Section in Nottingham City Council. Increasing the traffic flow, measured using embedded continuous monitoring loops in Beeston Road and Abbey Street, by three or four times and ignoring the road capacity limitations, were also clearly unrealistic. Therefore, it was decided to investigate another alternative to altering the traffic flow and/or speed for Beeston Road and/or Abbey Street.

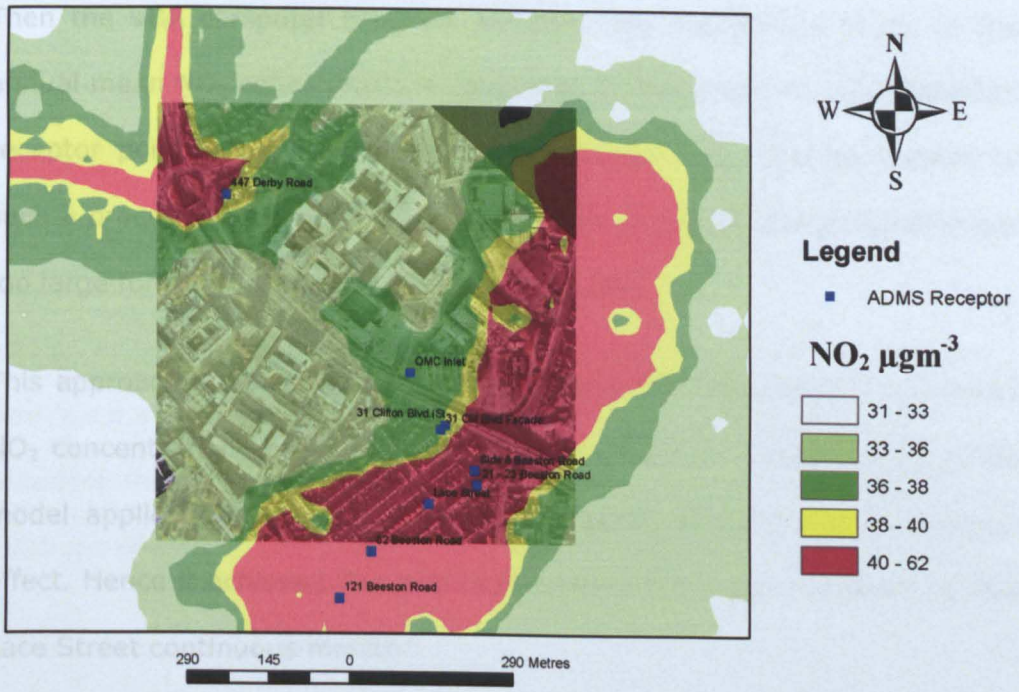

Figure 6.13 Ground Level 2006 Annual Mean NO_2 concentrations in the Dunkirk AQMA for the Two Traffic Scenarios Highlighted in Table 6.4

6.4.5.3 GIS-based Factor Approach

This approach involved applying a factor, the ratio of the monitored annual mean NO_2 concentration to the calculated annual mean NO_2 concentration at the Lace Street continuous monitor, to the base case scenario model output annual mean NO_2 concentrations. This was a challenge as the factor had to be applied only to the area in the Beeston Road canyon, not to all of the model application area (the Dunkirk AQMA).

A VBA computer program in MS Excel was coded to select automatically the output receptor points located inside the Beeston Road canyon area. To do this, GIS techniques were used to create a shape file for the Beeston Road canyon area, which was then converted into a set of point coordinates. Once this had been done, the VBA computer program automatically compared the coordinates of each output receptor point in the Dunkirk AQMA with this set of point coordinates, so that the receptor points located inside the Beeston Road canyon area could be identified automatically.

Then the VBA computer program automatically applied the factor to the annual mean NO_2 concentrations calculated by the model at each identified receptor point inside the Beeston Road canyon area. The automation of such a process was vital as the total number of output receptor points was too large for this factoring to be done manually.

This approach enables a modeller to increase the calculated annual mean NO_2 concentrations by any chosen factor throughout a subset area of the model application area that may have irregular boundaries, and canyon effect. Hence it achieved the goal of improving the macro-validation at the Lace Street continuous monitor.

6.5 Grid Design for the Base Case Scenario Model

The grid of the base case scenario model of the Dunkirk AQMA consisted of a set of output receptor points, at which the output air pollution concentrations were calculated by the air pollution model at a certain height above the ground surface. The gridded output concentrations were then used to create a contour map for the air pollution dispersion in the model application area. The first type of air pollution output grid in ADMS-Roads was the regular grid.

The regular grid in ADMS-Roads version 2.3 was a rectangular grid which varied in size from 1×1 to 100×100 receptor points (CERC, 2006a). The greater the regular grid size, the higher the resolution of the output concentrations contour map. However, the greater the regular grid size, the longer the model runtime. Therefore, there was a trade-off between the output data resolution and the model runtime.

The other type of air pollution output grid in ADMS-Roads version 2.3 was the intelligent grid. The intelligent grid was a regular grid with additional grid points close to the road sources, where the pollutant concentration gradients were the greatest (CERC, 2006a). The intelligent grid had two groups of these additional grid points. The number and locations of one group of these additional grid points depended on the relative emissions from each pair of intersecting roads. The number and locations of the other group of these additional grid points were specified by the number and locations of road sources defined in the model scenario.

Since a large number of road sources was defined in the base case scenario model, the use of a regular output grid was unsuitable. Therefore, the intelligent grid option was selected for the base case scenario model so that the rapidly changing NO_2 concentrations' gradient close to the main roads in the Dunkirk AQMA could be well captured.

Many trials were undertaken for the specification of the regular grid size of the base case scenario intelligent grid. As the base case scenario model had to run many times for the generation of the air pollution data at and above the ground surface, the model runtime was assigned a higher priority than that of the output data resolution. A regular grid size of 31×31 points was selected for the intelligent grid of the base case scenario model, in order to optimise both the model runtime and the output data resolution. This constituted 1089 regular grid output receptor points at any output height above the ground surface, as ADMS-Roads added an extra row or column of points at each edge of the regular grid.

A *.igp file, a special customisation text file in ADMS-Roads, was compiled for the customisation of the intelligent grid of the base case scenario model, in order to disable the automatic generation of the intelligent grid

points whose locations were dependent upon the relative emissions from each pair of intersecting roads. This meant that changing the emissions of the roads, to simulate the impacts of the implementation of NET Phase 2, would neither affect the number nor the locations of the output receptor points. This facilitated a direct comparison between the two cases, before and after the implementation of NET Phase 2, while making use of the above mentioned benefits of having an intelligent grid. The total number of additional intelligent grid points was 846 at any output height above the ground surface.

6.6 Height Limit and Step of the Air Pollution Output Receptor Points

Many runs of the Dunkirk AQMA base case scenario model were performed to specify the height limit of the air pollution plume above the ground surface. Initially, the height limit was defined as the height above the ground surface at which the air pollution vanishes. The gridded output option was disabled at the model interface to speed up the model run. Instead of the gridded output, many output receptor points were all defined at the single geographical location of the AQMS to output the 2006 annual mean NO_2 concentration at different heights above that point.

Many trials were undertaken for the identification of the height step between the successive output receptors above any single ground-level geographical location. The criterion for this identification was to have a significant drop in the calculated annual mean NO_2 concentrations between any two vertically successive output receptors. Therefore, the model initially was run with a small height step of 1 metre and the output annual mean NO_2 concentrations at the vertically successive receptors were

compared. It was found that a height step of 6 metres can satisfy the criterion. Hence, it was decided to increase the height of the vertically successive output receptors above the ground surface at the AQMS by 6 metres until the air pollution vanished.

Generally, the annual mean NO_2 concentration decreased as the height of the receptor points above the ground surface at the AQMS increased. At a height of 30 metres above the ground surface, the gradient of NO_2 decay with height became very small. Consequently, there was no point in increasing the output height beyond 30 metres as the annual mean NO_2 concentration would remain almost the same. Therefore, the height limit of the Dunkirk AQMA base case scenario model was set at 30 metres above the ground surface. Figure 6.14 and Figure 6.15 show the decay of the annual mean NO_x and NO_2 concentration with height at the AQMS. Figure 6.16 to Figure 6.21 show the contour maps of the gridded output 2006 annual mean NO_2 concentrations at 0 to 30 metres above the ground surface in the Dunkirk AQMA.

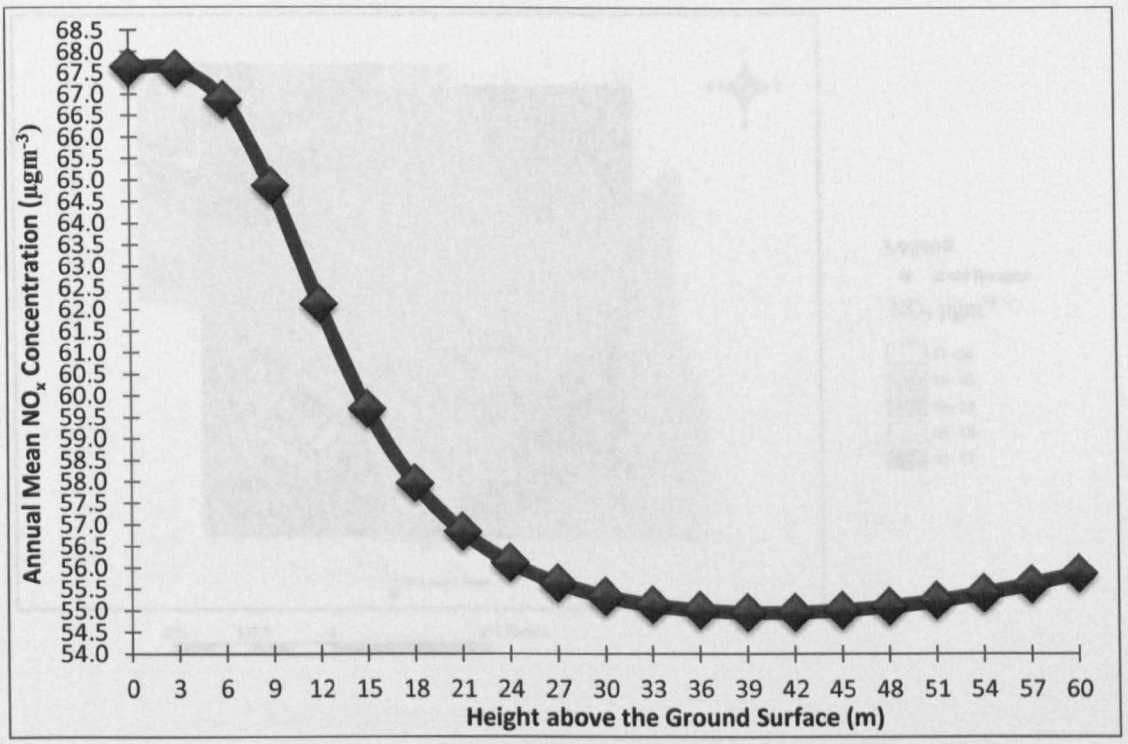

Figure 6.14 NO_X Decay with Height at the AQMS

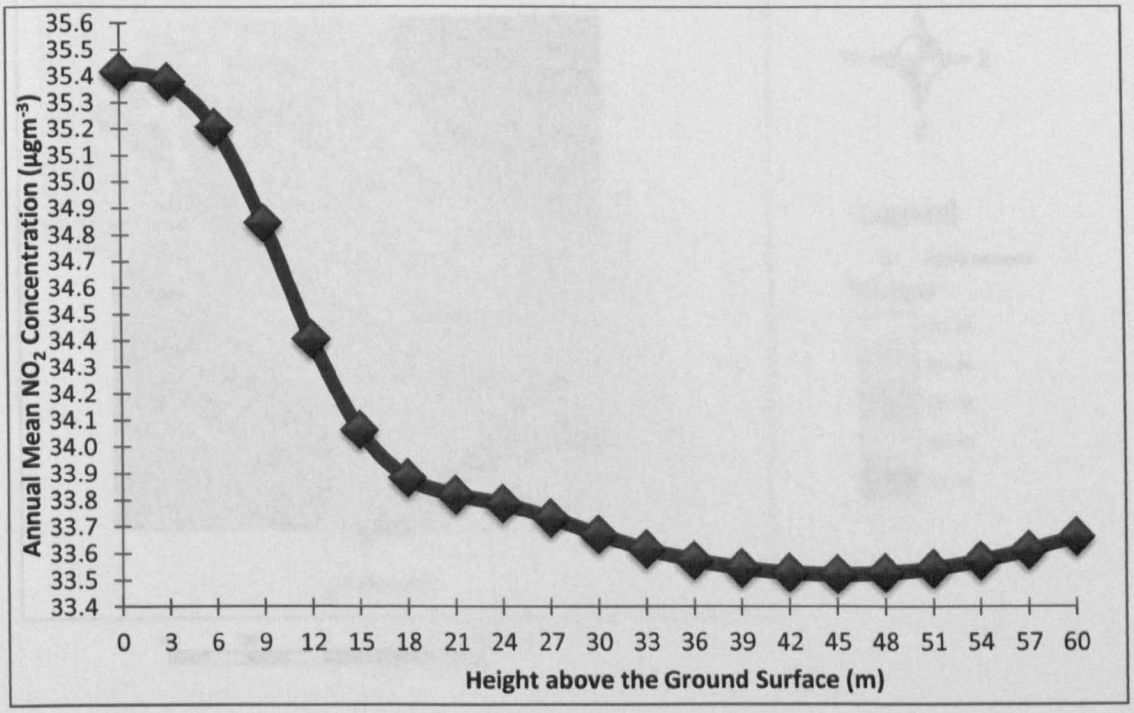

Figure 6.15 NO_2 Decay with Height at the AQMS

Figure 6.16 Contour Map of 2006 Ground-level Annual Mean NO_2 Concentrations in the Dunkirk AQMA

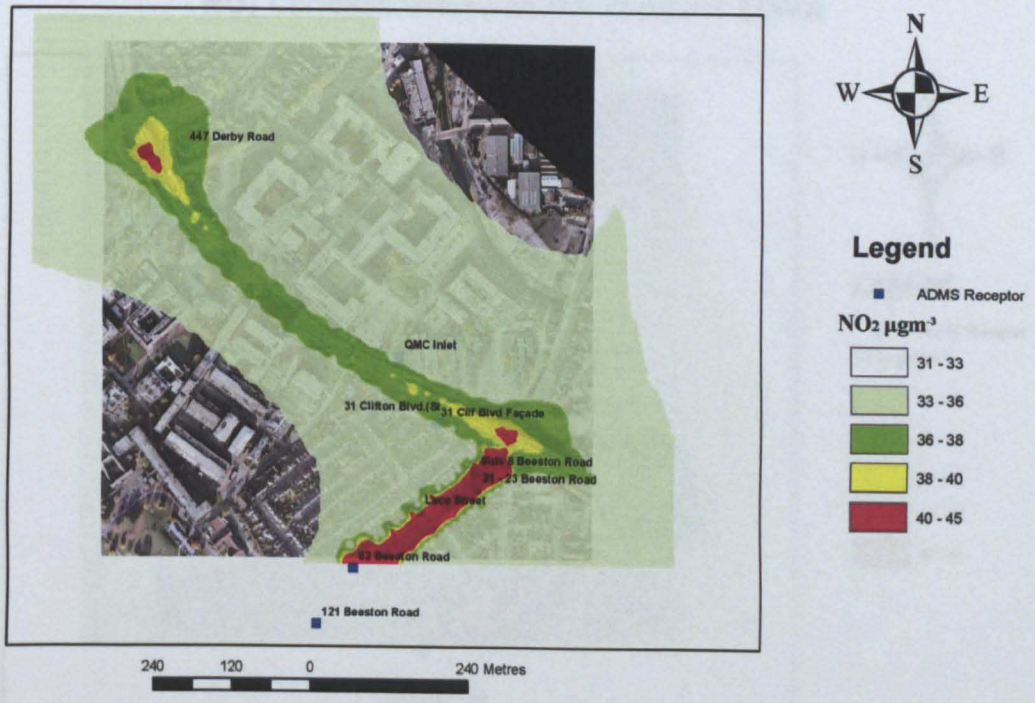

Figure 6.17 Contour Map of 2006 6 metres-height Annual Mean NO_2 Concentrations in the Dunkirk AQMA

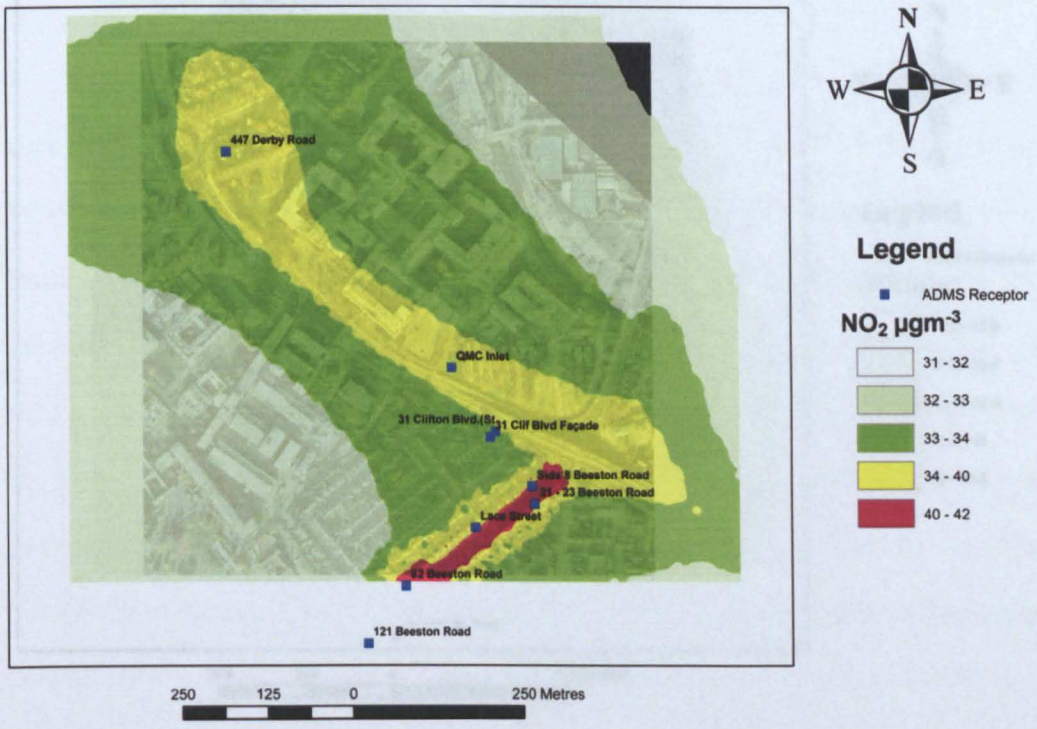

Figure 6.18 Contour Map of 2006 12 metres-height Annual Mean NO_2 Concentrations in the Dunkirk AQMA

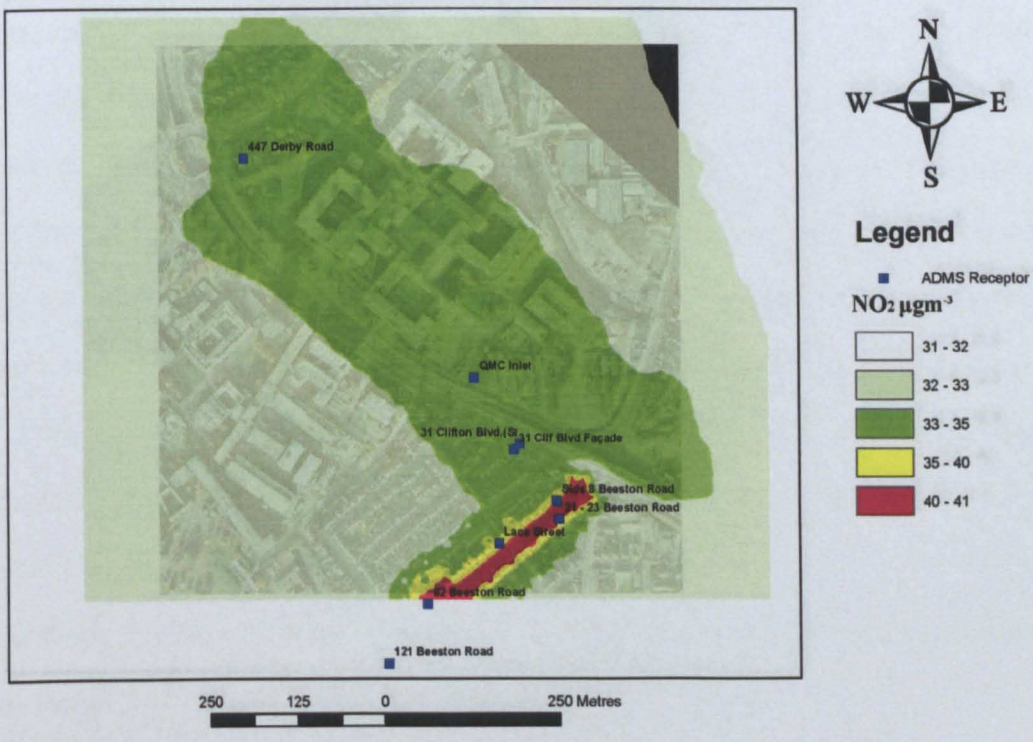

Figure 6.19 Contour Map of 2006 18 metres-height Annual Mean NO_2 Concentrations in the Dunkirk AQMA

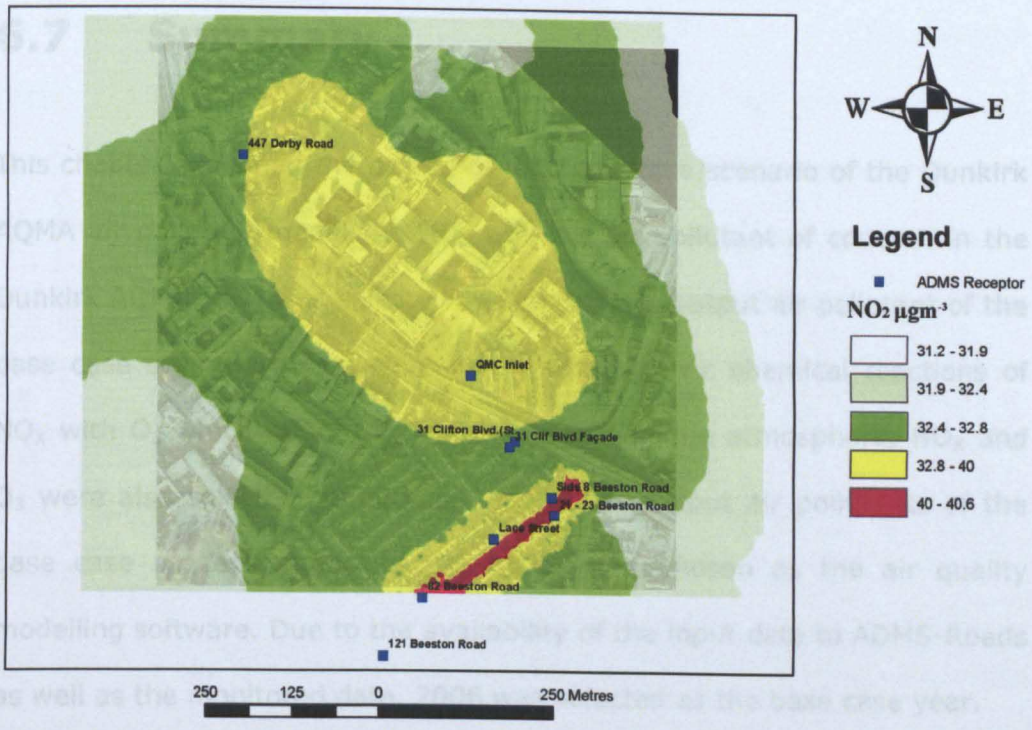

Figure 6.20 Contour Map of 2006 24 metres-height Annual Mean NO_2 Concentrations in the Dunkirk AQMA

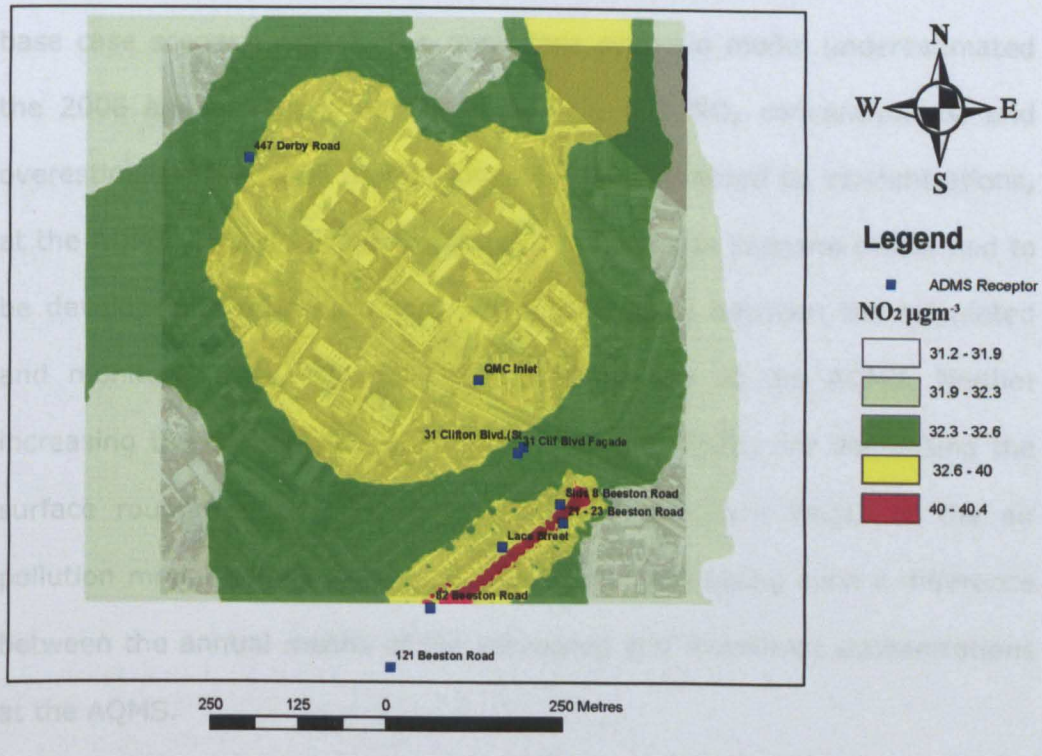

Figure 6.21 Contour Map of 2006 30 metres-height Annual Mean NO_2 Concentrations in the Dunkirk AQMA

6.7 Summary

This chapter explained the design of the base case scenario of the Dunkirk AQMA air pollution model. As NO_2 was the air pollutant of concern in the Dunkirk AQMA, NO_2 was selected as the primary output air pollutant of the base case scenario model. Due to the atmospheric chemical reactions of NO_X with O_3 which affect NO_2 concentrations in the atmosphere, NO_X and O_3 were also selected, in addition to NO_2, as output air pollutants of the base case scenario model. ADMS-Roads was chosen as the air quality modelling software. Due to the availability of the input data to ADMS-Roads as well as the monitored data, 2006 was selected as the base case year.

2006 air quality monitoring data from the AQMS located in the Dunkirk AQMA were obtained from Nottingham City Council for the validation of the base case scenario model. The base case scenario model underestimated the 2006 annual means of monitored NO_2 and NO_X concentrations, and overestimated the 2006 annual mean of the monitored O_3 concentrations, at the AQMS. Therefore, the design of the base case scenario model had to be developed in order to minimise the difference between the calculated and monitored NO_2, NO_X and O_3 concentrations at the AQMS. Neither increasing the primary NO_2 emissions from the traffic, nor decreasing the surface roughness and the minimum Monin-Obukhov length of the air pollution model output area, was effective in minimising such a difference between the annual means of the calculated and monitored concentrations at the AQMS.

Amending, by trial and error, the rural background concentrations of the base case scenario model, to account for poorly-defined or diffused urban emissions in the Dunkirk AQMA, effectively minimised the difference between the annual means of calculated and monitored NO_2, NO_X and O_3

concentrations at the AQMS, as shown in Table 6.1. In this research project, this was called the macro-calibration of the background concentrations of the base case scenario model. The comparison between the annual means of calculated and monitored air pollution concentrations was called, in this research project, the macro-validation of the base case scenario model. The results of the trial and error approach were used to derive Equations (6.1), (6.2) and (6.3) for the macro-calibration of NO_2, NO_X and O_3 background concentrations of a base case scenario model, without the need for the trial and error approach.

The RMSE, r and the slope of the regression best fit line through the origin were selected for the comparison of the two one-dimensional arrays of the 2006 hourly calculated and monitored NO_2 concentrations at the AQMS. This was called, in this research project, the micro-validation of the base case scenario. Using the macro-calibrated background concentrations only slightly improved the micro-validation results of the base case scenario model as shown in Figure 6.6. Therefore, it was decided to calibrate the NO_2, NO_X and O_3 background concentrations on an hourly basis. This was called, in this research project, the micro-calibration of the rural background concentrations of the base case scenario model.

The above macro-calibration equations were evolved to derive Equations (6.8), (6.9) and (6.10) for the micro-calibration of the NO_2, NO_X and O_3 background concentrations of the base case scenario model, based on the results of the macro-calibration analysis. Using the micro-calibrated background concentrations not only improved the macro-validation results, as shown in Table 6.2, but also significantly improved the micro-validation results, as shown in Figure 6.8. Therefore, it was decided to use these micro-calibrated background concentrations in the Dunkirk AQMA base

case scenario model. The inclusion of the traffic profiles in the base case scenario model could further improve the micro-validation by reducing the RMSE between the calculated and monitored hourly NO_2 concentrations by 28.4%.

The air quality predictions of the Dunkirk AQMA base case scenario model with rural background concentrations and a grid air pollution source in ADMS-Urban were compared to the air quality predictions of the Dunkirk AQMA base case scenario model with only calibrated background concentrations in ADMS-Roads. In terms of macro-validation, comparing Table 6.2 with Table 6.3, the ADMS-Roads model, with the micro-calibrated background concentrations only, was better than the ADMS-Urban model, with rural background concentrations and a grid source. In addition, in terms of micro-validation, comparing Figure 6.10 with Figure 6.8, the ADMS-Roads model, with the micro-calibrated background concentrations only, was much better than the ADMS-Urban model, with rural background concentrations and a grid source. In terms of macro-validation, comparing Table 6.1 (run 23, version 2.3) with Table 6.3, the ADMS-Roads model, this time with macro-calibrated background concentrations only, was better than the ADMS-Urban model, with rural background concentrations and a grid source. However, in terms of the micro-validation, comparing Figure 6.10 with Figure 6.6, the ADMS-Roads model, again with macro-calibrated background concentrations only, was almost as good as the ADMS-Urban model, with rural background concentrations and a grid source. According to both the macro and the micro-validation results as shown in Table 6.3 and Figure 6.11, running the ADMS-Urban model with the trajectory model of CRS made no difference to the above comparison between the ADMS-Roads model, with either macro or micro-calibrated background

concentrations, and the ADMS-Urban model, with rural background concentrations and a grid source.

Running the ADMS-Urban model of the base case scenario, with rural background concentrations, a grid source and either CRS or the trajectory model of CRS, required 44 minutes for the calculation of NO_2, NO_X and O_3 concentrations at a single output receptor point. In comparison, running the ADMS-Roads model of the base case scenario, with either macro-calibrated or micro-calibrated background concentrations, required 9 minutes for the calculation of NO_2, NO_X and O_3 concentrations at a single output receptor point. Therefore, for an output grid of 1935 receptor points repeated at six different heights above the ground surface, using ADMS-Roads with the background concentrations calibration technique developed in this chapter, could save up to 9.41 months of the model runtime.

Further NO_2 monitoring data, from diffusion tubes located in the Dunkirk AQMA in 2006, was obtained from the Pollution Control Section in Nottingham City Council. The Pollution Control Section also provided an estimate for the 2006 annual mean NO_2 concentration at the Lace Street continuous monitor. Macro-validation of the base case scenario model, with the macro-calibrated background concentrations, was attempted. The calculated annual mean NO_2 concentration agreed well with the monitored annual mean NO_2 concentrations from the diffusion tubes, except on Beeston Road. The Beeston Road diffusion tubes appeared to indicate that the annual mean NO_2 concentration was underestimated in the Beeston Road area, and the city council's estimate of the 2006 annual mean NO_2 concentration at the Lace Street continuous monitor indicated the amount of this underestimation.

The reconfiguration of Beeston Road in ADMS-Roads from a non-canyon road to a street canyon with a 6 metre canyon height did not effectively increase the calculated annual mean NO_2 concentrations at the diffusion tube receptor points on Beeston Road. Although altering the traffic flow and/or speed for Beeston Road and/or Abbey Street effectively increased the calculated annual mean NO_2 concentration at the Lace Street continuous monitor, it worsened the macro-validation at the AQMS, as shown in Table 6.4. Moreover, such an alteration of the Beeston Road and Abbey Street traffic flows and speeds added both Abbey Street, and a wide area around Beeston Road and Abbey Street, to the declared NO_2 Dunkirk AQMA as shown in Figure 6.13. This was confirmed as being incorrect by the Pollution Control Section in Nottingham City Council. Therefore, a VBA computer program was written by the author in MS Excel for the application of a multiplicative factor to the calculated annual mean NO_2 concentrations at the receptor points located inside the Beeston Road area only. The GIS functionality was used to input the irregular boundary of the Beeston Road area to the VBA computer program.

An intelligent grid of output receptor points was selected for the base case scenario model of the Dunkirk AQMA. The regular part of this intelligent grid had a size of 31×31 output receptor points for the balanced optimisation of both the model runtime and the output data resolution. A *.igp file was compiled to disable the automatic generation of the intelligent grid points whose locations were dependent upon the relative emissions from each pair of intersecting roads. This facilitated the direct comparison between the model results of different traffic emission scenarios before and after the implementation of NET Phase 2. A 30 metre height limit for the output NO_2 plume was selected based on the decay of the annual mean NO_2 concentrations with height at the AQMS as shown in

Figure 6.15. A height step of 6 metres was selected for the vertically successive intelligent grid output receptor points of the Dunkirk AQMA base case scenario model.

The calibration process effectively improved the accuracy of the annual mean and hourly NO_2 predictions and significantly reduced the runtime of the base case scenario model. This should improve the reliability of the air quality modelling of future scenarios based on the base case scenario. The grid design of the base case scenario model was suitable for capturing the rapidly changing NO_2 concentrations' gradient close to the principal roads in the Dunkirk AQMA. The height limit and height step were suitable for capturing the vertical dispersion of NO_2 concentrations above the ground surface, which is needed for the 3D visualisation of NO_2 dispersion in the Dunkirk AQMA 3D city model as discussed in Chapter 7.

Chapter 7

Development of the Technical Design of the 3D Air Pollution Dispersion Interface

7.1 Introduction

The purpose of this chapter is to give details of the development of the design of the 3D air pollution dispersion interface of this research decision-support system. As explained in Section 4.3, the proposed implementation of NET Phase 2 through the Dunkirk AQMA is the transport scheme used for all the initial development work in this research project. Hence, following on from Chapters 5 and 6, in this chapter the case study geographical focus continues to be the Dunkirk AQMA.

The application of 3D city models contributes to building a decision-support system for air quality-related transport planning. The 3D city model should help improve the visualisation and understanding of the air pollution dispersion in the urban environment. Being able to visualise the air quality in a 3D georeferenced virtual environment, both before and after the implementation of urban transport schemes, may help all those involved in, or potentially affected by, planning decisions, such as planners, decision-makers, local residents, environmental campaigners, etc, be they relevant professional experts or not, in all sorts of meeting contexts, such as in planning offices, public consultations, public inquiries, etc.

The link between the 3D city models and GIS databases provides a quickly created, and easily editable, 3D virtual environment to reflect automatically different transport planning options. Then, integrating the air pollution dispersion modelling may enable the air quality impacts of proposed transport schemes to be interactively visualised, demonstrated and evaluated.

Appleton et al.(2002) used 3D visual presentations developed from GIS databases to visualise the potential rural landscape after proposed future developments. These 3D visual presentations have been proven to be an effective means to convey future planning consequences to non-expert audiences, particularly those with no experience of GIS or mapping. Therefore, this research endeavoured to visualise the air pollution dispersion in 3D virtual environments, which are more understandable than the sort of 2D maps that are often used in environmental assessments.

The current convention with 2D maps is to use only a somewhat limited spectrum of colours to display the air pollution concentration values at a given height. Therefore, as the height changes, the values of the concentration levels to be displayed change; rather than changing the colour spectrum, the convention is to adjust the ranges of concentration values that the colours correspond to, which is potentially visually misleading. This problem is illustrated well by Figures 6.16 to 6.21. The colours alone (with a red, yellow, green hierarchy) appear to suggest that, for example, above 18 metres, the pollution levels increase (due to the yellow area increasing from Figure 6.19 to Figure 6.20, and then to Figure 6.21), though this is not the case when the legend detail is taken fully in account. The visualisation of air pollution dispersion in a 3D virtual environment may enable the viewer to recognise intuitively the change in the pollution concentrations with height in one view. Therefore, the

visualisation of air pollution dispersion in a 3D virtual environment may have the potential to encourage public participation in environmental decision-making. With a better understanding of the detrimental effect of traffic related pollution the public may be persuaded to take action.

7.2 Basic Considerations in 3D Interface Development

When developing the design of a 3D air pollution dispersion interface, it is important to consider both the concept of Level of Details (LOD) regarding the 3D city model components and the relevant HCI principles and guidelines, which are introduced in this section, and then are used in Section 7.4 and Section 7.5 to develop the design of the Dunkirk AQMA 3D air pollution dispersion interface.

Taking a fully user-centred approach is another consideration in the development of the 3D air pollution dispersion interface, so as to ensure that it meets its potential users' needs. As an approximation to such an ideal approach, ad-hoc demonstrations were made in a 3D virtual reality environment to the likes of supervisors (intended to represent transport planners), and to some students (intended to represent ordinary people). The feedback obtained during, and after, these demonstrations was taken into account in the development of the 3D air pollution dispersion interface from one stage to another, as presented in Section 7.5. In this research project, formal user consultation exercises were not undertaken as part of the development of the 3D air pollution dispersion interface, due to the availability of other research opportunities: firstly to test the transferability of the interface to other transport schemes in a different geographical location to the Dunkirk AQMA, as presented in Chapter 9, and secondly to

validate the future air quality predictions using yet another transport scheme, as presented in Chapter 10. However, with regard to future research, it is recommended in Section 11.2.3 to undertake more formal consultation exercises to contribute to further development of the 3D air pollution dispersion interface.

7.2.1 Level of Details of 3D City Model Components

The 3D city model is a very important part of the 3D geo-virtual environment (Döllner and Buchholz, 2005). 3D city models increase the accessibility of visualisation, navigation, analysis and management of geo-referenced datasets. Other parts of a virtual environment may include features and control data targeted at specific training and/or customer needs (Bildstein, 2005).

The main components of 3D city models are the ground terrain, static and dynamic 3D features, such as buildings and traffic, and photo-textures of building facades. However, buildings, traffic and vegetation are the most important contents of 3D city models when it comes to location recognition and orientation by the viewer (Zhu et al., 2005).

Bildstein (2005) introduced five LODs of 3D city models. LOD0 represents regional models consisting of 2.5D digital terrain model with aerial texture. LOD1 describes a city, or just a district of a city, and typically includes a simplified 3D representation of each building by extruding the building's ground plan to an average height without roof structure. LOD2 represents each textured 3D building with a roof structure, and differentiated heights within each building, in a city or a district. LOD3 renders the exterior architectural details of 3D buildings. Finally, LOD4 represents the interior

architectural details of 3D structures, such as room features, doors and staircases, and is primarily for a walk-through navigation mode.

The use of 3D city models determines the appropriate LOD of their individual components (Bildstein, 2005). In the same virtual scene, different components of the 3D city model may have different LODs according to the relative degree of interactivity of each component. Furthermore, the LOD of a component may depend on the context in which an end-user views that component. In other words, components which end-users of the application are going to interact with, but just to recognise them in a basic way in order to navigate smoothly through the virtual scene, can therefore be simplified or generalised, and so have a relatively low LOD. On the other hand, for a component of a direct use, end-users may need to be able to recognise more details of the component more realistically, in which case certain components may need to have a relatively high LOD.

Amongst low LOD components of the 3D city model, parts of the 3D city model which are hardly visible while navigating the virtual scene can be simplified further. However, prominent structures in the 3D city model, such as landmarks and long visible or eye-catching objects, should be of a relatively higher LOD (Bildstein, 2005).

7.2.2 Human Computer Interaction

The initial step towards the design of a good interface is to define the interface users' goals. The generic usage goal of a good interface is to display information in its most accessible, useful, intelligible and pleasing form (Sears and Jacko, 2008).

A number of universal principles of visual communication and organisation have been defined to design a good interface (Sears and Jacko, 2008). Firstly, asymmetry has to be provided to maintain contrast between interface elements such as weight, form and colour. That creates visual tension and drama, and so helps the graphics to reinforce the message.

Secondly, simplicity has to be maintained to offer the user an unambiguous, and easily understood, interface. Simplicity involves avoiding unnecessary decoration and not having too large number of components in the interface; less is more useful and understandable. That can be attained by assigning the appropriate LOD to each component and including only essential components in the interface.

The most important principle is that there are no rules to design a good interface, just guidelines, as the interface is context sensitive. Therefore, Sears and Jacko (2008) have introduced a number of guidelines to design a good interface. Firstly, visuals should help the observer understand relationships between interface components. Secondly, visuals should reinforce the message, by not only conveying the true message, but also by clarifying the message and making it more intelligible.

Colour is another important element to be customised correctly in order to design a good interface. It is the strongest emotional element in the visual communication (Sears and Jacko, 2008), and should be an integral part of the design programme used to reinforce the meaning, not just to decorate the view. Consequently, for a good interface design, using fewer colours is more useful and understandable.

The use of a colour scheme, composed of compatible colours, reinforces the visualisation of hierarchical information. Compatible colours are those of a monochromatic colour scheme or by using differing intensities of the

same hue (Sears and Jacko, 2008). Complementary colours, which are most opposite to each other in the colour scheme, should be used with extreme situations i.e. to signify highest and lowest bands of hierarchical data.

7.3 Design of Dunkirk AQMA 3D City Model

In order to acquire the ortho-image, a georeferenced raster coverage layer (Linder, 2006), and the DTM of the Dunkirk AQMA study area, Leica Photogrammetry Suite (LPS) software was used. LPS is a comprehensive digital photogrammetry package that defines the mathematical relationships between the photos in the aerial image block, the sensor that captured those photos at the time of exposure, and the ground (Leica, 2009). Therefore, LPS version 9.1 was used to integrate the Dunkirk AQMA coverage of stereoscopic aerial photographs, in order to build the ortho-image of the Dunkirk AQMA and then to extract the DTM of that area. Figure 7.1 depicts the ortho-image of the Dunkirk AQMA.

The main 3D features, which existed in the overlap zones of the Dunkirk AQMA coverage of aerial photographs, were extracted by Stereo Analyst for ERDAS IMAGINE 9.1. Stereo Analyst for ERDAS IMAGINE transformed the manually digitised 2D features from the block of aerial photographs into real-world dimensions by collecting 3D geographic information directly from imagery. The extracted features included the main 3D buildings in the study area, the footbridge over the A52 Clifton Boulevard and the Derby Road roundabout as shown in Figure 7.2.

Figure 7.1 Ortho-image of Dunkirk AQMA

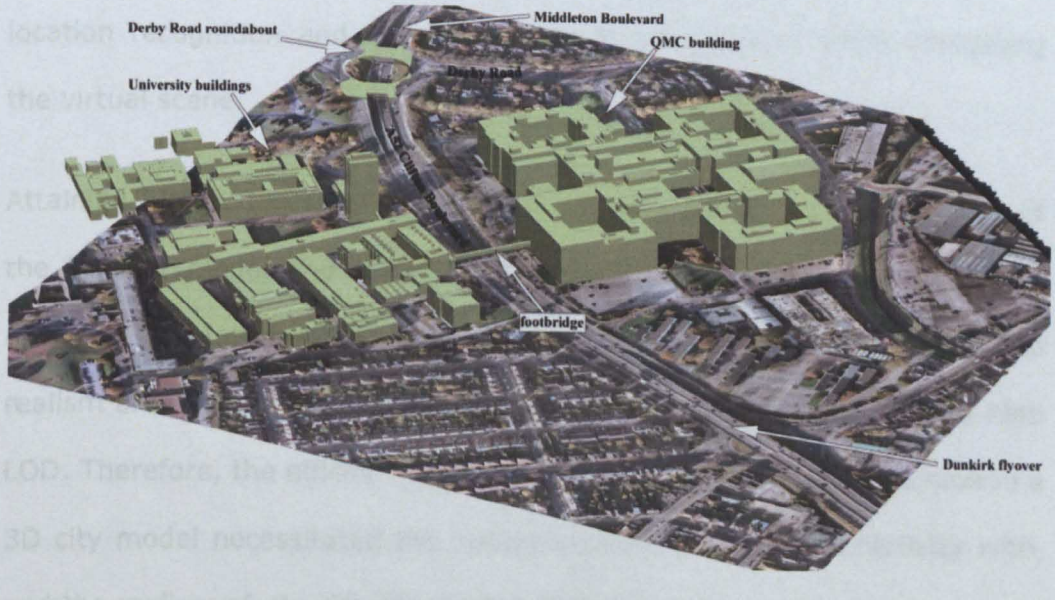

Figure 7.2 Initial Design of the Dunkirk AQMA 3D City Model

7.4 Further Development of the Design of the Dunkirk AQMA 3D City Model

In order to develop effective 3D visualisation of air pollution, a fundamental aspect of this research project was the deep integration of an air pollution dispersion model and 3D digital city models. Output data of the air pollution model of the Dunkirk AQMA was fused into the Dunkirk AQMA 3D city model to attain a 3D representation of the output air pollution data. The design of the Dunkirk AQMA 3D city model was developed to meet the LOD requirements to achieve an effective 3D visualisation of the air pollution dispersion in the Dunkirk AQMA.

Two main criteria were defined to develop the design of the Dunkirk AQMA 3D city model. Firstly, a good interface should provide the user with flexible access to the content according to the user's requirements (Sears and Jacko, 2008). Therefore, the first criterion was to maintain a smooth navigation in the virtual scene, and hence to ensure having a good degree of interactivity in the built-up virtual world. Secondly, a good level of location recognition and orientation should be provided while navigating the virtual scene.

Attaining a high degree of interactivity required simplifying the features of the 3D city model and assigning them a low LOD. On the other hand, achieving a high level of location recognition and orientation required realism and recognisable details, and so 3D city model's features of a high LOD. Therefore, the efficient visualisation of the air pollution dispersion in a 3D city model necessitated the optimisation of both the interactivity with, and the realism of, the 3D city model's features.

As far as the ground-level air pollution was concerned, adding many buildings to the virtual scene would obscure the visualisation of the air pollution underneath. That was because the air pollution dispersion modelling package used in this research, ADMS-Roads, models air pollution dispersion through, not only around, buildings.

In fact, the majority of commercially available traffic-induced air pollution modelling packages models air pollution dispersion through, not only around, buildings. Hence, the identified design criteria to develop the 3D air pollution dispersion interface of this research can be applied to integrate a broad range of commercially available air pollution models with 3D city models. Therefore, it was decided not to extract any more existing features than were initially extracted, as shown in Figure 7.2.

However, as far as location recognition and orientation was concerned, the 3D buildings in Figure 7.2 were assigned a high LOD to compensate for the absence of other 3D buildings in the study area. As far as the exposure to the air pollution was concerned, the emphasis was given to the outdoors environment. Therefore, LOD4 was deemed unsuitable to represent the 3D buildings of the study area. Instead, a LOD somewhere between LOD2 and LOD3, according to data availability, was selected to represent these buildings in the 3D city model.

The application of a photo-realistic texture to the 3D buildings of the study area overburdened the virtual scene. Consequently, the draping of such a texture prevented smooth navigation in the virtual environment. Therefore, it was decided to take the texture off the facades of the study area 3D buildings, so that a good degree of interactivity in the created virtual world could be maintained. To compensate for the absence of photo-realistic textures, a dynamic 3D traffic layer was added to the 3D city model. The

traffic layer enhanced the location recognition and orientation while navigating the virtual scene, which also compensated further for the absence of other 3D buildings in the study area.

The traffic layer was composed of 3D vehicle objects associated to traffic paths. The traffic paths were 3D polylines digitised over the DTM of the study area by using the 3D Analyst extension of ArcGIS. This digitisation enabled the X, Y and Z coordinates of the vertices of each traffic path to be derived from the DTM of the study area. Then, every 3D vehicle object moved along its associated traffic path that followed the terrain surface to give a realistic traffic animation in the 3D city model. Each 3D vehicle object was modelled as a 3D point shape file, with its Z coordinate interpolated from the study area DTM by the 3D Analyst at the start point of the associated traffic path. Then, a 3D symbology was assigned to every 3D point shape file to give the 3D point its realistic vehicular shape.

The virtual traffic animation was looped so that the virtual vehicles automatically continued to animate throughout the entire observation time of the 3D city model. One challenge was to prevent the virtual vehicles that followed the same traffic path from appearing to interfere with each other during the animation. This challenge was resolved by changing the start animation point of, allocating a different traffic path for, and changing the end animation time of, every virtual vehicle.

Another challenge was to stop the virtual vehicles that followed different traffic paths from colliding with each other during the animation. This challenge was overcome by assigning different animation speeds to virtual vehicles that moved along different traffic paths. Figure 7.3 shows the second design stage of the Dunkirk AQMA 3D city model with the virtual traffic included.

Figure 7.3 Second Design Stage of the Dunkirk AQMA 3D City Model

The modelling of the dynamic 3D traffic layer started in ArcGIS. However, a further challenge arose when moving the virtual traffic over the Derby Road roundabout. The associated traffic path was interpolated from the study area DTM, and hence it followed the terrain surface not the Derby Road roundabout surface. Consequently, the virtual traffic moved underneath the Derby Road roundabout, not over it as it should in reality! With no option in ArcGIS to digitise a traffic path over the Derby Road roundabout feature, the Derby Road roundabout object and the erroneous traffic path were exported to AutoCAD Civil 3D. In AutoCAD Civil 3D, the erroneous traffic path was fixed to follow the Derby Road roundabout surface, not the terrain surface underneath.

The inclusion of the Dunkirk flyover in the 3D city model, as discussed in the following paragraphs, and the need to move the virtual traffic over the Dunkirk flyover – another example of the road surface being above the terrain surface – led to changing the majority of the 3D traffic modelling from ArcGIS to AutoCAD Civil 3D. Macros in AutoCAD Civil 3D, VBA user-written computer programming codes which extend the functionality of AutoCAD, helped to semi-automate the modelling, editing and optimisation

of the 3D traffic layer, further justifying the change of the 3D virtual traffic modelling from ArcGIS to AutoCAD Civil 3D.

As far as the traffic-induced air pollution was concerned, the number of 3D vehicles of the dynamic 3D traffic layer was amended so that it was proportional to the amount of displayed air pollution. Consequently, the observer could intuitively understand the relationship between moving traffic and the traffic-induced air pollution.

To further improve the animation realism of the dynamic 3D virtual traffic, the Dunkirk flyover was modelled and added to the 3D city model. Then the virtual traffic was animated over the Dunkirk flyover. As the extraction of a realistic 3D object for the Dunkirk flyover from the study area block of aerial photographs was very difficult, if not impossible, AutoCAD Civil 3D was used to model the flyover.

A 3D model of the Dunkirk flyover was accurately and quickly modelled in CAD by using 3D solid objects, the basic 3D CAD shapes which can be aggregated in different combinations to build any complex 3D feature, on many layers for optimisation. The number of layers in CAD was determined according to the number of potential LODs which the flyover might take in the virtual scene. Then, the 3D CAD object of the flyover was successfully georeferenced and integrated with the 3D city model of the Dunkirk AQMA.

A dynamic link was maintained between the Dunkirk flyover in the 3D city model and the original CAD model of the flyover. The flyover was optimised by turning on or off a layer in CAD which altered the LOD of the flyover in the virtual scene through the dynamic link between the flyover CAD and virtual objects. The optimisation of the flyover CAD model continued until the optimum LOD of the virtual flyover was determined. The optimum LOD

was that which achieved a good degree of realism of the virtual flyover, while not overburdening the 3D virtual scene.

The next challenge was that the Derby Road roundabout was extracted from the study area block of aerial photographs without its ramps for traffic moving between the Derby Road roundabout and Clifton/Middleton Boulevard. The Derby Road roundabout ramps are features which gradually rise from one surface level to another. The extraction of such features from aerial photographs was found to be very difficult, if not impossible, to achieve.

The lack of Derby Road roundabout ramps caused the virtual traffic to fly unrealistically, for example when moved from the level of the bottom of a ramp to the level of the top of that ramp. Therefore, the Derby Road roundabout was remodelled in CAD and was displayed in the Dunkirk AQMA 3D city model with the inclusion of the roundabout ramps. Figure 7.4 shows the third design stage of the Dunkirk AQMA 3D city model after the inclusion of the Dunkirk flyover and the Derby Road roundabout ramps.

Figure 7.4 Third Design Stage of the Dunkirk AQMA 3D City Model

Yet another challenge was to model in the Dunkirk AQMA 3D city model the additional features corresponding to the implementation of NET Phase 2. The modelling process comprised two steps. The first step was to do with the modelling of the 3D viaduct carrying the tram line over the QMC site and Clifton Boulevard. The second step was to do with creating the path lines of the tram over the viaduct, adding the 3D tram objects to the virtual scene, and finally animating the 3D tram objects along the created path lines.

In the first step, the challenge was that there is no existing viaduct constructed in the Dunkirk AQMA. Therefore, there were no means of extracting this future feature from the study area block of aerial photographs. Initially, there was the issue of the exact location of the future viaduct in the 3D city model. To resolve this issue, hard copies of some proposed landscape and cross-section plans for the NET Phase 2 Chilwell via QMC and Beeston route were obtained from the NET Project Team in Nottingham City Council, as shown in Figure 7.5 and Figure 7.6.

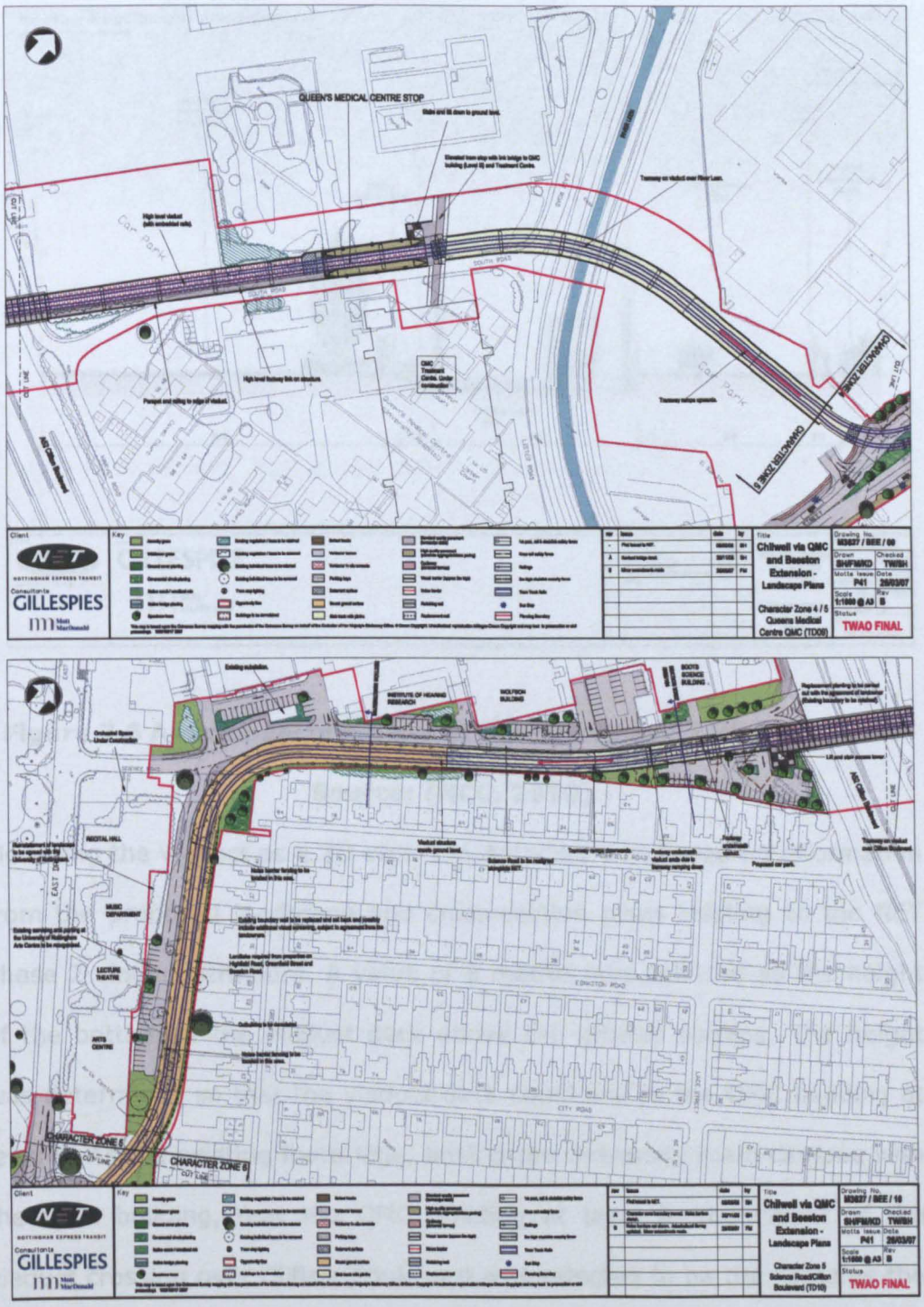

Figure 7.5 Landscape Plans of the NET Phase 2 Viaduct in the Dunkirk AQMA
Source: (NCC, 2010)

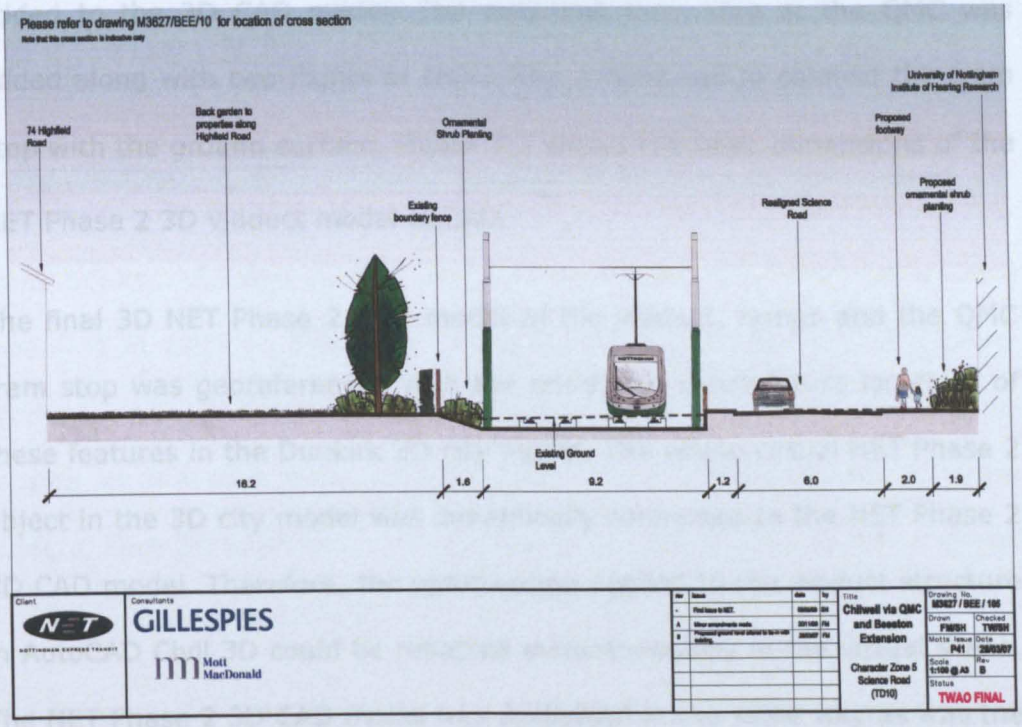

Figure 7.6 A cross-section view of the NET Phase 2 Viaduct in the Dunkirk AQMA
Source: (NCC, 2010)

Modelling the viaduct as a 3D object in AutoCAD was based on information from the proposed landscape and cross-section plans relating to the NET Phase 2 viaduct structure. A value of 6 metres was selected as the height of the bottom of the viaduct deck above the ground surface. The height was determined so that the viaduct deck could link to the QMC building at level B. As the existing footbridge, linking the University main campus with the QMC building, met the QMC building at level B, the height of the viaduct crossing over Clifton Boulevard was selected to be the same as the height of the footbridge, thus ensuring sufficient clearance above Clifton Boulevard. A value of one metre was used for the depth of the viaduct deck. The width of the viaduct was obtained from the plans, as shown in Figure 7.6, as 9.2 metres.

A series of columns to support the viaduct deck was added to the 3D viaduct model in CAD. Two ramps at the start and end of the viaduct were

added to the 3D CAD model. The proposed tram stop at the QMC was added along with two flights of stairs with a hand rail to connect the tram stop with the ground surface. Figure 7.7 shows the basic dimensions of the NET Phase 2 3D viaduct model in CAD.

The final 3D NET Phase 2 CAD model of the viaduct, ramps and the QMC tram stop was georeferenced with the envisaged exact future locations of these features in the Dunkirk 3D city model. The whole virtual NET Phase 2 object in the 3D city model was dynamically connected to the NET Phase 2 3D CAD model. Therefore, the optimisation applied to the viaduct structure in AutoCAD Civil 3D could be reflected instantaneously in the virtual scene. The NET Phase 2 3D CAD model was optimised in the same way as was the Dunkirk flyover CAD model described earlier in this section.

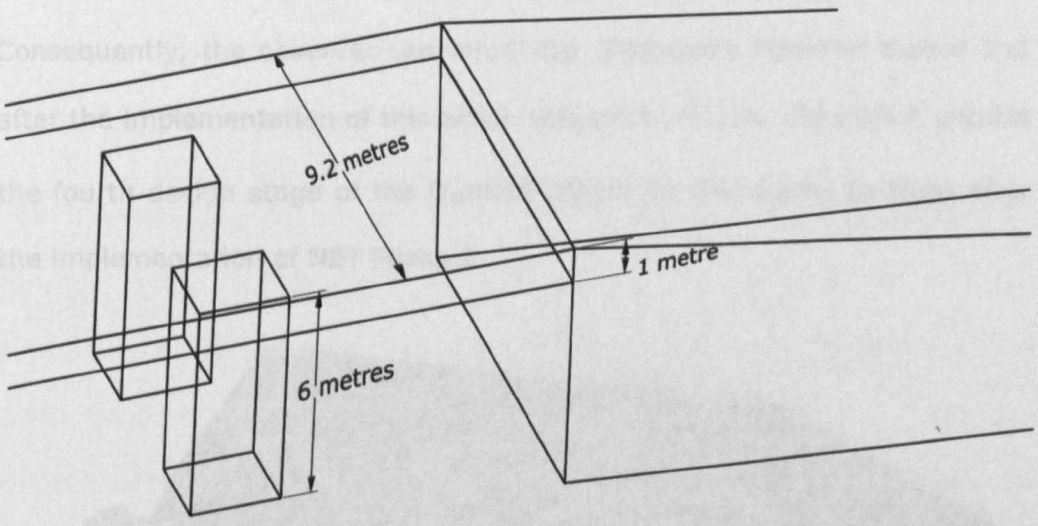

Figure 7.7 Basic Dimensions of the NET Phase 2 Viaduct Model in CAD

The whole virtual NET Phase 2 object was assigned a different colour to that of other features in the virtual scene. That was primarily to maintain asymmetry and to create a contrast between the viaduct as a future (currently non-existent) structure and other present structures in the Dunkirk AQMA study area.

In the second step of modelling the additional features corresponding to the implementation of NET Phase 2 in the Dunkirk AQMA 3D city model, dynamic 3D tram objects were added to the virtual scene and animated over the whole NET Phase 2 feature. Two path lines were created for two tram objects moving in two opposite directions. The path lines were modelled in CAD so that they followed the top surface of the viaduct structure, not the terrain surface underneath. Two 3D point shapes were located at the start point of each path line to represent the 3D tram objects. Each 3D point was animated along its associated path line and was assigned 3D symbology to give the point its true 3D tram shape.

The dynamic 3D tram objects enhanced the visualisation of the Dunkirk AQMA study area after the implementation of NET Phase 2 and further maintained asymmetry between present and future conditions. Consequently, the observer can intuitively distinguish between before and after the implementation of this urban transport scheme. Figure 7.8 depicts the fourth design stage of the Dunkirk AQMA 3D city model to show after the implementation of NET Phase 2.

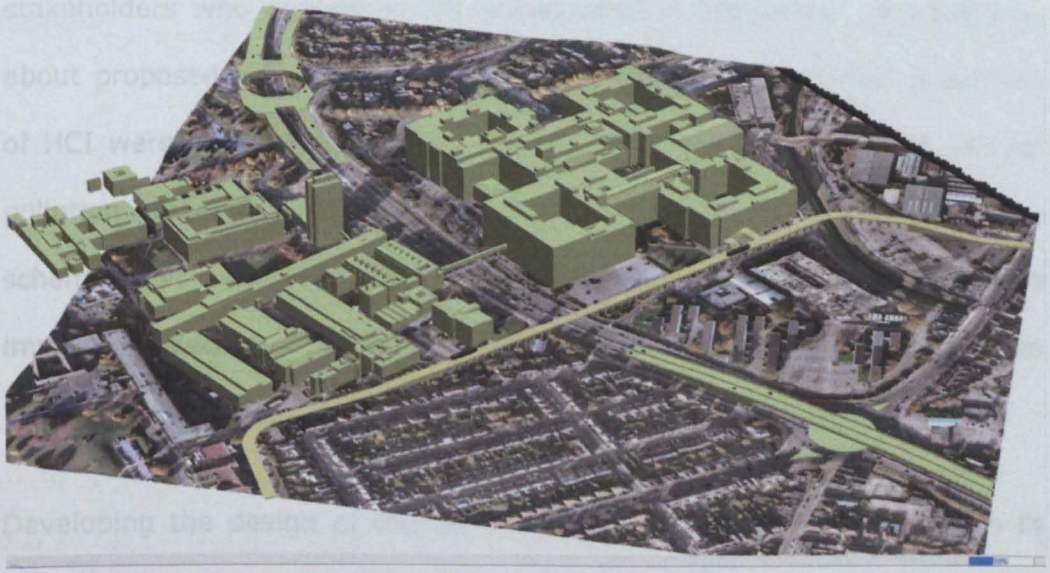

Figure 7.8 Fourth Design Stage of the Dunkirk AQMA 3D City Model

7.5 Development of the Design of the 3D Air Pollution Dispersion Interface

Initially, in Section 1.1, the aim of a good 3D air pollution dispersion interface was defined in this research project to be to display the output data of an air pollution dispersion model at and above the ground surface in one virtual scene. This single virtual scene should be accessible and intelligible enough so that the observer can intuitively recognise and easily understand the air quality impacts, at and above the ground surface, of the implementation of identified urban transport schemes. Achieving this requires the design of an informative, and in meanwhile a simple, interface to visualise the air pollution dispersion, at and above the ground surface, before and after the implementation of urban transport schemes.

The users of the 3D air pollution dispersion interface of this research project could be decision-makers, transport planners and all the stakeholders who constitute the participants in the public consultations about proposed urban transport schemes. Some principles and guidelines of HCI were selected to develop the design of the Dunkirk AQMA 3D air pollution dispersion interface. Contrast, simplicity and using a colour scheme that reinforces the hierarchy of information were the most important selected principles and guidelines of HCI, as discussed in Section 7.2.2.

Developing the design of the 3D air pollution dispersion interface ran in parallel to the development of the design of the Dunkirk AQMA 3D city model. Therefore, the initial design alternatives of the 3D air pollution

dispersion interface did not display the air pollution data in the later design stages of the 3D city model.

The interface design started by using VirtualGIS to display the 3D city model of the Dunkirk AQMA study area as shown in Figure 7.9. However, VirtualGIS could only display the 3D traffic layer in a static way, not in a dynamic way. Additionally, VirtualGIS could not display the air pollution dispersion data in the 3D city model due to some technical limitations. Therefore, it was decided to move on to another software package to visualise the air pollution dispersion in the Dunkirk AQMA 3D city model.

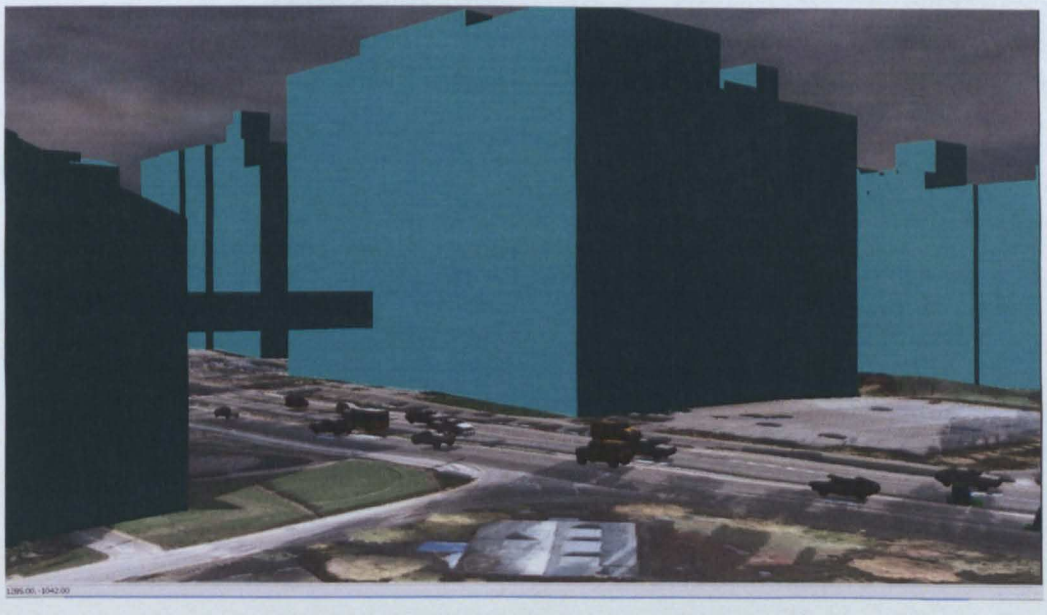

Figure 7.9 VirtualGIS Dunkirk AQMA 3D City Model

3D Analyst of ArcGIS 9.2 was used to display the air pollution dispersion in the Dunkirk AQMA 3D city model. That involved a number of technical challenges to assign the appropriate air pollution concentration to each point of the air pollution model grid with its elevation interpolated from the DTM of the study area. These challenges were resolved through the development of 3D Analyst of ArcGIS 9.2 using visual basic computer programming.

The second interface design displayed a 2D contour map of the ground-level air pollution concentrations. This 2D contour map was draped over the 3D terrain surface of the 3D city model with an offset value of 1 metre between the air pollution contour map and the terrain surface as shown in Figure 7.10. That was to avoid the intersection between the contour map and the terrain surface. Additionally, the terrain surface was assigned a rendering priority less than that of the contour map, so that the contour map was always rendered on the top of the terrain surface.

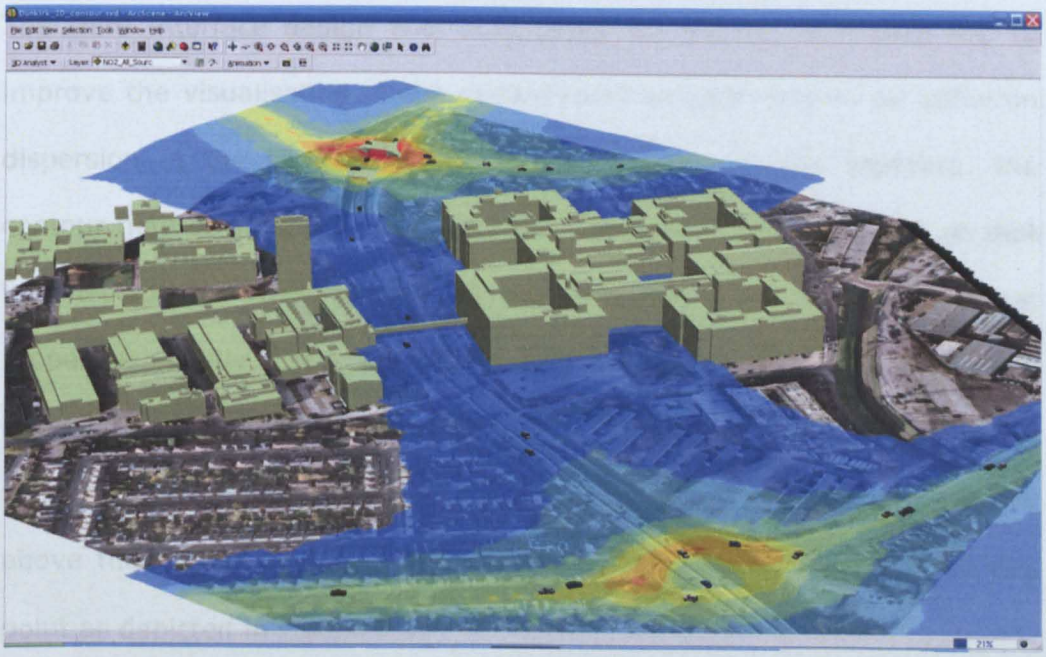

Figure 7.10 2D Contour Map Interface

A colour scheme was attached to the contour map to signify hierarchically the amount of air pollution concentrations. Eight colours were used in the colour scheme. However, after consulting the Pollution Control Section in Nottingham City Council, it was decided that such a number of colours was too many. It is felt that using eight colours to visualise the hierarchy of the air pollution concentrations distracts, rather than impresses, the observer. Therefore, the Pollution Control Section recommended the use of only 4 to 5 colours for visualisation in the contour map of the air pollution dispersion, as presented in Figures 6.16 to 6.21. However this approach becomes

potentially visually misleading when displaying the air pollution concentrations at a number of heights, as shown in Figures 6.16 to 6.21, and as discussed in Section 7.1. Furthermore, this interface did not display the air pollution dispersion data at a number of heights above the ground surface in the same view. So, this interface design did not achieve the visualisation goal of this research project. Consequently, it was decided to move on to another interface design for the air pollution dispersion visualisation in 3D city models.

The third interface design was built using 3D Analyst of ArcGIS 9.2 to improve the visualisation of the ground-level contour map of air pollution dispersion in the Dunkirk AQMA 3D city model. In this interface, the contour map of ground-level air pollution dispersion was displayed so that it reflected the value of the air pollution by combining two different properties. Firstly, the hierarchy of the air pollution concentrations was reflected by assigning a colour scheme to the contour map. Secondly, the value of air pollution at each point was also reflected by assigning a height above the ground surface equal to the air pollution concentration at this point as depicted in Figure 7.11.

Therefore, the surface of the air pollution contour map was not parallel to the ground surface, because the contour map surface was created using the air pollution concentration values rather than the ground level elevations. Therefore, an offset value of 8.5 metres, determined by trial and error, was applied between the contour map surface and the ground surface to avoid the intersection between the two surfaces.

Eight colours were assigned to the colour scheme of the air pollution contour map, although previously this had been confirmed as being too extensive by the Pollution Control Section. The large offset between the air

pollution contour map and the ground surface created the illusion of a spatial shift in the location of the contour map in the perspective viewing projection. Furthermore, in the stereo viewing projection, the ground-level air pollution contour map floated high above the ground surface. This confused the observer by creating the illusion of having the air pollution at such heights above the ground surface whereas, in fact, the displayed air pollution was calculated at the ground level, as with the floating surface created by Wang (2005) and Wang et al. (2008) which was reviewed in Section 3.6.

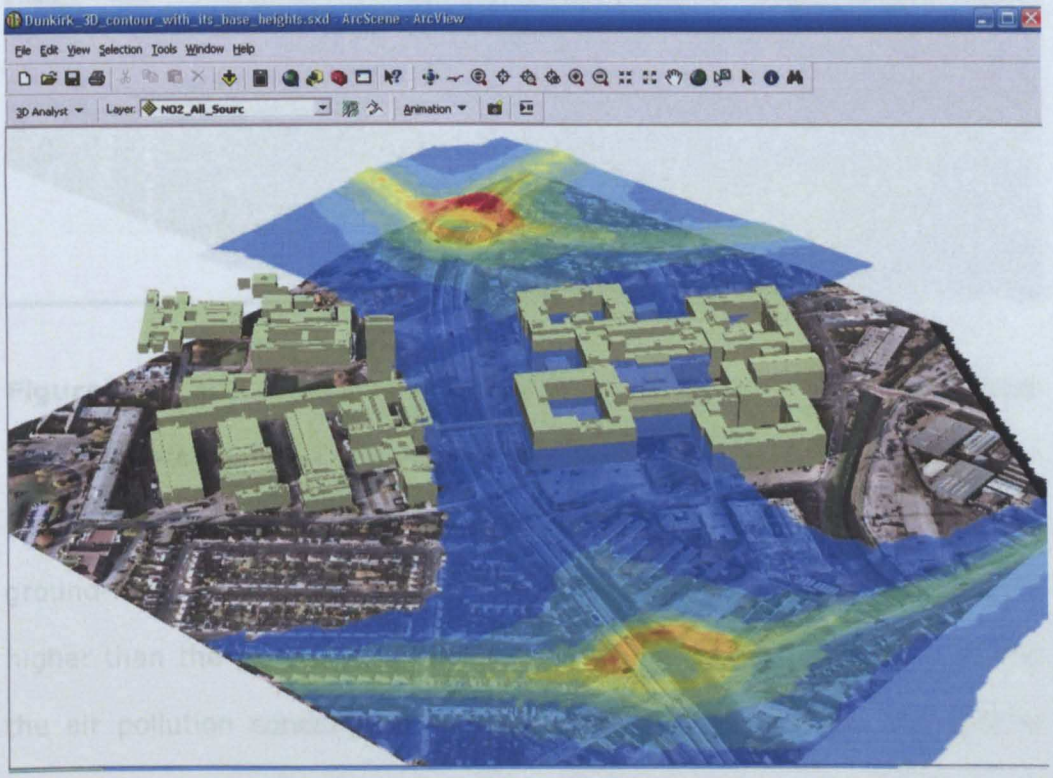

Figure 7.11 3D Contour Map Interface

Therefore the interface design moved on again. Beginning the original interface design work undertaken in this research project, in the fourth interface design, the height at each point in the air pollution contour map was the ground-level air pollution concentration plus the ground surface level at that point. This improved the parallelism between the contour map

and the ground surface, and consequently reduced the necessary offset between the two surfaces as shown in Figure 7.12.

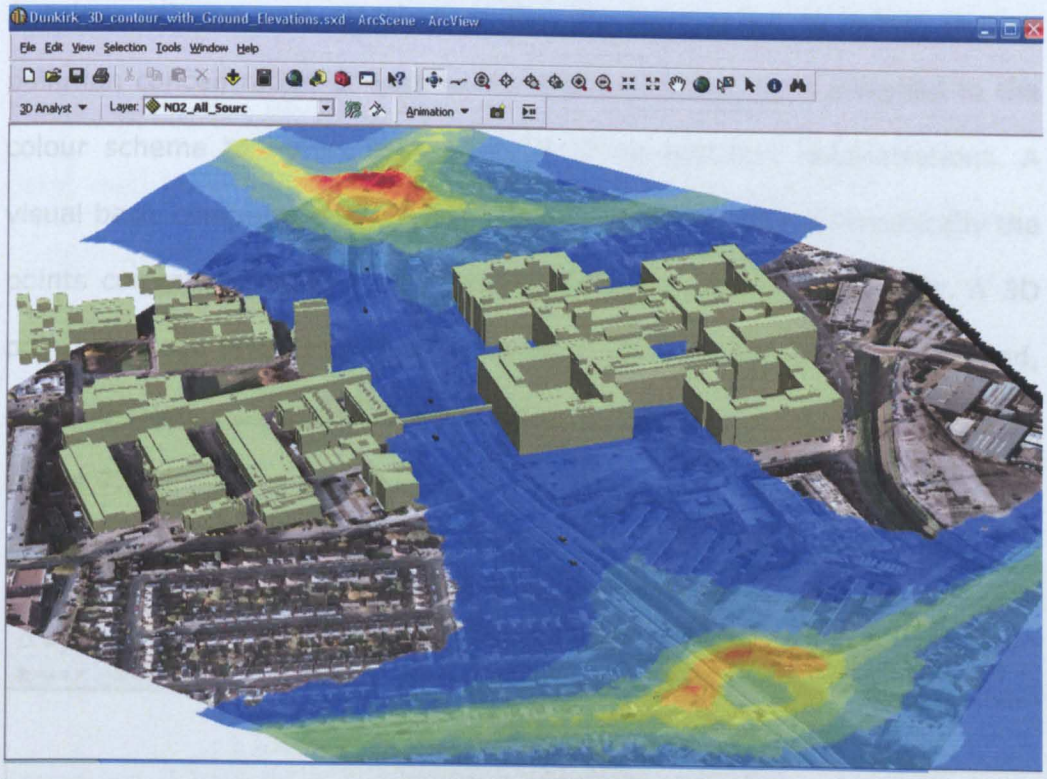

Figure 7.12 3D Contour Map with Ground Level Elevations Interface

This interface removed the illusion of a spatial shift in the location of the contour map in the perspective viewing projection. However, again the ground-level air pollution contour map was confusingly displayed at a level higher than the ground level. Additionally, this interface could not display the air pollution concentrations data at other heights above the ground surface in the same view. Therefore, it was necessary to move on to another interface design.

The fifth interface design displayed the air pollution data at and above the ground surface in one view. That was done by running the air pollution model to give the air pollution data at many levels at and above the ground level. A 3D point array was created at the output receptor points of the air

pollution model, with every receptor point having a value for the air pollution concentration.

A colour scheme was attached to the 3D point array to reflect the air pollution concentration at each point. Twelve colours were assigned to the colour scheme to reflect the hierarchy of air pollution concentrations. A visual basic computer program was developed to retrieve automatically the points corresponding to every colour band from the whole dataset. A 3D point coverage layer was created for each point set for each colour band, and the layer was assigned the colour of that colour band as shown in Figure 7.13.

Figure 7.13 3D Point Array with Many Layers Interface

The positive feedback regarding this interface design was that the air pollution data at and above the ground surface was displayed in one view. Therefore, this interface design had one clear advantage over the previous four interface designs. On the other hand, there was negative feedback

about this interface design regarding the very large number of points, as mentioned in Section 6.4.4, which had the effect of making the visualisation rather confusing. Additionally, using a colour scheme composed of twelve colours was found confusing and the interface lost its simplicity. Adding twelve shape files to the virtual scene for the twelve point sets overburdened the virtual scene and hindered a smooth navigation through the scene.

Consequently, for a sixth interface design, the functionality of 3D Analyst of ArcGIS 9.2 was used to represent the whole air pollution dataset, at and above the ground surface, as one 3D point shape file in the virtual scene. Again, a colour scheme composed of twelve colours was assigned to the point shape file to reflect the hierarchy of air pollution concentrations at each point in the 3D point array as depicted in Figure 7.14.

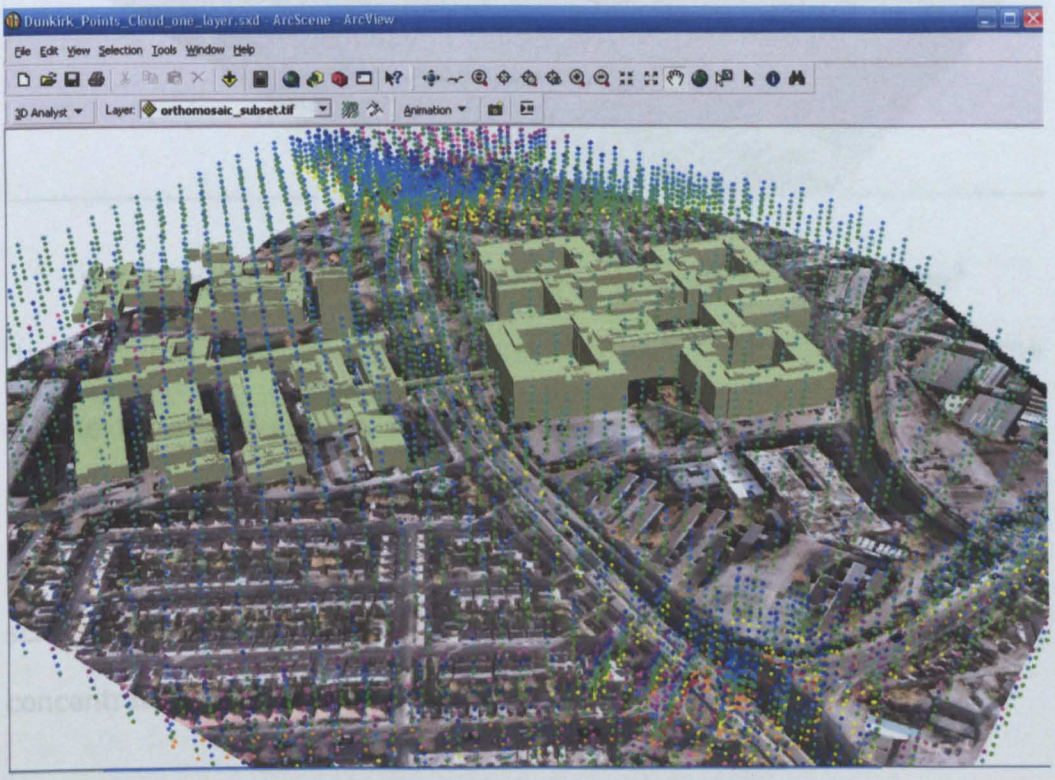

Figure 7.14 3D Point Array with One Layer Interface

This interface design depicted in Figure 7.14 introduced a new option. This new option was the ability to limit the displayed points of the point array to any user-specified range of air pollution concentrations. Figure 7.15 shows the 3D point array displaying only the points at which the air pollution concentration is greater than 40 $\mu g/m^3$, the AQO of NO_2.

Figure 7.15 Points at which NO_2 is Greater Than 40 $\mu g/m^3$

However, the interface design shown in Figure 7.14 did not tackle the complexity issues raised above about having a large number of points and colours. Therefore, another interface design for the 3D point array (the seventh interface design so far) was built with a monochromatic colour scheme and points graduated in size according to the air pollution concentration as shown in Figure 7.16.

For the interface design depicted in Figure 7.16, the assigned monochromatic colour scheme comprised only four shades of the colour grey. For every point in the 3D point array, the darker was the point

colour, and the greater was the diameter of the 3D point, the higher was the NO_2 concentration at that point, as depicted in Figure 7.16. This interface design maintained the option of limiting the displayed points to a user-specified range of air pollution concentrations.

Figure 7.16 3D Point Array with One Monochromatic Layer with Graduated Point Size Interface

However, the interface design depicted in Figure 7.16 did not tackle the complexity arising from using a large number of points. Furthermore, visualising points of varying size in stereo viewing projection gave a wrong perception of the point location in the 3D virtual space. The points bigger in size seemed closer to the observer than smaller points, although these big points were in fact further away than the small points. That confused the observer and hindered recognising the correct spatial locations of different air pollution concentrations in the stereo viewing projection. Hence, the interface design had still not achieved sufficient simplicity to provide the observer with a correct and intuitive understanding of the 3D air pollution dispersion, so the development of the interface design continued.

The eighth interface design tackled the complexity of having a large number of points (small components) in the 3D point array interface by pooling the large number of points into a smaller number of larger components. A 3D planar surface was interpolated between the points relevant to each band of air pollution concentrations. Then, the number of the air pollution components in the interface design reduced to the number of air pollution concentration bands. A colour scheme was assigned to the resultant surfaces to reflect the hierarchy of air pollution concentration bands, as shown in Figure 7.17 and Figure 7.18.

In some cases, the points relevant to one air pollution concentrations band were located in spatially separate groups. Therefore, the surface connecting these points together covered the spaces in-between such groups of points, and the points in these spaces were not relevant to that air pollution concentrations band. Consequently, instead of being an improvement, this interface design conveyed a false impression of the air pollution dispersion. Furthermore, the resultant surfaces interfered with each other, which necessitated displaying them one by one in the virtual scene. This was a real step backwards relative to this research project's goal of displaying the air pollution data at different levels at and above the ground surface in the same view. Consequently, the development of the interface design continued further.

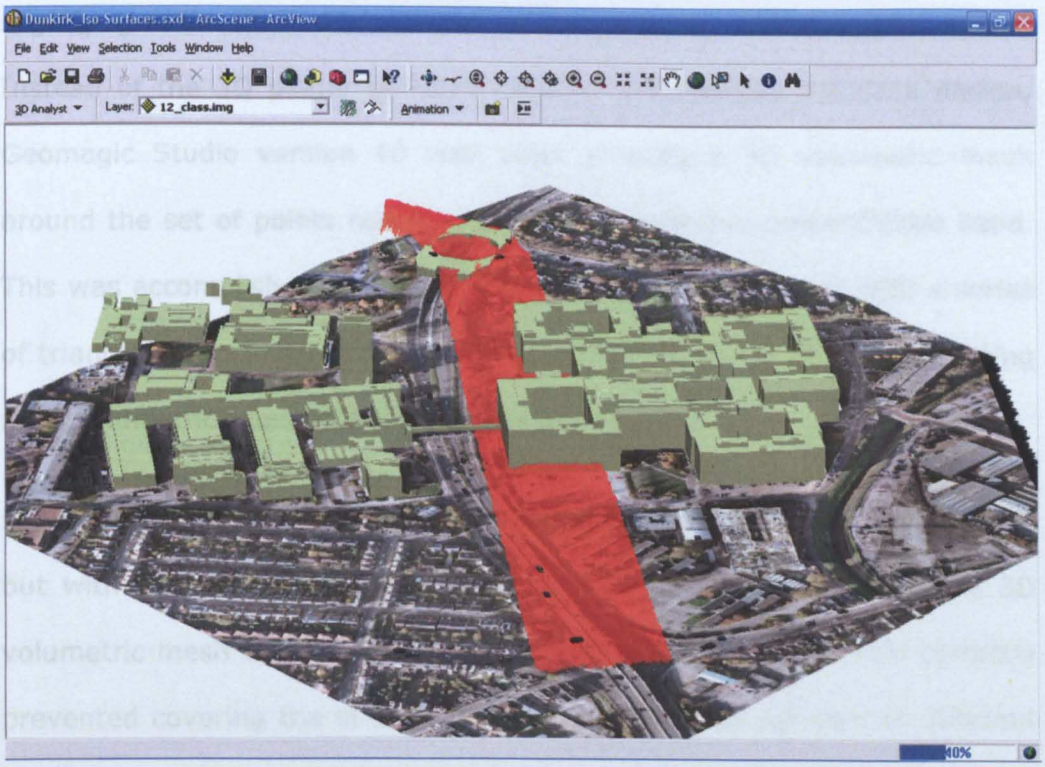

Figure 7.17 44-51 µg/m^3 Surface Interface

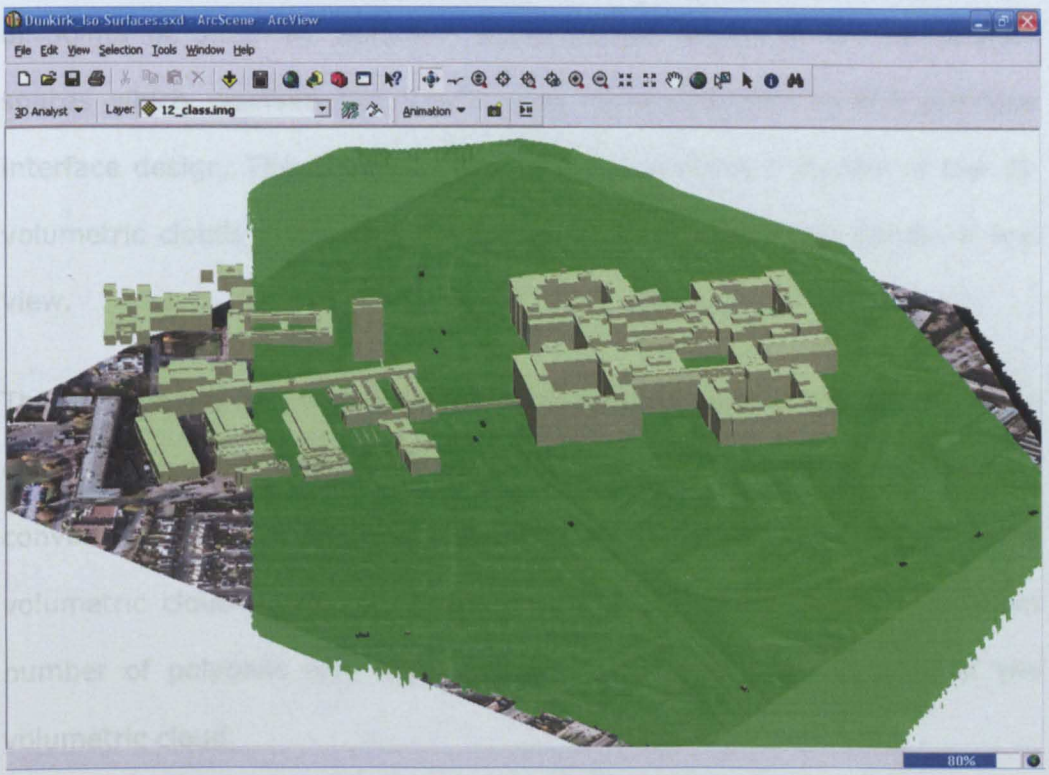

Figure 7.18 35-36 µg/m^3 Surface Interface

The ninth interface design reduced the large number of points in the 3D point array interface down to a number of 3D components which was

slightly greater than the number of air pollution concentration bands. Instead of the 3D planar surfaces used in the previous interface design, Geomagic Studio version 10 was used to wrap a 3D volumetric mesh around the set of points relevant to each air pollution concentration band. This was accomplished by connecting the points of every set with a series of triangles to form an external 3D surface and internal 3D webs, creating a 3D volumetric 'cloud' for every set of points.

For a set of points relevant to a certain air pollution concentration band, but with the points located in spatially separate groups, a separate 3D volumetric mesh was wrapped around each group of points. This correctly prevented covering the in-between spaces, which are relevant to different air pollution concentration bands. Therefore, the volumetric clouds of these groups of points did not interfere with the volumetric clouds of the group(s) of points of other air pollution concentration bands in the in-between spaces which resolved the interference issue identified in the previous interface design. Therefore this development enabled a display of the 3D volumetric clouds relevant to all air pollution concentration bands in one view.

The functionality of Geomagic Studio was used to convert every volumetric cloud to polygons. Then, Geomagic Studio was used again to optimise the converted volumetric cloud by reducing the number of polygons so that the volumetric cloud would not overburden the virtual scene. This optimum number of polygons was large enough to preserve the 3D form of the volumetric cloud.

A challenge arose when wrapping a 3D volumetric mesh around a group of points which totally surrounded another group of points belonging to a different air pollution concentration band. The external volumetric cloud

interfered with the internal volumetric cloud. To resolve this challenge, Geomagic Studio was used to trim the external volumetric cloud by subtracting the internal cloud from the external cloud. This gave the external volumetric cloud its correct hollow-core shape, and hence it did not interfere any more with the internal volumetric cloud. The optimised 3D volumetric clouds for all the air pollution concentration bands were exported from Geomagic Studio in DXF format for the integration with the Dunkirk AQMA 3D city model in 3D Analyst of ArcGIS 9.2.

The volumetric clouds in 3D Analyst of ArcGIS 9.2 were assigned a monochromatic colour scheme of four shades of the colour grey, to reflect the hierarchy of NO_2 concentration bands. The darker was the cloud colour, the higher was the NO_2 concentration of this cloud. In addition, the 3D volumetric clouds were assigned a 50% degree of transparency in order not to obscure parts of the virtual scene located behind and underneath. The transparency of these 3D volumetric clouds maintained a good degree of location recognition and orientation while navigating the virtual scene. Figure 7.19, Figure 7.20 and Figure 7.21 display screenshots of the incremental representation of the 3D volumetric clouds relevant to individual bands of 2006 NO_2 concentrations in the Dunkirk AQMA virtual scene. Figure 7.22 shows a screenshot of the display of the 3D volumetric clouds relevant to all the 2006 NO_2 concentration bands in one view.

Figure 7.19 One 2006 NO_2 concentration band

Figure 7.20 Two 2006 NO_2 concentration bands

Figure 7.21 Three 2006 NO_2 concentration bands

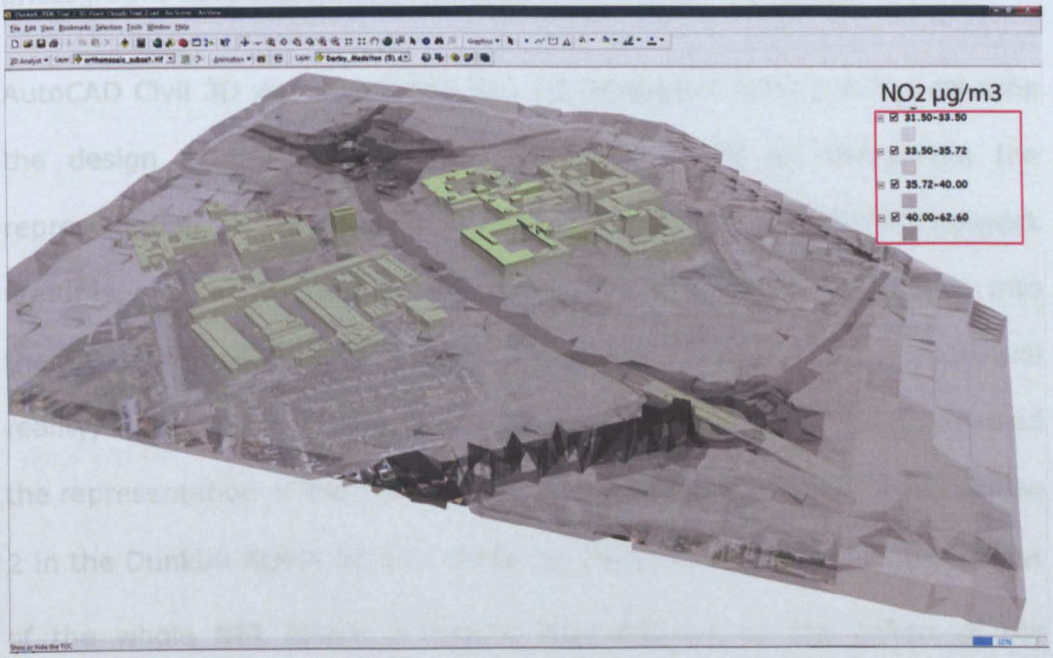

Figure 7.22 All 2006 NO_2 concentration bands

The 3D volumetric clouds interface design achieved the goal of this chapter to develop a good 3D air pollution dispersion interface, as discussed at the start of this section. Therefore, this design was selected to be the 3D air pollution dispersion interface of this research decision-support system.

7.6 Summary

This chapter explained the details of developing the design of the 3D air pollution dispersion interface. The main elements of this interface were the 3D city model of the Dunkirk AQMA and the numerical output NO_2 concentrations. Maintaining a smooth navigation and a good level of location recognition and orientation were the two criteria used to design the Dunkirk AQMA 3D city model so that an effective visualisation of the air pollution dispersion could be attained. A mid-range LOD, between LOD2 and LOD3, was selected to represent the featured 3D buildings of the Dunkirk AQMA, which were extracted from a block of stereoscopic aerial photographs covering the Dunkirk AQMA, in the 3D city model.

AutoCAD Civil 3D was integrated with 3D Analyst of ArcGIS 9.2 to develop the design of the Dunkirk AQMA 3D city model to incorporate the representation of a dynamic traffic layer and certain major road network features, such as the Dunkirk flyover and the Derby Road roundabout, into the 3D city model. Such a deep integration between CAD and virtual reality, which was identified as a challenge by Whyte et al. (2000), enabled the representation of the future viaduct, ramps and tram stop of NET Phase 2 in the Dunkirk AQMA 3D city model as depicted in Figure 7.8. The colour of the whole NET Phase 2 feature was different to the colour of the remaining features in order to distinguish intuitively between the present (existing) features and future additional features.

The intuitive 3D visualisation of NO_2 concentrations at and above the ground surface in a single virtual scene was the aim of the 3D air pollution dispersion interface, which was identified as a challenge ahead by Wang et al. (2008). Some principles and guidelines of HCI were selected to develop the design of the Dunkirk AQMA 3D air pollution dispersion interface in

order to achieve this goal. Contrast, simplicity and using a colour scheme that reinforces the hierarchy of information were the most important selected principles and guidelines of HCI.

The design of the Dunkirk AQMA 3D air pollution dispersion interface evolved from the 3D visualisation of the ground-level contour map of NO_2 concentrations, as shown in Figure 7.10, Figure 7.11 and Figure 7.12, to the 3D visualisation of NO_2 concentrations at and above the ground surface as a 3D point array in a single virtual scene, as shown in Figure 7.13, Figure 7.14 and Figure 7.16. The large number of points in the 3D point array was found not to be particularly intuitively meaningful, so the research was progressed to the 3D visualisation of NO_2 concentrations at and above the ground surface as a much smaller number of 3D planar surfaces. However, these surfaces interfered with each other when displayed together in the virtual scene so the research was progressed further to the representation of the NO_2 concentrations by 3D volumetric clouds as shown in Figure 7.22. The 3D volumetric clouds interface achieved the above mentioned goal of the 3D air pollution dispersion visualisation in 3D city models.

Chapter 8

Application of the Decision-Support System to the Future NET Phase 2 Implementation

8.1 Introduction

The aim of this chapter is the application of the developed decision-support system to the implementation of NET Phase 2 through the Dunkirk AQMA in order to predict and visualise its future air quality impacts in the Dunkirk AQMA. This also demonstrates the use of the decision-support system to investigate the future additional traffic flow/speed changes that would be needed, as well as those anticipated due to the implementation of NET Phase 2, to relate conceptually to the Dunkirk AQMA being totally revoked in 2021. The aim of this chapter is achieved by the investigation of five main objectives:

1. The projection of the air pollution input data for the Dunkirk AQMA base case scenario model from 2006 to 2021.
2. The creation of the 2021 3D air pollution dispersion interfaces for the 2021 Do-Minimum and Do-Something NET Phase 2 traffic scenarios, as defined in Section 5.5.
3. The investigation of the effectiveness of alternative versions of the 2021 Do-Something NET Phase 2 traffic scenario, to relate conceptually to totally revoking the Dunkirk AQMA in 2021.

4. The creation of the 2021 3D air pollution dispersion interfaces for the effective alternative NET Phase 2 traffic scenarios.
5. The investigation of the impact on the modelled 2021 air quality of assuming the full anticipated future emission reductions due to improved vehicle technology and better fuel standards.

8.2 Projection of Air Pollution Input Data to 2021 Assuming Full Future Technology Benefits

In order to build the 2021 Do-Minimum and Do-Something air quality scenarios, the traffic and emission data of the base case scenario had to be projected from 2006 to 2021. The traffic data was projected from 2006 to 2021, as presented in Chapter 5. The total pollutant concentration calculated by the air pollution model at a receptor point is made up of three main components: background concentrations, traffic-induced emissions and industry-induced emissions. Therefore, this section explains the projection of these three components from 2006 to 2021, assuming the full anticipated future emission reductions due to improved vehicle technology and better fuel standards.

8.2.1 Projection of Background Concentrations

The micro-calibrated background concentrations of the Dunkirk AQMA base case scenario model were projected from 2006 to 2021 using The Year Adjustment Calculator. The Year Adjustment Calculator is a simple MS Excel tool available for download from the website of the UK Air Quality

Archive (AEA, 2008). This MS Excel tool incorporates updated year adjustment factors from those published in DEFRA (2003) and are suitable for use with the DEFRA (2003) update. The year adjustment factors have been calculated as the likely changes in air pollution concentrations resulting from changes in emissions. This incorporates the expected impact of changes in activity, such as traffic movements, and changes in emission factors, due to the use of improved vehicle technology and fuel standards in the future, for both traffic and stationary sources.

Year Adjustment Calculator, version 2.2a, is primarily designed for five types of pollutant: NO_2 background, NO_2 roadside, NO_x background, PM_{10} primary background and PM_{10} secondary background. This tool enables the user to choose a parameter, to type in a measured or modelled concentration for a given year, and to select a year for future projection. The tool then automatically does the calculation and presents the predicted concentration. Predicted concentrations by this tool are based on analyses from a base year of 2004, and projections should never be made backwards to the relevant year, only forwards from a base year to the relevant year.

O_3 background was not included in the Year Adjustment Calculator although it did affect the calculated total NO_2 concentrations, because it was not included in the analyses used for building this tool. The impact of changing O_3 background concentrations on the calculated total NO_2 concentrations was explained during the calibration process of the base case scenario model as shown in Sections 06.4.1 and 6.4.2. Therefore, it was decided to project the O_3 background concentrations from 2006 to 2021 as well. As NO_2 background concentrations are expected to decrease in the future as predicted by the Year Adjustment Calculator, future O_3 background levels, consumed in the conversion of NO to NO_2 in the

background, may increase. Hence, 2021 O_3 background concentrations were calculated by adding the difference between 2006 and 2021 NO_2 background concentrations to 2006 O_3 background concentrations.

The Year Adjustment Calculator was used to derive the year adjustment factors for the NO_2 and NO_x background concentrations. The year of the reading was entered as 2006, and the year of the projection was entered as 2021. The value of the 2006 reading was entered as 1.0 and the 2021 reading was read off. Because the value of the 2006 reading was entered as 1.0, the value of the 2021 reading was considered as an adjustment factor which could be multiplied by any value of 2006 concentrations to result in a projected 2021 concentration. This facilitated the automation of the projection of the hourly sequential 2006 background concentrations to 2021 in Ms Excel.

The 2006 micro-calibrated background concentrations file was imported into MS Excel. Then, the 2021 year adjustment factors for the NO_2 and NO_x background concentrations were read off from The Year Adjustment Calculator as 0.83 and 0.72 respectively. For each hour of the 2006 data, the micro-calibrated NO_2 and NO_x background concentrations were multiplied by 0.83 and 0.72 respectively. In addition, for each hour of the 2006 data, the 2021 O_3 background concentration was automatically estimated from the 2006 O_3 and NO_2 micro-calibrated background concentrations, assuming a linear relationship, as follows:

$$\text{2021 } O_3 \text{ background}_i = \text{2006 } O_3 \text{ background}_i + (1 - 0.83) \times \text{2006 } NO_2 \text{ background}_i, \quad \textbf{(8.1)}$$

where i ranges from 1 to 8760, the total number of hours in year 2006. It was important to maintain the structure of the projected 2021 hourly

sequential background concentrations file so that it could be read by the air pollution model.

8.2.2 Projection of Traffic-induced Emissions

Traffic-induced emissions were projected from 2006 to 2021 using the built-in emission factors of ADMS-Roads. The emission year was altered from 2006 to 2021 in the model interface. This fully reflected the future impacts of using improved vehicle technology and better fuel standards on the 2021 traffic-generated emissions which are calculated from the forecast 2021 traffic flow and speed data. It was assumed that the 2006 proportion of primary NO_2 in NO_X as NO_2 emissions (10%) is the same in 2021, assuming no increase in the popularity of diesel cars due to the anticipated wide use of cleaner vehicles in the future. The 2006 hourly and monthly traffic profiles file, *.fac, was used for the year 2021 assuming no change in the future traffic profiles.

8.2.3 Industry-induced Emissions

The industry-induced emissions of NO_x as NO_2 were generated by the three industrial point sources which were defined in the 2006 Dunkirk AQMA base case scenario model, as stated in Section 6.3. As traffic-induced air pollution was the main focus of the research project, the air quality impacts of changes in the future industry-induced emissions were not considered. Therefore, it was decided to keep the industrial emission rates in 2021 the same as in 2006.

8.3 Predicted 2021 Air Quality in the Dunkirk AQMA

The forecast 2021 traffic flow and speed data for the 2021 Do-Minimum traffic scenario were used, along with the projected 2021 air pollution input data, for running ADMS-Roads for 2021 air pollution modelling of the Dunkirk AQMA. The 2021 annual mean NO_2 concentrations were calculated by ADMS-Roads at the output receptor points of the intelligent grid described in Section 6.5. The GIS-based factor, explained in Section 6.4.5.3, was applied to the 2021 calculated annual mean NO_2 concentrations in the Beeston Road area. Figure 8.1 shows the contour map of 2021 ground-level annual mean NO_2 concentrations for the 2021 Do-Minimum traffic scenario in the Dunkirk AQMA. This process was repeated with the 2021 traffic flow and speed data for the 2021 Do-Something NET Phase 2 traffic scenario. Figure 8.2 shows the contour map of 2021 ground-level annual mean NO_2 concentrations for the 2021 Do-Something traffic scenario in the Dunkirk AQMA.

Figure 8.1 Contour Map of Do-Minimum 2021 Ground-level Annual Mean NO_2 Concentrations in the Dunkirk AQMA

Figure 8.2 Contour Map of Do-Something 2021 Ground-level Annual Mean NO_2 Concentrations in the Dunkirk AQMA

Figure 8.3 compares the modelled 2006 ground-level NO_2 concentrations in Figure 6.16 to the predicted 2021 ground-level NO_2 concentrations in Figures 8.1 and 8.2.

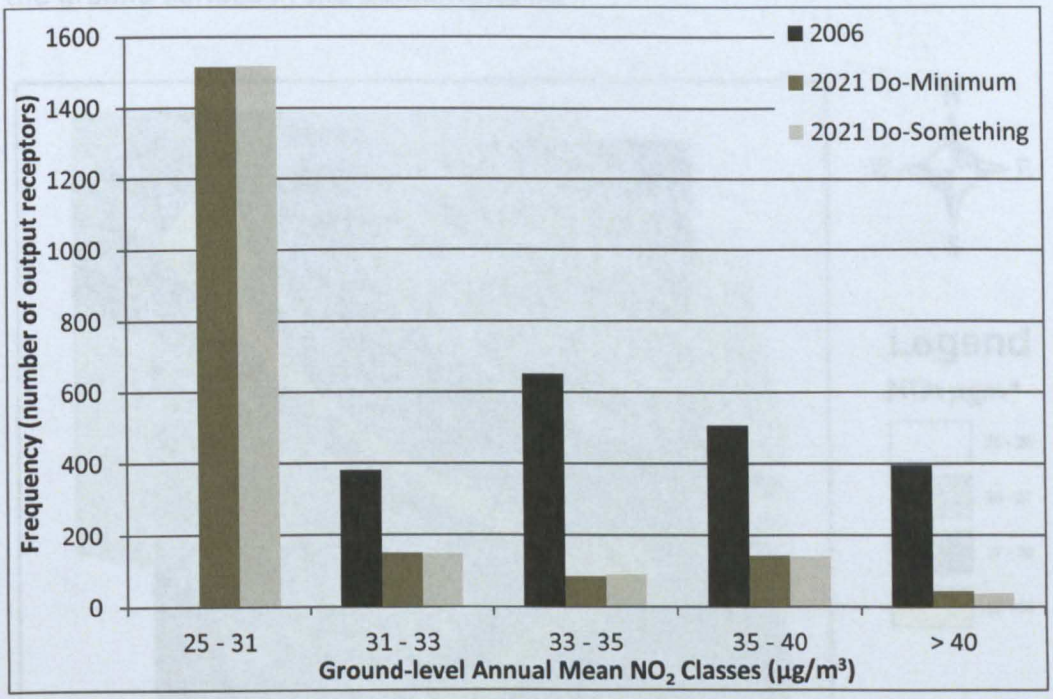

Figure 8.3 Comparison of Modelled Ground-level 2006 to 2021 Annual Mean NO_2 Concentrations

As is clearly evident both from comparing Figure 8.1 and Figure 8.2 (with identical legends) and from considering Figure 8.3, the predicted 2021 ground-level NO_2 concentrations for the 2021 Do-Minimum and Do-Something NET Phase 2 traffic scenarios, within the limitations of the average speed average flow model, were very similar. This indicated that the air quality impact of the implementation of NET Phase 2 in the Dunkirk AQMA would not be significant at all. Hence, it was decided to generate just one set of output NO_2 concentrations above the ground surface for both the 2021 Do-Minimum and Do-Something NET Phase 2 traffic scenarios. ADMS-Roads was run to output the 2021 annual mean NO_2 concentrations at 6 to 30 metres above the ground surface with a 6 metre height step. At each output height above the ground surface, the GIS-based factor, explained in

Section 6.4.5.3, was applied to the 2021 calculated annual mean NO_2 concentrations in the Beeston Road area. Figure 8.4 to Figure 8.8 show the output contour maps of the 2021 annual mean NO_2 concentrations above the ground surface in the Dunkirk AQMA.

Figure 8.4 Contour Map of 2021 Do-Minimum/Do-Something 6 metres-height Annual Mean NO_2 Concentrations in the Dunkirk AQMA

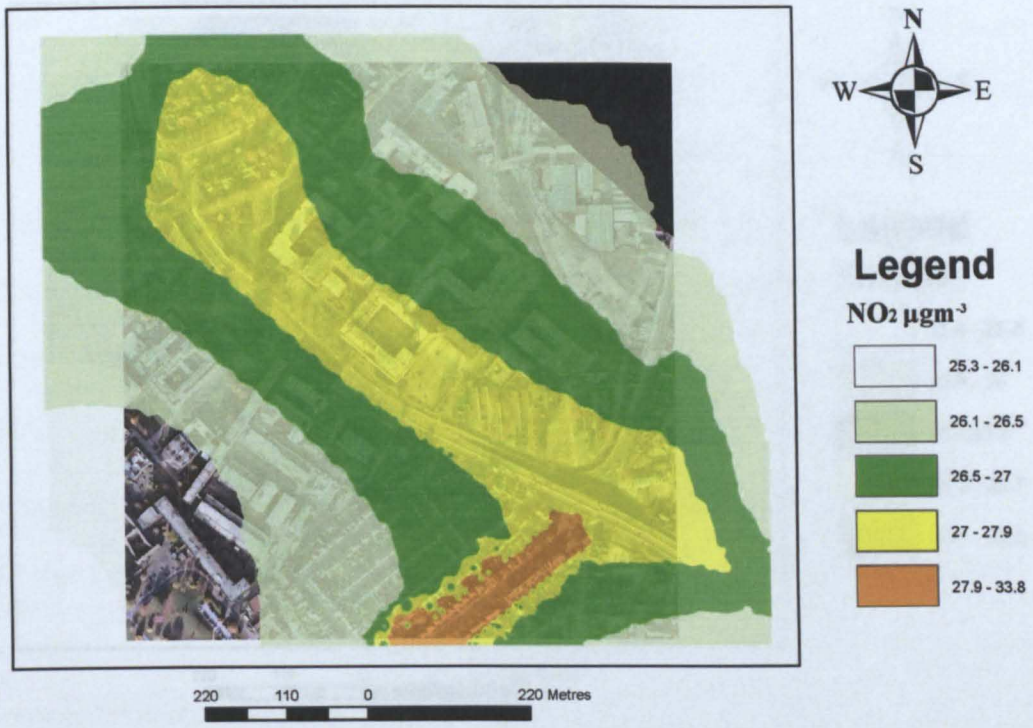

Figure 8.5 Contour Map of 2021 Do-Minimum/Do-Something 12 metres-height Annual Mean NO_2 Concentrations in the Dunkirk AQMA

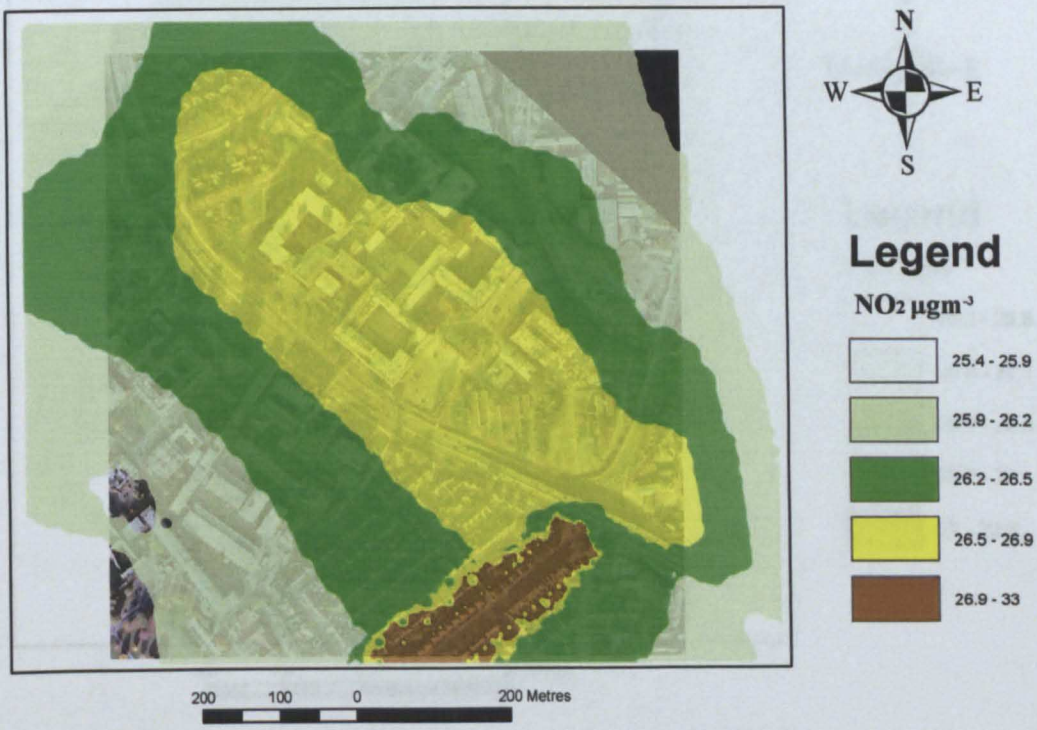

Figure 8.6 Contour Map of 2021 Do-Minimum/Do-Something 18 metres-height Annual Mean NO_2 Concentrations in the Dunkirk AQMA

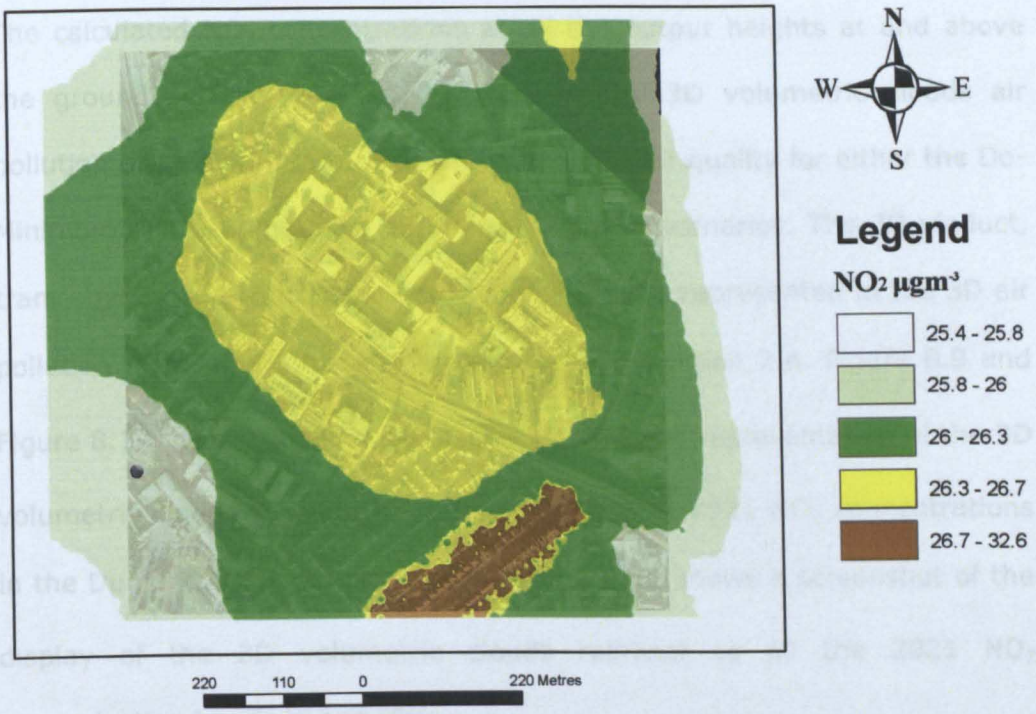

Figure 8.7 Contour Map of 2021 Do-Minimum/Do-Something 24 metres-height Annual Mean NO_2 Concentrations in the Dunkirk AQMA

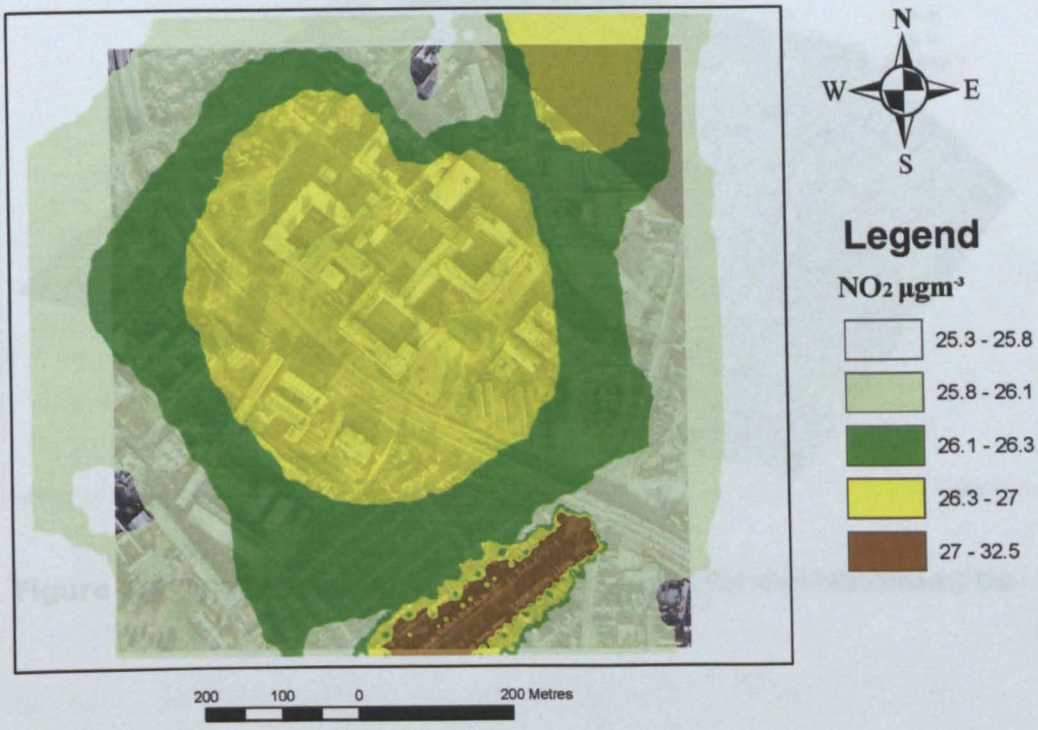

Figure 8.8 Contour Map of 2021 Do-Minimum/Do-Something 30 metres-height Annual Mean NO_2 Concentrations in the Dunkirk AQMA

The calculated NO_2 concentrations at all the output heights at and above the ground surface were used to create the 3D volumetric clouds air pollution dispersion interface to show the 2021 air quality for either the Do-Minimum or Do-Something NET Phase 2 traffic scenarios. The 3D viaduct, tram objects and tram stop of NET Phase 2 were represented in the 3D air pollution dispersion interface, as explained in Section 7.4. Figure 8.9 and Figure 8.10 display screenshots of the incremental representation of the 3D volumetric clouds relevant to individual bands of 2021 NO_2 concentrations in the Dunkirk AQMA 3D city model. Figure 8.11 shows a screenshot of the display of the 3D volumetric clouds relevant to all the 2021 NO_2 concentration bands in one view.

Figure 8.9 One 2021 NO_2 concentration band for Do-Minimum/Do-Something Scenarios

Figure 8.10 Two 2021 NO_2 concentration bands for Do-Minimum/Do-Something Scenarios

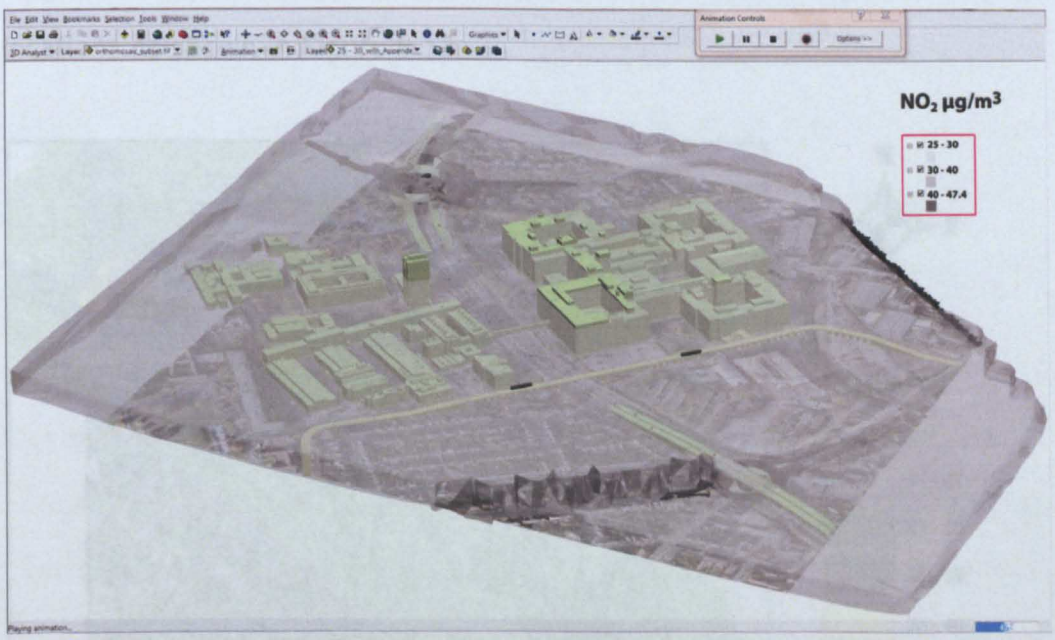

Figure 8.11 All 2021 NO_2 concentration bands for Do-Minimum/Do-Something Scenarios

8.4 Alternative Versions of the 2021 NET Phase 2 Traffic Scenario

Although the predicted 2021 air pollution levels were much lower than the modelled 2006 air pollution levels as shown in Figure 8.3, The AQO for the

annual mean NO_2 concentration, of 40 $\mu g/m^3$, was still exceeded at just two ground-level locations in the 2021 Do-Something NET Phase 2 traffic scenario as shown in Figure 8.2. Therefore, it was decided to investigate the development of alternative versions of the 2021 Do-Something traffic scenario in order to work out, according to modelling, what the 2021 traffic flow and/or speed data would need to be so that the AQO for the annual mean NO_2 concentration could be achieved at these two ground-level locations in 2021. In modelling terms, this could conceptually relate to the Dunkirk AQMA being totally revoked in 2021. As it took a relatively long runtime for the generation of a gridded output, the output grid option was turned off in the ADMS-Roads interface, and instead just two individual output receptors were defined, one at each of these two ground-level locations as shown in Figure 8.12.

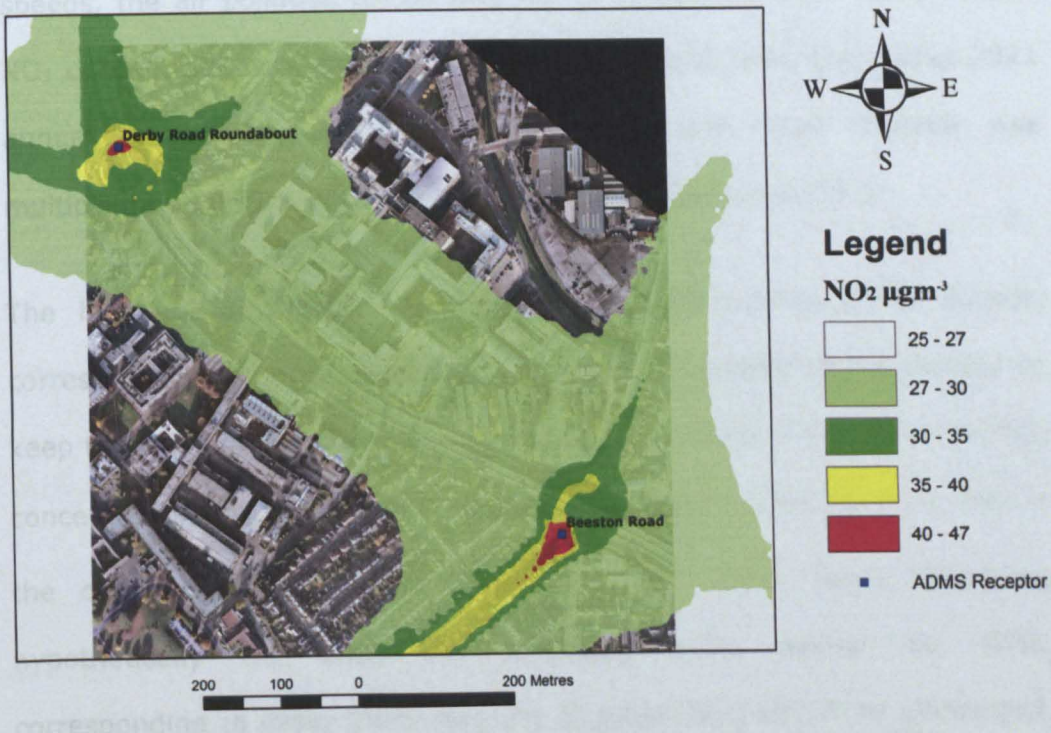

Figure 8.12 Two Test Receptors in the Areas Breaching the AQO of the Annual Mean NO_2 Concentration for the 2021 Do-Something Scenario

8.4.1 Traffic Speed Amendment Only Scenarios

The first stage of this investigation was into the air pollution model's sensitivity to changing only the traffic speed data in the 2021 Do-Something traffic scenario. The 2021 Do-Something traffic speeds for all the roads defined in the air pollution model were amended hypothetically by -50%, -75%, +10%, +25%, +50%, +60%, +75% and +85% while the 2021 Do-Something traffic flows were unchanged. The reductions in the traffic speed correspond to an increase in the traffic density, and hence sufficient road capacity was assumed to be available. The traffic speed was also increased hypothetically for other scenarios, thus effectively ignoring the speed limit in the Dunkirk AQMA. After each amendment of the traffic speeds, the air pollution model was run to output the 2021 annual mean NO_2 concentrations at the two test receptors. Each time, the output 2021 annual mean NO_2 concentration at the Beeston Road receptor was multiplied by the GIS-based factor, explained in Section 6.4.5.3.

The hypothetical reduction in the 2021 Do-Something traffic speeds, corresponding to longer journey times, and increased traffic density to keep the traffic flow unchanged, increased the calculated annual mean NO_2 concentrations at the two test receptors as shown in Figure 8.13. This is the opposite effect to that desired. On the other hand, increasing hypothetically the 2021 Do-Something traffic speeds by 50%, corresponding to lower traffic density, to keep the traffic flow unchanged, reduced the calculated annual mean NO_2 concentrations very slightly at the two test receptors, but not by enough to achieve the AQO of the annual mean NO_2 concentration at the two test receptors.

Increasing the 2021 Do-Something traffic speeds by more than 50% slightly increased the calculated annual mean NO_2 concentrations at the two test receptors. Increasing the 2021 Do-Something traffic speeds by more than 85% was found to be practically infeasible due to the speed limits of ADMS-Roads built-in emission factors. Therefore, it was concluded that changing the future traffic speeds only is not enough to achieve the AQO of the annual mean NO_2 concentration at the two test receptors.

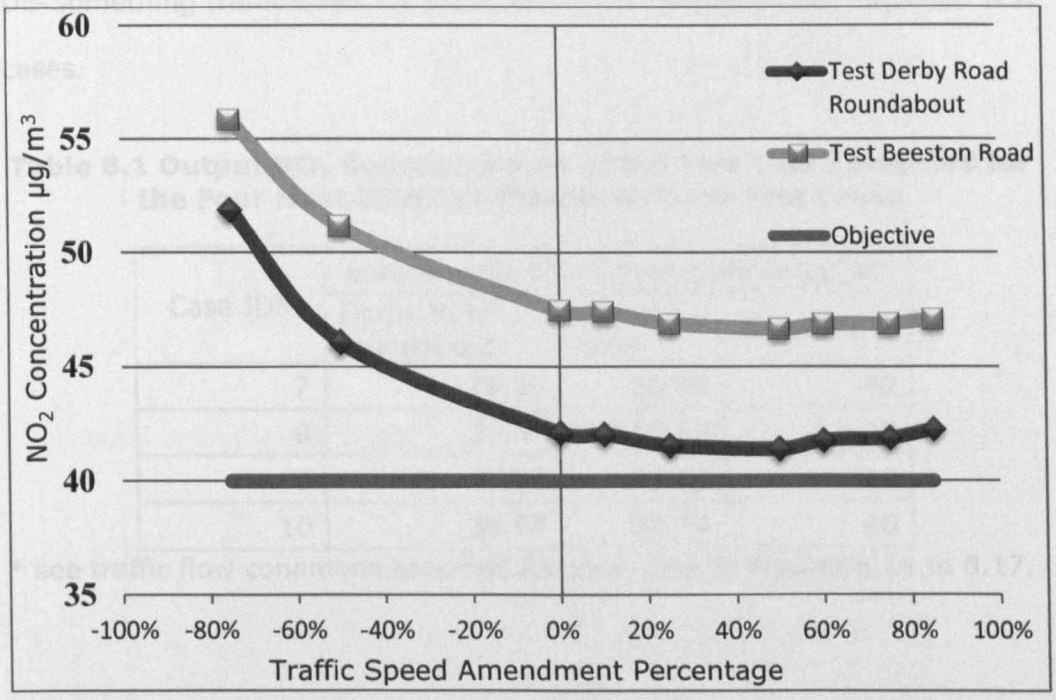

Figure 8.13 Annual Mean NO_2 Concentrations versus the Change in the Traffic Speeds Only at the Two Test Receptors

8.4.2 Traffic Flow Amendment Only Scenarios

The second stage of this investigation was into the air pollution model's sensitivity to changing only the traffic flows in the 2021 Do-Something traffic scenario. The 2021 Do-Something traffic flows for all the principal roads in the Dunkirk AQMA were amended many times, involving various flow reduction arrangements, while always keeping the traffic speeds unchanged, which corresponds to lower traffic density on these roads. For each case tested, the amended (reduced) traffic flows were input into the

air pollution model which was run to output the 2021 annual mean NO_2 concentrations at the two test receptors. Each time, the output 2021 annual mean NO_2 concentration at the Beeston Road receptor was multiplied by the GIS-based factor, described in Section 6.4.5.3. Table 8.1 shows the output annual mean NO_2 concentrations at the two test receptors for the four most effective flow reduction cases that were tested. Figure 8.14 to Figure 8.17 show the reductions made to the original 2021 Do-Something traffic flows for these four most effective flow reduction test cases.

Table 8.1 Output NO_2 Concentrations at the Two Test Receptors for the Four Most Effective Flow Reduction Test Cases

Case ID*	annual mean NO_2 concentrations $\mu g/m^3$		
	Derby Road roundabout	Beeston Road	Objective
7	39.94	39.86	40
8	39.94	39.52	40
9	39.99	39.99	40
10	39.99	39.74	40

* see traffic flow conditions assumed for each case in Figures 8.14 to 8.17.

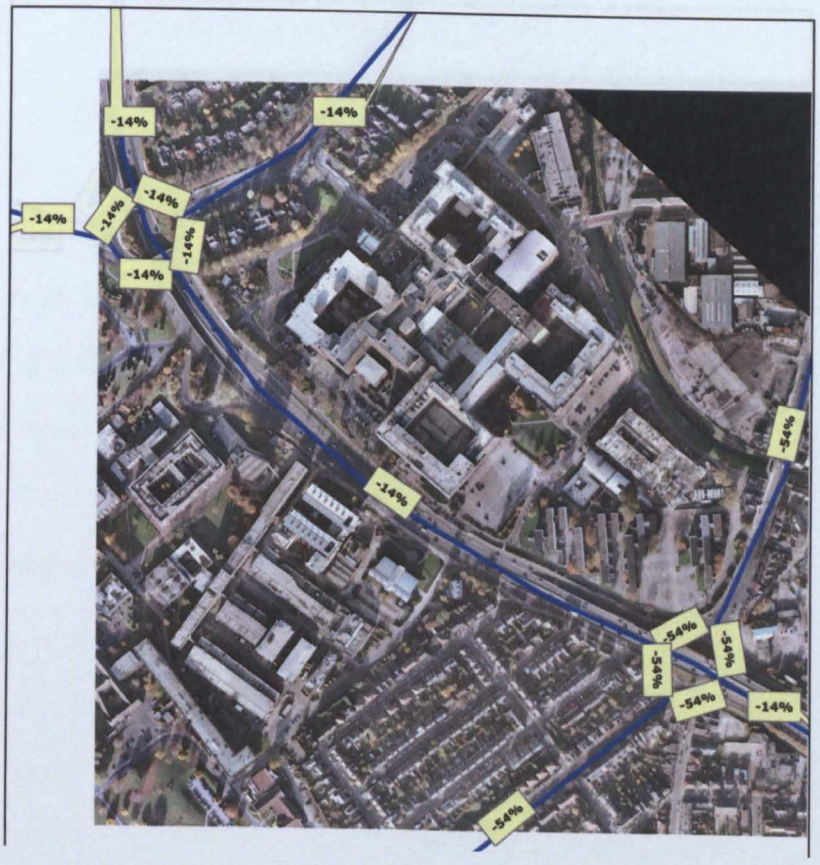

Figure 8.14 Percentages of Traffic Flow Reductions for Case 7

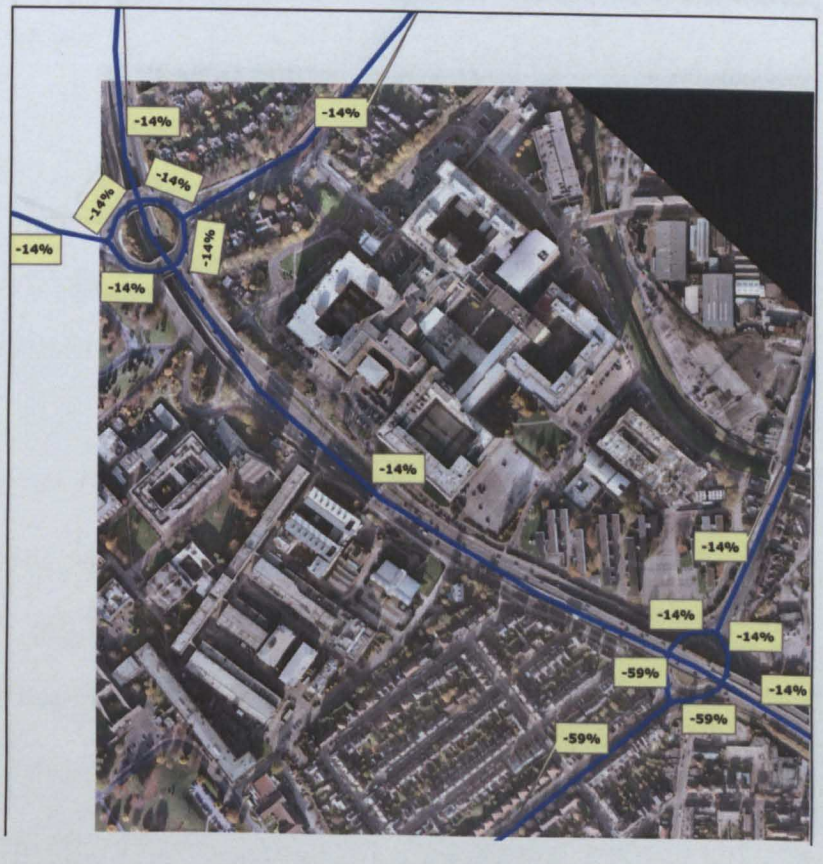

Figure 8.15 Percentages of Traffic Flow Reductions for Case 8

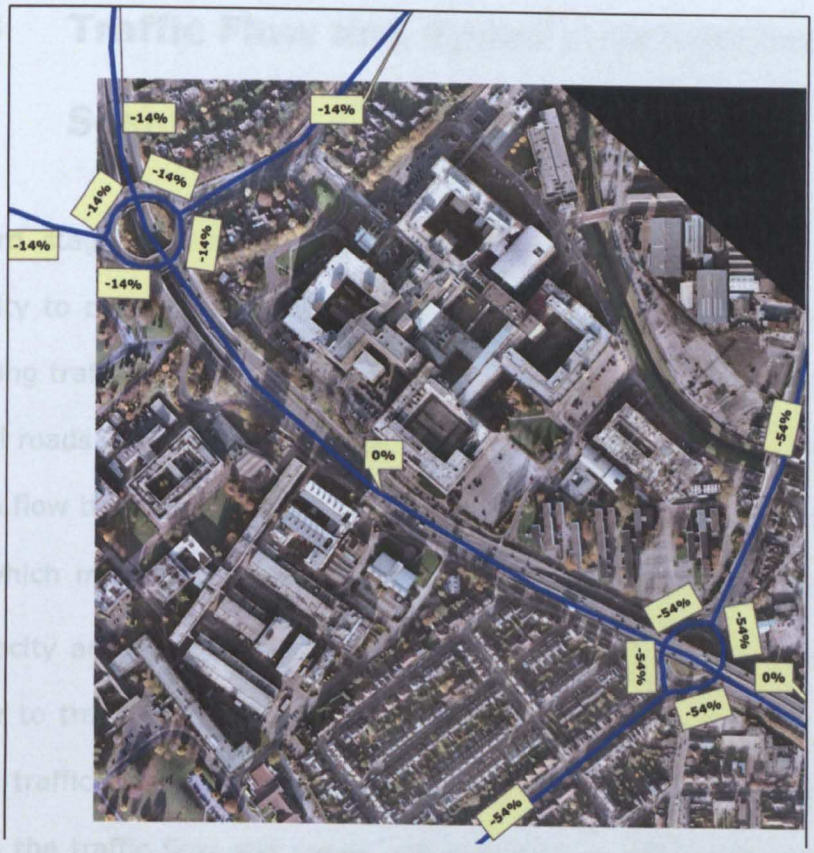

Figure 8.16 Percentages of Traffic Flow Reductions for Case 9

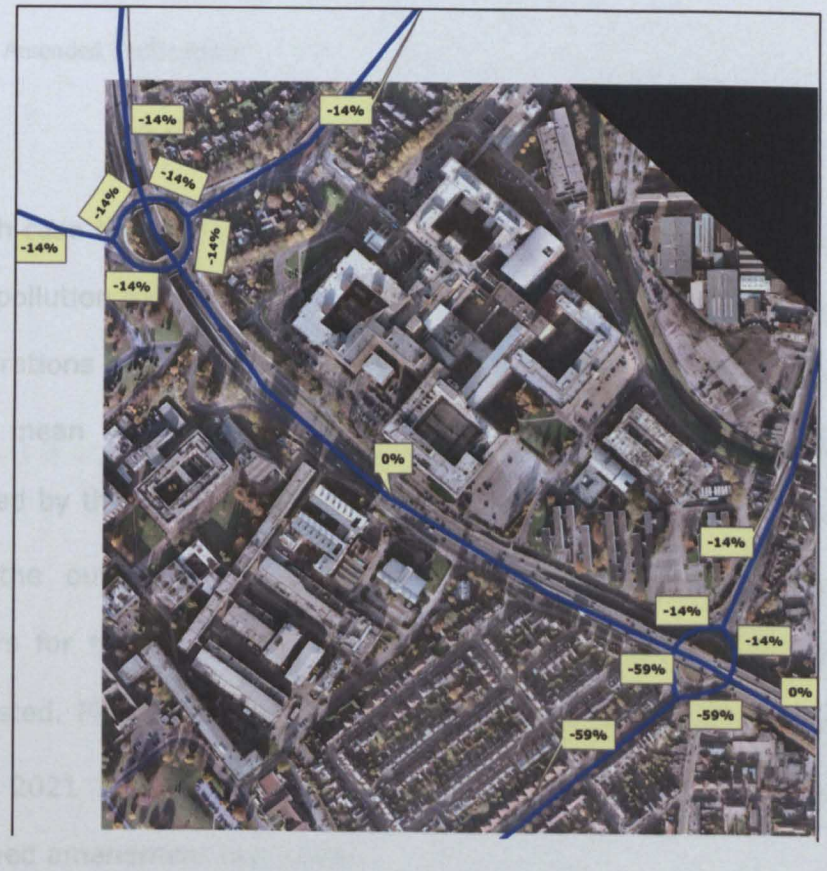

Figure 8.17 Percentages of Traffic Flow Reductions for Case 10

8.4.3 Traffic Flow and Speed Amendment Scenarios

The third stage of this investigation was into the air pollution model's sensitivity to changing both the traffic flows and speeds in the 2021 Do-Something traffic scenario. The 2021 Do-Something traffic flows for all the principal roads in the Dunkirk AQMA were reduced a number of times, and for each flow the corresponding traffic speed was increased using Equation (8.2), which might hypothetically correspond to various improvements in the capacity and attractiveness of NET Phase 2 which, due to modal shift from car to tram, might yield various reductions in traffic density. Hence, for the traffic scenarios investigated in this section, the relationship between the traffic flow and speed was assumed to follow the top part of Figure 5.10.

$$\text{2021 Amended Traffic Speed} = \text{2021 Original Traffic Speed} \times \frac{\text{2021 Original Traffic Flow}}{\text{2021 Amended Traffic Flow}} \qquad \textbf{(8.2)}$$

For each case tested, the amended traffic flows and speeds were input into the air pollution model which was run to output the 2021 annual mean NO_2 concentrations at the two test receptors. Each time, the output 2021 annual mean NO_2 concentration at the Beeston Road receptor was multiplied by the GIS-based factor, explained in Section 6.4.5.3. Table 8.2 shows the output annual mean NO_2 concentrations at the two test receptors for the four most effective flow/speed amendment cases that were tested. Figure 8.18 to Figure 8.21 show the reductions made to the original 2021 Do-Something traffic flows for these four most effective flow/speed amendment test cases.

Table 8.2 Output NO_2 Concentrations at the Two Test Receptors for the Four Most Effective Flow/Speed Amendment Test Cases

Case ID*	annual mean NO_2 concentrations $\mu g/m^3$		
	Derby Road roundabout	Beeston Road	Objective
11	39.97	39.99	40
12	39.97	39.94	40
13	39.99	39.99	40
14	39.99	39.95	40

* see traffic flow conditions assumed for each case in Figures 8.18 to 8.21.

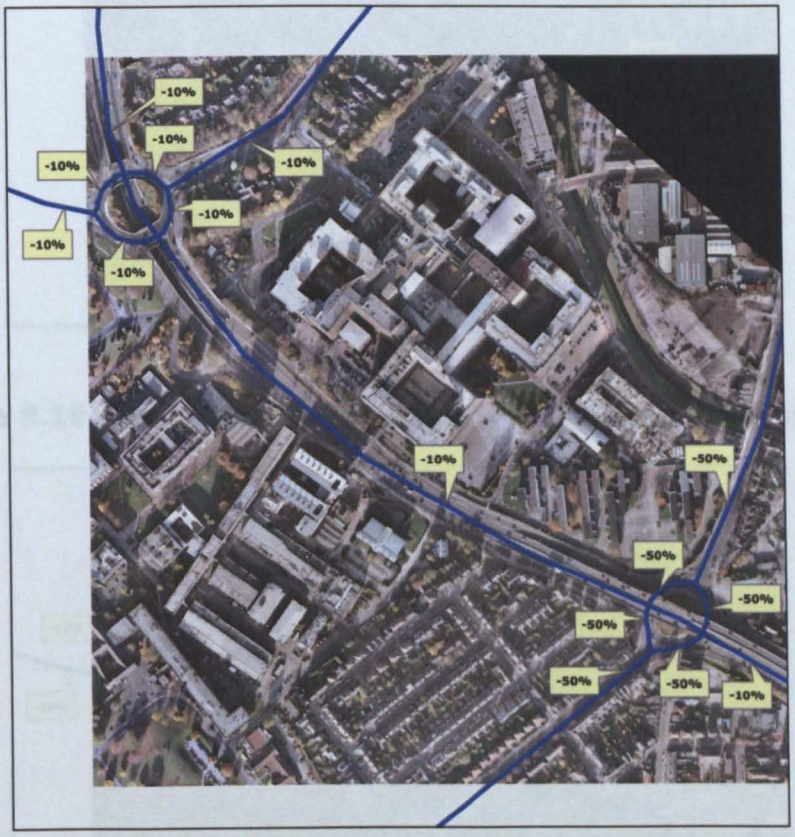

Figure 8.18 Percentages of Traffic Flow Reductions for Case 11

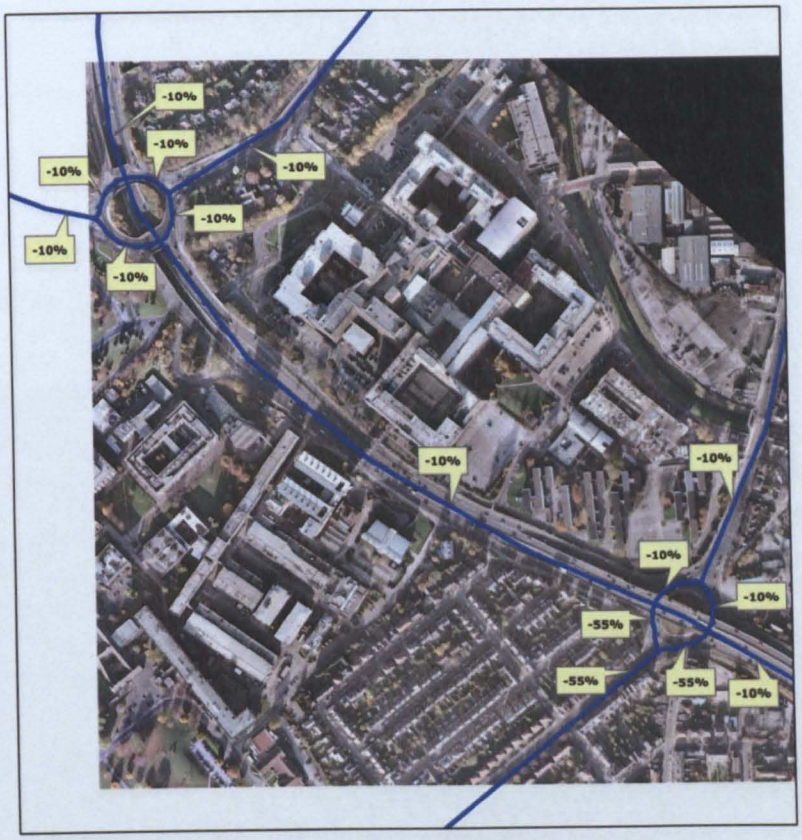

Figure 8.19 Percentages of Traffic Flow Reductions for Case 12

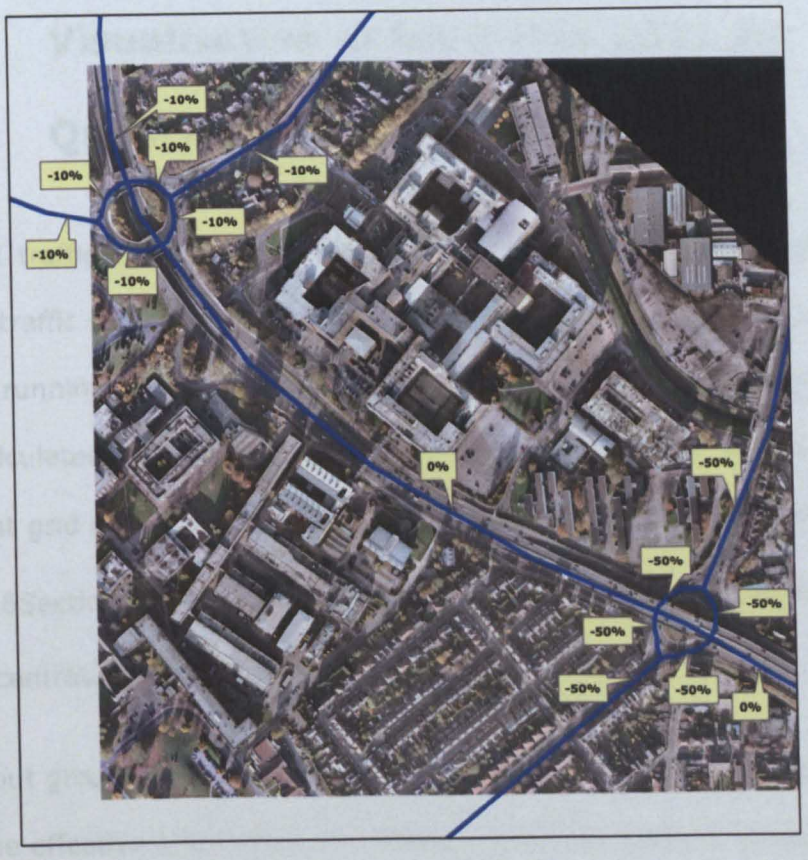

Figure 8.20 Percentages of Traffic Flow Reductions for Case 13

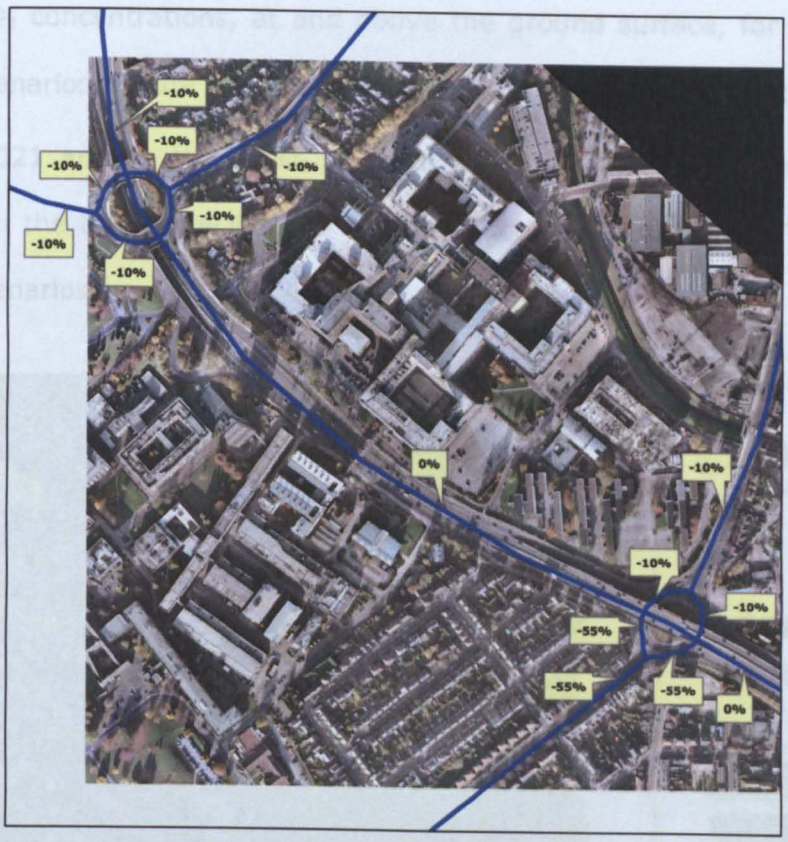

Figure 8.21 Percentages of Traffic Flow Reductions for Case 14

8.4.4 Visualisation of Enhanced 2021 Air Quality in Dunkirk AQMA

The 2021 traffic flow and speed data for the most effective alternative NET Phase 2 traffic scenarios were used along with the 2021 air pollution input data for running ADMS-Roads. The 2021 annual mean NO_2 concentrations were calculated by ADMS-Roads at the output receptor points of the intelligent grid described in Section 6.5. The GIS-based factor, explained in Chapter 6Section 6.4.5.3, was applied to the 2021 calculated annual mean NO_2 concentrations in the Beeston Road area.

The output ground-level annual mean NO_2 concentrations were very similar for all the effective alternative NET Phase 2 traffic scenarios, cases 7 to 14. Therefore, it was decided to generate just one set of the output annual

mean NO_2 concentrations, at and above the ground surface, for all these traffic scenarios. Figure 8.22 to Figure 8.27 show the output contour maps of the 2021 annual mean NO_2 concentrations, at and above the ground surface in the Dunkirk AQMA, for all the effective alternative NET Phase 2 traffic scenarios.

Figure 8.22 Contour Map of 2021 Ground-level Annual Mean NO_2 Concentrations in the Dunkirk AQMA for the Effective Alternative NET Phase 2 Traffic Scenarios

Figure 8.23 Contour Map of 2021 6 metres-height Annual Mean NO_2 Concentrations in the Dunkirk AQMA for the Effective Alternative NET Phase 2 Traffic Scenarios

Figure 8.24 Contour Map of 2021 12 metres-height Annual Mean NO_2 Concentrations in the Dunkirk AQMA for the Effective Alternative NET Phase 2 Traffic Scenarios

Figure 8.25 Contour Map of 2021 18 metres-height Annual Mean NO_2 Concentrations in the Dunkirk AQMA for the Effective Alternative NET Phase 2 Traffic Scenarios

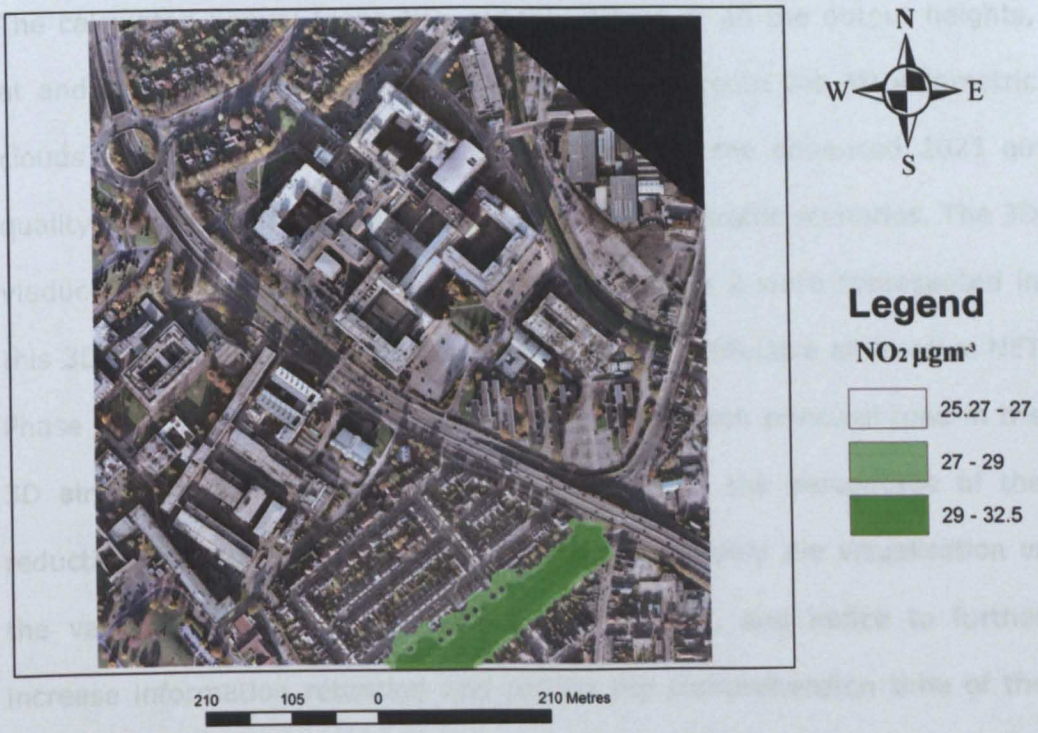

Figure 8.26 Contour Map of 2021 24 metres-height Annual Mean NO_2 Concentrations in the Dunkirk AQMA for the Effective Alternative NET Phase 2 Traffic Scenarios

Figure 8.27 Contour Map of 2021 30 metres-height Annual Mean NO_2 Concentrations in the Dunkirk AQMA for the Effective Alternative NET Phase 2 Traffic Scenarios

The calculated annual mean NO_2 concentrations at all the output heights, at and above the ground surface, were used to create the 3D volumetric clouds air pollution dispersion interfaces to show the enhanced 2021 air quality for all the effective alternative NET Phase 2 traffic scenarios. The 3D viaduct, tram objects and tram stop of NET Phase 2 were represented in this 3D air pollution dispersion interface. For each effective alternative NET Phase 2 traffic scenario, it was decided to colour each principal road in the 3D air pollution dispersion interface according to the percentage of the reduction in its traffic flows. This was done to simplify the visualisation of the various percentages of traffic flow reduction, and hence to further increase information retention and reduce the comprehension time of the 3D air pollution dispersion interfaces for these traffic scenarios.

The GIS functionality of ArcGIS 9.2 was used to create 2D polygons for the principal roads considered in the air pollution model of the Dunkirk AQMA.

These polygons were split into roads on the ground level and roads on ramps. The base heights of the roads on the ground level were interpolated from the DTM of the Dunkirk AQMA in ArcGIS 9.2. The functionality of AutoCAD Civil 3D was used to convert the 2D polygons of the roads on ramps to 3D polygons by using the CAD models of the ramps. Figure 8.28 to Figure 8.35 display screenshots of the 3D air pollution dispersion interfaces for the effective alternative NET Phase 2 traffic scenarios.

Figure 8.28 3D Air Pollution Dispersion Interface for Case 7

Figure 8.29 3D Air Pollution Dispersion Interface for Case 8

Figure 8.30 3D Air Pollution Dispersion Interface for Case 9

Figure 8.31 3D Air Pollution Dispersion Interface for Case 10

Figure 8.32 3D Air Pollution Dispersion Interface for Case 11

Figure 8.33 3D Air Pollution Dispersion Interface for Case 12

Figure 8.34 3D Air Pollution Dispersion Interface for Case 13

Figure 8.35 3D Air Pollution Dispersion Interface for Case 14

8.5 Projection of Air Pollution Input Data to 2021 Assuming Partial Future Technology Benefits

The impacts of the introduction of NET Phase 2 in the Dunkirk AQMA were not considered in the air pollution modelling of either the 2021 Do-Minimum traffic scenario or the 2006 base case scenario. Although the traffic flows of the 2021 Do-Minimum scenario were higher than the traffic flows of the 2006 base case scenario, the predicted 2021 Do-Minimum air quality was much better than the 2006 air quality. This was shown by the size of the area where NO_2 levels exceeded the annual mean AQO in the Dunkirk AQMA. This area was much smaller in 2021 than it was in 2006 as indicated by the NO_2 ground-level contour maps in Figure 6.16 and Figure 8.1. Therefore, it was decided to investigate the impact of assuming less than the full anticipated future emission reductions due to improved vehicle

technology and better fuel standards, on the 2021 Do-Minimum air quality in the Dunkirk AQMA.

8.5.1 Projection of Air Pollution Input Data to 2021 Assuming 50% Future Technology Benefits

The background concentrations and the traffic-induced emissions were projected from 2006 to 2021 only allowing for 50% of the anticipated future emission reductions due to technological advances in vehicle manufacturing and the fuel industry. The new hourly sequential background concentrations of NO_2, NO_X and O_3 were calculated by using the micro-calibrated 2006 background concentrations and the fully projected 2021 background concentrations as follows:

$$50\%\ \text{background}_i = \frac{background_{2021\ fully\ projected\ i} + background_{2006\ i}}{2}, \quad \textbf{(8.3)}$$

where i ranges from 1 to 8760, the total number of hours in a year. 2013 was selected as the modelling year for emissions in the air pollution model as it is half-way between 2006 and 2021. This effectively projected the traffic-induced emissions from 2006 to 2021 only allowing for 50% of the anticipated future emission reductions due to using improved vehicle technology and better fuel standards. The 2006 values of the industry-induced emissions, and the monthly and hourly traffic profiles, were used in 2021 with no future projection.

The modified 2021 air pollution data were used with the 2021 traffic data of the Do-Minimum scenario, and the dummy emissions modelling year of 2013, to run ADMS-Roads. Figure 8.36 shows the ground-level contour map of the 2021 annual mean NO_2 concentrations in the Dunkirk AQMA.

The comparison between Figure 8.1 and Figure 8.36 implied a significant variation in the modelled air quality impact depending on the extent of assumed future emission reductions due to improved vehicle technology and better fuel standards.

Figure 8.36 50% Projected 2021 Ground-level Annual Mean NO_2 Concentrations in the Dunkirk AQMA

8.5.2 Projection of Air Pollution Input Data to 2021 Assuming Zero Future Technology Benefits

In order to confirm as much as possible the significance of assuming the full anticipated future emission reductions due to improved vehicle technology and better fuel standards, the 2021 Do-Minimum air quality was predicted assuming no allowance for these anticipated future emission reductions. In addition to the industry-induced emissions, and the monthly and hourly traffic profiles, the background concentrations and the traffic-

induced emissions were not projected from 2006 to 2021. In this case, the 2006 micro-calibrated background concentrations were used in the 2021 Do-Minimum scenario. The 2006 traffic emission factors were used for the 2021 Do-Minimum scenario by selecting 2006 as the modelling year in the air pollution model. The resulting air pollution data were used with the 2021 traffic data of the Do-Minimum NET Phase 2 traffic scenario to run ADMS-Roads. Figure 8.37 shows the ground-level contour map of the 2021 annual mean NO_2 concentrations in the Dunkirk AQMA.

Figure 8.37 Non-projected 2021 Ground-level Annual Mean NO_2 Concentrations in the Dunkirk AQMA

Comparing Figure 8.1, Figure 8.36 and Figure 8.37 confirmed the significant variation in the modelled air quality impact depending on the extent of assumed future emission reductions due to improved vehicle technology and better fuel standards.

8.6 Summary

In this chapter, the developed decision-support system in this research project was applied to predict and visualise the future air quality impacts of the implementation of NET Phase 2 in the Dunkirk AQMA. This necessitated the projection of the air pollution input data for the Dunkirk AQMA base case scenario model from 2006 to 2021. The Year Adjustment Calculator was used for the projection of the micro-calibrated background concentrations from 2006 to 2021.

The 2006 monthly and hourly traffic profiles were used for the 2021 air quality predictions, thus assuming no change in the future traffic profiles. The air quality impacts of the future industry-induced emissions in the Dunkirk AQMA were outside the scope of this research project. Therefore, it was decided to use the 2006 industrial emission rates of NO_X as NO_2 for the 2021 Do-Minimum and Do-Something air quality scenarios.

The comparison between the ground-level contour maps of the 2021 annual mean NO_2 concentrations for the 2021 Do-Minimum and Do-Something traffic scenarios, shown in Figure 8.1 and Figure 8.2, implied that the air quality impact of the implementation of NET Phase 2 would not be significant at all in the Dunkirk AQMA. Therefore, it was decided to generate just one set of the output 2021 annual mean NO_2 concentrations above the ground surface for both the 2021 Do-Minimum and Do-Something NET Phase 2 traffic scenarios. Figure 8.11 depicts a screenshot of the 3D volumetric clouds air pollution dispersion interface for either the Do-Minimum or the Do-Something 2021 NO_2 air quality in the Dunkirk AQMA.

The effectiveness of many alternative versions of the 2021 Do-Something NET Phase 2 traffic scenario was investigated, to relate conceptually to revoking totally the Dunkirk AQMA in 2021. The alternative 2021 NET Phase 2 traffic scenarios were generated by changing only the traffic speed, then changing only the traffic flow, and finally changing both the traffic flow and speed, for all the principal roads in the Dunkirk AQMA. Changing the traffic speed only was not enough to achieve the annual mean NO_2 AQO at the two locations exceeding this AQO in the original 2021 Do-Something scenario.

Changing the traffic flow only resulted in four effective alternative NET Phase 2 traffic scenarios, shown in Figure 8.14 to Figure 8.17. Changing both the traffic flow and speed resulted in four other effective alternative NET Phase 2 traffic scenarios, shown in Figure 8.18 to Figure 8.21. Changing both the traffic flow and speed meant that the required traffic flow reductions were 4% less than for the corresponding traffic flow only scenarios.

The principal roads in the 3D air pollution dispersion interfaces for the effective alternative NET Phase 2 traffic scenarios were each coloured according to the required percentage reduction in their traffic flows. This simplified the visualisation of the traffic flow reduction percentage, which varied from one road to another in the same traffic scenario. Figure 8.28 to Figure 8.35 display screenshots of the 3D air pollution dispersion interfaces of the effective alternative NET Phase 2 traffic scenarios. The modelled air quality benefits of assuming the full anticipated future emission reductions due to improved vehicle technology and better fuel standards significantly outweighed the adverse air quality impacts of the forecast future traffic growth in the Dunkirk AQMA. This was confirmed by comparing Figure 8.1,

Figure 8.36 and Figure 8.37, in which the less was the consideration of the air quality benefits of these future assumptions, the larger was the 2021 area within the Dunkirk AQMA where the AQO of annual mean NO_2 concentrations was exceeded.

Chapter 9

Transferability of the Decision-support System to Other Future Transport Schemes

9.1 Introduction

The aim of this chapter is to evaluate the transferability of the decision-support system resulting from this research to two other transport schemes different from the transport scheme which was used in the initial development of the decision-support system. Therefore, research was undertaken into the use of the developed decision-support system for the prediction and visualisation of the potential air quality impacts of the future Turning Point East and Broadmarsh Shopping Centre Extension transport schemes, which were introduced in Section 2.7 and selected in Section 4.3. This also included the investigation of the contribution of these two transport schemes to possibly revoking the Nottingham City Centre AQMA in the future. The aim of this chapter was achieved by the investigation of eight main objectives:

1. The identification of the air pollution model application area.
2. The set-up of the base case scenario.
3. The geospatial data processing of the road network.
4. The calibration and validation of the base case scenario model.
5. The description of the grid design and height limit and step determination of the air pollution model output receptors.

6. The creation of the 3D air pollution dispersion interface for the base case scenario.
7. The future projection of the traffic and air pollution data of the base case scenario to after the implementation of the Turning Point East and Broadmarsh Shopping Centre Extension transport schemes.
8. The prediction and visualisation of the future air quality impacts of these two transport schemes in the 3D city model of the City Centre air pollution model application area.

The two transport schemes featured in this chapter are specifically different to each other and to the NET Phase 2 implementation through the Dunkirk AQMA schemes, in that whereas the latter is concerned with adding substantial new transport infrastructure (for an additional mode of transport) to the existing infrastructure, the Turning Point East scheme is concerned with changing the operation of certain roads, and the Broadmarsh Shopping Centre Extension scheme is concerned with changing the road network in one part of the city centre. Modelling the air quality impacts of the two transport schemes featured in this chapter requires many more roads to be considered in ADMS-Roads than was the case in the Dunkirk AQMA context, which generated the research to be described in Section 9.4.

9.2 Air Pollution Model Application Area

The areas containing the roads directly affected by the implementation of the Turning Point East and the Broadmarsh Shopping Centre Extension transport schemes partially coincide with the City Centre AQMA, as shown in Figure 2.2, and the two continuous air quality monitoring stations in the city centre (the AURN and the Carter Gate monitoring stations described in

Section 2.4) are nearby. Therefore, the initial boundary of the air pollution model application area was drawn so that it contained the roads directly affected by the two transport schemes, all of the City Centre AQMA, and the locations of the two continuous air quality monitoring stations, as shown by the darker shaded area in Figure 9.1. Hence the air pollution model would be validated against air pollution monitoring data measured within the model application area (DEFRA, 2009).

To get precise air quality predictions inside the initial model application area, the traffic emission contributions of the road segments located within 200 metres from this area had to be considered in the air pollution model (DMRB, 2007). Therefore, the final boundary of the air pollution model application area was drawn so that it included the initial model application area and the 200-metre buffer zone around this area, as shown by the lighter shaded area in Figure 9.1.

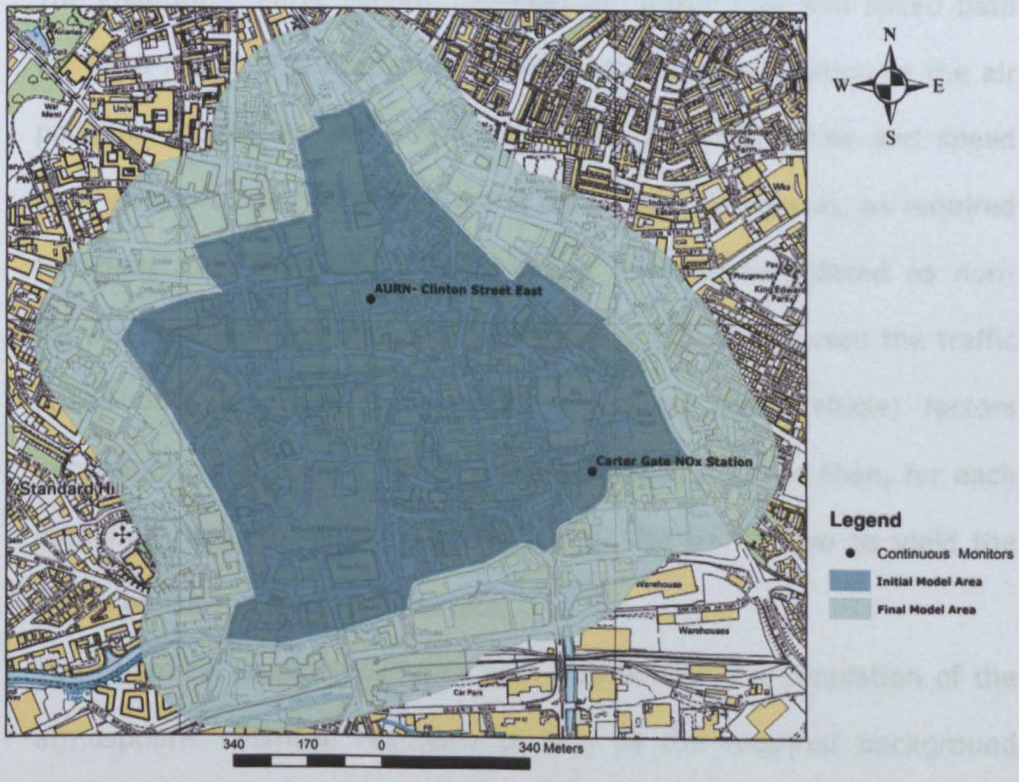

Figure 9.1 Central Nottingham Air Pollution Model Application Area

9.3 Set-up of Base Case Scenario Modelling

As NO_2 was the air pollutant of concern in the City Centre AQMA, NO_2 was selected as the primary output air pollutant of the air pollution model. Due to the atmospheric chemical reactions between NO_X and O_3 which affect NO_2 concentrations in the atmosphere, NO_X and O_3 were also selected as output air pollutants of the air pollution model. Discussions with the Pollution Control Section in Nottingham City Council were undertaken to help with the identification of the set-up of the base case scenario in ADMS-Roads. These consultations resulted in the following set-up:

- 2006 was selected as the base case year due to the availability of air pollution data required for running and validating the air pollution model.
- The Pollution Control Section provided the traffic flow and speed data for 78 A roads, 5 B roads and 25 C roads for consideration in the air pollution model. For each of these roads, the traffic flow and speed data were provided for the LDV and HDV traffic categories, as required for input to ADMS-Roads. These roads were all considered as non-canyon streets in the air pollution model. ADMS-Roads used the traffic speed data to identify the traffic emissions (per vehicle) factors according to the built-in 2003 DMRB database, in order then, for each modelled road, to multiply the factor by the traffic flow to yield the traffic emissions (per second) rate.
- The Chemical Reaction Scheme was selected for the simulation of the atmospheric chemical reactions of NO_x as the required background concentrations of NO_x, NO_2 and O_3 were available.

- Surface roughness = 1.0, latitude = 52° and minimum Monin-Obukov length = 30.
- Three point sources were defined in the base case scenario and other future scenarios: London Road Heat Station, EON Ratcliffe power station and the chimney of Daleside Dyers & Finishers Ltd. The emitted pollutant was NO_x as NO_2. As the chemical reactions option was selected, ADMS-Roads assumed that 10% of NO_x as NO_2 emissions was NO_2.
- The 2006 hourly sequential meteorological data measured by the Nottingham Watnall Weather Station was used for all air quality modelling scenarios. The meteorological data included 10 parameters: Station Number, Year, Day, Hour, Temperature, Wind Speed, Wind Direction, Precipitation, Cloud Cover and Degree of Humidity. The wind speed was measured at 10 metres height and the wind sector size was 10°. Figure 6.2 shows the 2006 wind rose. It was assumed that the weather conditions in the Watnall and City Centre areas of Nottingham were identical at all times.
- The 2006 hourly sequential concentrations, measured by the Rochester air quality monitoring station, were used as background levels in the base case scenario model. This is an AURN station sited at a rural site distant from urban air pollution, as shown in Figure 6.3, and hence DEFRA recommends using its monitoring data as background levels for modelling urban air quality in the UK to avoid double counting issues. The background concentrations comprised NO_x, NO_2, O_3, PM_{10} and SO_2 concentrations.
- The base case scenario model was configured to output the modelled 2006 hourly calculated and annual mean NO_x, NO_2 and O_3

concentrations at the sites of the AURN and Carter Gate continuous monitoring stations, described in Section 2.4.

9.4 Geospatial Data Processing of the Road Network

The roads for which traffic flow and speed data were provided by the Pollution Control Section, were defined by the origin and destination of each road. However, ADMS-Roads requires the geographical coordinates of the vertices of each road's centreline. As there were so many roads and as some were long roads, the conventional digitisation of these roads on a digital map in a GIS system would have been labour-intensive and would have taken a long time. Moreover, the digitisation of the long roads required zooming in, zooming out and panning across many map views while digitising a single road. This was not supported by the ArcGIS-ADMS link, which was supplied by CERC with the ADMS-Roads software.

The CERC helpdesk advised to split every long road into many shorter roads so that each of them could be digitised in one map view. However, this meant increasing the already large number of roads to the extent that the number of roads exceeded the maximum number of roads that could be defined in ADMS-Roads, which is 150. Furthermore, the conventional digitisation of these roads required familiarity with the names and centreline locations of the roads on the map. The lack of such familiarity increased further the complexity and the time required for looking up and digitising the centrelines of these roads on a digital map.

To overcome this digitisation problem, a tool was created by the author with Python, an object-oriented computer programming language, in

ArcGIS 9.2 to import the geographical coordinates of the vertices of the roads' centrelines into ADMS-Roads without any digitisation. The centreline of each road was automatically generated by inputting the road's origin and destination into the 'From-To' utility of Google Earth (Google, 2009). The generated centrelines in Google Earth were saved in a KML format, the native file format for Google Earth. The tool simultaneously read the KML files of all the roads and converted them to polyline shape files. Then, the tool automatically clipped every polyline shape file with the polygon shape file of the final air pollution model application area, to leave only the parts of the polyline shape file located inside this area. The clipped polyline shape files were automatically projected by the tool from the Google Earth coordinate system to the coordinate system of the air pollution model application area polygon shape file by using a describe ArcObject, a computer object in ArcGIS 9.2 which was used internally by the tool.

For a given road, a high LOD corresponded to a large number of vertices, which means a more accurate representation of the road centreline, but a longer model runtime. In order to avoid the high LOD of the original road centrelines in Google Earth, for every projected polyline shape file, the tool automatically read the coordinates of the vertices which were not within an input tolerance, a user-specified minimum allowable distance between the vertices. The tolerance determined the LOD of the processed roads by controlling the number of every road's centreline vertices to be read. This was accomplished by skip reading the vertices that were a smaller distance apart than the input tolerance for every projected polyline shape file. Then, the tool automatically wrote the read vertices' coordinates, along with the relevant road name, to an output table. The output table of the vertices' coordinates was imported into the emissions inventory file which

enabled the road centrelines geospatial data to be imported automatically into ADMS-Roads. Figure 9.2 displays the flowchart of this new GIS tool.

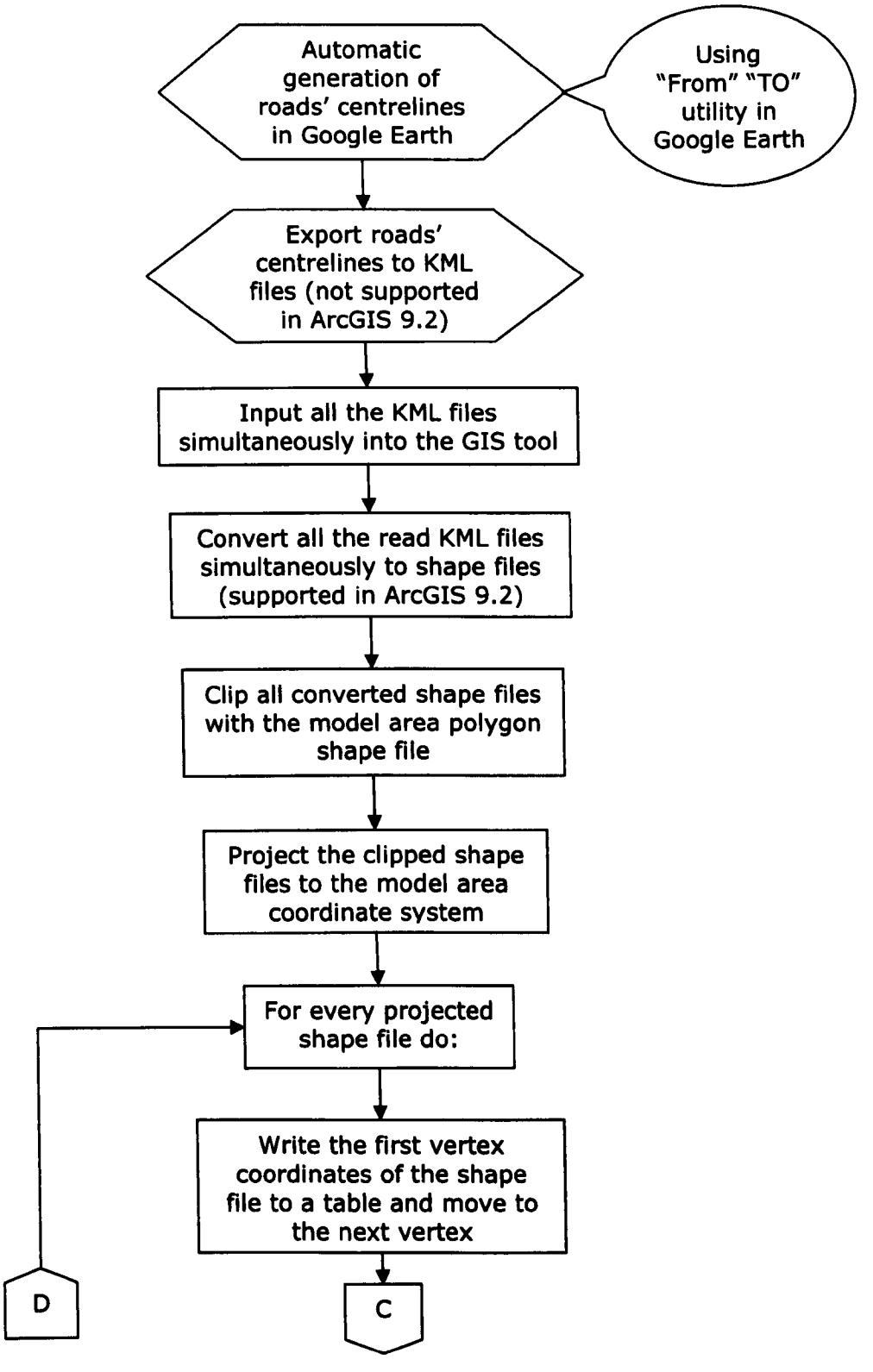

Figure 9.2a Flowchart of the New GIS Tool

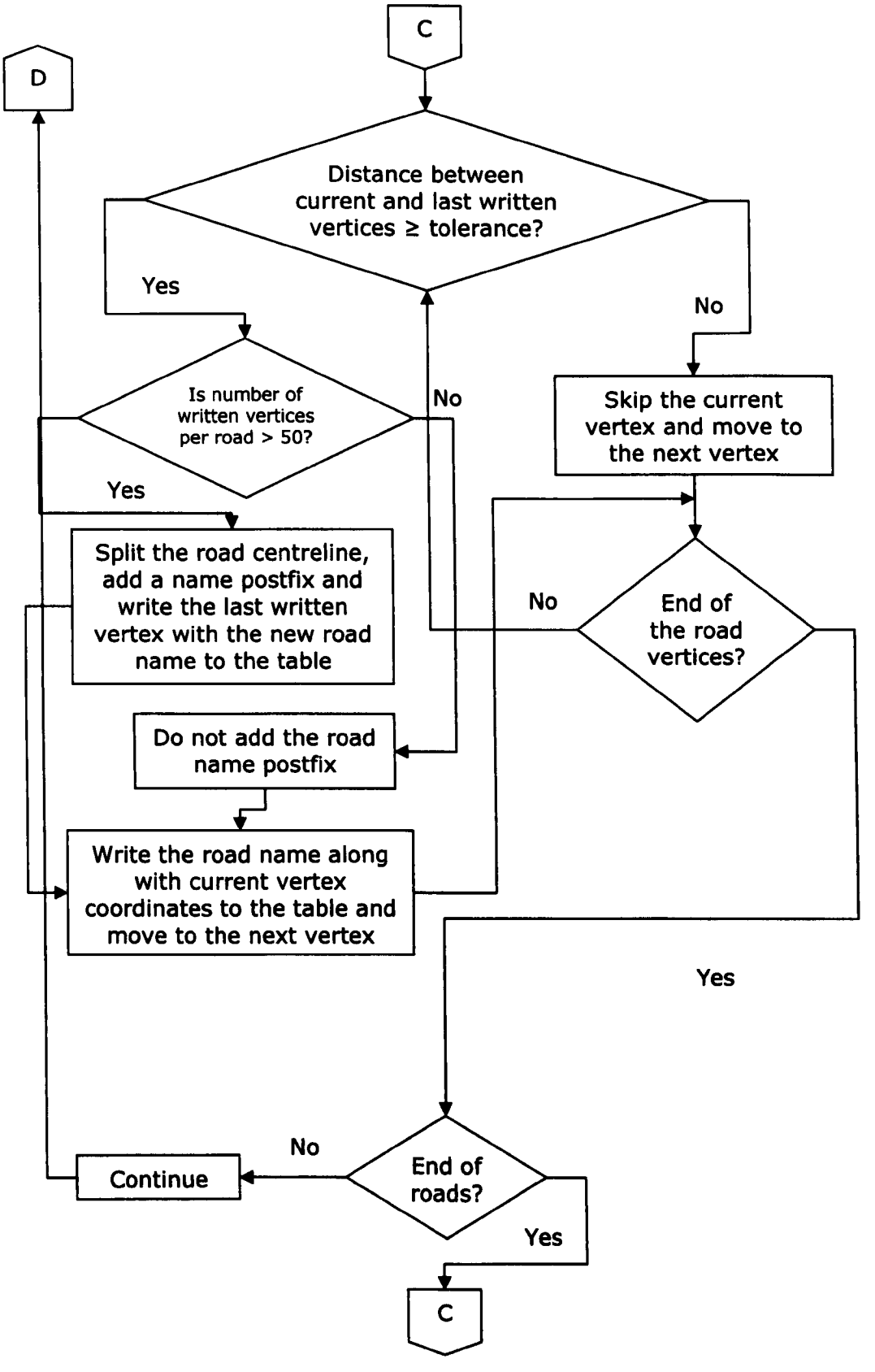

Figure 9.2b Flowchart of the New GIS Tool (continued)

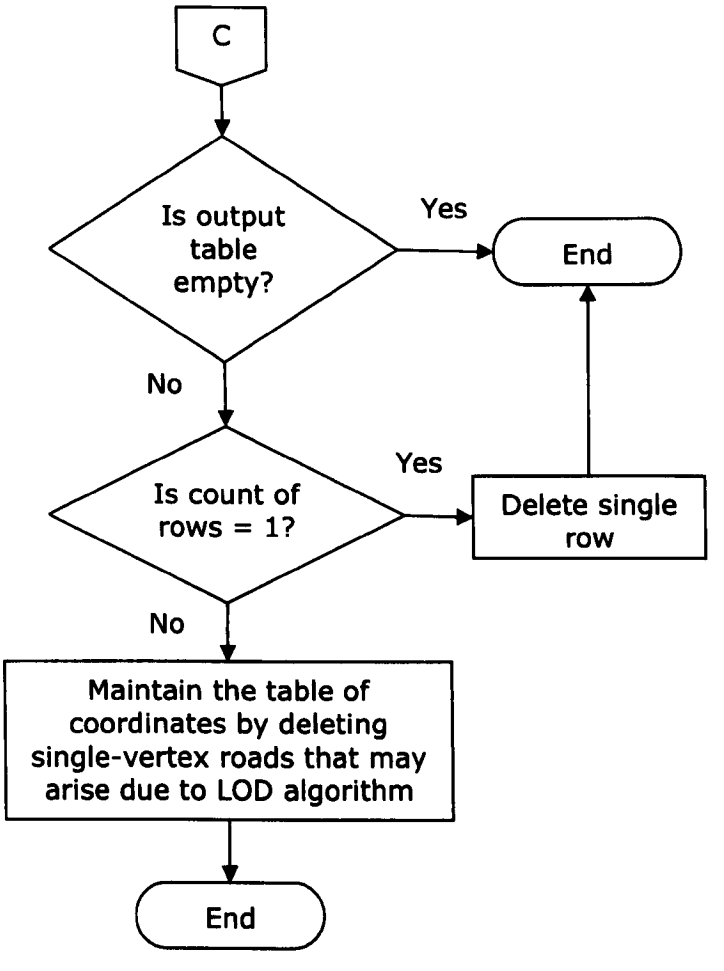

Figure 9.2c Flowchart of the New GIS Tool (continued)

The new GIS tool complied with the ADMS-Roads technical requirements in terms of the maximum allowable number of vertices (50) for any one road. If the number of the road vertices exceeded 50, the tool would automatically split the road and start a new segment of the road with the same road's name plus a name postfix. This was done because ADMS-Roads does not allow many roads to be defined under the same name. Moreover, the vertex counter started again from 1 for every new segment of the same road.

The implementation of the LOD algorithm, shown in Figure 9.2b, resulted in many single-vertex roads in the output table of road vertices' coordinates. This necessitated intervention using Python in the new GIS tool to

automate the maintenance of the output table of coordinates after the implementation of the LOD algorithm. The output table maintenance algorithm, shown in Figure 9.2c, automatically removed the single-vertex roads from the output table and tackled the raised error in two special cases. The first special case was having an empty output table when all the processed roads do not intersect with the model application area polygon shape file. The second special case was having one single-vertex road in the output table.

A help file, displaying a brief description of each item of the input data to the tool, was attached to the graphical user interface of the new GIS tool as shown in Figure 9.3. The new GIS tool provided a friendly graphical user interface for the tool console during the runtime. The runtime tool console printed the name of every processed road along with the number of its extracted vertices according to the required LOD after being processed successfully. Furthermore, the new GIS tool gave the user insight into the processing by printing the start, end and the results of each processing stage to the tool output console during the runtime as shown in Figure 9.4. Figure 9.5 displays the tool output road centrelines for the roads for which the traffic emissions were considered in the air pollution model.

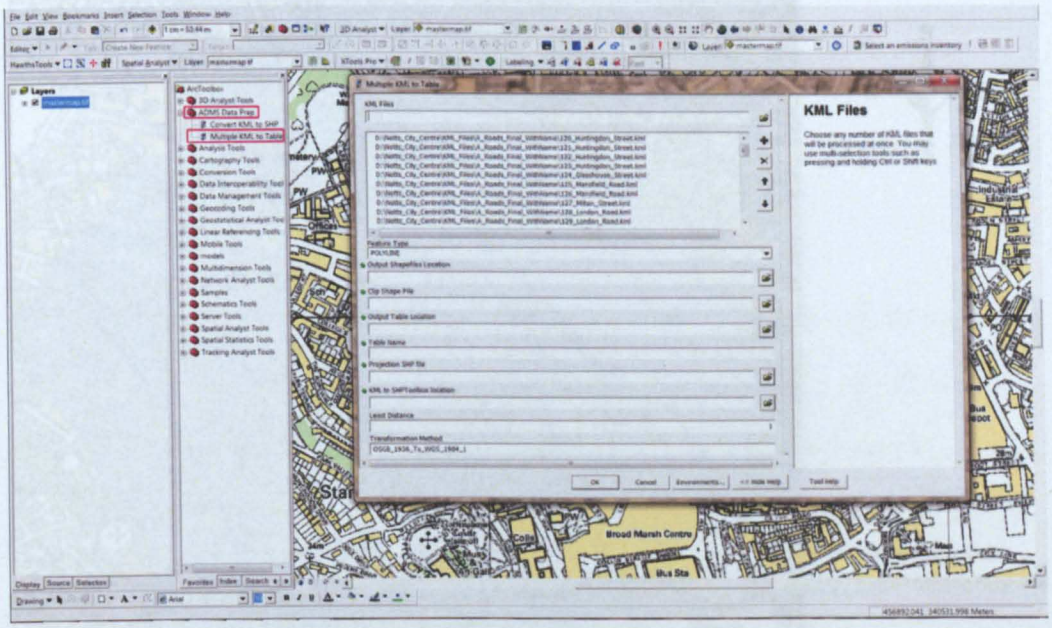

Figure 9.3 Data Entry Graphical User Interface of the New GIS Tool

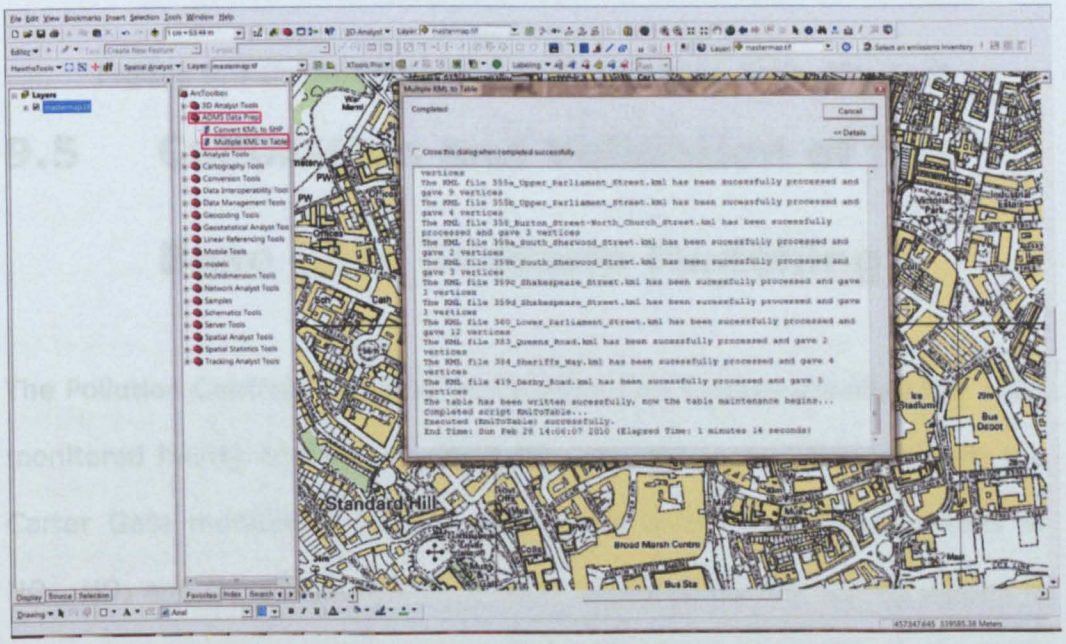

Figure 9.4 Runtime Console of the New GIS Tool

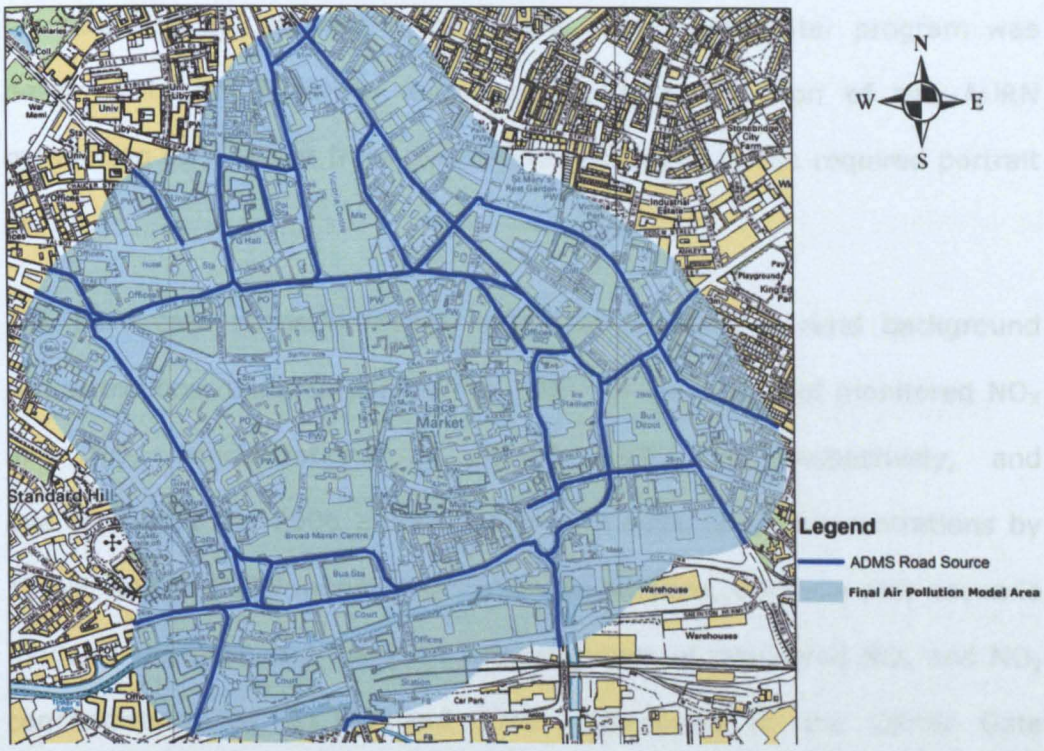

Figure 9.5 Output Road Centrelines of the New GIS Tool

9.5 Calibration and Validation of the Base Case Scenario Modelling

The Pollution Control Section in Nottingham City Council provided the 2006 monitored hourly and annual mean NO_X and NO_2 concentrations from the Carter Gate monitoring station. The hourly levels and annual means of NO_X, NO_2 and O_3, which were monitored by the AURN monitoring station in 2006, were downloaded from the UK Air Quality Archive. The downloaded hourly concentrations had a landscape layout which displayed the 24 day-hours in 24 columns and the 365 year-days in 365 rows. However, a portrait layout, consisting of one column and 8760 rows for 8760 year-hours, was required for the downloaded data, in order to facilitate the comparison between the hourly monitored concentrations and the hourly calculated concentrations for the base case scenario at the AURN. The large amount of downloaded data impeded its manual transformation from the

landscape to the portrait layout. Hence, a VBA computer program was designed in MS Excel to automate the transformation of the AURN monitoring data layout from the original landscape to the required portrait layout.

The base case scenario model, with the uncalibrated rural background concentrations, underestimated the 2006 annual means of monitored NO_X and NO_2 concentrations by 45.4% and 26% respectively, and overestimated the 2006 annual mean of monitored O_3 concentrations by 17.6%, at the AURN monitoring station. In addition, the base case scenario model underestimated the 2006 annual means of monitored NO_X and NO_2 concentrations by 31.1% and 23% respectively at the Carter Gate monitoring station, as implied by the results of run 1 in Table 9.1. This indicated the need for the calibration of the base case scenario model.

As O_3 concentrations were not monitored by the Carter Gate monitoring station, the AURN-monitored NO_X, NO_2 and O_3 concentrations were used for the investigation of the applicability of the Chapter 6 macro and micro-calibration strategies to the base case scenario model. The Carter Gate-monitored NO_X and NO_2 concentrations were kept independent of the calibration process for the validation of air quality predictions of the base case scenario model at the Carter Gate monitoring station.

9.5.1 Macro-calibration and Validation of the Base Case Scenario Modelling

The 2006 annual mean NO_2, NO_X and O_3 concentrations calculated using the uncalibrated rural background concentrations were substituted, along with the 2006 annual means of the AURN-monitored NO_2, NO_X and O_3 concentrations, into Equations (6.1), (6.2) and (6.3) to evaluate the

macro-calibration adjustment values for the rural background concentrations. Using the macro-calibrated background concentrations greatly improved the macro-validation results of the base case scenario model at both the AURN and Carter Gate monitoring stations, as indicated by the results of run 2 in Table 9.1.

9.5.2 Micro-calibration and Validation of the Base Case Scenario Modelling

The uncalibrated rural background concentrations were used for running the base case scenario model in order to output the 2006 hourly calculated NO_2 concentrations at the AURN and Carter Gate monitoring stations. This was for the micro-validation of the base case scenario model before any calibration as shown in Figure 9.6 and Figure 9.7. Then for the micro-validation after the macro-calibration, the base case scenario model was run with the macro-calibrated background concentrations to output the 2006 hourly calculated NO_2 concentrations at the AURN and Carter Gate monitoring stations. Figure 9.8 and Figure 9.9 illustrate the micro-validation results of running the macro-calibrated base case scenario model.

Table 9.1 Macro-calibration Results of the City Centre Base Case Scenario Model

RUN 1	Background	Δ background	Calculated Concentrations at AURN	Δ Calculated	Target concentrations at AURN	Calculated Concentrations at Carter Gate	Target concentrations at Carter Gate
NO_2	0	0	24.86	0	33.6	30.34	39.4
NO_x	0	0	34.16	0	62.56	59.16	85.9
O_3	0	0	44.84	0	38.54		
RUN 2	**Background**	**Δ background**	**Calculated Concentrations at AURN**	**Δ Calculated**	**Target concentrations at AURN**	**Calculated Concentrations at Carter Gate**	**Target concentrations at Carter Gate**
NO_2	+1.406	+1.406	35.38	+10.517	33.6	39.20	39.4
NO_x	+28.41	+28.41	62.57	+28.407	62.56	87.57	85.9
O_3	-2.571	-2.571	32.85	-11.982	38.54		
RUN 8	**Background**	**Δ background**	**Calculated Concentrations at AURN**	**Δ Calculated**	**Target concentrations at AURN**	**Calculated Concentrations at Carter Gate**	**Target concentrations at Carter Gate**
NO_2	+3.406	+2.000	36.76	+11.898	33.6	40.75	39.4
NO_x	+28.41	0	62.57	+28.407	62.56	87.57	85.9
O_3	-1.571	+1.000	34.54	-10.299	38.54		
RUN 9	**Background**	**Δ background**	**Calculated Concentrations at AURN**	**Δ Calculated**	**Target concentrations at AURN**	**Calculated Concentrations at Carter Gate**	**Target concentrations at Carter Gate**
NO_2	+3.406	0	37.23	+12.371	33.6	41.31	39.4
NO_x	+28.41	0	62.57	+28.407	62.56	87.57	85.9
O_3	-0.500	+1.071	36.01	-8.823	38.54		

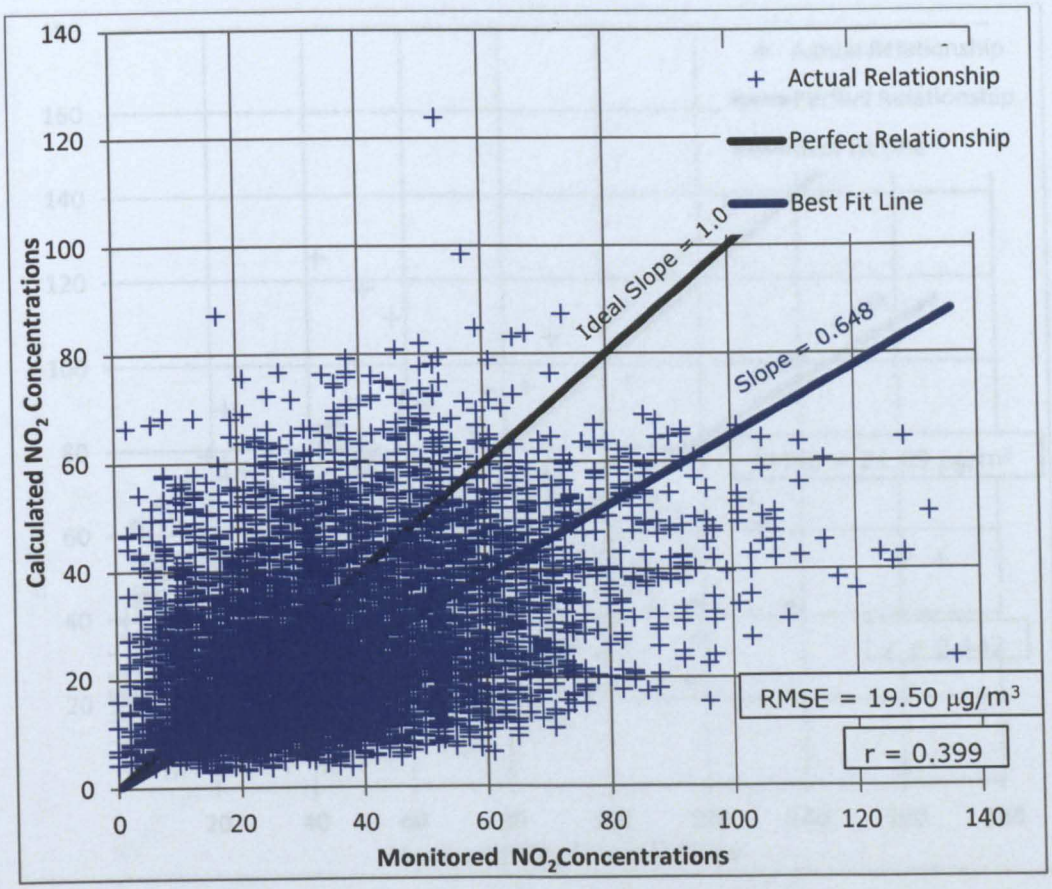

Figure 9.6 Scatter Diagram of Hourly NO_2 Concentrations at the AURN Station before Calibration

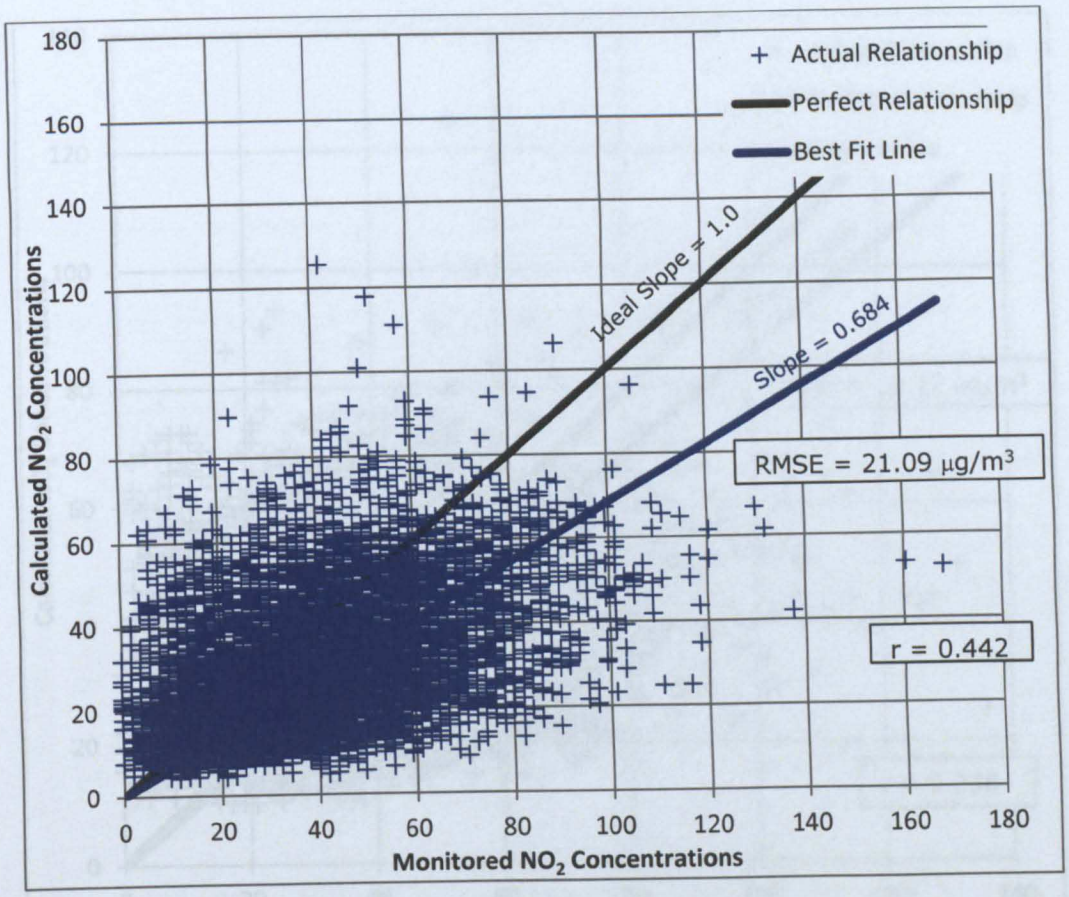

Figure 9.7 Scatter Diagram of Hourly NO_2 Concentrations at the Carter Gate Station before Calibration

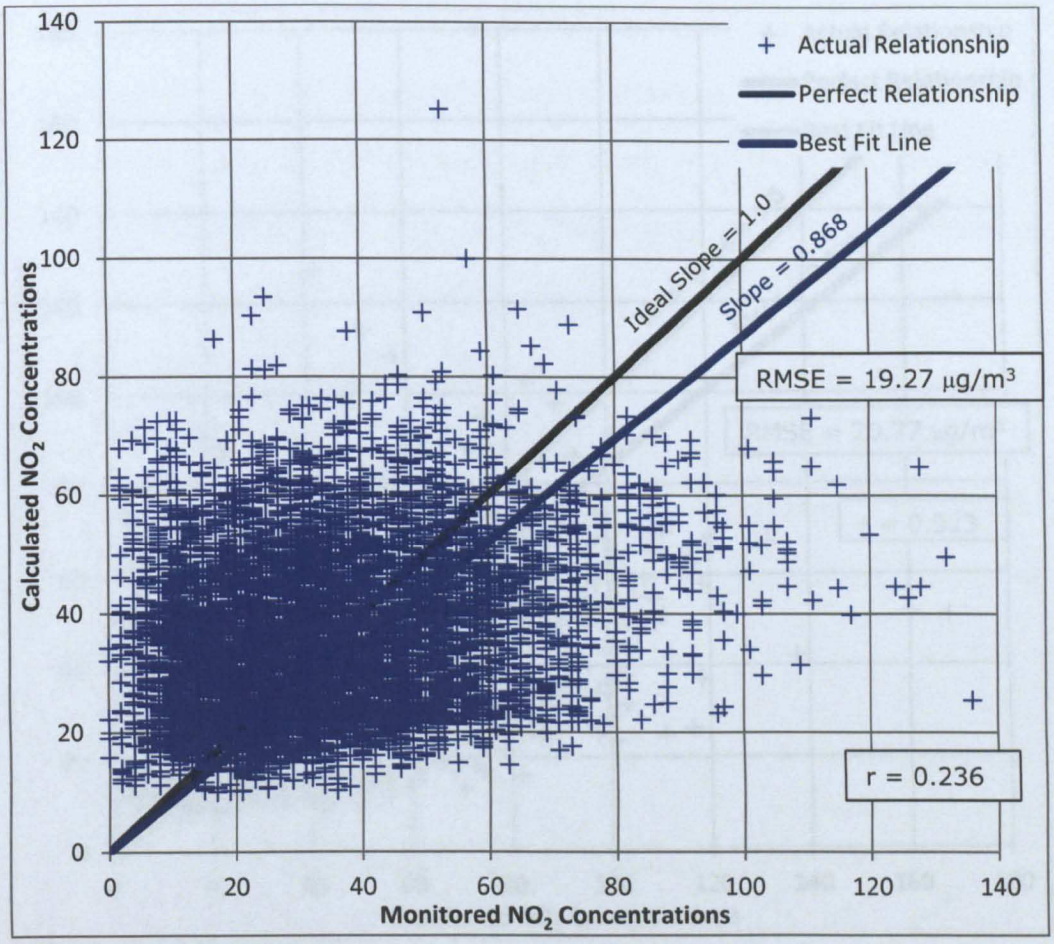

Figure 9.8 Scatter Diagram of Hourly NO_2 Concentrations at the AURN Station after Macro-calibration

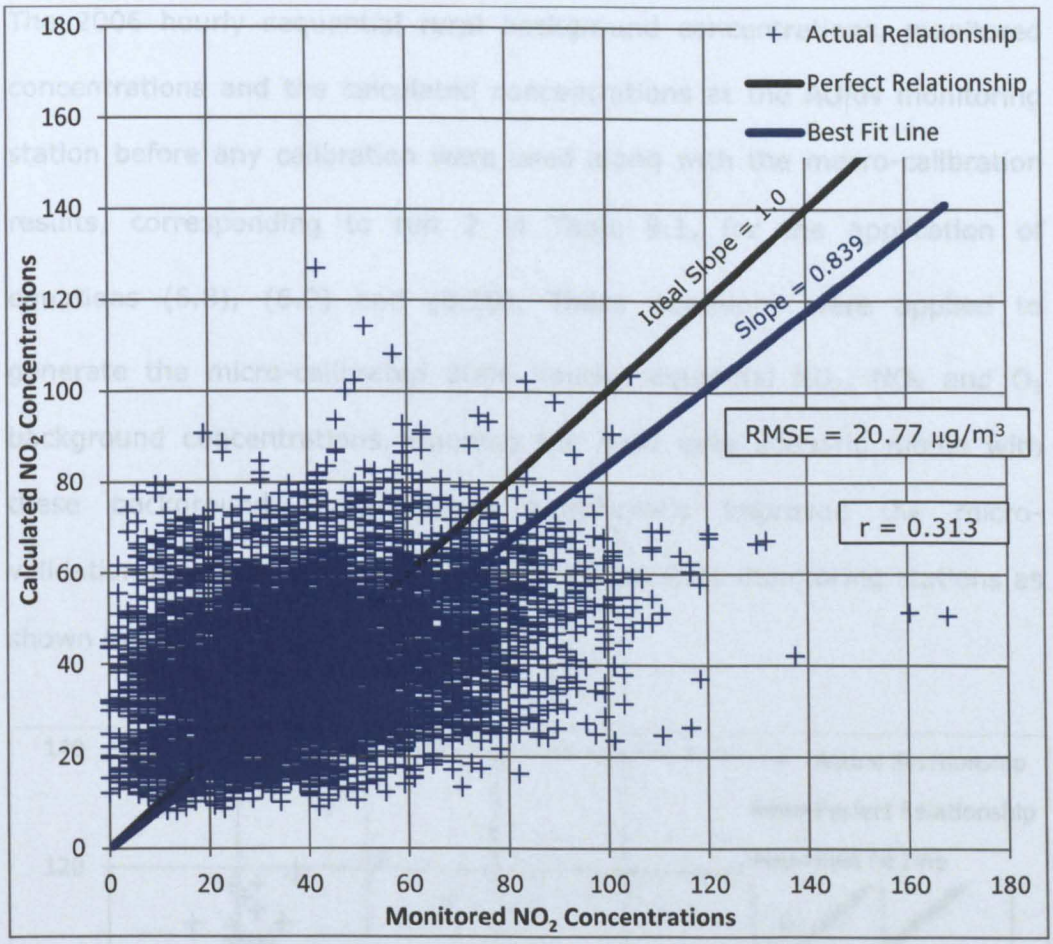

Figure 9.9 Scatter Diagram of Hourly NO_2 Concentrations at the Carter Gate Station after Macro-calibration

The macro-calibration of the base case scenario model slightly improved the micro-validation results at the AURN monitoring station, as implied by the comparison between the values of RMSE in Figure 9.6 and Figure 9.8. In addition, the comparison between the values of RMSE in Figure 9.7 and Figure 9.9 confirmed this slight improvement in the micro-validation results of the macro-calibrated base case scenario model at the independent receptor point of the calibration process, the Carter Gate monitoring station. This indicated the need for the application of the micro-calibration strategy in order to improve effectively the micro-validation results of the base case scenario model.

The 2006 hourly sequential rural background concentrations, monitored concentrations and the calculated concentrations at the AURN monitoring station before any calibration were used along with the macro-calibration results, corresponding to run 2 in Table 9.1, for the application of equations (6.8), (6.9) and (6.10). These equations were applied to generate the micro-calibrated 2006 hourly sequential NO_2, NO_X and O_3 background concentrations. Running the base case scenario model with these background concentrations significantly improved the micro-validation results at both the AURN and Carter Gate monitoring stations as shown in Figure 9.10 and Figure 9.11.

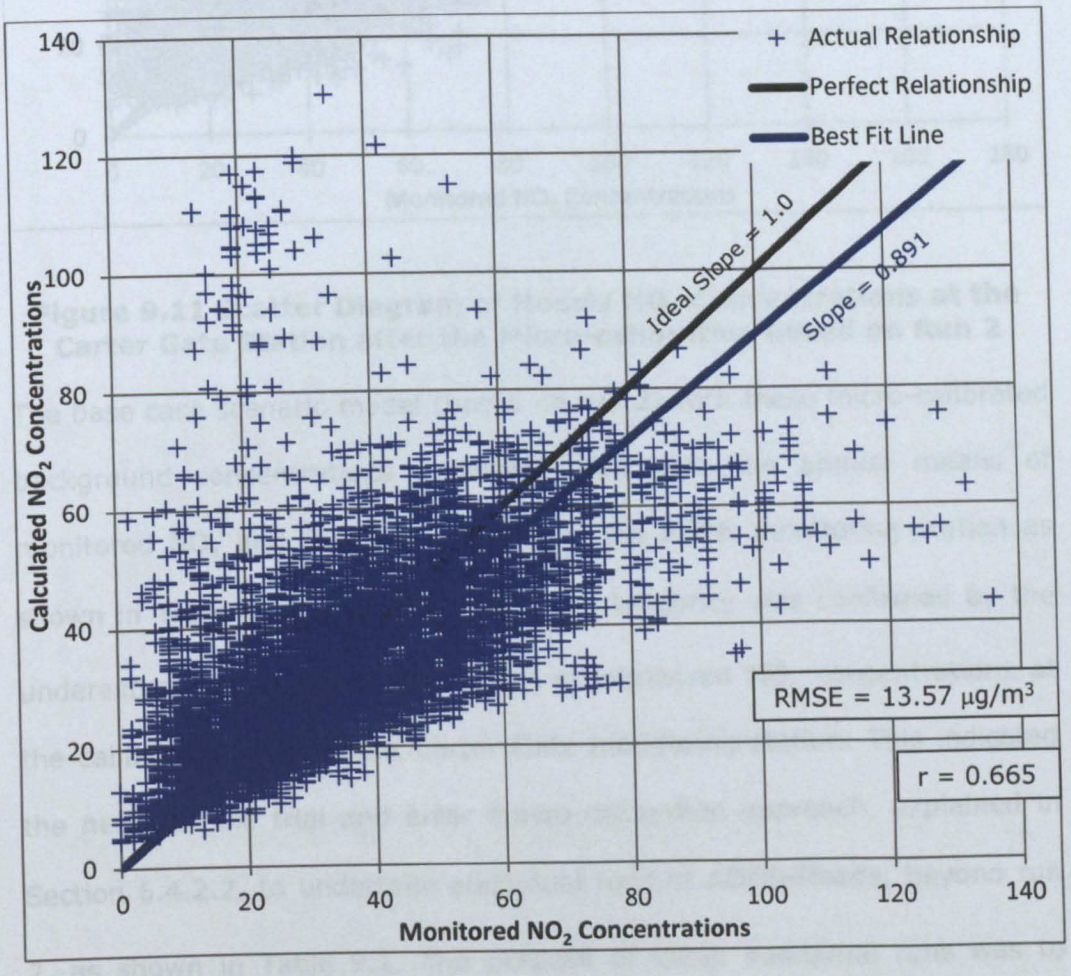

Figure 9.10 Scatter Diagram of Hourly NO_2 Concentrations at the AURN Station after the Micro-calibration based on Run 2

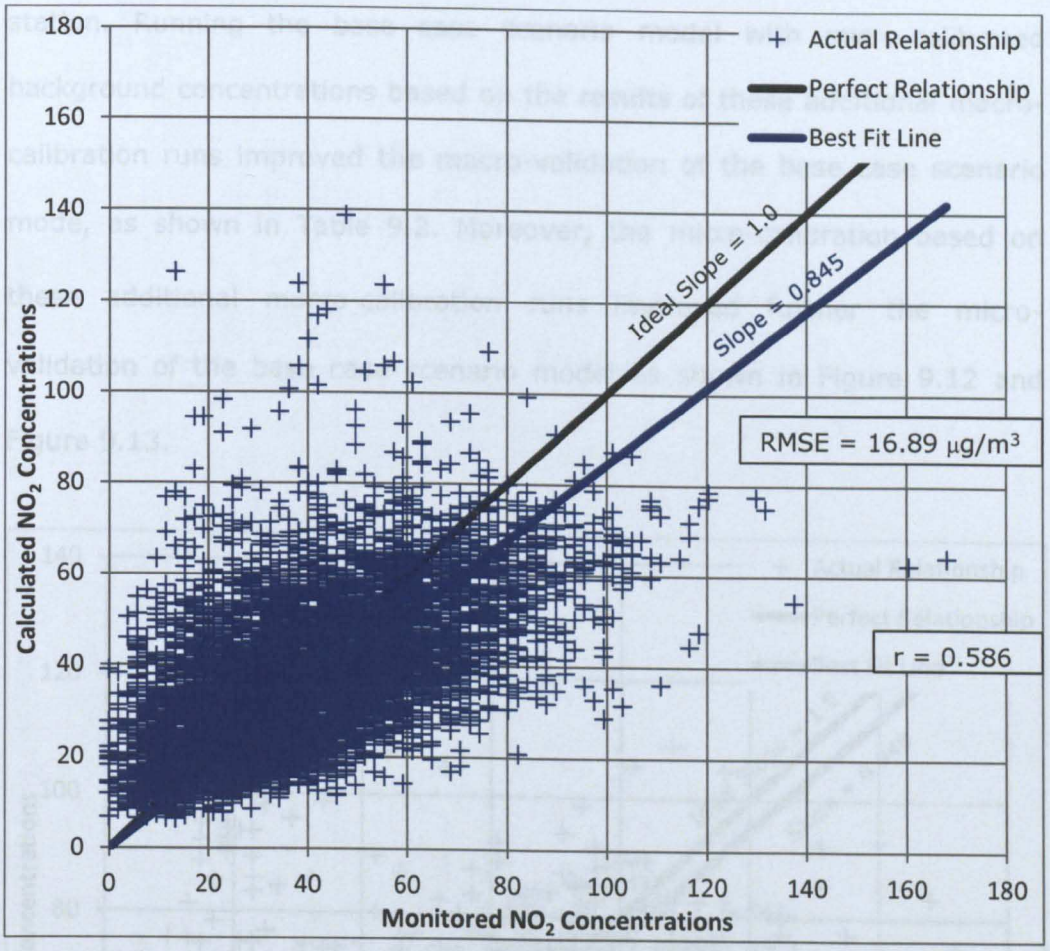

Figure 9.11 Scatter Diagram of Hourly NO_2 Concentrations at the Carter Gate Station after the Micro-calibration based on Run 2

The base case scenario model (based on run 2) with these micro-calibrated background concentrations underestimated both the annual means of monitored NO_2 and O_3 concentrations at the AURN monitoring station as shown in Table 9.2. This underestimation tendency was confirmed by the underestimation of the annual mean of monitored NO_2 concentrations at the calibration-independent Carter Gate monitoring station. This indicated the need for the trial and error macro-calibration approach, explained in Section 6.4.2.2, to undertake additional runs of ADMS-Roads, beyond run 2, as shown in Table 9.1. The purpose of these additional runs was to overestimate the annual mean NO_2 and O_3 concentrations after the macro-calibration, so that they would be well estimated after the micro-calibration based on these additional macro-calibration runs, at the AURN monitoring

station. Running the base case scenario model with micro-calibrated background concentrations based on the results of these additional macro-calibration runs improved the macro-validation of the base case scenario mode, as shown in Table 9.2. Moreover, the micro-calibration based on these additional macro-calibration runs improved further the micro-validation of the base case scenario model as shown in Figure 9.12 and Figure 9.13.

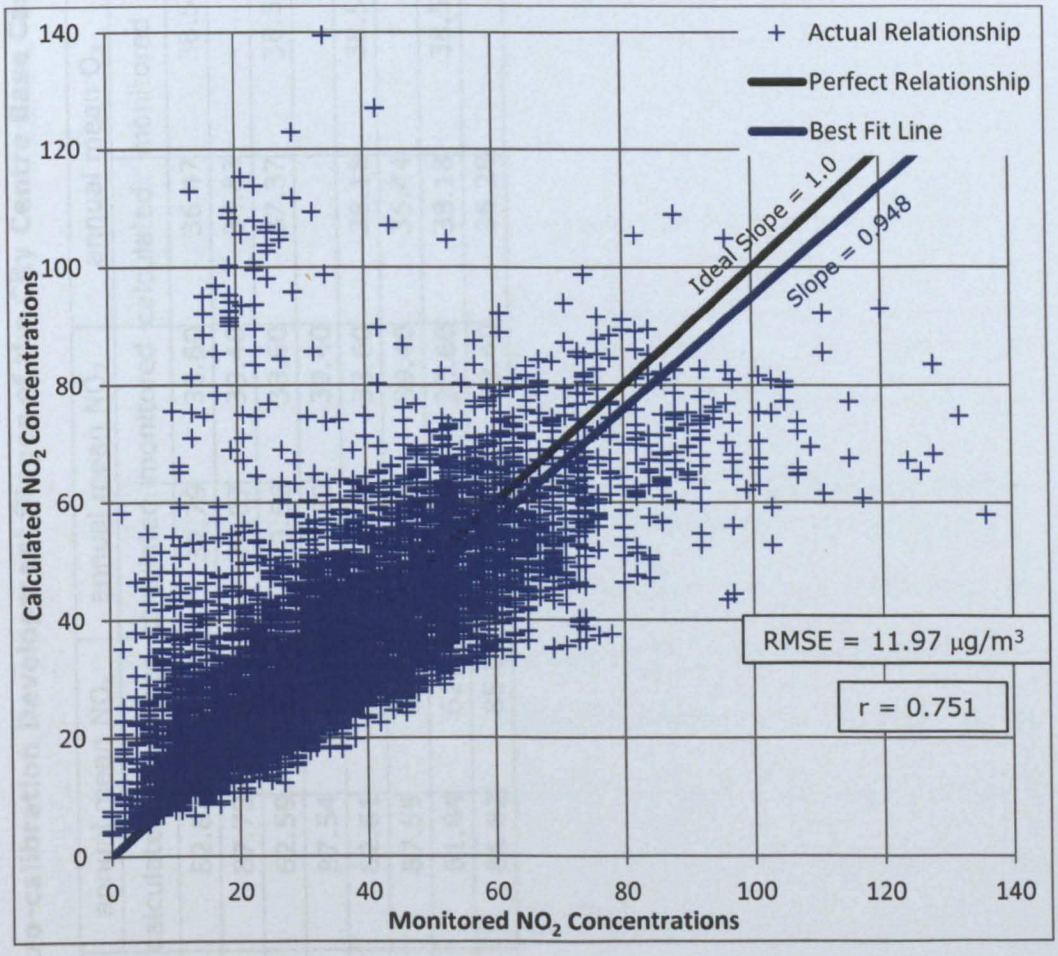

Figure 9.12 Scatter Diagram of Hourly NO_2 Concentrations at the AURN Station after the Micro-calibration based on Run 9

Table 9.2 Micro-calibration Development Stages of the City Centre Base Case Scenario Model

case description	Receptor name	annual mean NO_x		annual mean NO_2		annual mean O_3		uncalibrated RMSE	macro-calibrated RMSE	micro-calibrated RMSE
		calculated	monitored	calculated	monitored	calculated	monitored			
based on run 2	AURN	62.81	62.56	32.79	33.60	36.47	38.54	19.50	19.27	13.57
	Carter Gate	87.73	85.90	36.87	39.40	34.83		21.09	20.77	16.89
based on run 8	AURN	62.59	62.56	33.66	33.60	37.37	38.54	19.50	19.27	12.16
	Carter Gate	87.54	85.90	37.80	39.40			21.09	20.77	15.82
based on run 9	AURN	62.61	62.56	34.13	33.60	38.18	38.54	19.50	19.27	11.97
	Carter Gate	87.55	85.90	38.29	39.40	36.44		21.09	20.77	15.70
Based on run 9 adjusted	AURN	61.84	62.56	33.27	33.60	38.18	38.54	19.50	19.27	9.61
	Carter Gate	86.82	85.90	37.60	39.40	36.28		21.09	20.77	14.74

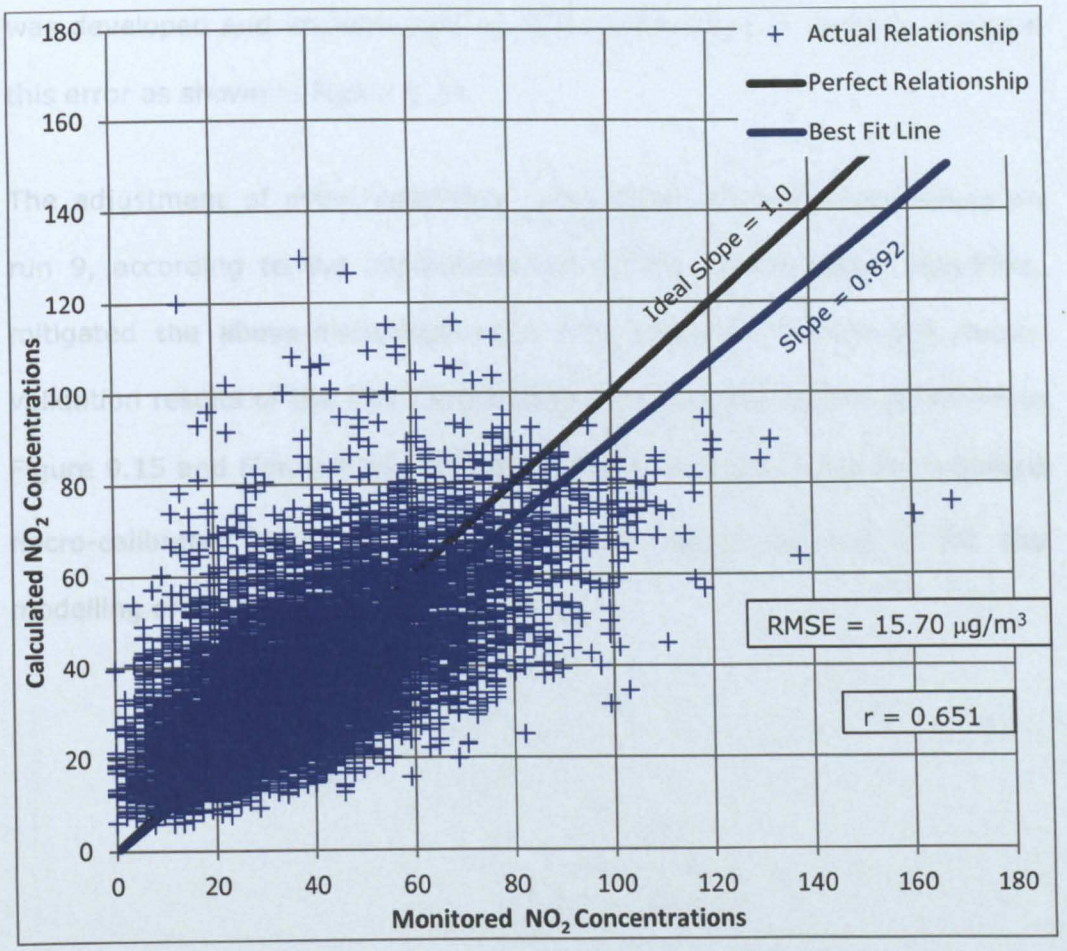

Figure 9.13 Scatter Diagram of Hourly NO_2 Concentrations at the Carter Gate Station after the Micro-calibration based on Run 9

The micro-calibration development, from run 2 to run 9, increased the error between the calculated and monitored NO_2 concentrations at many hours, as implied by the comparison between the scatter in the overestimated points on the upper left side of Figure 9.10 and Figure 9.12. This increase in the error at many hours was also indicated by the comparison between the scatter in the overestimated points on the upper left side of Figure 9.11 and Figure 9.13. The potential reason for such unexpected behaviour of the micro-calibration process at these hours was explained in Section 6.4.2.2. However the number of these hours from the air pollution model of the city centre was higher than that from the air pollution model of the Dunkirk AQMA. Therefore, a mathematical algorithm

was developed and implemented by VBA in MS Excel in order to mitigate this error as shown in Figure 9.14.

The adjustment of micro-calibrated background concentrations based on run 9, according to the implementation of this mathematical algorithm, mitigated the above-mentioned error and improved further the micro-validation results of the City Centre base case scenario model as shown in Figure 9.15 and Figure 9.16. Therefore, it was decided to use the adjusted micro-calibrated background concentrations based on run 9 for the modelling of future air quality scenarios.

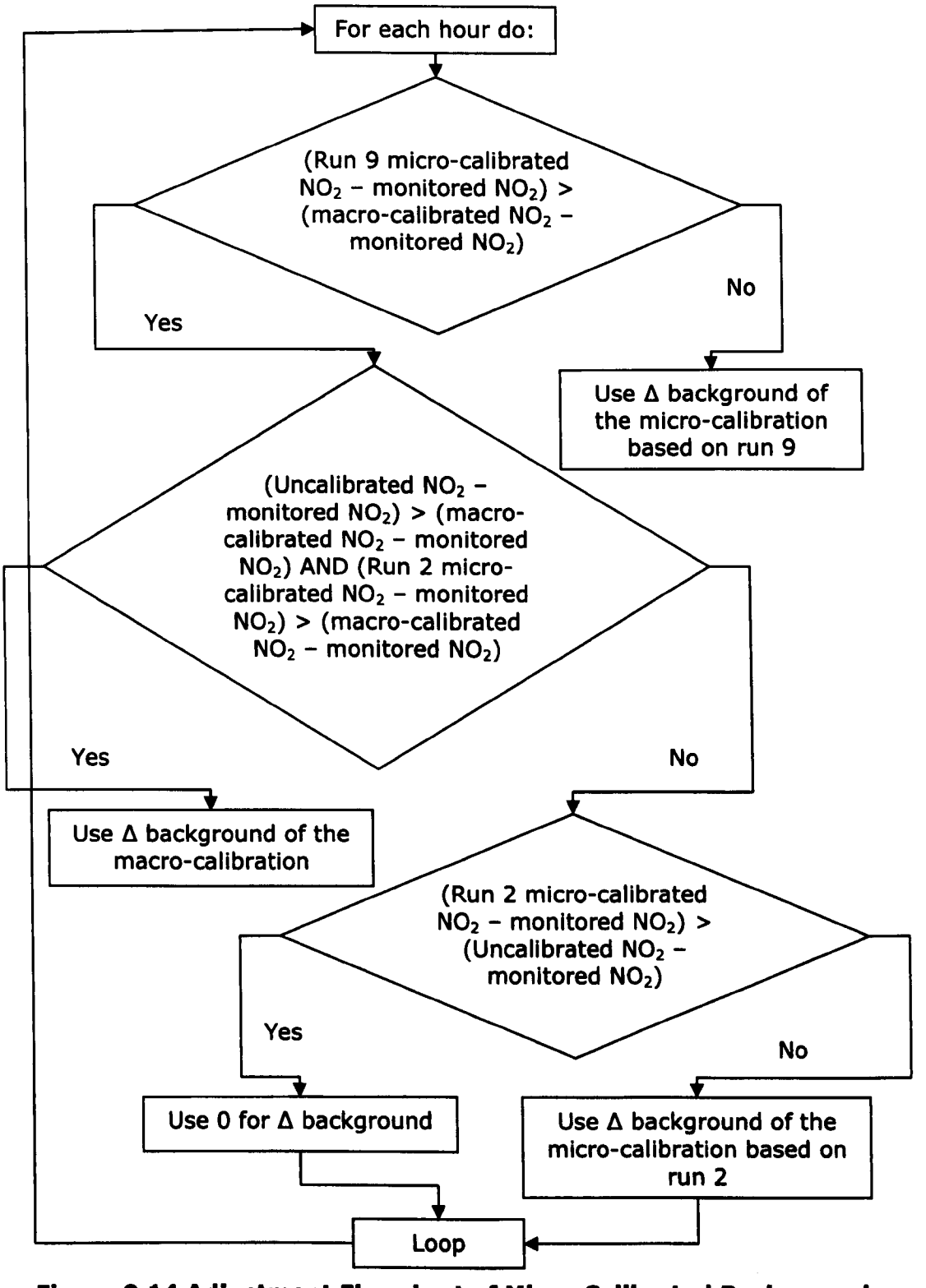

Figure 9.14 Adjustment Flowchart of Micro-Calibrated Background Concentrations based on Run 9

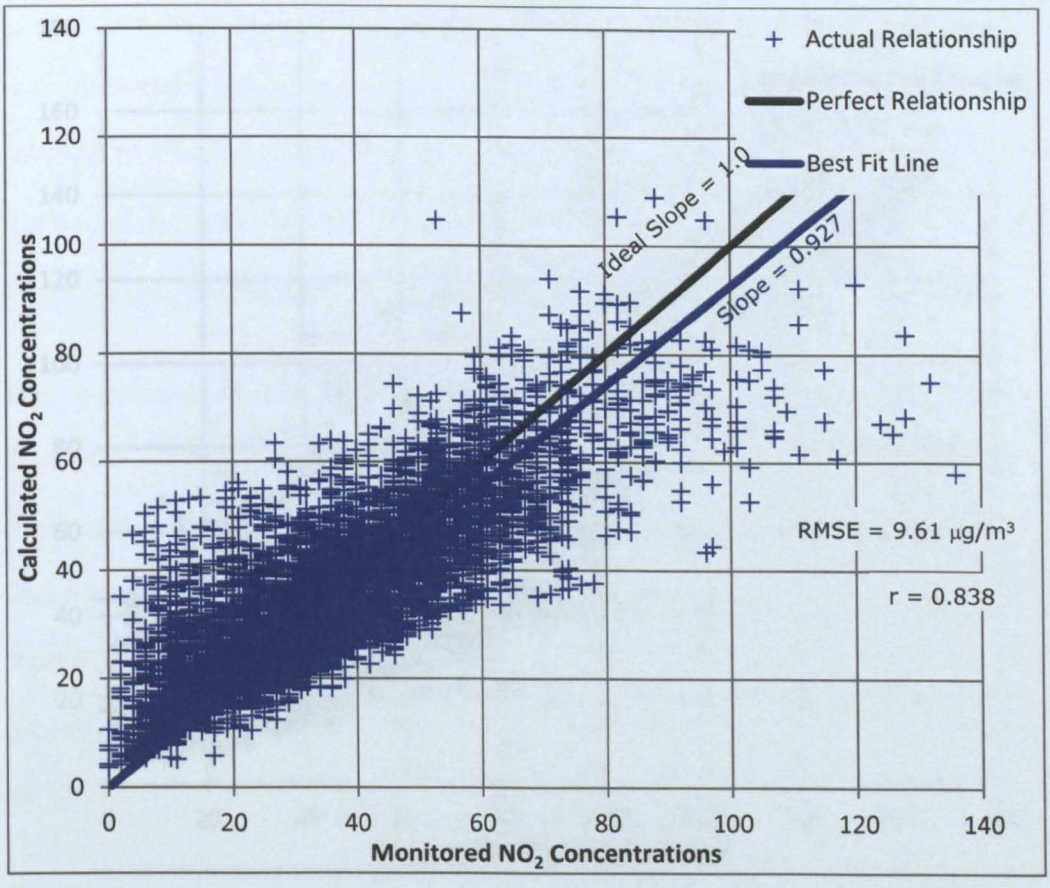

Figure 9.15 Scatter Diagram of Hourly NO_2 Concentrations at the AURN Station after the Micro-calibration based on Run 9 Adjusted

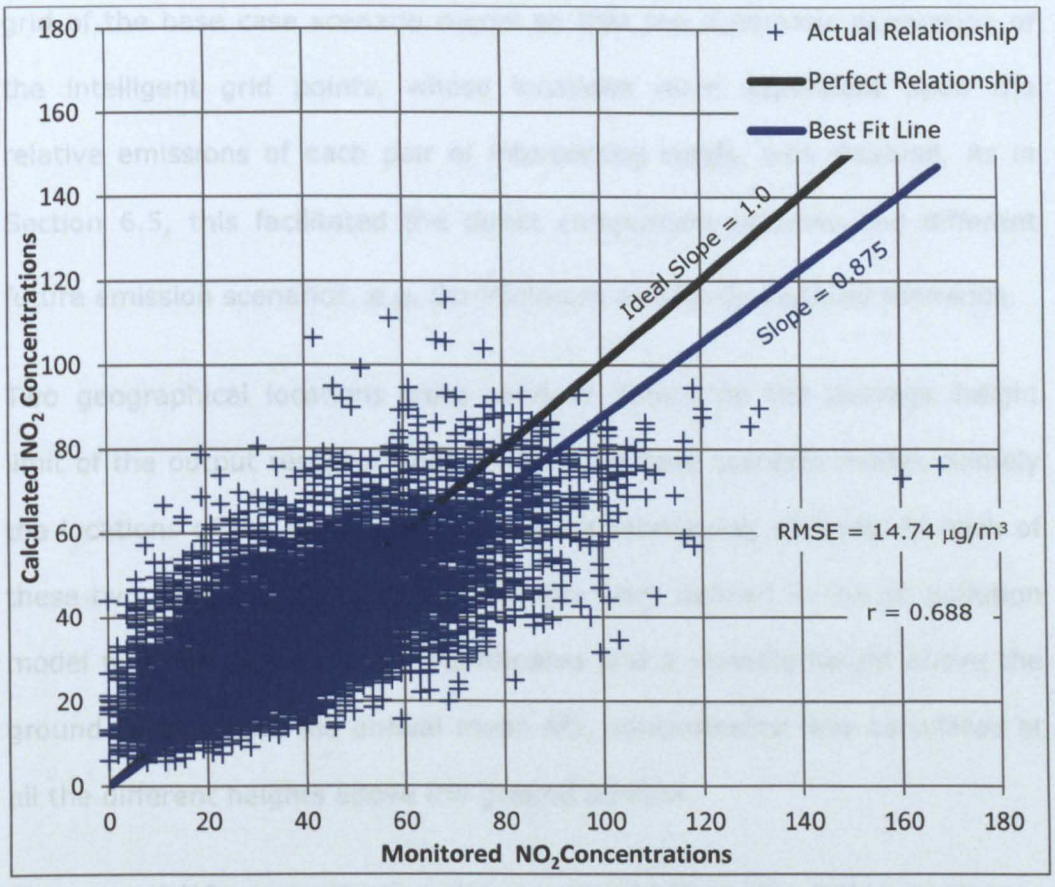

Figure 9.16 Scatter Diagram of Hourly NO_2 Concentrations at the Carter Gate Station after the Micro-calibration based on Run 9 Adjusted

9.6 Grid Design and Height Limit and Step of the Air Pollution Output Receptor Points

As the City Centre base case scenario model comprised a large number of road sources, the intelligent grid option was selected for the base case scenario model to capture better the rapidly changing NO_2 concentrations' gradient close to the road sources. As in Section 6.5, a regular grid size of 31×31 points was selected for the intelligent grid of the base case scenario model, in order to optimise both the model runtime and the output data resolution. A *.igp file was compiled for the customisation of the intelligent

grid of the base case scenario model so that the automatic generation of the intelligent grid points, whose locations were dependent upon the relative emissions of each pair of intersecting roads, was disabled. As in Section 6.5, this facilitated the direct comparison between the different future emission scenarios, e.g. Do-Minimum and Do-Something scenarios.

Two geographical locations were used to determine the average height limit of the output receptor grids of the base case scenario model, namely the locations of the AURN and Carter Gate monitoring stations. At each of these two locations, many receptor points were defined in the air pollution model with the same x and y coordinates and a variable height above the ground surface, and the annual mean NO_2 concentration was calculated at all the different heights above the ground surface.

The rate of NO_2 concentration decay with height at the AURN monitoring station started to get very small at a height of 40 metres above the ground surface as shown in Figure 9.17. This suggested a height limit of 40 metres at the AURN monitoring station. On the other hand, at the Carter Gate monitoring station, the annual mean NO_2 concentration decreased with height until a height of 20 metres above the ground surface as shown in Figure 9.18. Above this height, at this location, NO_2 industrial emissions from the nearby elevated chimney of London Road Heat Station slightly increased the annual mean NO_2 concentration by less than 1 $\mu g/m^3$. This suggested another height limit of 20 metres at the Carter Gate monitoring station.

Therefore, an average height limit of 30 metres was selected for the entire air pollution model application area. This was because the large savings in the model runtime, due to the reduction in the height limit from 40 to 30 metres, significantly outweighed the small rise in annual mean NO_2

concentration at the AURN monitoring station due to such a reduction in the height limit (0.2 $\mu g/m^3$). Consistent with Section 6.6, a height step of 6 metres was selected to increase the output height of successive air pollution model runs until reaching the average height limit above the ground surface. Figure 9.19 to Figure 9.24 show the contour maps of the gridded output 2006 annual mean NO_2 concentrations at 0 to 30 metres above the ground surface.

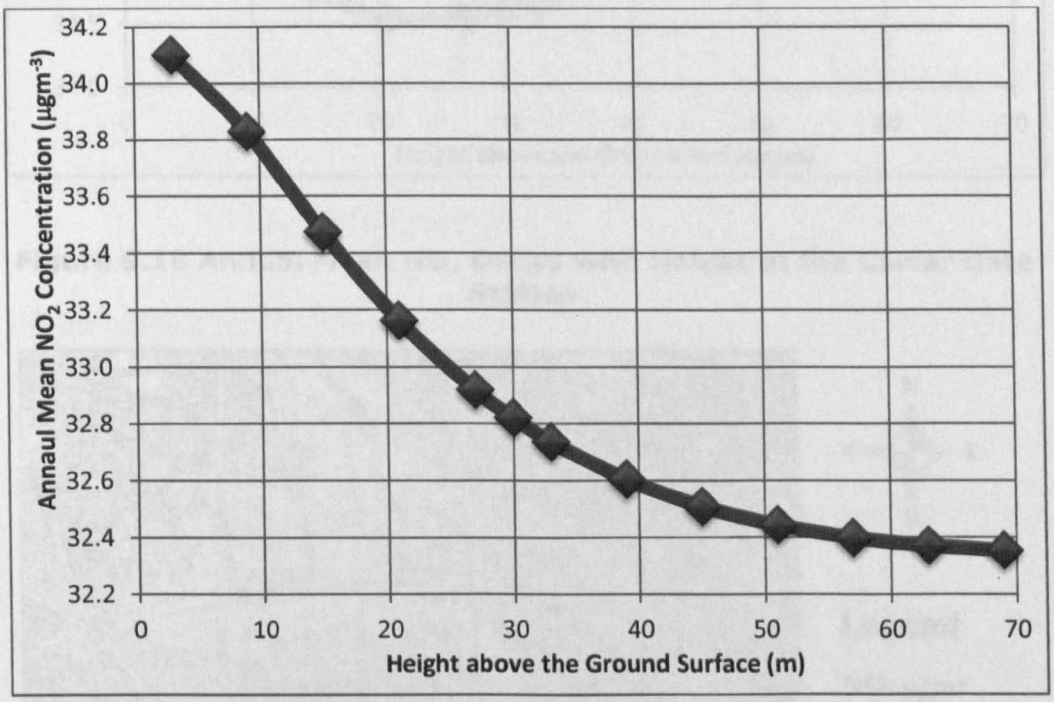

Figure 9.17 Annual Mean NO_2 Decay with Height at the AURN Station

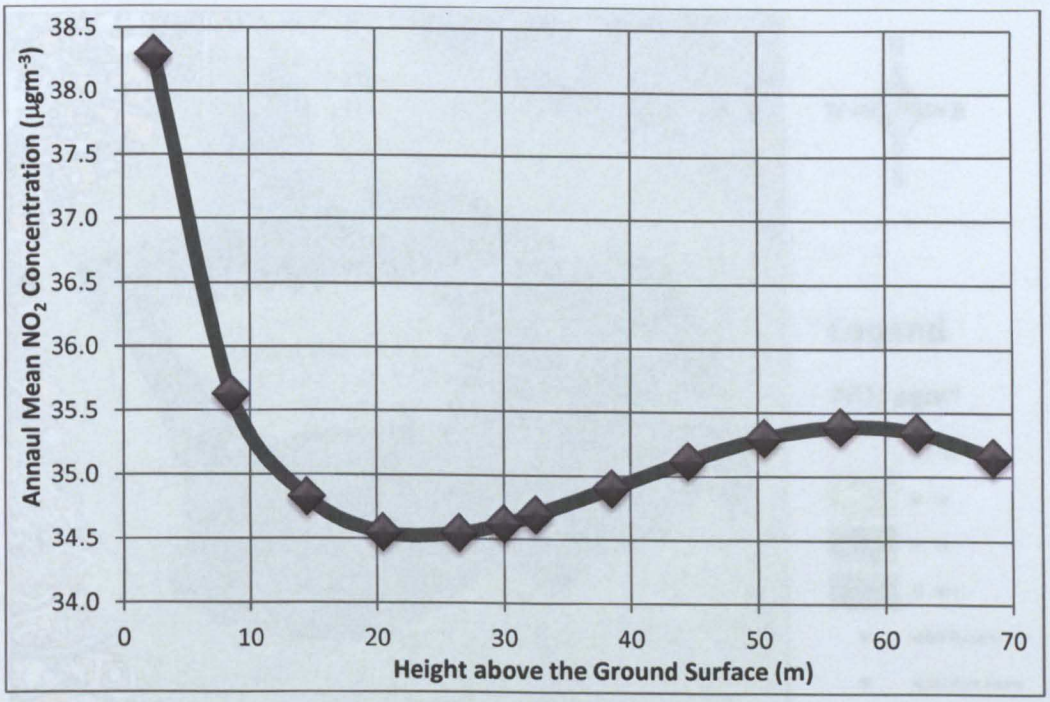

Figure 9.18 Annual Mean NO_2 Decay with Height at the Carter Gate Station

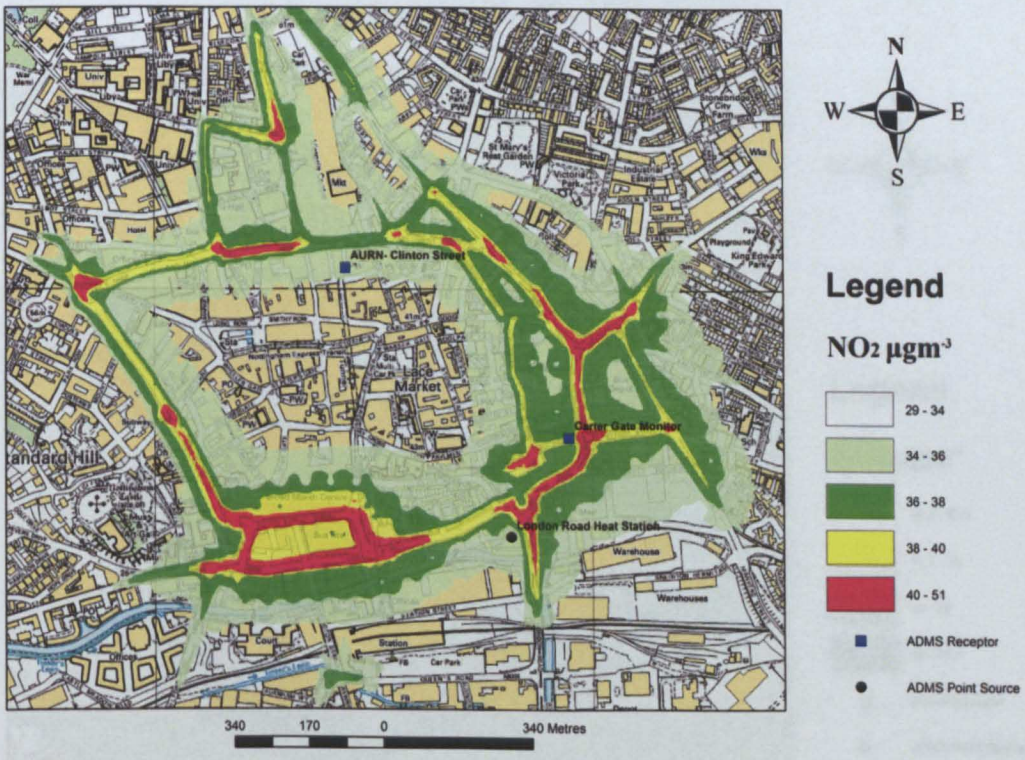

Figure 9.19 Contour Map of 2006 Ground-level Annual Mean NO_2 Concentrations in the City Centre

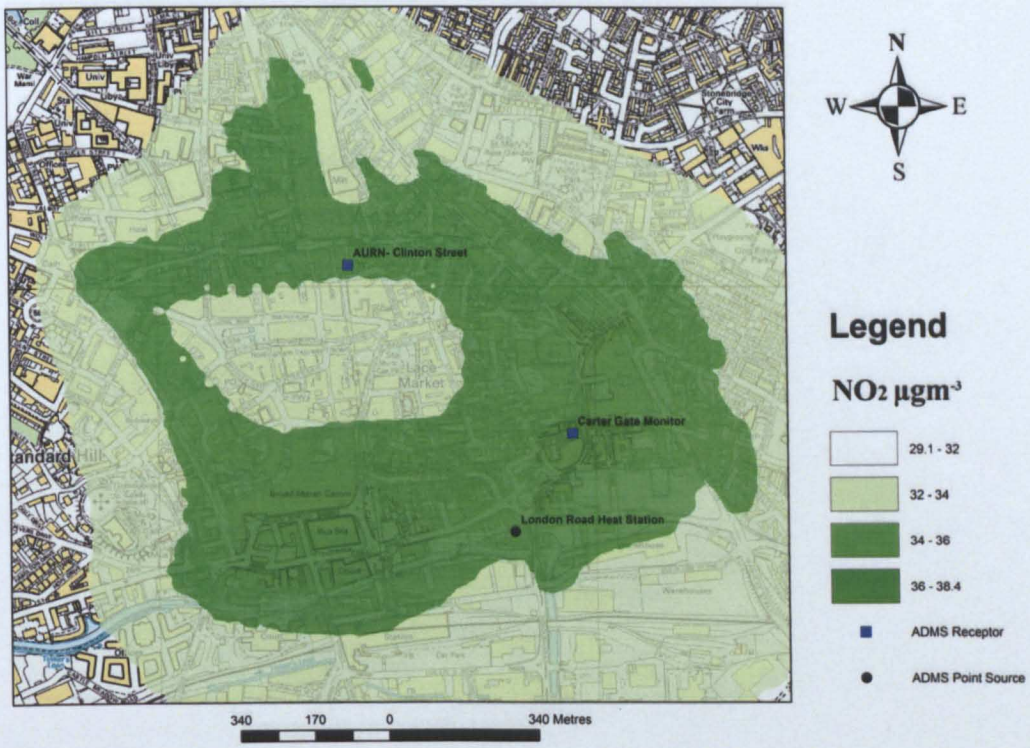

Figure 9.20 Contour Map of 2006 6 metres-height Annual Mean NO_2 Concentrations in the City Centre

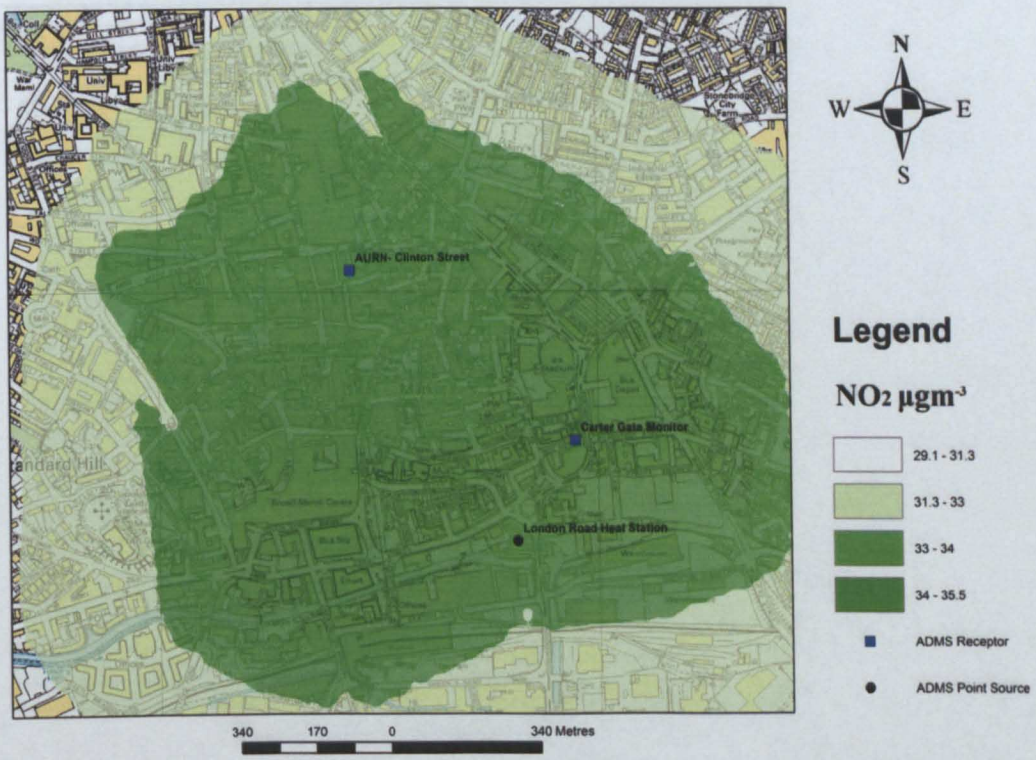

Figure 9.21 Contour Map of 2006 12 metres-height Annual Mean NO_2 Concentrations in the City Centre

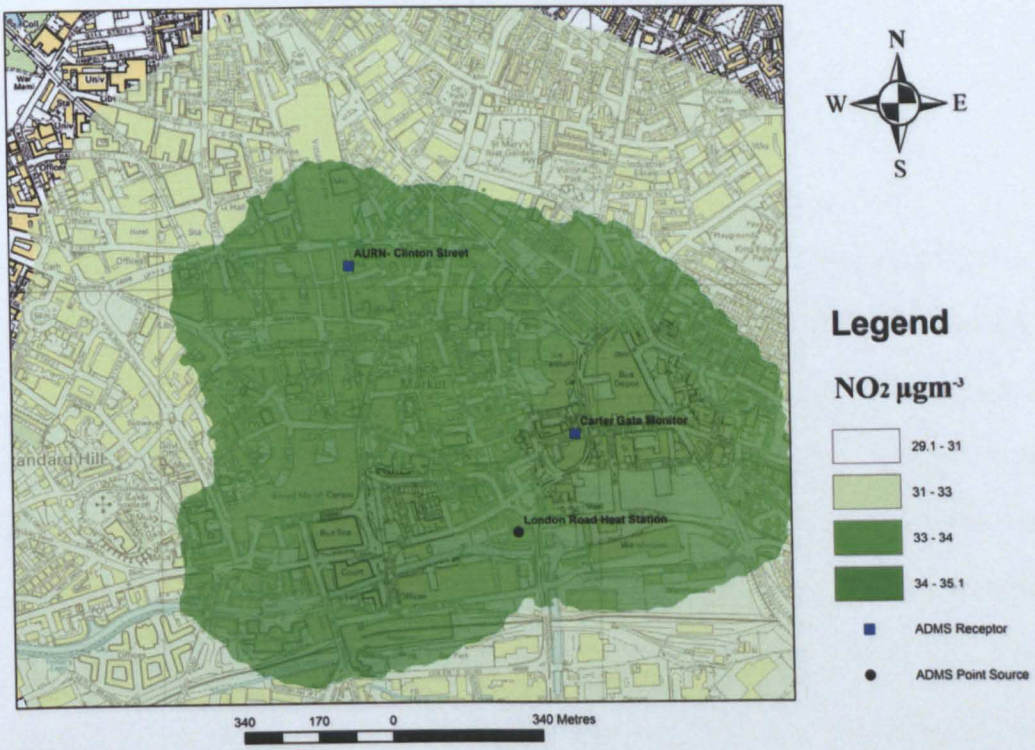

Figure 9.22 Contour Map of 2006 18 metres-height Annual Mean NO_2 Concentrations in the City Centre

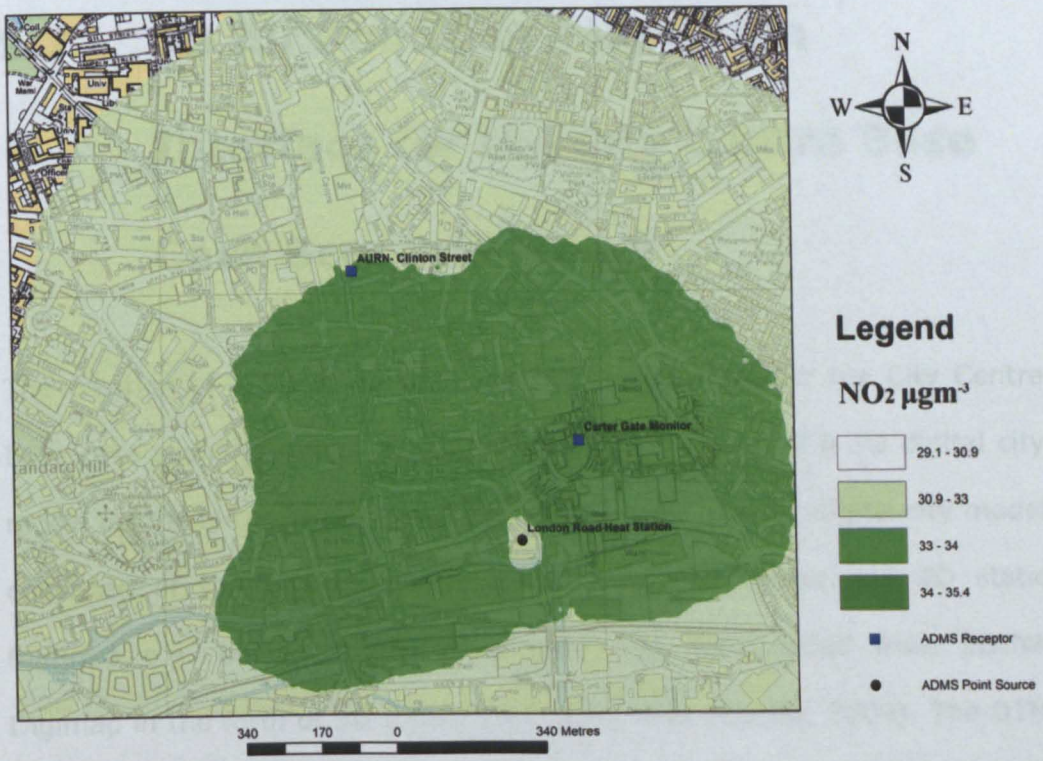

Figure 9.23 Contour Map of 2006 24 metres-height Annual Mean NO_2 Concentrations in the City Centre

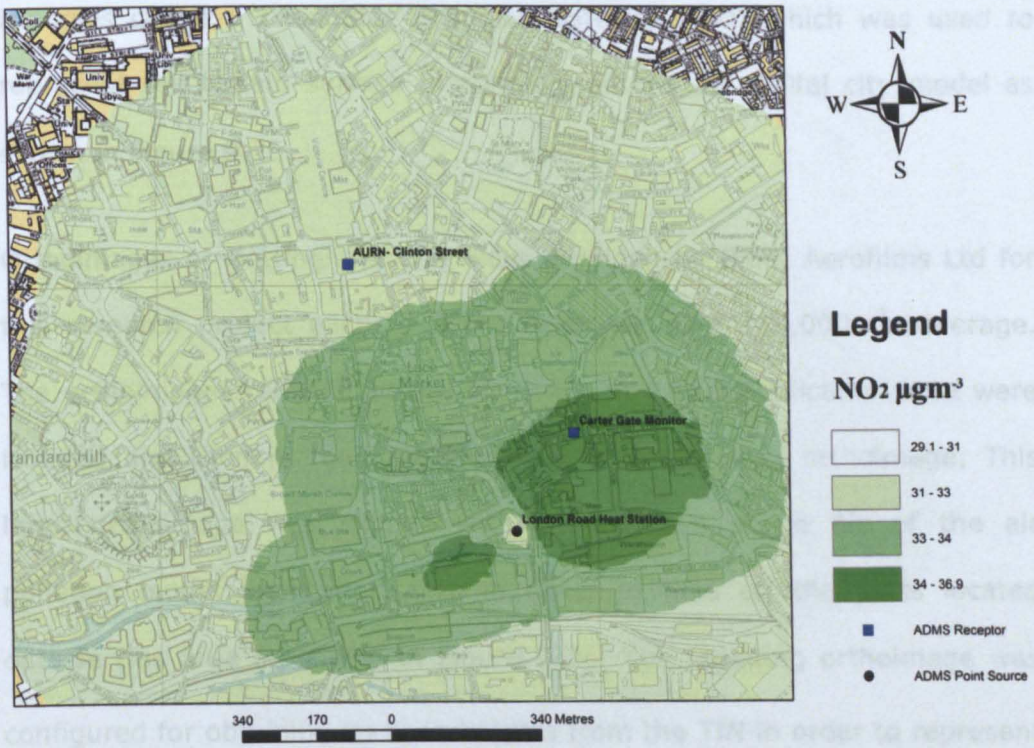

Figure 9.24 Contour Map of 2006 30 metres-height Annual Mean NO_2 Concentrations in the City Centre

9.7 3D Air Pollution Dispersion Interface for the City Centre Base Case Scenario Model

The creation of a 3D air pollution dispersion interface for the City Centre base case scenario model started off with the creation of a 3D digital city model for the air pollution model application area. The 3D digital city model consisted of three components: a DTM, an orthoimage and 3D static features e.g. buildings. The DTM data was downloaded from EDINA Digimap in the form of 3D topographic point data (EDINA, 2009). The DTM data was clipped with the polygon shape file of the final air pollution model application area in order to leave only the 3D points existing inside this area. The functionality of 3D Analyst of ArcGIS 9.2 was used in order to get these 3D points connected with a series of edges to form a network of

triangles called a Triangular Irregular Network (TIN) which was used to represent the terrain surface morphology in the 3D digital city model as shown in Figure 9.25.

Orthoimages of Nottingham City were provided by Blom Aerofilms Ltd for this research project each in 10cm resolution and 250,000m^2 coverage. The orthoimages relevant to the air pollution model application area were isolated and then merged together into a single large orthoimage. This large orthoimage was clipped with the polygon shape file of the air pollution model application area in order to take off the parts located outside this area as shown in Figure 9.26. The resulting orthoimage was configured for obtaining its base heights from the TIN in order to represent realistically the terrain surface in the 3D digital city model.

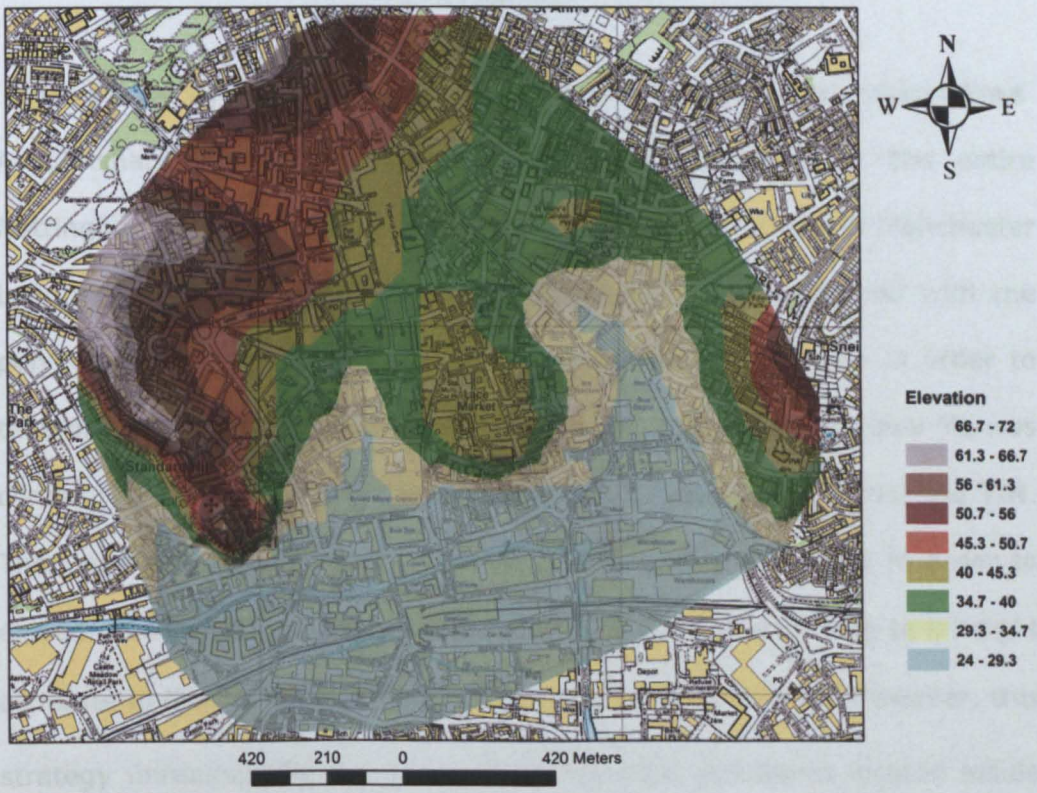

Figure 9.25 TIN of the Air Pollution Model Output Area

Figure 9.26 Orthoimage of the Air Pollution Model Application Area

A 2D shape file for the footprint of buildings located in the entire Nottingham urban area was downloaded from the University of Manchester Landmap Service (Landmap, 2009). The shape file was clipped with the polygon shape file of the air pollution model application area in order to take off the buildings located outside this area. The resulting shape file was configured so that the buildings obtained their base heights from the TIN. Then, the functionality of 3D Analyst of ArcGIS 9.2 was used in order to extrude the buildings vertically above the TIN surface according to a height attribute in the buildings shape file as shown in Figure 9.27. However, this strategy unrealistically represented the elevated structures located inside the air pollution model application area as walls. Therefore, the 2D polygons of these elevated structures were isolated and exported to

AutoCAD Civil 3D where they were designed as realistic 3D elevated structures.

Figure 9.27 A Screenshot of the 3D Digital City Model of the Air Pollution Model Application Area

As indicated by the comparison between Figure 9.19 and Figure 9.20, the contour band of 2006 NO_2 concentrations exceeding the AQO of annual mean NO_2 concentrations, 40 $\mu g/m^3$, disappeared at 6 metres above the ground surface. Therefore, these critical NO_2 concentrations would be represented in the 3D air pollution dispersion interface by a 2D planar surface, which was not the case with the 2006 Dunkirk AQMA 3D air pollution dispersion interface. However, the true vertical and horizontal spatial extensions of these high NO_2 concentrations are always highly important for air pollution exposure-related studies and policies. Therefore, a specific investigation was undertaken in order to identify the height limit of the cloud representing these high NO_2 concentrations. One ground-level receptor point was defined at the centroid of every ground-level contour zone of NO_2 exceedances i.e. at the centroid of every red contour zone in Figure 9.19. For each of these zones, many other receptors were defined at

the same x and y coordinates as the ground-level centroidal receptor point and at many different heights above the ground surface.

Since the 6-metres height NO_2 contour map did not show any exceedances, the height of additional receptors varied from 1 metre to 5 metres above the ground surface. In some contour zones, the AQO for NO_2 continued to be exceeded until 2 metres above the ground surface. The calculated annual mean NO_2 concentrations at some other contour zones continued to exceed the AQO for NO_2 until 3 metres above the ground surface. In the other contour zones the AQO for NO_2 continued to be exceeded until 4 metres above the ground surface. Hence, it was decided to select 4 metres as the height limit of the cloud that represented annual mean NO_2 concentrations exceeding the AQO for NO_2.

The base of this cloud was determined by importing the gridded output concentrations file of the 2006 ground-level annual mean NO_2 concentrations into a spreadsheet. The grid points, at which NO_2 concentrations were greater than 40 $\mu g/m^3$, were selected and exported to another separate spreadsheet. In the separate spreadsheet, many additional grid points were created by copying x and y coordinates of the exported grid points and assigning heights of 1, 2, 2.5, 3, and 4 metres above the ground surface. The resulting set of additional grid points was too large to be defined in the air pollution model interface as output receptor points. Moreover, it was impossible to create a grid from this large set of points defined at variable heights above the ground surface. Hence, another technique was used to read the three coordinates and attributes of every additional grid point: name, x, y and height above the ground surface, from an external comma-delimited text file to define an output receptor point on the fly during the air pollution model runtime.

The calculated NO_2 concentrations at all the output heights, 0 – 30 metres above the ground surface, including the intermediate heights between 0 and 6 metres, were integrated with the 3D city model of the air pollution model application area in order to create the 2006 3D volumetric clouds air pollution dispersion interface. Figure 9.28 displays a screenshot of the 3D air pollution dispersion interface.

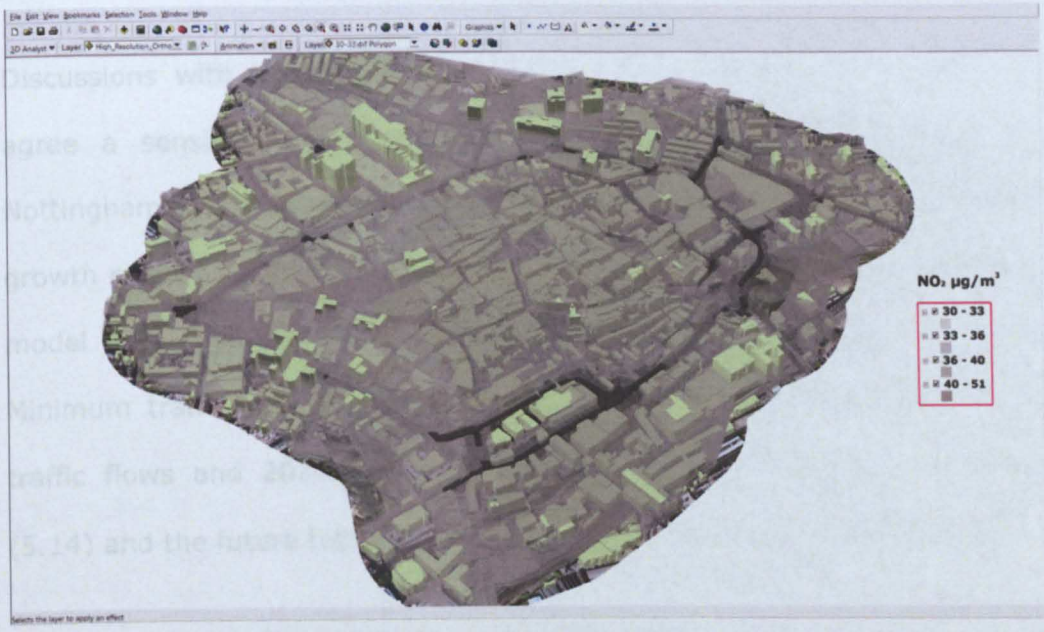

Figure 9.28 Screenshot of 2006 3D Air Pollution Dispersion Interface for the City Centre

9.8 Future Traffic Scenarios for City Centre Area Modelling

From discussions with Nottingham City Council, it was discovered that the Turning Point East scheme is actually set to be implemented in two phases. Nottingham City Council confirmed that all the impacts of this transport scheme to do with traffic movements would result from the first phase. Therefore, this chapter considered the air quality impacts of only the first phase of the Turning Point East scheme. The anticipated implementation year of Turning Point East Phase One is 2011. On the other hand,

Nottingham City Council confirmed that they envisaged the implementation year of the Broadmarsh Extension scheme to be 2014. Therefore, 2014 was selected as the future emission year to predict and evaluate the air quality impacts of both the Turning Point East Phase One and Broadmarsh Extension schemes.

9.8.1 Do-Minimum Scenario

Discussions with Nottingham City Council were undertaken in order to agree a sensible annual average traffic growth rate assumption for Nottingham City Centre from 2006 to 2014. A 2% annual average traffic growth rate was agreed to project the traffic flows of the 2006 air pollution model base case scenario to the 2014 Do-Minimum scenario. 2014 Do-Minimum traffic speeds were estimated from 2006 traffic speeds, 2006 traffic flows and 2014 Do-Minimum traffic flows according to Equation (5.14) and the future traffic density assumption described in Section 5.8.

9.8.2 Do-Something Scenario

The consultations with Nottingham City Council resulted in the identification of the roads where traffic flows are expected to be directly affected by the implementation of both the Turning Point East Phase One and Broadmarsh Extension schemes as shown in Figure 9.29. Nottingham City Council provided the anticipated 2011 traffic flows for the roads to be directly affected by the implementation of Turning Point East Phase One. A 2% annual average traffic growth rate was used to project these traffic flows from 2011 to 2014.

Nottingham City Council provided the anticipated 2014 traffic flows for the roads to be directly affected by the implementation of the Broadmarsh

Extension scheme. Traffic flows for the remaining roads, which are expected to be largely unaffected by the implementation of either Turning Point East Phase One or the Broadmarsh Extension scheme, were projected by a 2% annual average growth rate from 2006 to 2014. For all the roads defined in the air pollution model, 2014 Do-Something traffic speeds were estimated from 2006 traffic speeds, 2006 traffic flows and 2014 Do-Something traffic flows according to equation (5.14) and the future traffic density assumption described in Section 5.8.

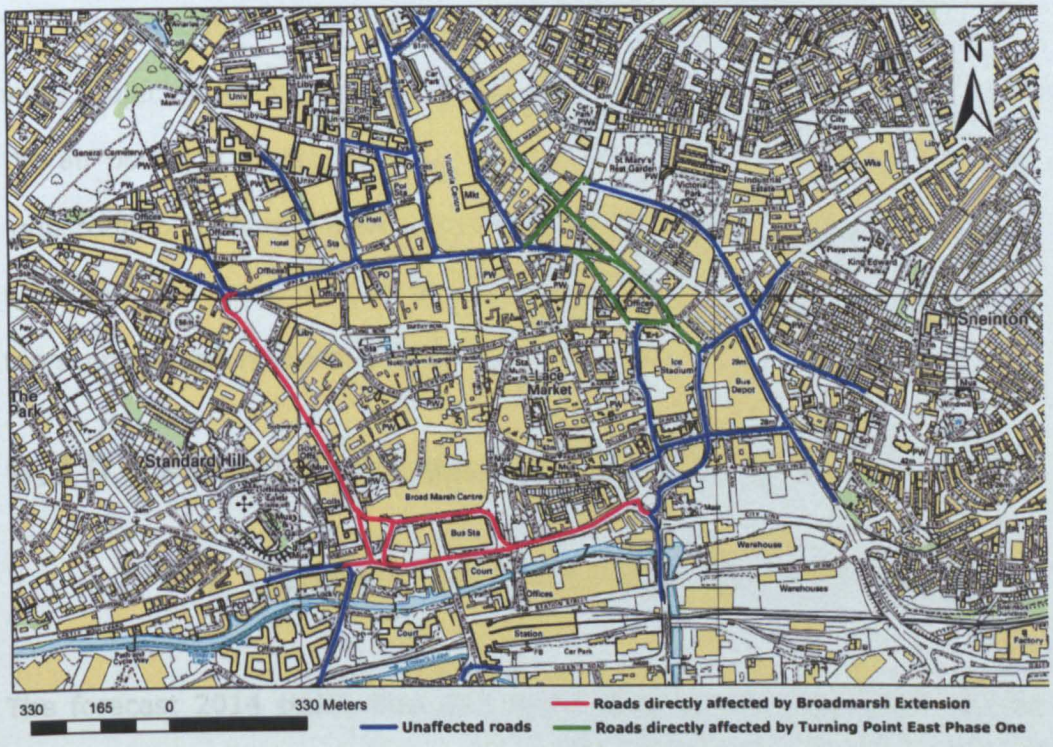

Figure 9.29 Roads Affected by The Proposed Transport Schemes in the City Centre

9.9 Projection of Air Pollution Input Data to 2014

In order to build the 2014 Do-Minimum and Do-Something air quality scenarios, the air pollution input data for the City Centre base case scenario model had to be projected from 2006 to 2014. The micro-

calibrated background concentrations of the City Centre base case scenario model were projected from 2006 to 2014 using The Year Adjustment Calculator as explained in Section 8.2.1. In addition, for each hour of the 2006 hourly sequential background concentrations, the 2014 O_3 background concentration was estimated automatically in a spreadsheet from the 2006 O_3 and NO_2 micro-calibrated background concentrations according to equation (8.1) with 0.83 replaced with the 2014 year factor for NO_2 background concentrations.

The traffic-induced emissions of the City Centre base case scenario model were projected from 2006 to 2014 by altering the emission year to 2014 in the air pollution model interface. 2006 NO_X as NO_2 emissions of the three industrial point sources defined in the City Centre base case scenario model were kept the same in 2014 as industry-induced air pollution was outside the scope of this research project.

9.10 Prediction and Visualisation of 2014 Air Quality in the City Centre Area

The forecast 2014 traffic flow and speed data for the 2014 Do-Minimum traffic scenario were used, along with the projected 2014 air pollution input data, for running ADMS-Roads for 2014 air pollution modelling of the City Centre Area. The 2014 annual mean NO_2 concentrations was calculated by ADMS-Roads at the output receptor points of the intelligent grid described in Section 9.6. Figure 9.30 to Figure 9.35 show the contour maps of 2014 annual mean NO_2 concentrations for the 2014 Do-Minimum scenario at and above the ground surface. This process was repeated using the forecast 2014 traffic flow and speed data for the 2014 Do-Something traffic scenario. Figure 9.36 to Figure 9.41 show the contour maps of 2014 annual

mean NO_2 concentrations for the 2014 Do-Something scenario at and above the ground surface.

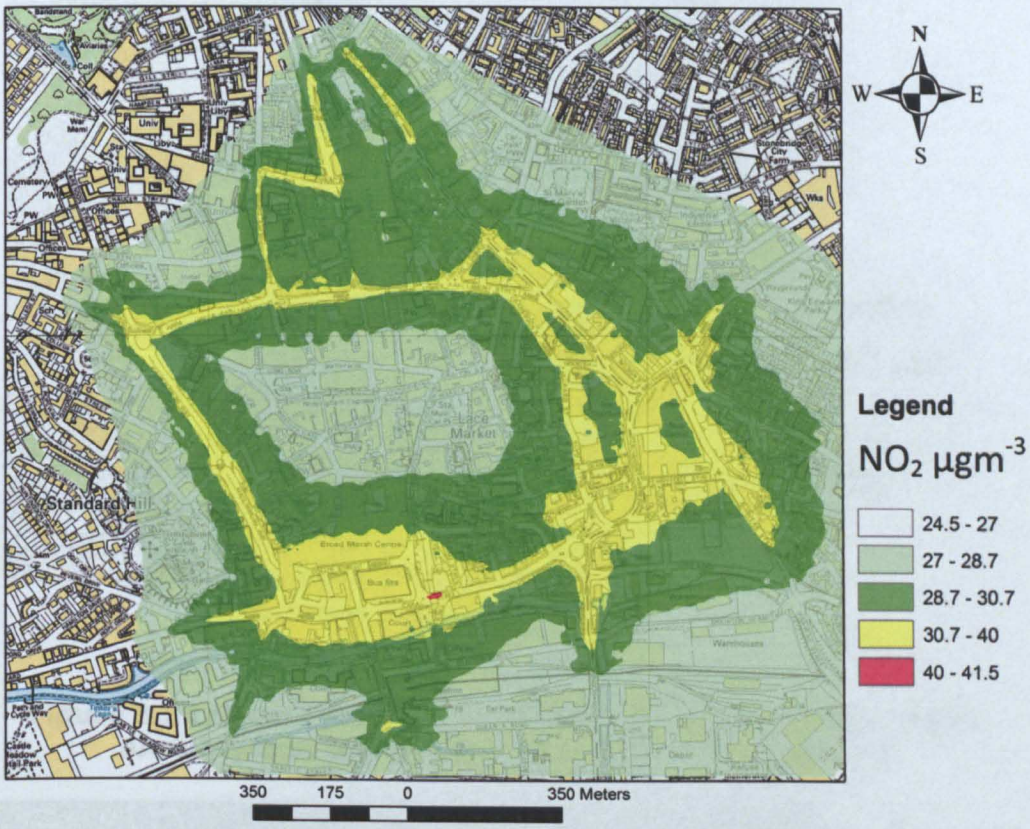

Figure 9.30 Contour Map of Do-Minimum 2014 Ground-level Annual Mean NO_2 Concentrations in the City Centre

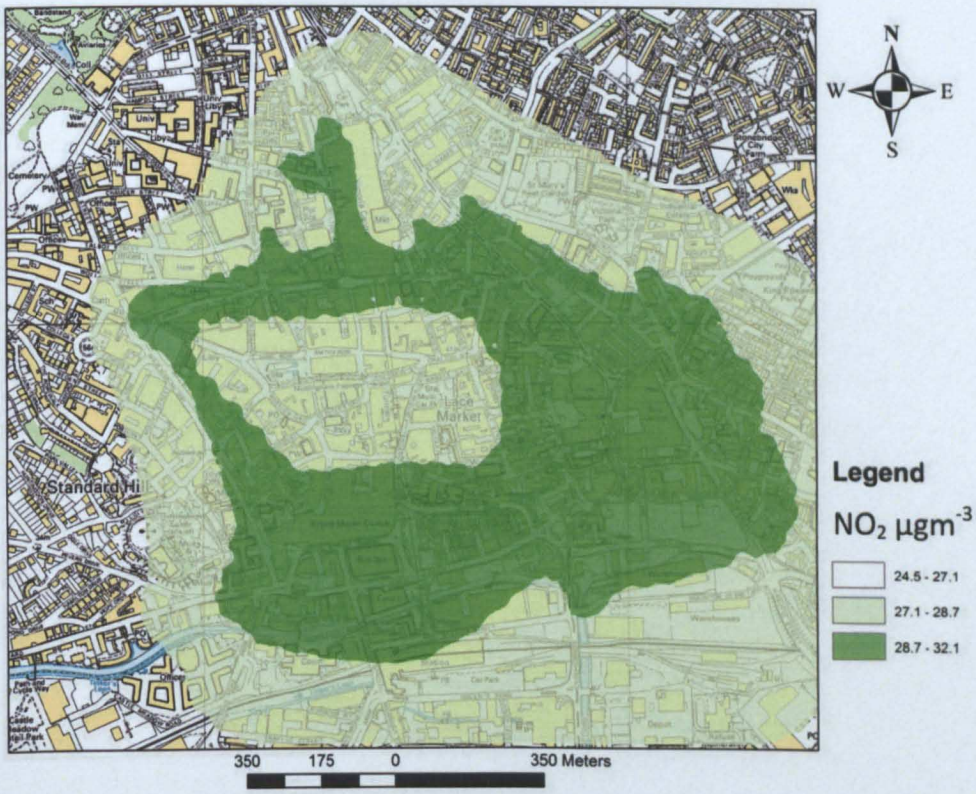

Figure 9.31 Contour Map of Do-Minimum 2014 6 metres-height Annual Mean NO_2 Concentrations in the City Centre

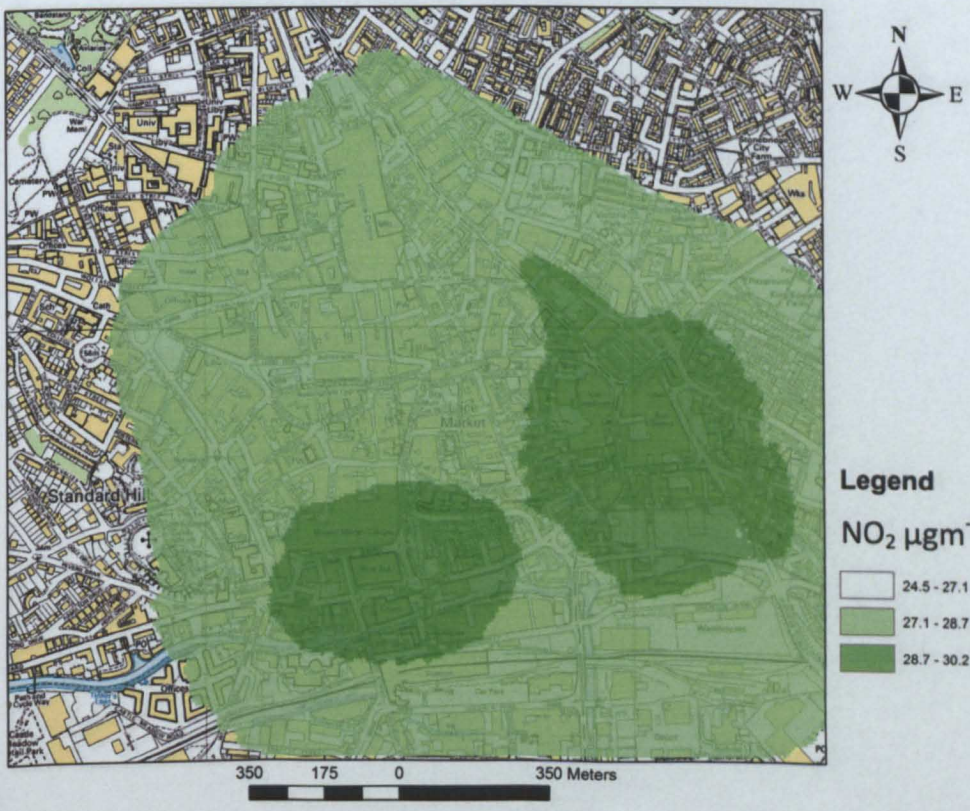

Figure 9.32 Contour Map of Do-Minimum 2014 12 metres-height Annual Mean NO_2 Concentrations in the City Centre

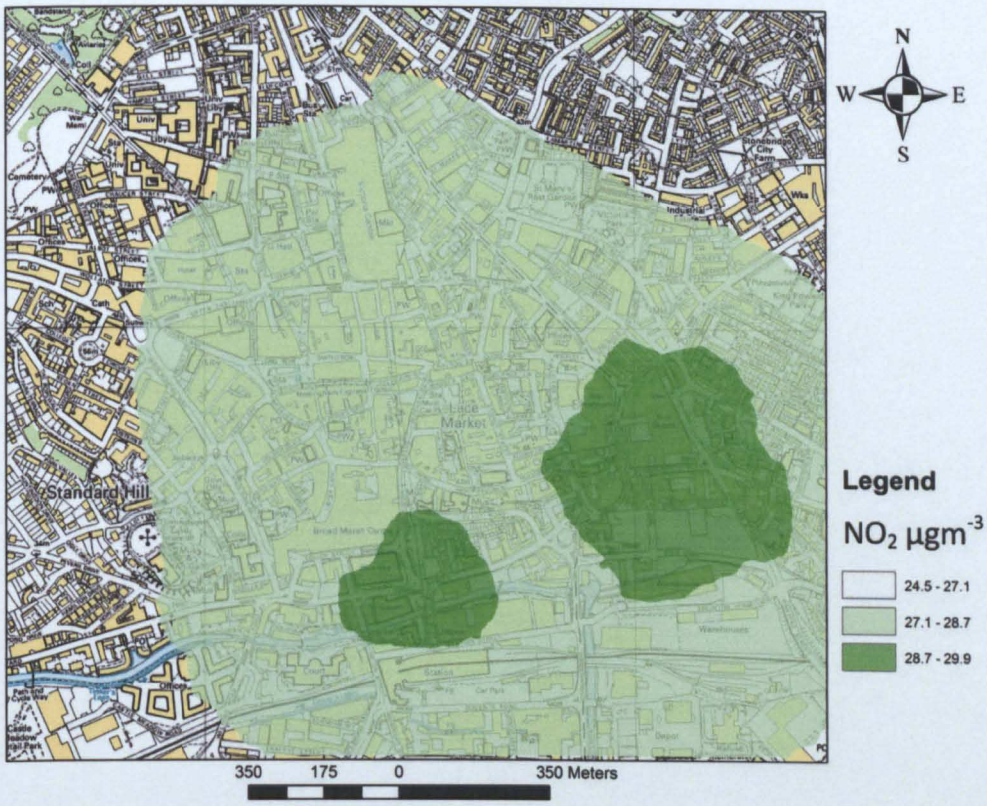

Figure 9.33 Contour Map of Do-Minimum 2014 18 metres-height Annual Mean NO_2 Concentrations in the City Centre

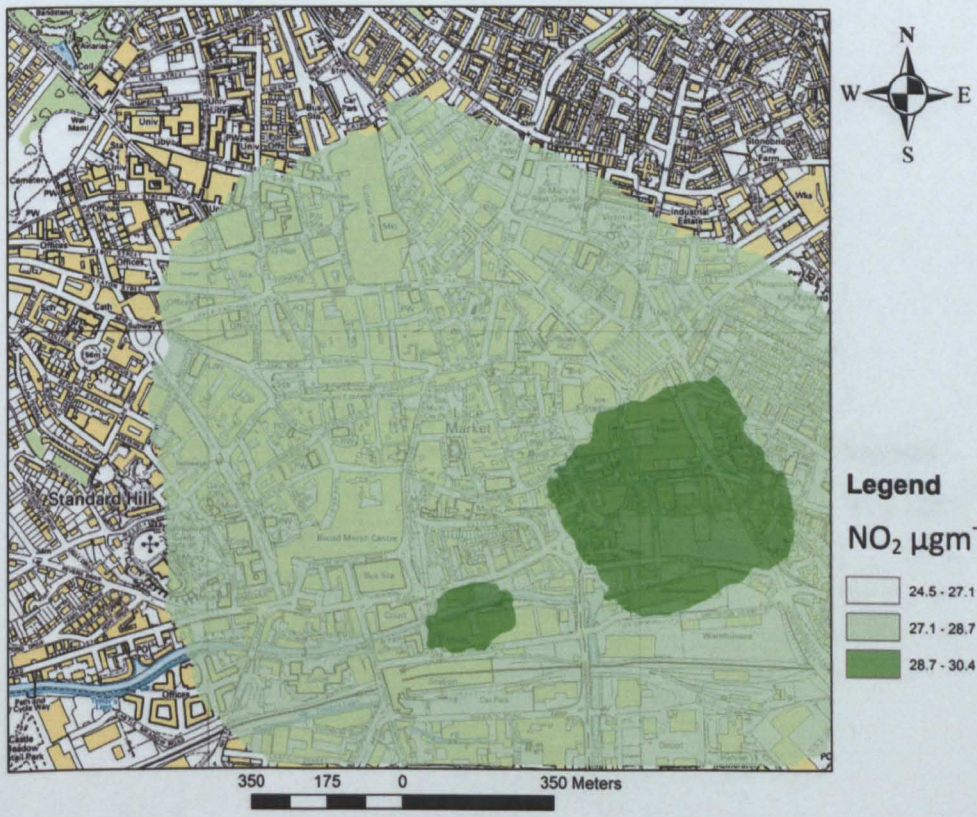

Figure 9.34 Contour Map of Do-Minimum 2014 24 metres-height Annual Mean NO_2 Concentrations in the City Centre

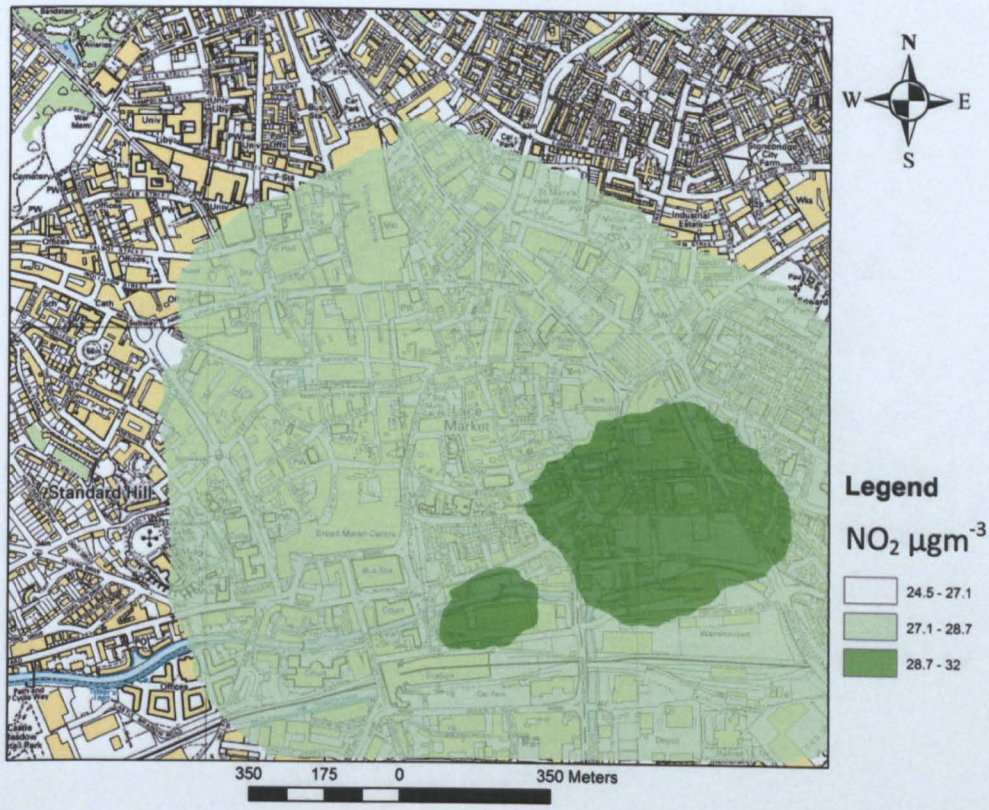

Figure 9.35 Contour Map of Do-Minimum 2014 30 metres-height Annual Mean NO_2 Concentrations in the City Centre

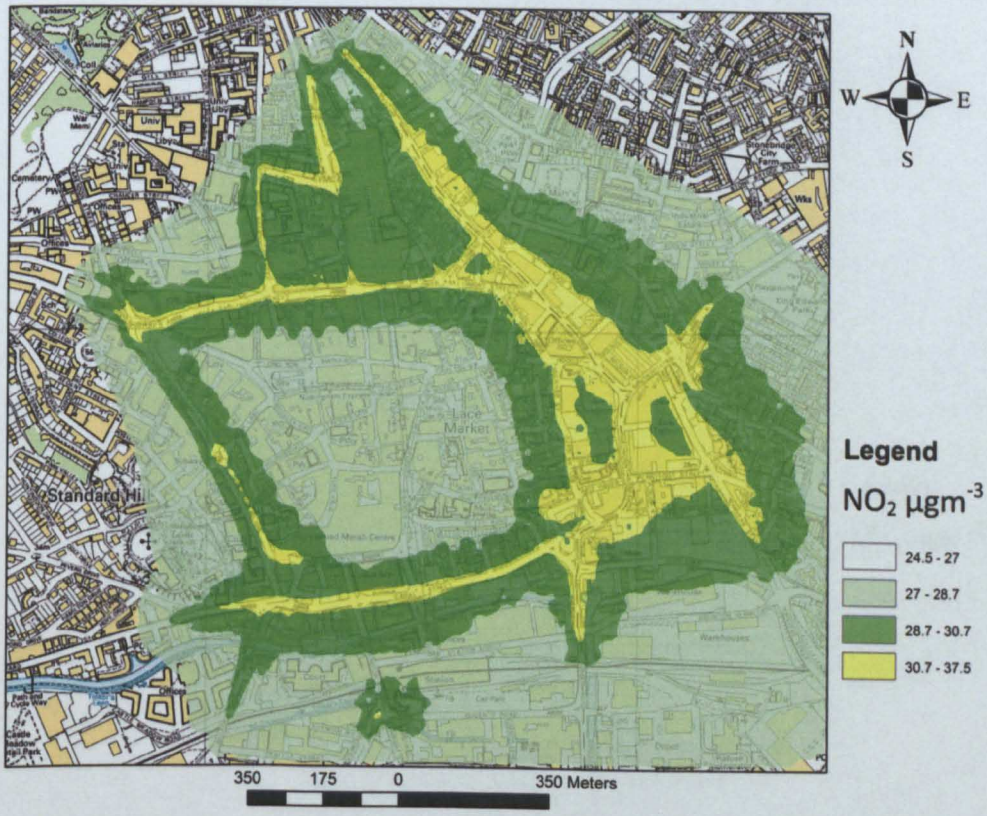

Figure 9.36 Contour Map of Do-Something 2014 Ground-level Annual Mean NO_2 Concentrations in the City Centre

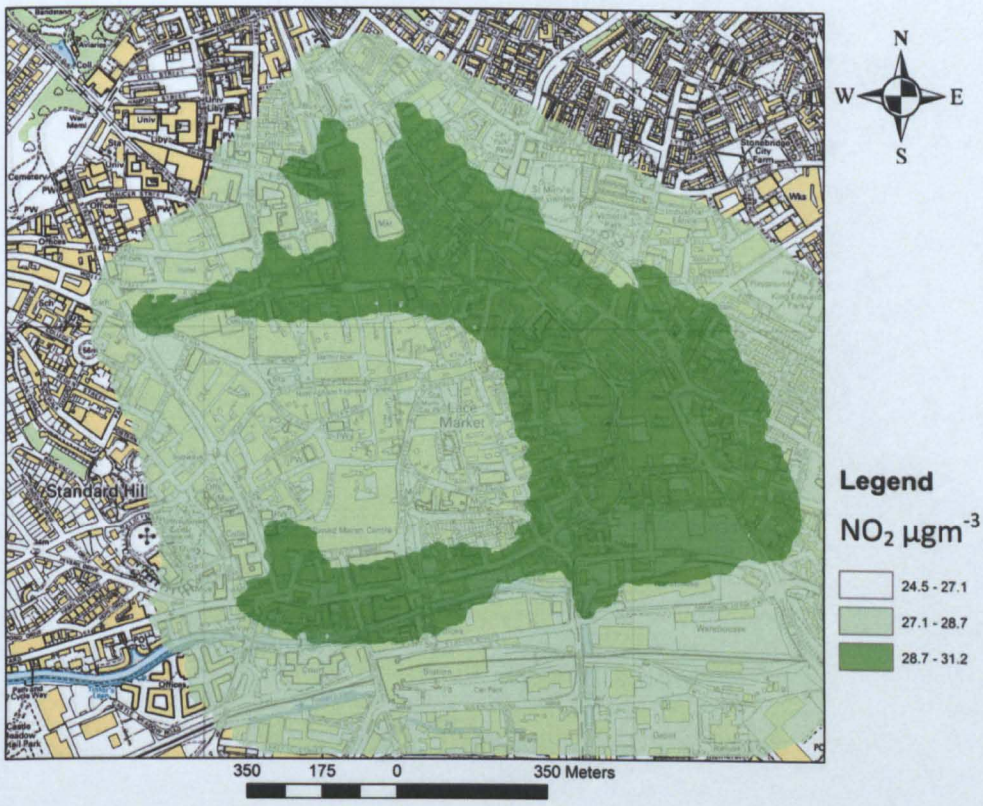

Figure 9.37 Contour Map of Do-Something 2014 6 metres-height Annual Mean NO_2 Concentrations in the City Centre

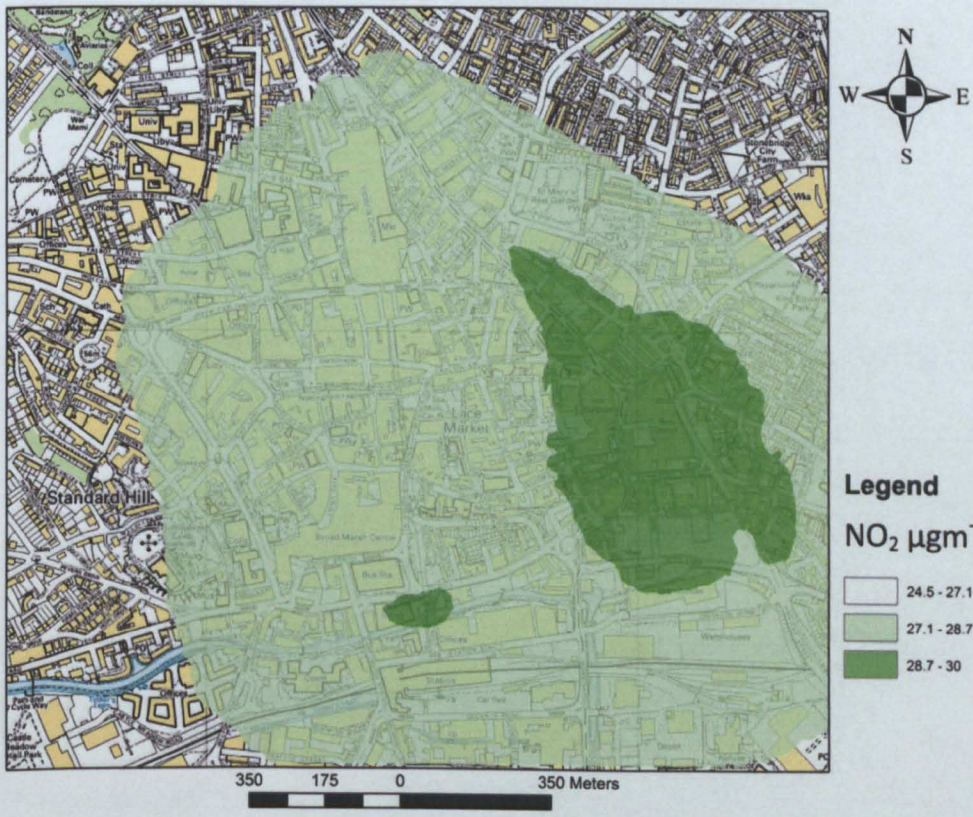

Figure 9.38 Contour Map of Do-Something 2014 12 metres-height Annual Mean NO_2 Concentrations in the City Centre

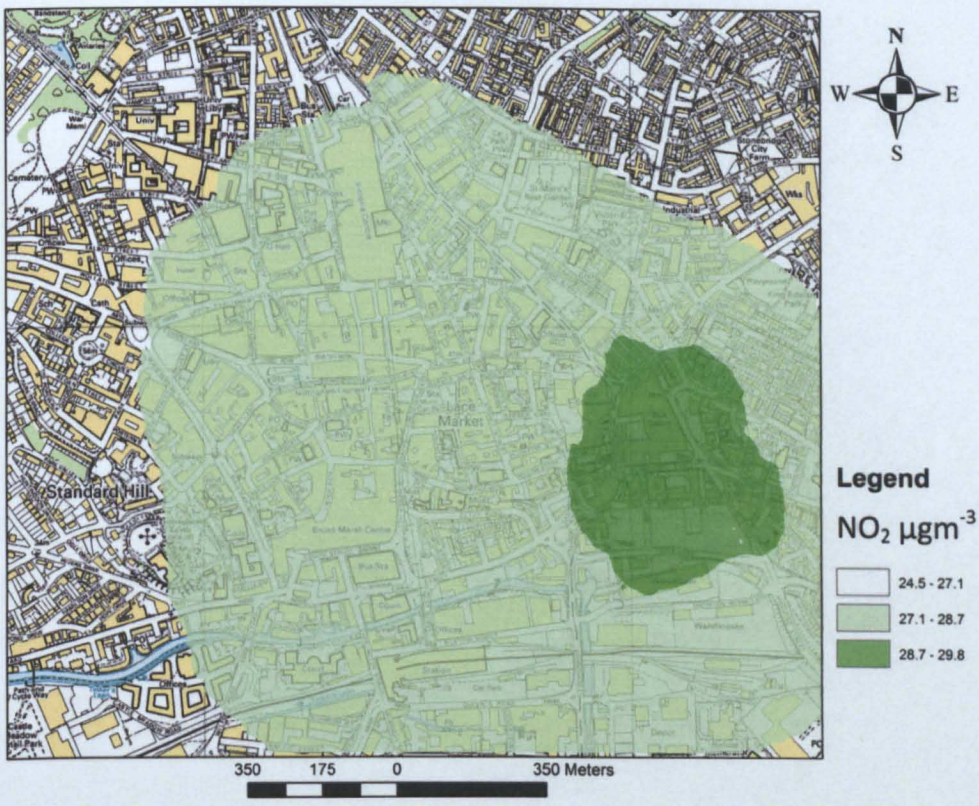

Figure 9.39 Contour Map of Do-Something 2014 18 metres-height Annual Mean NO_2 Concentrations in the City Centre

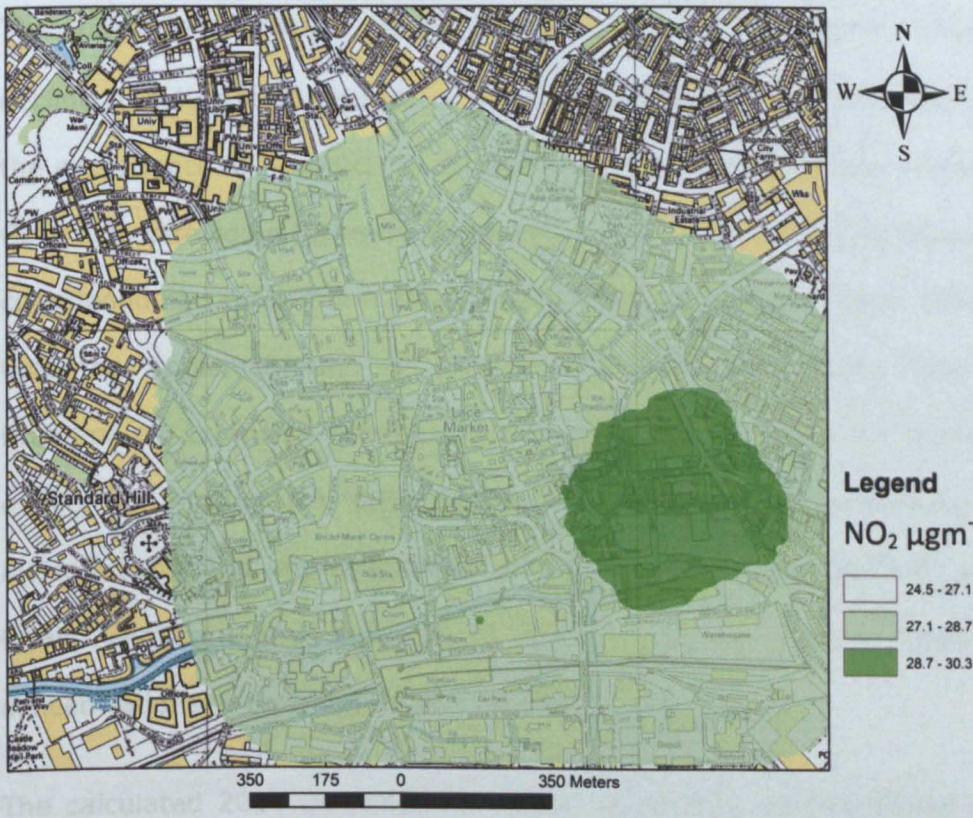

Figure 9.40 Contour Map of Do-Something 2014 24 metres-height Annual Mean NO_2 Concentrations in the City Centre

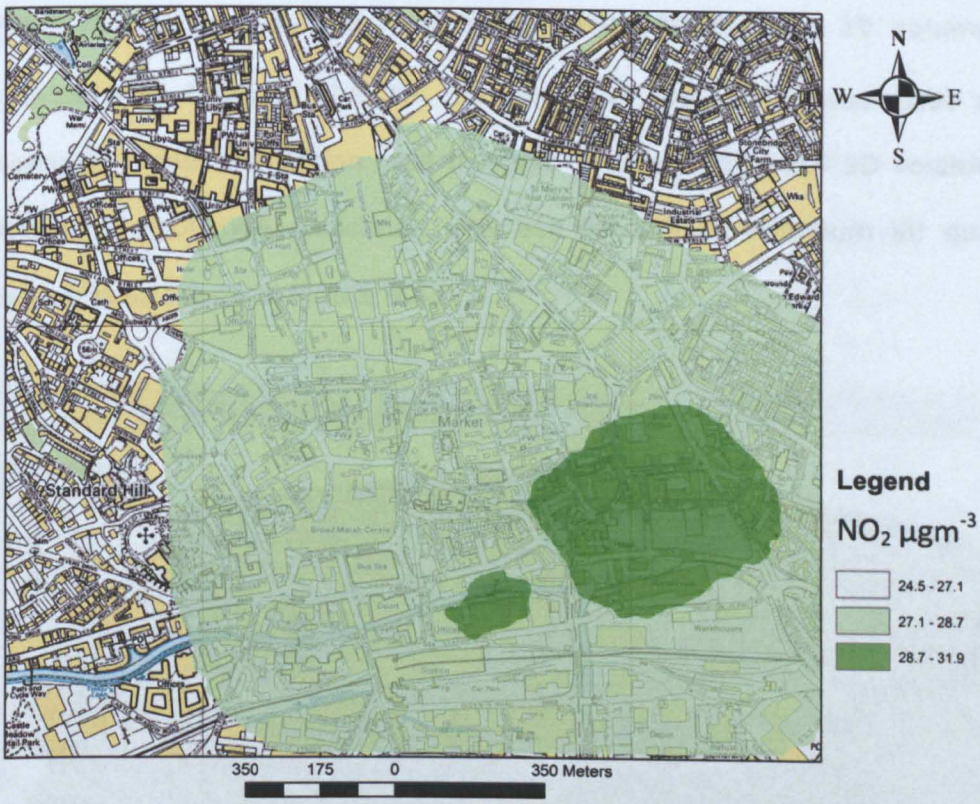

Figure 9.41 Contour Map of Do-Something 2014 30 metres-height Annual Mean NO_2 Concentrations in the City Centre

The comparison between Figure 9.19 and Figure 9.30 indicated that the decline in future background concentrations would substantially decrease the exceedance of the AQO for annual mean NO_2 concentrations in the City Centre despite some future traffic growth being anticipated. Comparing the corresponding Do-Minimum and Do-Something NO_2 contour maps indicated that the implementation of the Turning Point East Phase One and Broadmarsh Extension schemes would effectively improve the future air quality in Nottingham City Centre. Furthermore, the modelling also indicated that the implementation of these two transport schemes would totally eliminate any exceedances of the AQO for annual mean NO_2 concentrations in Nottingham City Centre.

The calculated 2014 Do-Minimum annual mean NO_2 concentrations at all the 6 metre-apart output heights, at and above the ground surface, were turned into 3D volumetric clouds for three concentration bands as was

done in Section 7.5 with four concentration bands. The 3D volumetric clouds were fused in the 3D city model of the City Centre base case scenario model application area in order to create the 2014 3D volumetric clouds air pollution dispersion interface for the Do-Minimum air quality scenario as shown in Figure 9.42.

Figure 9.42 Screenshot of 2014 Do-Minimum 3D Air Pollution Dispersion Interface for the City Centre

The creation of the 2014 3D air pollution dispersion interface for the Do-Something air quality scenario required development of the 3D city model of the base case scenario model application area, in order to take account of changes in Nottingham City Centre's built environment which would be expected due to the implementation of the Turning Point East Phase One and Broadmarsh Extension schemes. Hence, there would be an intuitive visual distinction between the 3D air pollution dispersion interfaces for the Do-Minimum and Do-Something air quality scenarios.

The discussions with Nottingham City Council confirmed that the implementation of the Turning Point East Phase One scheme would not involve any modifications to Nottingham City Centre's built environment,

but that the implementation of the Broadmarsh Extension scheme would involve the demolition of existing buildings in order to extend the Broadmarsh Shopping Centre to four proposed new blocks as shown in Figure 9.43. The average heights of these new blocks were provided by Nottingham City Council as 20 metres for blocks A, C and D and 15 metres for block B.

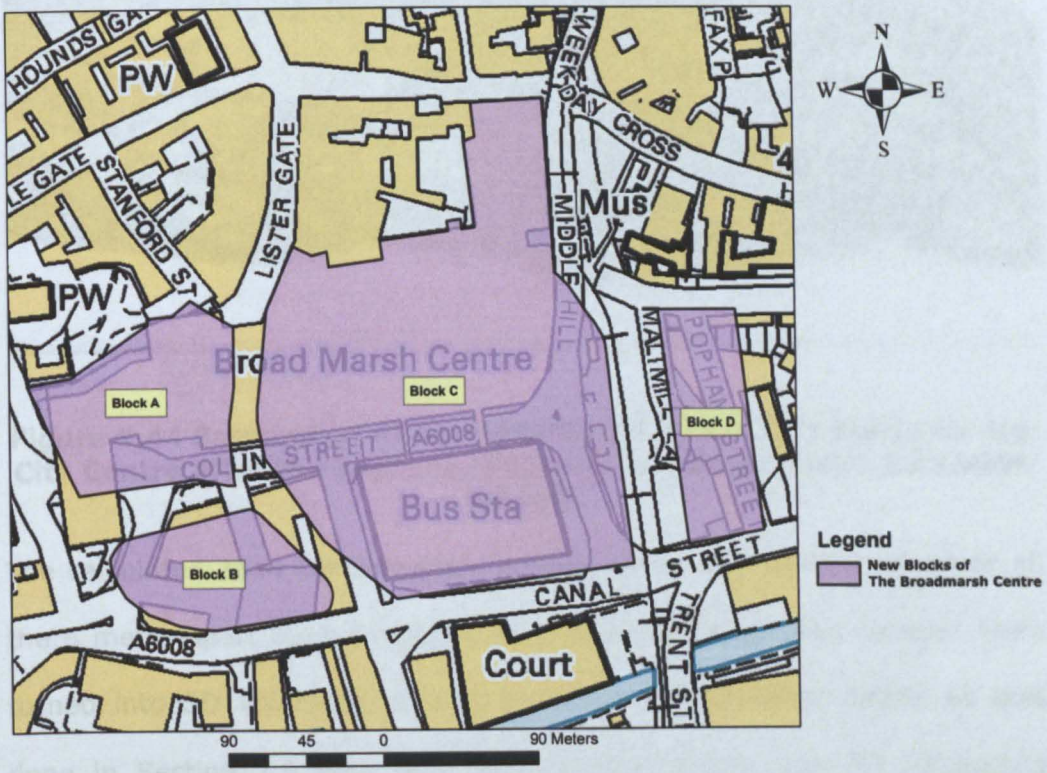

Figure 9.43 Four Proposed New Blocks of the Broadmarsh Shopping Centre

3D models of the new blocks were created in AutoCAD Civil 3D. Existing blocks in the 3D city model were imported into AutoCAD Civil 3D, where the ones interfering with the four new blocks were deleted. The remaining existing blocks and the new blocks were exported to the 3D city model in order to represent the built environment in Nottingham City Centre after the extension of the Broadmarsh Shopping Centre. The colour of the four new blocks was different from the colour of the remaining blocks in order

to distinguish intuitively between the present (existing) blocks and the future blocks of the Broadmarsh Shopping Centre as shown in Figure 9.44.

Figure 9.44 Screenshot of the Updated 3D digital City Model for the City Centre after the Implementation of the Broadmarsh Extension Scheme

The calculated 2014 Do-Something annual mean NO_2 concentrations at all the 6 metre-apart output heights, at and above the ground surface, were turned into 3D volumetric clouds for three concentration bands as was done in Section 7.5 with four concentration bands. The 3D volumetric clouds were fused in the updated 3D city model in order to create the 2014 3D volumetric clouds air pollution dispersion interface for the Do-Something air quality scenario as shown in Figure 9.45.

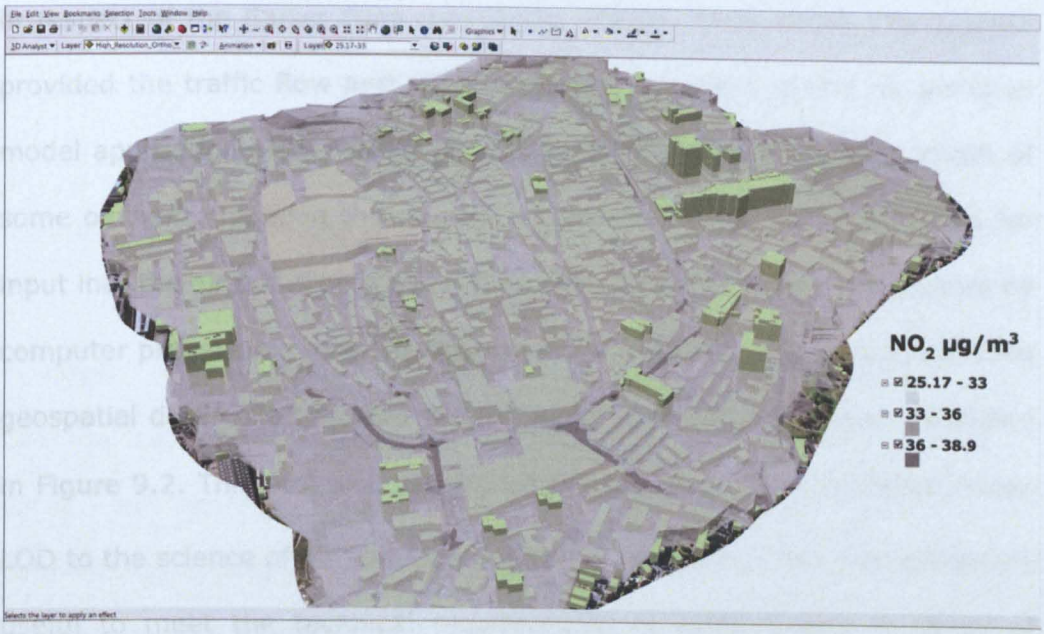

Figure 9.45 Screenshot of 2014 Do-Something 3D Air Pollution Dispersion Interface for the City Centre

9.11 Summary

This chapter evaluated the applicability of the decision-support system developed in this research project to the Turning Point East Phase One and Broadmarsh Shopping Centre Extension transport schemes. This involved the prediction and visualisation of the future air quality impacts of these two transport schemes. This also included the investigation of these two transport schemes' contribution to possibly revoking the Nottingham City Centre AQMA. The air pollution model application area contained the roads directly affected by the implementation of these two transport schemes, all of the City Centre AQMA and a 200-metre buffer zone as shown in Figure 9.1.

Due to the availability of both the input data to ADMS-Roads and the air pollution monitoring data, 2006 was selected as the base case year. 2006 air quality monitoring data was obtained from the UK Air Quality Archive in respect of the AURN monitoring station, and from Nottingham City Council

in respect of the Carter Gate monitoring station. Nottingham City Council provided the traffic flow and speed data for 108 roads in the air pollution model application area. The large number of roads, and the long length of some of them, impeded the manual digitisation of the road centrelines for input into the air pollution model. Therefore, a new GIS tool was created by computer programming with Python in ArcGIS 9.2 in order to automate the geospatial data collection and processing of the road centrelines as shown in Figure 9.2. This tool also introduced the concept of the modelled roads' LOD to the science of air pollution dispersion modelling. This was extremely useful to meet the technical requirements of ADMS-Roads in terms of ensuring that the vertices of each road centreline were at least 1 metre apart.

The base case scenario model underestimated the 2006 annual mean of monitored NO_2 and NO_X concentrations, and overestimated the 2006 annual mean of the monitored O_3 concentrations at the AURN monitoring station. This tendency was confirmed at the Carter Gate monitoring station where the base case scenario model underestimated the 2006 annual means of monitored NO_2 and NO_X concentrations. This indicated the need for the calibration of the base case scenario model. As O_3 concentrations were not monitored by the Carter Gate monitoring station, the AURN monitoring data were used for the investigation of the applicability of the Chapter 6 macro and micro-calibration strategies to the base case scenario model. The Carter Gate monitored data were kept independent of the calibration process for the validation of air pollution predictions of the base case scenario model.

The application of equations (6.1), (6.2) and (6.3), derived from the macro-calibration of the Dunkirk AQMA air pollution model, greatly

improved the macro-validation results of the City Centre base case scenario model at both the AURN and Carter Gate monitoring stations, as indicated by the results of run 2 in Table 9.1. The application of the micro-calibration strategy improved the micro-validation results of the City Centre base case scenario model as shown in Figure 9.12 and Figure 9.13. However, either the imprecise model simulation of actual atmospheric chemical reactions between NO_X and O_3 or imprecise monitoring data at some hours increased the error between calculated and monitored NO_2 concentrations after the micro-calibration at these hours. Therefore, a mathematical algorithm was created and implemented by VBA in MS Excel in order to mitigate this error as shown in Figure 9.14. The application of this mathematical algorithm mitigated the error and improved further the micro-validation results of the City Centre base case scenario model as shown in Figure 9.15 and Figure 9.16.

The output grid design of the Dunkirk AQMA base case scenario model was replicated for the output grid design of the City Centre base case scenario model in this chapter. The application of the height limit strategy of the Dunkirk AQMA base case scenario model at the AURN and Carter Gate monitoring stations resulted in an average height limit of 30 metres with a 6-metre step for the City Centre base case scenario output grid.

The DTM, orthoimage and 3D features of the 3D digital city model of the base case scenario model application area were created and integrated with calculated NO_2 concentrations at and above the ground surface in order to build the 3D volumetric clouds air pollution dispersion interface for the City Centre base case scenario model. However, the ground-level contour band exceeding the AQO of annual mean NO_2 concentrations disappeared at the next output height, so the 3D volumetric cloud

representing the critical ground-level NO_2 concentrations would only be displayed as a ground-level 2D planar surface. Therefore, a specific investigation was carried out and a new strategy was introduced in order to give this cloud realistic vertical and horizontal shape in the 3D air pollution dispersion interface.

Discussions with Nottingham City Council resulted in the identification of the roads on which traffic movement is likely to be directly affected by the implementation of the Turning Point East Phase One and the Broadmarsh Shopping Centre Extension schemes as shown in Figure 9.29. Nottingham City Council provided the anticipated future traffic flows for these roads when these two transport schemes are expected to be implemented. The anticipated implementation years are 2011 for the Turning Point East Phase One scheme and 2014 for the Broadmarsh Extension scheme. Therefore, 2014 was selected as the modelling year of the Do-Minimum and Do-Something future traffic scenarios. A 2% annual average traffic growth rate was used to project the traffic flows of the City Centre base case scenario model to the 2014 Do-Minimum traffic scenario. This traffic growth rate was also used to project the base case scenario traffic flows of roads expected to be largely unaffected by the implementation of these two transport schemes to the 2014 Do-Something traffic scenario.

The micro-calibrated background concentrations and the traffic-induced emissions of the City Centre base case scenario model were projected from 2006 to 2014 in the same way as described in Section 8.2. The 2006 industrial emission rates were used in the 2014 air quality scenarios with no projection, as this kind of emissions was outside the scope of this research project. Comparing the corresponding (in terms of height) 2014 Do-Minimum and Do-Something NO_2 contour maps indicated that the implementation of the two transport schemes would effectively improve the

future air quality in Nottingham City Centre, and also would totally eliminate any exceedances of the AQO for annual mean NO_2 concentrations in Nottingham City Centre.

The calculated 2014 Do-Minimum annual mean NO_2 concentrations at and above the ground surface were integrated with the 3D city model of the City Centre base case scenario model application area to build the 2014 Do-Minimum 3D volumetric clouds air pollution dispersion interface as shown in Figure 9.42. The 3D city model of the City Centre base case scenario model was developed to include representation of the four new blocks of the Broadmarsh Shopping Centre after its extension in 2014. After the integration with the calculated 2014 Do-Something annual mean NO_2 concentrations at and above the ground surface, the updated 3D city model provided an intuitive distinction between the 2014 3D volumetric clouds air pollution dispersion interfaces of the Do-Minimum and Do-Something air quality scenarios. These four new blocks were assigned a different colour to the colour of the remaining blocks in the 2014 Do-Something 3D air pollution dispersion interface as shown in Figure 9.45. This provided a contrast so a viewer may distinguish intuitively between the present (existing) blocks and future blocks of the Broadmarsh Shopping Centre.

Therefore, relating to the aim of this chapter, the decision-support system initially developed for modelling and visualising the air quality impacts of the implementation of NET Phase 2 in the Dunkirk AQMA needed the further development presented in this chapter in order to be applicable to the Turning Point East Phase One and Broadmarsh Shopping Centre Extension transport schemes in Nottingham City Centre.

Chapter 10

Validation of Future Air Quality Predictions Using the Decision-support System

10.1 Introduction

The aim of this chapter is to attempt a fuller validation of the research decision-support system, by using it to model an already fully implemented transport scheme, in order to try to assess the accuracy of future air quality predictions made using this research decision-support system. This involves taking the base year (for modelling before the implementation of the scheme) to be some years ago, and the future modelling year (for modelling after the implementation of the scheme) to be a more recent past time, so that not only can the before implementation modelling be validated against monitored base year data, but validation of the after implementation modelling against monitored more recent past data can also be attempted. Therefore, with a base year of 2003 and a future modelling year of 2006, research was undertaken into the use of the developed decision-support system for the prediction, and then validation, of the air quality impacts of the completed Turning Point North transport scheme, which was introduced in Section 2.6.3 and selected for this purpose in Section 4.3.

Therefore, in this chapter, it is important to remember that all the before and after modelling, i.e. the 2003 base case scenario modelling and the

prediction of the 2006 air quality, was done as if 'time now' is 2003. For the validation of the results of the 2006 air quality modelling against 2006 monitored data, the 'time now' is obviously shifted to 2006. The aim of this chapter was attained by the investigation of seven main objectives.

1. The identification of the air pollution model application area.
2. The set-up of the base case scenario.
3. The geospatial data processing of the road network.
4. The calibration and validation of the base case scenario model.
5. The description of the output grid design which allows the validation of the spatial distribution of air quality predictions.
6. The future projection of the traffic and air pollution data of the base case scenario to after the implementation of the Turning Point North transport scheme at a more recent past time for which air quality monitoring data is available.
7. The prediction of the future air quality impacts of the implementation of this urban transport scheme, and the validation of these future air quality predictions against the available air quality monitoring data.

10.2 Air Pollution Model Application Area

The final air pollution model application area in Figure 9.1 was selected as the model application area of this air pollution model. This was to facilitate the validation of the base case scenario model against monitoring data from the continuous air quality monitoring stations located in Nottingham City Centre as explained in Section 9.2. The selection of this air pollution model application area also enabled the validation of the spatial distribution of air quality predictions for the Do-Something air quality scenario which will be discussed in Section 10.9.

10.3 Set-up of Base Case Scenario Modelling

As the research decision-support system uses NO_2 in order to assess the air quality impacts of proposed urban transport schemes, and as NO_2 was the air pollutant of concern in the City Centre AQMA, NO_2 was selected as the primary output air pollutant of the air pollution model. Due to the atmospheric chemical reactions between NO_X and O_3 which affect NO_2 concentrations in the atmosphere, NO_X and O_3 were also selected as output air pollutants of the air pollution model. Discussions with the Pollution Control Section in Nottingham City Council were undertaken to help with the identification of the set-up of the base case scenario in ADMS-Roads. These consultations resulted in the following set-up:

- 2003 was selected as the base case year for modelling the air quality before the implementation of the Turning Point North scheme because of data availability for that year for running, calibrating and validating the air pollution model.
- The Pollution Control Section provided the traffic flow and speed data for 206 roads for consideration in the air pollution model. For each of these roads, the traffic flow and speed data were provided for the LDV and HDV traffic categories, as required for input to ADMS-Roads. These roads were all considered as non-canyon streets in the air pollution model. ADMS-Roads used the traffic speed data to identify the traffic emissions (per vehicle) factors according to the built-in 2003 DMRB database, in order then, for each modelled road, to multiply the factor by the traffic flow to yield the traffic emissions (per second) rate.

- The Chemical Reaction Scheme was selected for the simulation of the atmospheric chemical reactions of NO_x as the required background concentrations of NO_x, NO_2 and O_3 were available.
- Surface roughness = 1.0, latitude = 52° and minimum Monin-Obukhov length = 30.
- Three point sources were defined in the base case scenario and other future scenarios: London Road Heat Station, EON Ratcliffe power station and the chimney of Daleside Dyers & Finishers Ltd. The emitted pollutant was NO_x as NO_2. As the chemical reactions option was selected, ADMS-Roads assumed that 10% of NO_x as NO_2 emissions was NO_2.
- The 2003 hourly sequential meteorological data measured by the Nottingham Watnall Weather station was used for all air quality modelling scenarios. The meteorological data included 10 parameters: Station Number, Year, Day, Hour, Temperature, Wind Speed, Wind Direction, Precipitation, Cloud Cover and Degree of Humidity. The wind speed was measured at 10 metres height and the wind sector size was 10°. Figure 10.1 shows the 2003 wind rose. It was assumed that the weather conditions in the Watnall and City Centre areas of Nottingham were identical at all times.
- The 2003 hourly sequential rural background concentrations, measured by the Rochester air quality monitoring station shown in Figure 6.3, were downloaded from NAEI (2009) and used in the base case scenario model. The background concentrations comprised NO_x, NO_2, O_3 and SO_2 concentrations.
- The base case scenario model was configured to output the modelled 2003 hourly calculated and annual mean NO_x, NO_2 and O_3 concentrations at only the site of the AURN monitoring station,

described in Section 2.4, as the Carter Gate monitoring station only began operation in 2004.

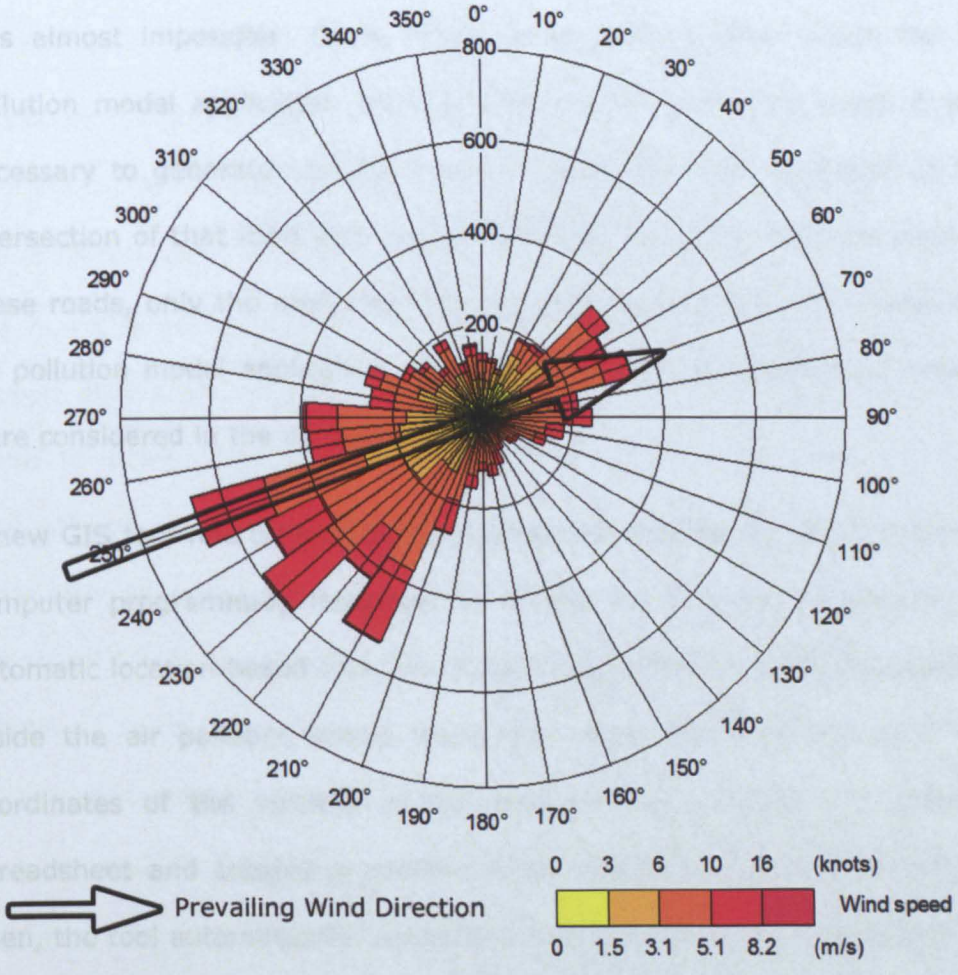

Figure 10.1 2003 Wind Rose

10.4 Geospatial Data Processing of the Road Network

The roads for which traffic flow and speed data were provided by the Pollution Control Section, were not identifiable by name. The road corresponding to each data record was instead defined by the coordinates of the vertices of its centreline written to a spreadsheet. As the number of these roads (206) was very large and exceeded the maximum number of roads (150) that could be defined in ADMS-Roads, it was necessary to

consider only the road segments located inside the air pollution model application area. With such a large number of unnamed roads, the manual selection of roads located inside the air pollution model application area was almost impossible. Some roads were partly located inside the air pollution model application area, and hence, for each such road, it was necessary to generate one more vertex along the road centreline at the intersection of that road with the boundary of this area. Then for each of these roads, only the road segments, from the end of the road inside the air pollution model application area to this additionally generated vertex, were considered in the air pollution model.

A new GIS tool was created by the author with Python, an object-oriented computer programming language, in ArcGIS 9.2 in order to perform an automatic location-based selection of the road centreline segments existing inside the air pollution model application area. The new tool read the coordinates of the vertices of the road centrelines from the external spreadsheet and created a polyline shape file for every road centreline. Then, the tool automatically clipped the road centreline shape files with the polygon shape file of the air pollution model application area in order to leave only the road centreline segments located inside this area. For roads only partly located inside the air pollution model application area, such a clipping of the road centreline shape files automatically generated additional centreline vertices at the intersections of those roads with the boundary of this area. Finally, the tool wrote the coordinates of the vertices of all the resulting road centreline segments inside the air pollution model application area to an output table which was subsequently exported to the emissions inventory file of ADMS-Roads. Figure 10.2 displays the flowchart of this new GIS tool.

As explained in Section 9.4, the new GIS tool complied with the ADMS-Roads technical requirements in terms of having a maximum of 50 vertices for any one road. The new GIS tool implemented the LOD and the associated output table maintenance algorithms described in Section 9.4, as shown in Figures 10.2b and 10.2c respectively. A help file, displaying a brief description of each item of the input data to the tool, was attached to the graphical user interface of the new GIS tool as shown in Figure 10.3. The new GIS tool provided a friendly graphical user interface for the tool console during the runtime. The runtime tool console printed the assigned name to every processed road along with its read vertices, from the external spreadsheet, and the number of written vertices to the output table after applying the LOD algorithm. Moreover, the new GIS tool gave the user insight into the processing by printing the start, end and the results of each processing stage to the tool output console during the runtime as shown in Figure 10.4. Figure 10.5 displays the tool output road centrelines which their traffic emissions were considered in the air pollution model.

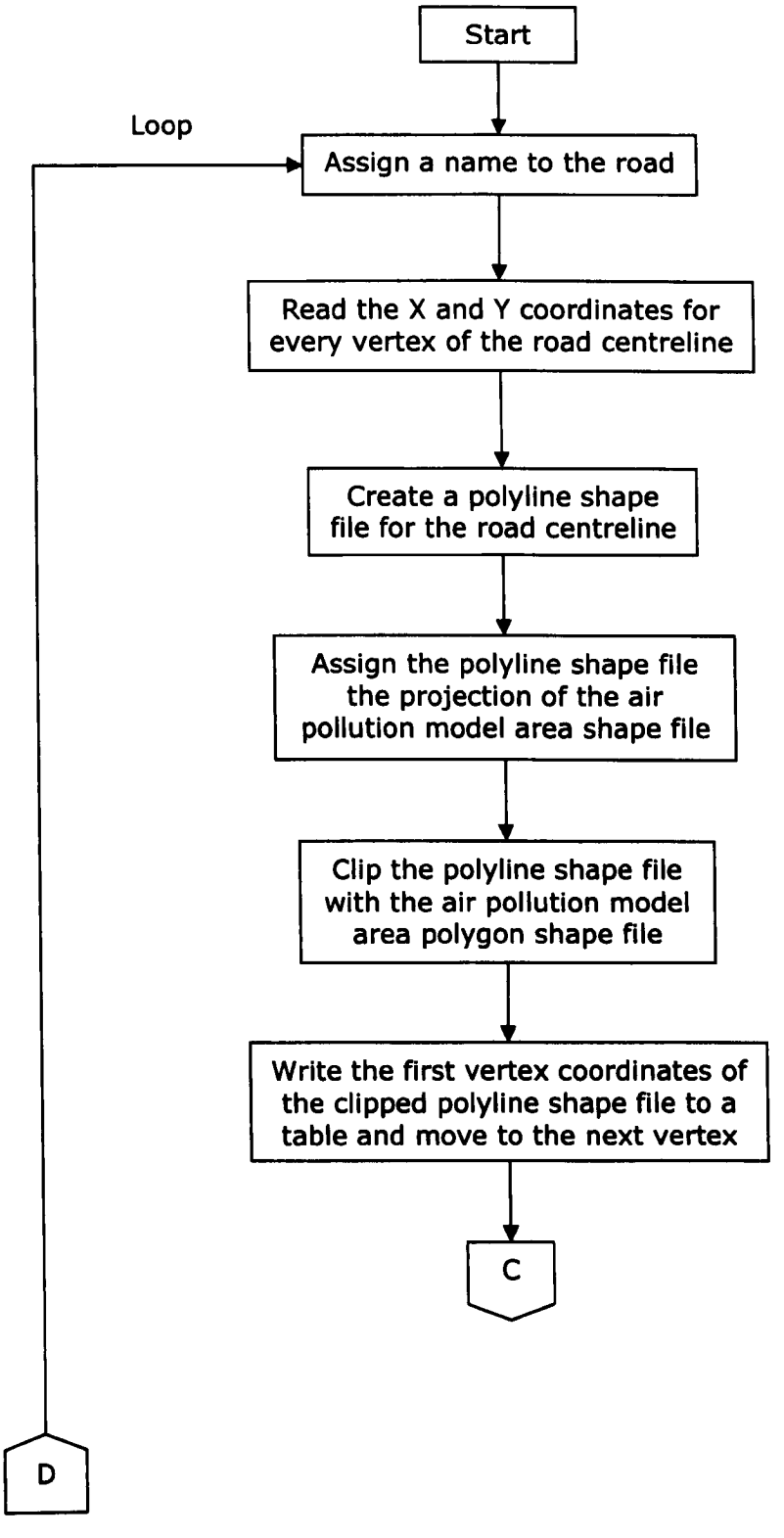

Figure 10.2a Flowchart of the New GIS Tool

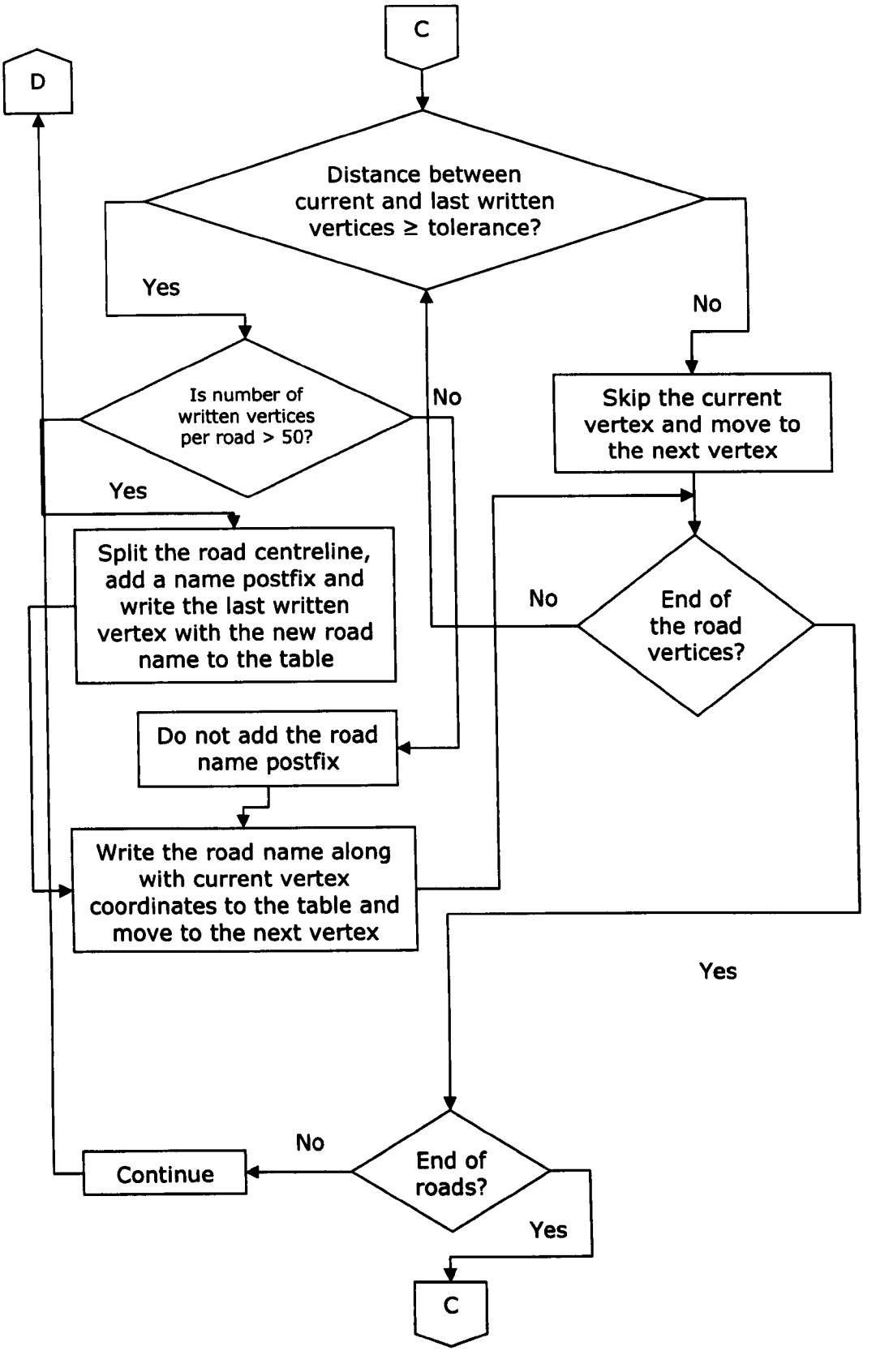

Figure 10.2b Flowchart of the New GIS Tool (continued)

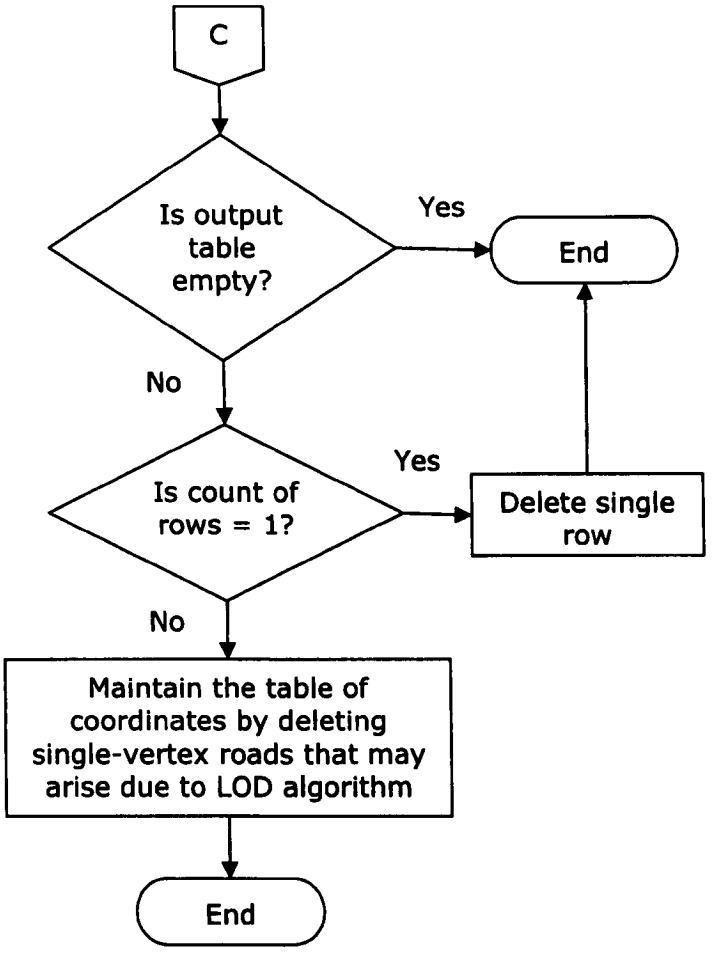

Figure 10.2c Flowchart of the New GIS Tool (continued)

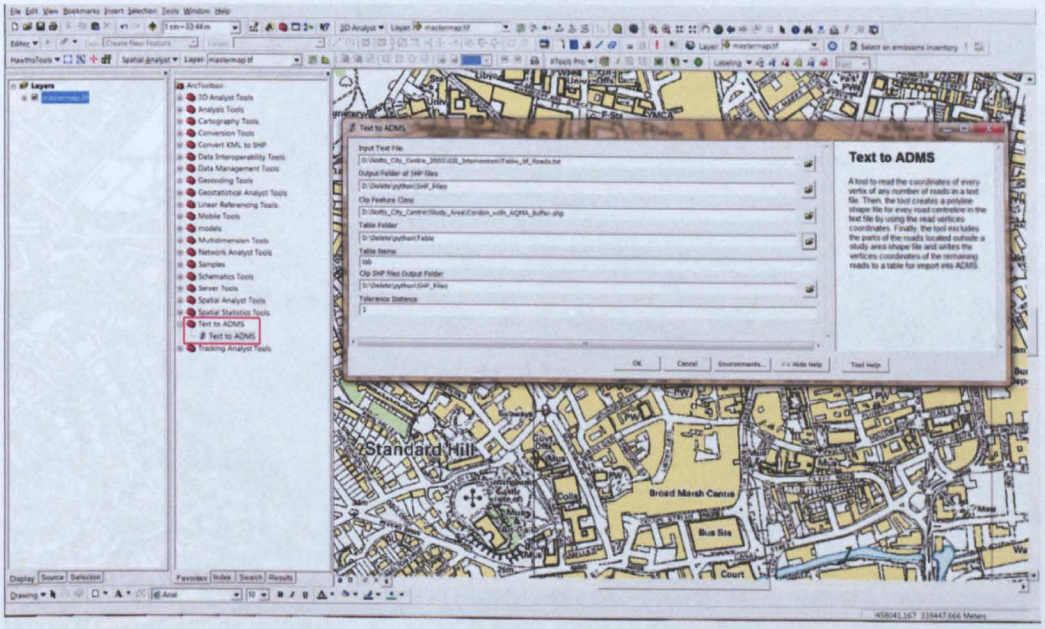

Figure 10.3 Data Entry Graphical User Interface of the New GIS Tool

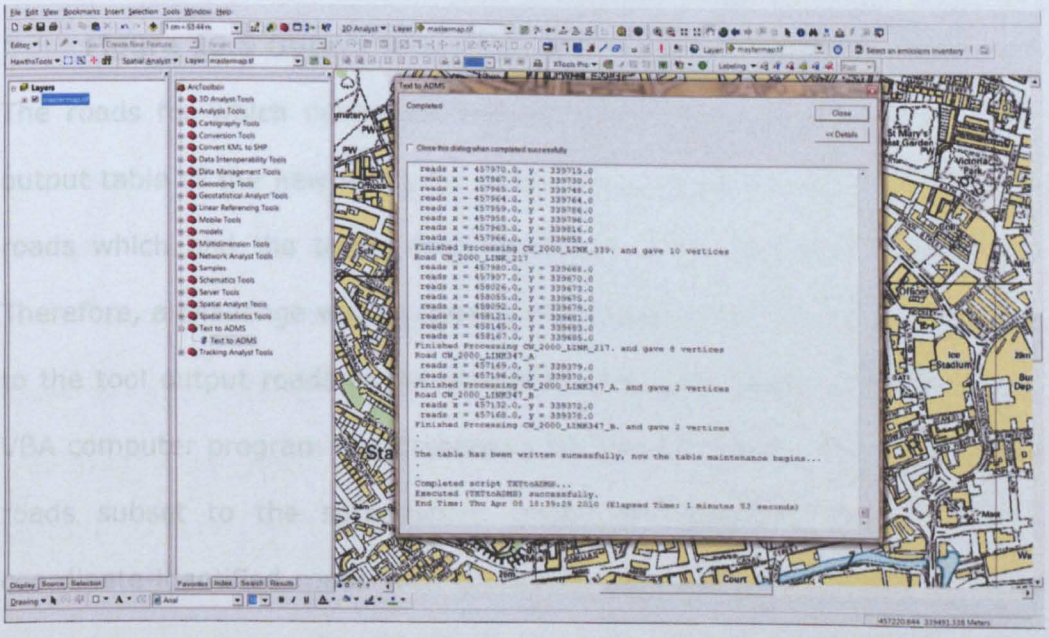

Figure 10.4 Runtime Console of the New GIS Tool

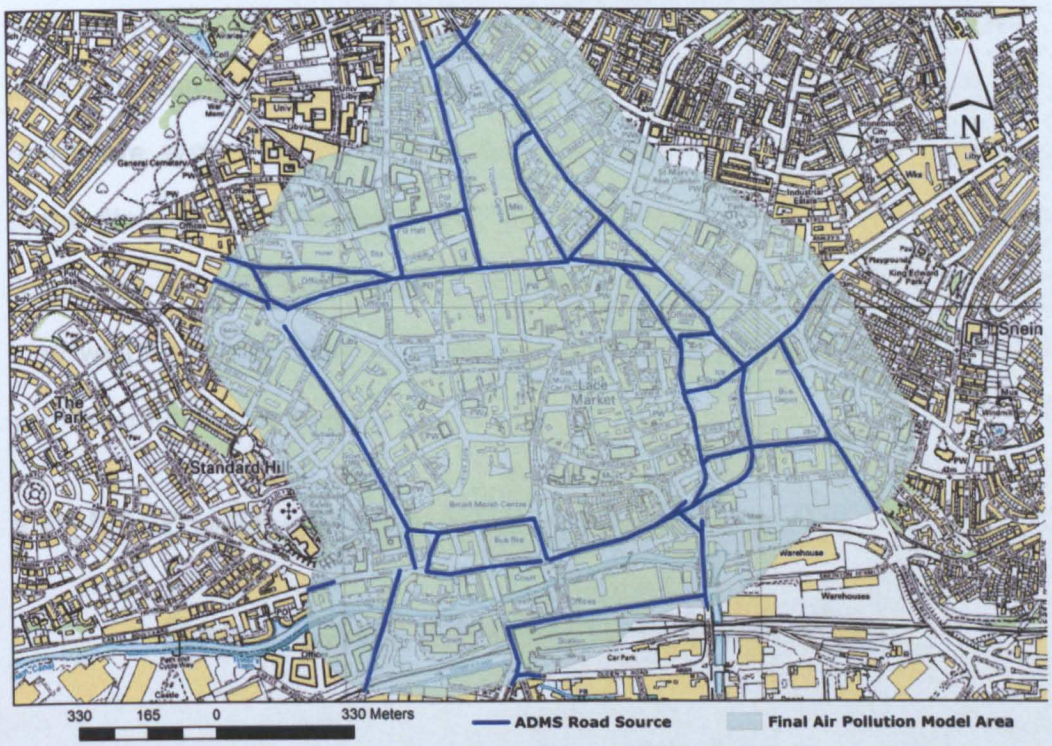

Figure 10.5 Output Road Centrelines of the New GIS Tool

The roads for which centreline vertices' coordinates were written to the output table of the new GIS tool, were only a subset of the original set of roads which had the traffic data attributes in the external spreadsheet. Therefore, a challenge was to append the appropriate traffic data attributes to the tool output roads in the emissions inventory file of ADMS-Roads. A VBA computer program was created in MS Excel in order to link the output roads subset to the spreadsheet which contained the original set of coordinate-identified roads with the traffic data attributes. Then, the VBA computer program automatically appended the appropriate traffic data attributes from that spreadsheet to the corresponding road in the output roads subset.

Another challenge was the determination of the width of every road for which the centreline was located inside the air pollution model application area. The road widths were required as input data to the air pollution model. To overcome this challenge, the output clipped shape files from the

new GIS tool were merged together into a single polyline shape file. Then, the single polyline shape file was projected from the British National Grid coordinate system to the Google Earth Coordinate System. This projected shape file was converted to a KML file, the file format accepted by Google Earth. The KML file was imported and displayed in Google Earth where the road width corresponding to each road centreline was measured for input into the air pollution model.

10.5 Calibration and Validation of the Base Case Scenario Modelling

No 2003 air quality monitoring data was available from the Carter Gate monitoring station as it only started operating in 2004. The hourly levels and annual means of NO_X, NO_2 and O_3, which were monitored by the AURN monitoring station in 2003, were downloaded from the UK Air Quality Archive. The downloaded hourly concentrations had the landscape layout issue described in Section 9.5. Therefore, the VBA computer program explained in Section 9.5 was used for the automatic transformation of this monitoring data layout from the original landscape to the required portrait layout.

Many records were missing in the 2003 hourly sequential background concentrations monitored by the Rochester air quality monitoring station. The missing data extended over many consecutive hours of 2003. This interrupted the running of the air pollution model as the model used the chemical reaction scheme which required the availability of background concentrations for each hour of the modelled year. Therefore, for each period of missing data, the missing records of background concentrations were filled in with the average of the last available and first available

hourly concentrations, before and after that period of missing data. However, it was difficult to do that manually due to the disparate locations of missing data records in the very large background concentrations dataset. Hence, a VBA computer program was created in MS Excel in order to automate the process of filling in the missing records of background concentrations.

The base case scenario model, with the uncalibrated rural background concentrations, underestimated the 2003 annual means of monitored NO_X and NO_2 concentrations by 27.85% and 16.26% respectively, and overestimated the 2003 annual mean of monitored O_3 concentrations by 34.51%, at the AURN monitoring station, as implied by the results of run 1 in Table 10.1. This indicated the need for the calibration of the base case scenario model.

10.5.1 Macro-calibration and Validation of the Base Case Scenario Modelling

The 2003 annual mean NO_2, NO_X and O_3 concentrations calculated using the uncalibrated rural background concentrations were substituted, along with the 2003 annual means of the AURN-monitored NO_2, NO_X and O_3 concentrations, into equations (6.1), (6.2) and (6.3) to evaluate the macro-calibration adjustment values for the rural background concentrations. Using the macro-calibrated background concentrations greatly improved the macro-validation results of the base case scenario model at the AURN monitoring station, as indicated by the results of run 2 in Table 10.1.

Table 10.1 Macro-calibration Results of the City Centre Base Case Scenario Model

RUN 1	Background	Δ background	calculated Concentrations at AURN	Δ Calculated	Target concentrations at AURN
NO_2	0	0	30.44	0	36.35
NO_x	0	0	46.69	0	64.71
O_3	0	0	44.47	0	33.06
RUN 2	**Background**	**Δ background**	**calculated Concentrations at AURN**	**Δ Calculated**	**Target concentrations at AURN**
NO_2	+0.95	+0.95	36.24	5.80	36.35
NO_x	+18.02	+18.02	64.71	18.02	64.71
O_3	-4.66	-4.66	34.94	-9.52	33.06
RUN 14	**Background**	**Δ background**	**calculated Concentrations at AURN**	**Δ Calculated**	**Target concentrations at AURN**
NO_2	+0.50	-0.45	31.20	0.76	36.35
NO_x	+2.40	-15.62	49.09	2.40	64.71
O_3	-2.00	+2.66	42.29	-2.18	33.06
RUN 15	**Background**	**Δ background**	**calculated Concentrations at AURN**	**Δ Calculated**	**Target concentrations at AURN**
NO_2	+0.72	+0.22	31.36	0.92	36.35
NO_x	+2.40	0	49.09	2.40	64.71
O_3	-2.00	0	42.35	-2.11	33.06

Table 10.1 Macro-calibration Results of the City Centre Base Case Scenario Model (continued)

RUN 16	Background	Δ background	calculated Concentrations at AURN	Δ Calculated	Target concentrations at AURN
NO_2	+0.72	0	31.33	0.89	36.35
NO_x	+2.30	-0.10	48.99	2.30	64.71
O_3	-2.00	0	42.38	-2.08	33.06
RUN 17	**Background**	**Δ background**	**calculated Concentrations at AURN**	**Δ Calculated**	**Target concentrations at AURN**
NO_2	+0.72	0	31.26	0.82	36.35
NO_x	+2.00	-0.30	48.69	2.00	64.71
O_3	-2.00	0	42.46	-2.01	33.06

10.5.2 Micro-calibration and Validation of the Base Case Scenario Modelling

The uncalibrated rural background concentrations were used for running the base case scenario model in order to output the 2003 hourly calculated NO_2 concentrations at the AURN monitoring station. This was for the micro-validation of the base case scenario model before any calibration as shown in Figure 10.6. Then for the micro-validation after the macro-calibration, the base case scenario model was run with the macro-calibrated background concentrations to output the 2003 hourly calculated NO_2 concentrations at the AURN monitoring station. Figure 10.7 illustrates the micro-validation results of running the macro-calibrated base case scenario model.

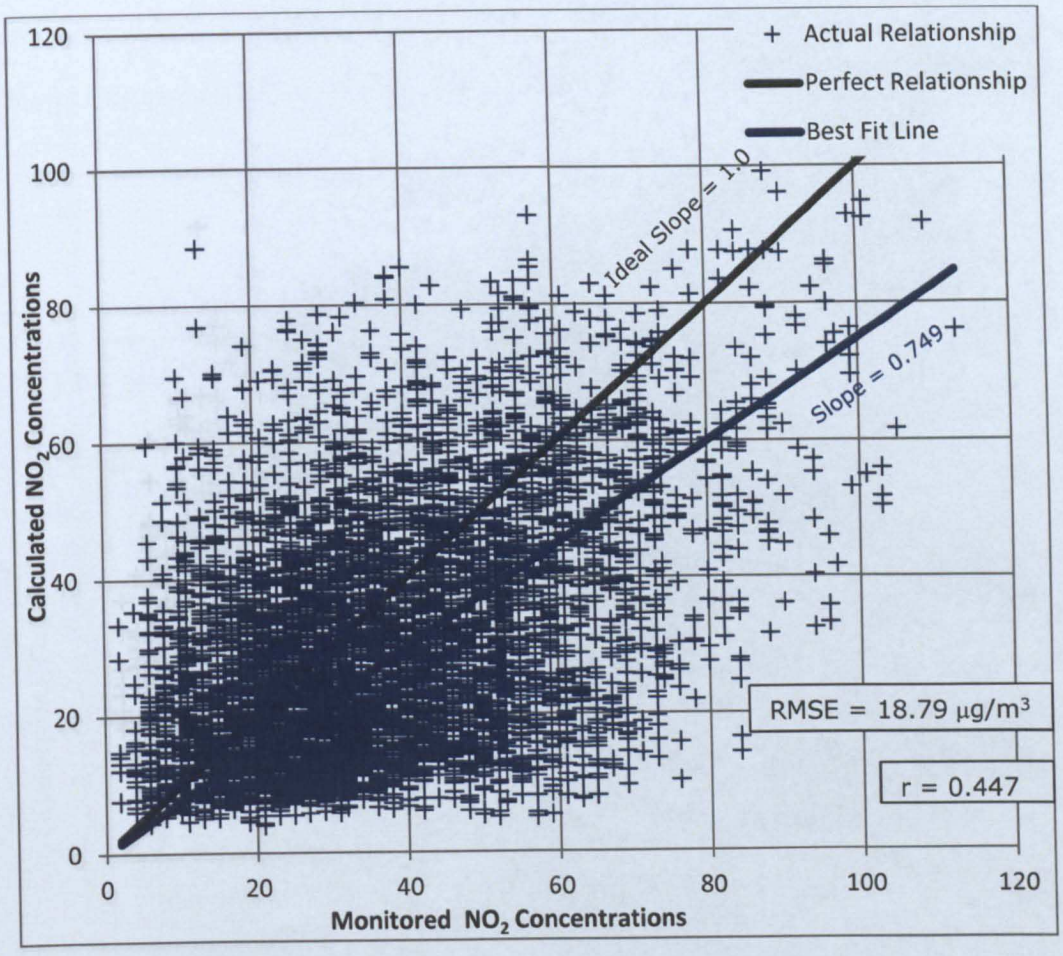

Figure 10.6 Scatter Diagram of Hourly NO_2 Concentrations at the AURN Station before Calibration

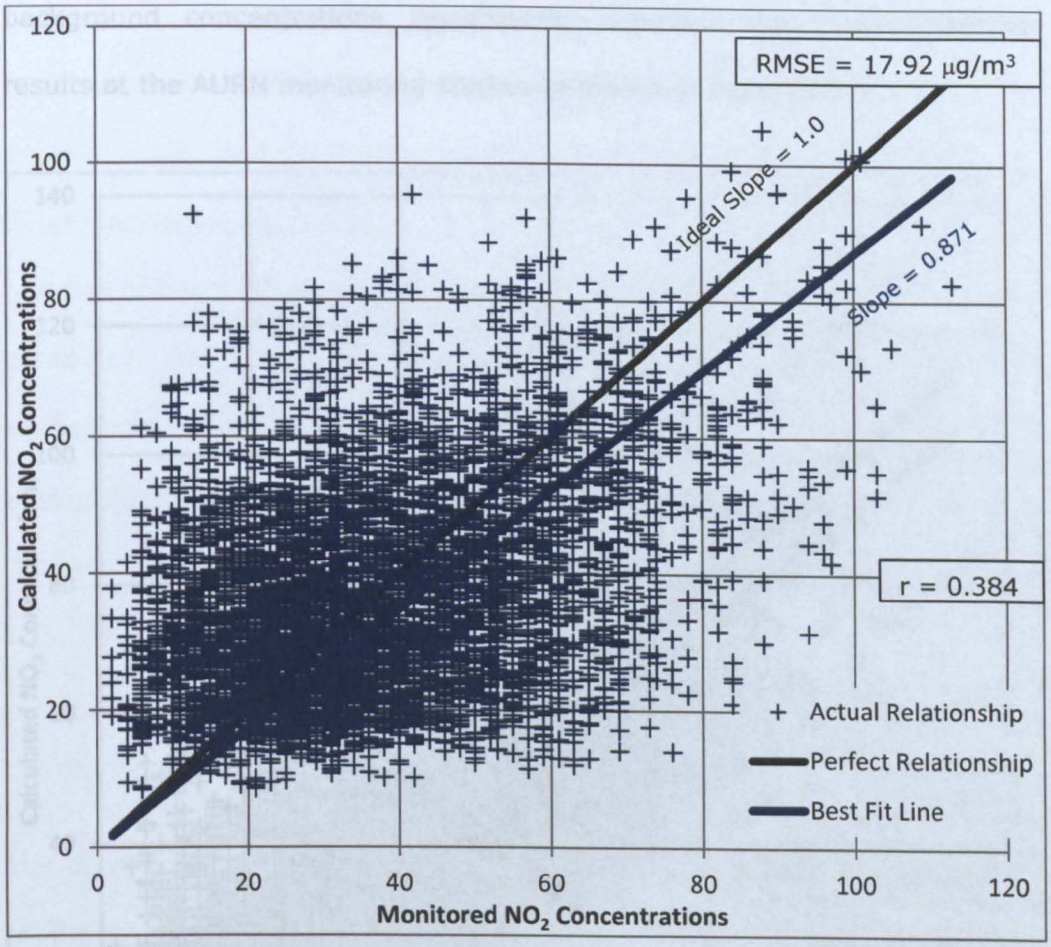

Figure 10.7 Scatter Diagram of Hourly NO_2 Concentrations at the AURN Station after Macro-calibration

The macro-calibration of the base case scenario model slightly improved the micro-validation results at the AURN monitoring station, as implied by the comparison between Figure 10.6 and Figure 10.7. This indicated the need for the application of the micro-calibration strategy in order to improve effectively the micro-validation results of the base case scenario model. The 2003 hourly sequential rural background concentrations, monitored concentrations and the calculated concentrations before any calibration were used along with the macro-calibration results, corresponding to run 2 in Table 10.1, for the application of equations (6.8), (6.9) and (6.10). These equations were applied to generate of the micro-calibrated 2003 hourly sequential NO_2, NO_X and O_3 background concentrations. Running the base case scenario model with these

background concentrations significantly improved the micro-validation results at the AURN monitoring station as shown in Figure 10.8.

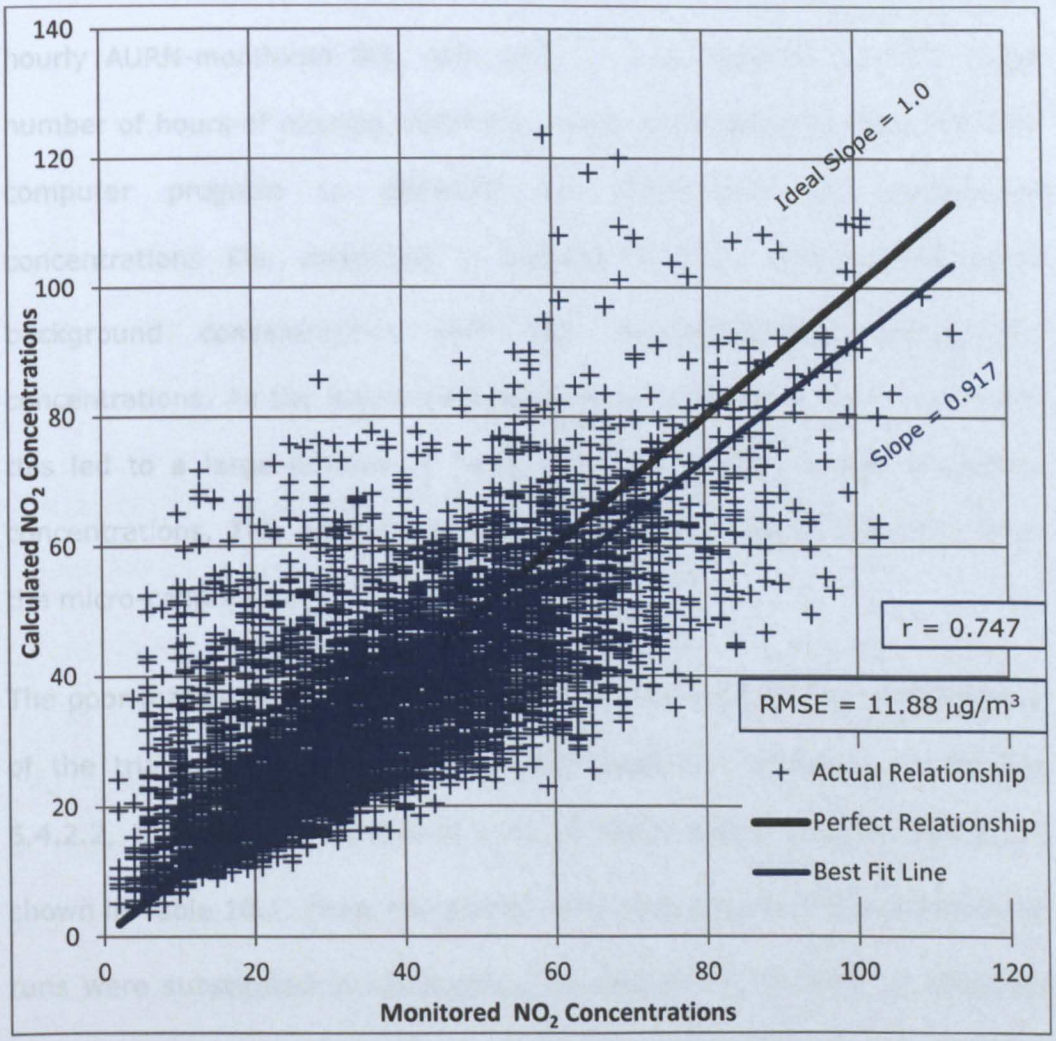

Figure 10.8 Scatter Diagram of Hourly NO_2 Concentrations at the AURN Station after the Micro-calibration based on Run 2

The base case scenario model (based on run 2) with these micro-calibrated background concentrations underestimated the annual mean of monitored NO_2 concentration, and overestimated the annual mean of monitored O_3 concentrations, at the AURN monitoring station as shown in Table 10.2. Additionally, this time, the base case scenario model with these micro-calibrated background concentrations overestimated the annual mean of monitored NO_X concentrations at the AURN monitoring station as shown in Table 10.2. A potential reason for such an overestimation of the annual

mean of monitored NO_X concentrations, which did not happen before in the micro-calibration of the 2006 base case scenario model presented in Section 9.5.2, was the relatively large number of missing hours of 2003 hourly AURN-monitored NO_X, NO_2 and O_3 concentrations. For the large number of hours of missing AURN-monitored concentrations data, the VBA computer program to generate the micro-calibrated background concentrations file, described in Section 6.4.2.2, replaced the rural background concentrations with the macro-calibrated background concentrations. As the macro-calibration is not precise on the micro level, this led to a large number of hours with less precise hourly calculated concentrations. This possibly caused the poor NO_X macro-validation after the micro-calibration.

The poor macro-validation of NO_X, NO_2 and O_3 concentrations required use of the trial and error macro-calibration approach, explained in Section 6.4.2.2, to undertake additional runs of ADMS-Roads, beyond run 2, as shown in Table 10.1. Then, the macro-calibration results of these additional runs were substituted in equations (6.8) and (6.10) in order to generate the 2003 hourly sequential micro-calibrated NO_2 and O_3 background concentrations. However, the overestimation of the 2003 annual mean of monitored NO_X concentrations at the AURN monitoring station necessitated the alteration of equation (6.9) in order to take the same general form as equations (6.8) and (6.10) as follows:

$$\Delta NO_{x\,background\,i} = \frac{(NO_{x\,monitored\,i} - NO_{x\,uncalibrated\,i})}{(\overline{NO}_{x\,macro} - \overline{NO}_{x\,uncalibrated})} \times \Delta NO_{x\,macro\,background,} \quad \textbf{(10.1)}$$

where $\Delta NO_{x\,background\,i}$ is the adjustment value for the rural NO_x background concentration for the hour i. $NO_{x\,monitored\,i}$ is the monitored hourly NO_x concentration for the hour i. $NO_{x\,uncalibrated\,i}$ is the calculated hourly NO_x

concentration for the hour i using the uncalibrated rural background concentrations. The value of i ranged from 1 to 8760, which was the total number of hours in the year 2003. $\overline{NO_{x\,macro}}$ is the annual mean NO_x concentration calculated using the macro-calibrated background concentrations. $\overline{NO_{x\,uncalibrated}}$ is the annual mean NO_2 concentration calculated using the uncalibrated rural background concentrations (46.69 $\mu g/m^3$). $\Delta NO_{x\,macro\,background}$ is the macro-calibration adjustment value for the rural NO_x background concentrations, as given in the column headed 'Background' in Table 10.1.

The macro-calibration results of the additional runs were substituted in equation (10.1) in order to generate the 2003 hourly sequential micro-calibrated NO_x background concentrations. Running the base case scenario model with these micro-calibrated background concentrations incrementally improved the macro-validation of the base case scenario model as shown in Table 10.2. Moreover, the micro-calibration based on the last of these additional macro-calibration runs (run 17) improved further the micro-validation of the base case scenario model as shown in Figure 10.9.

The micro-calibration development, from run 2 to run 17, increased the error between the calculated and monitored NO_2 concentrations at some hours, as implied by the comparison between the scatter in the overestimated points on the upper left side of Figures 10.8 and 10.9. A potential reason for such unexpected behaviour of the micro-calibration development at these hours was explained in Section 9.5.2. Therefore, the micro-calibrated background concentrations based on run 17 were adjusted by the implementation of the VBA computer program for which the flowchart was illustrated in Figure 9.14. This reduced the above-mentioned error and improved further the micro-validation results of the City Centre

base case scenario model as shown in Figure 10.10. Therefore, it was decided to use the adjusted micro-calibrated background concentrations based on run 17 for the modelling of the future air quality scenario.

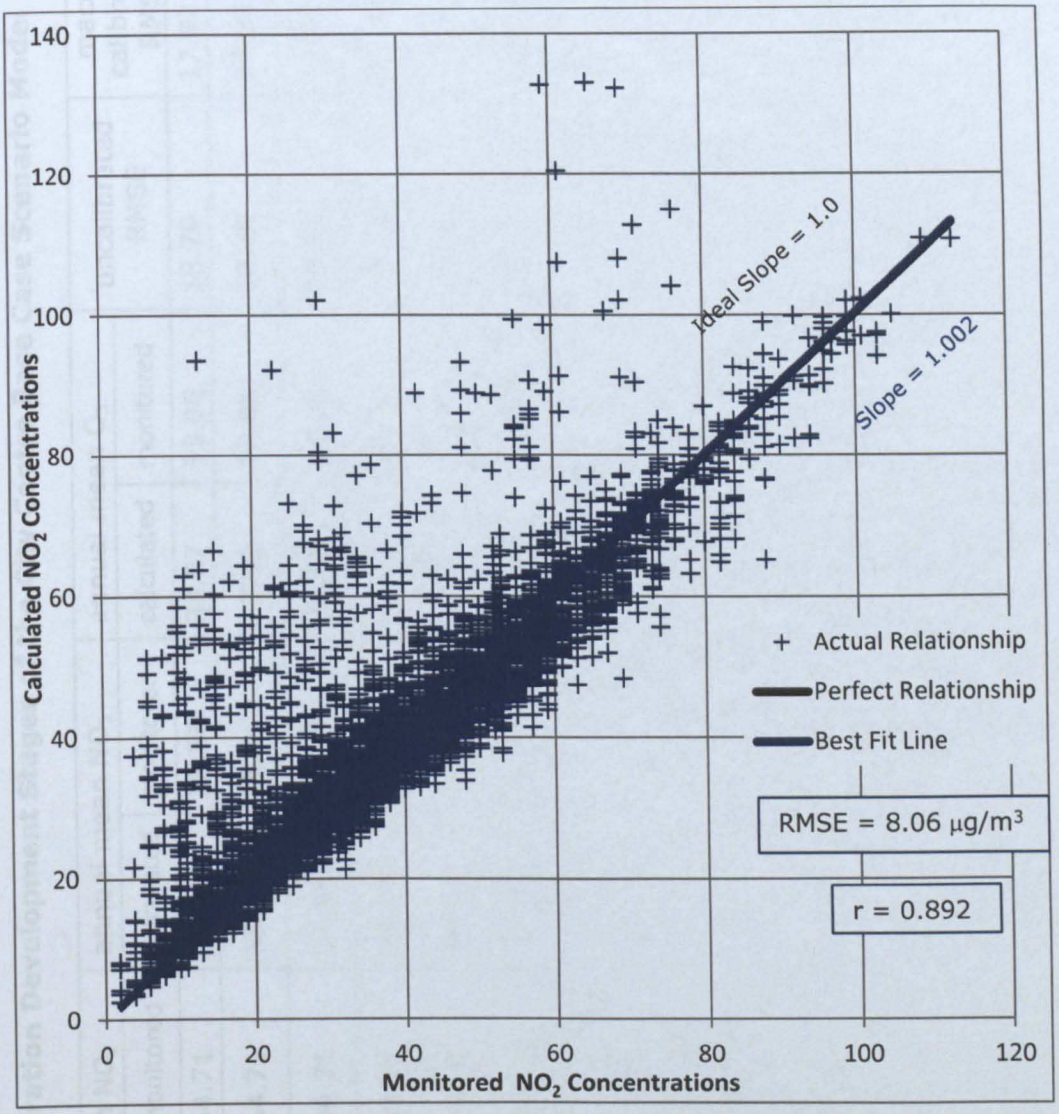

Figure 10.9 Scatter Diagram of Hourly NO_2 Concentrations at the AURN Station after the Micro-calibration based on Run 17

Table 10.2 Micro-calibration Development Stages of the City Centre Base Case Scenario Model

case description	Receptor name	annual mean NO_x		annual mean NO_2		annual mean O_3		uncalibrated RMSE	macro-calibrated RMSE	micro-calibrated RMSE
		calculated	monitored	calculated	monitored	calculated	monitored			
based on run 2	AURN	69.08	64.71	35.68	36.35	34.57	33.06	18.79	17.92	11.88
based on run 14	AURN	65.29	64.71	35.29	36.35	33.11	33.06	18.79	17.92	9.19
based on run 15	AURN	65.23	64.71	35.94	36.35	33.01	33.06	18.79	17.92	8.37
based on run 16	AURN	65.20	64.71	36.06	36.35	32.92	33.06	18.79	17.92	8.25
based on run 17	AURN	65.12	64.71	36.40	36.35	32.69	33.06	18.79	17.92	8.06
based on run 17 adjusted	AURN	64.51	64.71	36.08	36.35	33.21	33.06	18.79	17.92	6.75

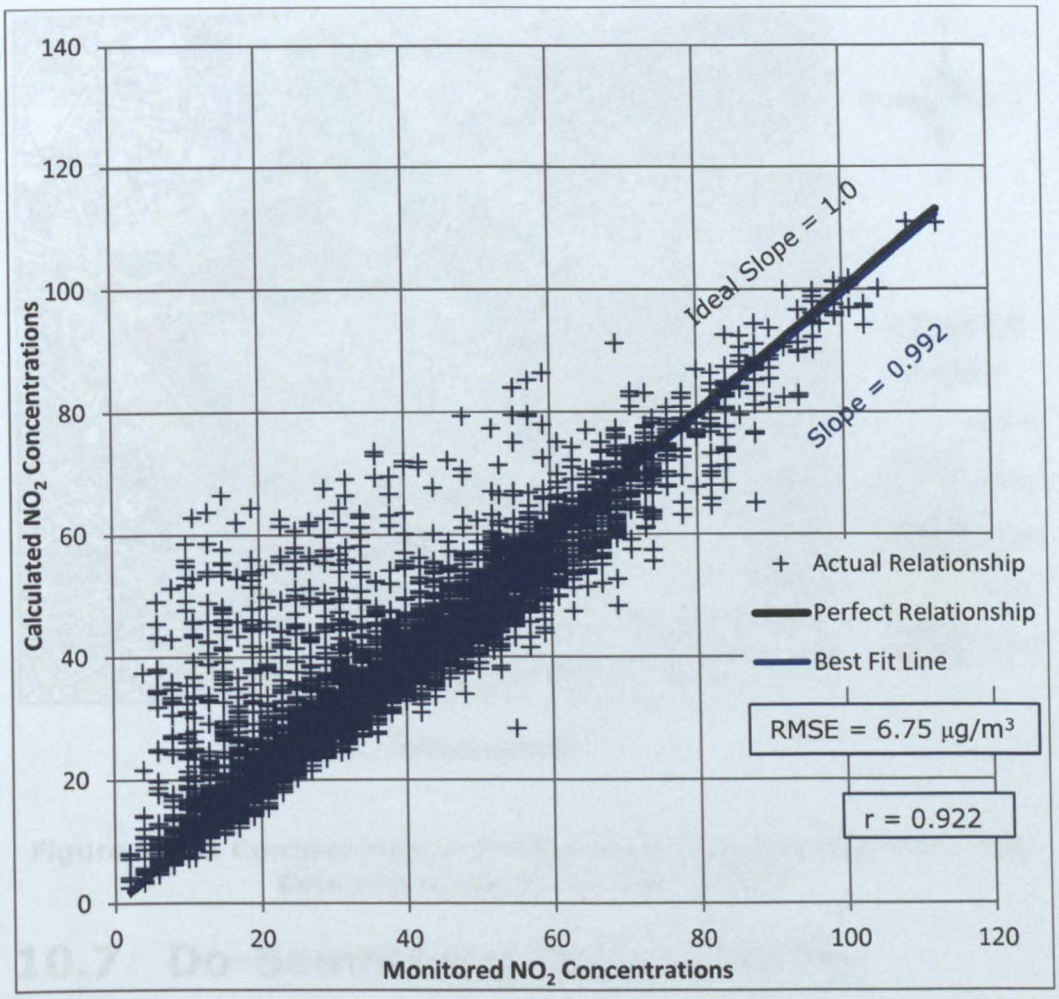

Figure 10.10 Scatter Diagram of Hourly NO_2 Concentrations at the AURN Station after the Micro-calibration based on Run 17 Adjusted

10.6 Grid Design of Output Receptors

The grid design described in Section 9.6 was applied for the design of this air pollution model output grid of receptors. This allowed the validation of the spatial distribution of air quality predictions of the Do-Something air quality scenario as will be discussed in Section 10.9. Figure 10.11 displays the 2003 ground-level contour map of the gridded output annual mean NO_2 concentrations.

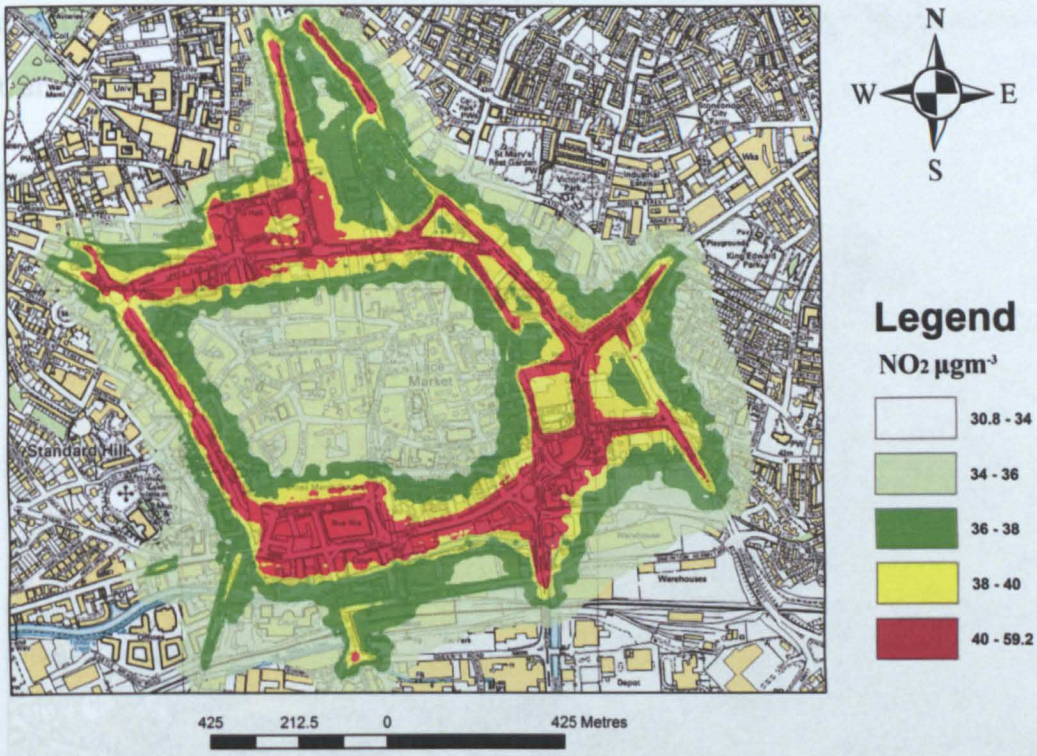

Figure 10.11 Contour Map of 2003 Ground-level Annual Mean NO_2 Concentrations in the City Centre

10.7 Do-Something Future Traffic Scenario

As 2006 was the implementation year of the Turning Point North scheme (NCC and NCC, 2006), 2006 was selected as the future modelling year of the Do-Something scenario. Discussions with Nottingham City Council were undertaken in order to determine a sensible traffic growth rate in Nottingham City Centre from 2003 to 2006, assuming that the determination was being made in 2003. A 1.4% annual average traffic growth rate was agreed to project the traffic flows of the 2003 air pollution model base case scenario to 2006. Then, for the roads directly affected by the implementation of the Turning Point North scheme, a 90% reduction was applied to their projected 2006 traffic flows as recommended by Nottingham City Council. Figure 10.12 shows the roads considered to be

directly affected by the implementation of the Turning Point North transport scheme.

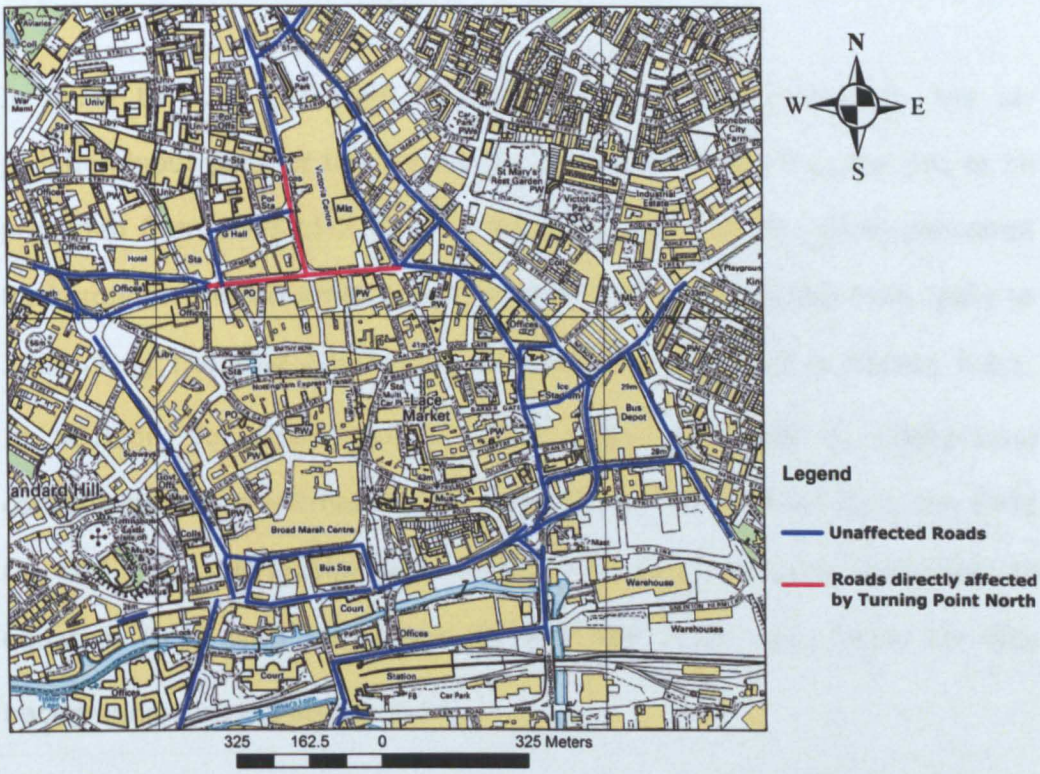

Figure 10.12 Roads Affected by Turning Point North Scheme

For the roads which were expected to be largely unaffected by the implementation of the Turning Point North scheme, Nottingham City Council advised the use of the 2003 traffic speeds for the 2006 Do-Something traffic scenario. This was due to the small traffic growth rate, and the short time span, from 2003 to 2006. Hence, the changes in the traffic speed, due to the small changes in the traffic flow from 2003 to 2006, would be very slight and could be ignored. For roads directly affected by the implementation of the Turning Point North scheme, the large reduction in the traffic flow could conceivably have led to a significant increase in the traffic speed on these roads. However, the traffic speed rise on these roads was limited by the urban speed limit, obtained from Nottingham City Council.

10.8 Projection of Air Pollution Input Data to 2006

In order to build the 2006 Do-Something air quality scenario, the air pollution input data for the City Centre base case scenario model had to be projected from 2003 to 2006. The adjusted NO_X and NO_2 micro-calibrated background concentrations based on run 17 were projected from 2003 to 2006 using The Year Adjustment Calculator as explained in Section 8.2.1. In addition, for each hour of 2003 data, the 2006 O_3 background concentration was estimated automatically in a spreadsheet from the 2003 O_3 and NO_2 micro-calibrated background concentrations according to equation (8.1) with 0.83 replaced with the 2006 year factor for NO_2 background concentrations (0.94).

The traffic-induced emissions of the City Centre base case scenario model were projected from 2003 to 2006 by altering the emission year to 2006 in the air pollution model interface. The Pollution Control Section in Nottingham City Council confirmed that the 2003 NO_X as NO_2 emissions of the three industrial point sources defined in the base case scenario model were the same in 2006. Therefore, the 2003 NO_X as NO_2 industrial emission rates were used in the 2006 Do-Something air quality scenario.

10.9 Prediction and Validation of 2006 Air Quality in the City Centre Area

Assuming that 'time now' is 2003, the forecast 2006 traffic flow and speed data for the 2006 Do-Something traffic scenario were used along with the projected 2006 air pollution input data for running ADMS-Roads for 2006

air pollution modelling of the City Centre Area. The 2006 annual mean NO_2, NO_x and O_3 concentrations and the 2006 hourly sequential NO_2 concentrations were calculated by ADMS-Roads at the AURN and Carter Gate monitoring stations. Shifting 'time now' to 2006, the calculated 2006 NO_2 concentrations were compared to the 2006 monitored NO_2 concentrations at these two locations for the validation of the future air quality predictions after the implementation of the Turning Point North transport scheme as shown in Table 10.3, Figure 10.13 and Figure 10.14.

Table 10.3 Macro-validation of the 2006 Future Air Quality Predictions at the AURN and Carter Gate Monitoring Stations

Receptor	annual mean NO_x ($\mu g/m^3$)		annual mean NO_2 ($\mu g/m^3$)		annual mean O_3 ($\mu g/m^3$)	
	Calculat-ed	Monito-red	Calculat-ed	Monitore-d	Calculat-ed	Monitore-d
AURN	51.54	62.56	31.98	33.60	36.28	38.54
Carter Gate	73.94	85.90	37.15	39.40	33.22	

The comparison between the results based on run 17 adjusted in Table 10.2 and the results in Table 10.3 implied that the projection of the 2003 base case scenario to the 2006 Do-Something scenario worsened the accuracy of the macro-validation of the annual mean NO_2 concentration at the AURN monitoring station by 1.35 $\mu g/m^3$. Such a rise in the difference between the annual means of calculated and monitored NO_2 concentrations indicated modelling underestimation. This underestimation tendency on the macro level was confirmed by the underestimation of the 2006 annual mean of monitored NO_2 concentrations at the Carter Gate monitoring station as shown in Table 10.3.

On the micro level, the projection of the 2003 base case scenario to the 2006 Do-Something scenario increased the RMSE between the hourly calculated and monitored NO_2 concentrations at the AURN monitoring

station by 15.63 μg/m^3 as implied by the comparison between Figure 10.10 and Figure 10.13. In addition, this projection increased the drift of the actual relationship between the hourly calculated and monitored NO_2 concentrations from the perfect straight-line relationship by 86.66%, as indicated by the values of r in Figures 10.1 and 10.13. Furthermore, this projection increased the underestimation tendency on the micro level by 23.4%, as indicated by the slopes of the regression through the origin best fit lines in Figures 10.1 and 10.13.

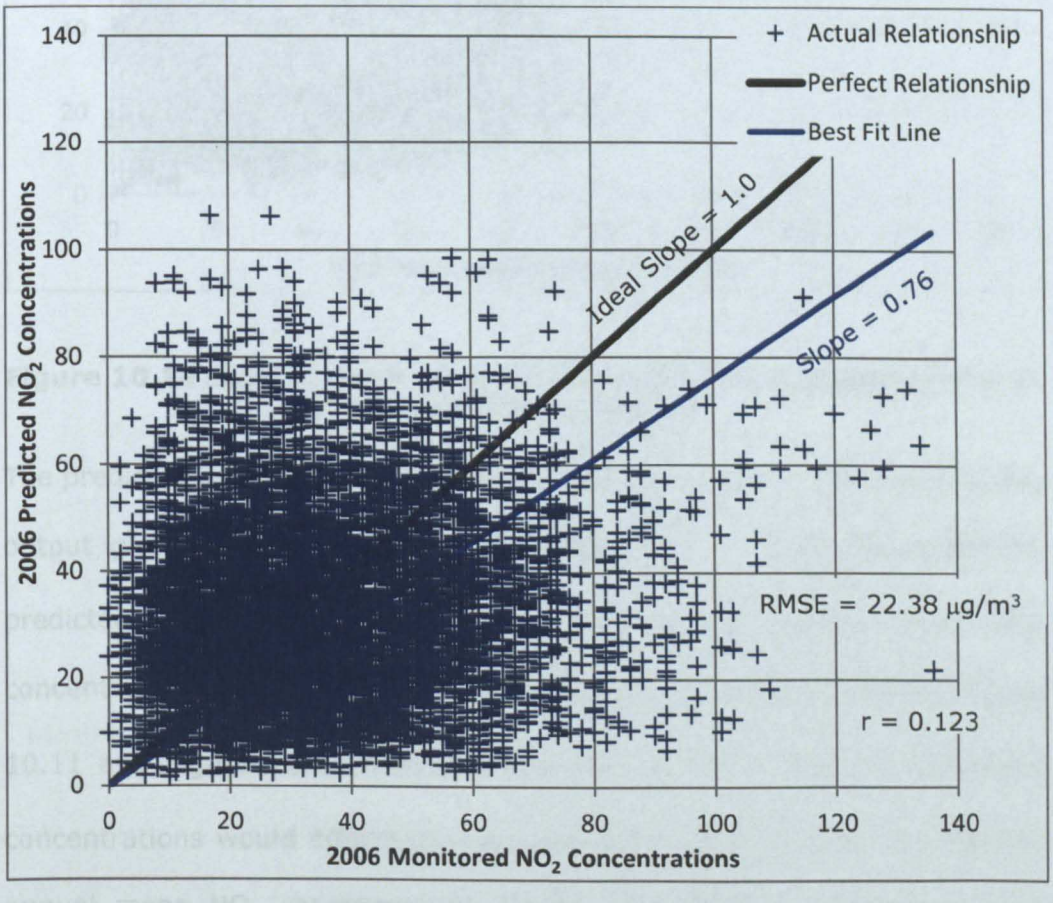

Figure 10.13 Scatter Diagram of Hourly 2006 NO_2 Concentrations at the AURN Station

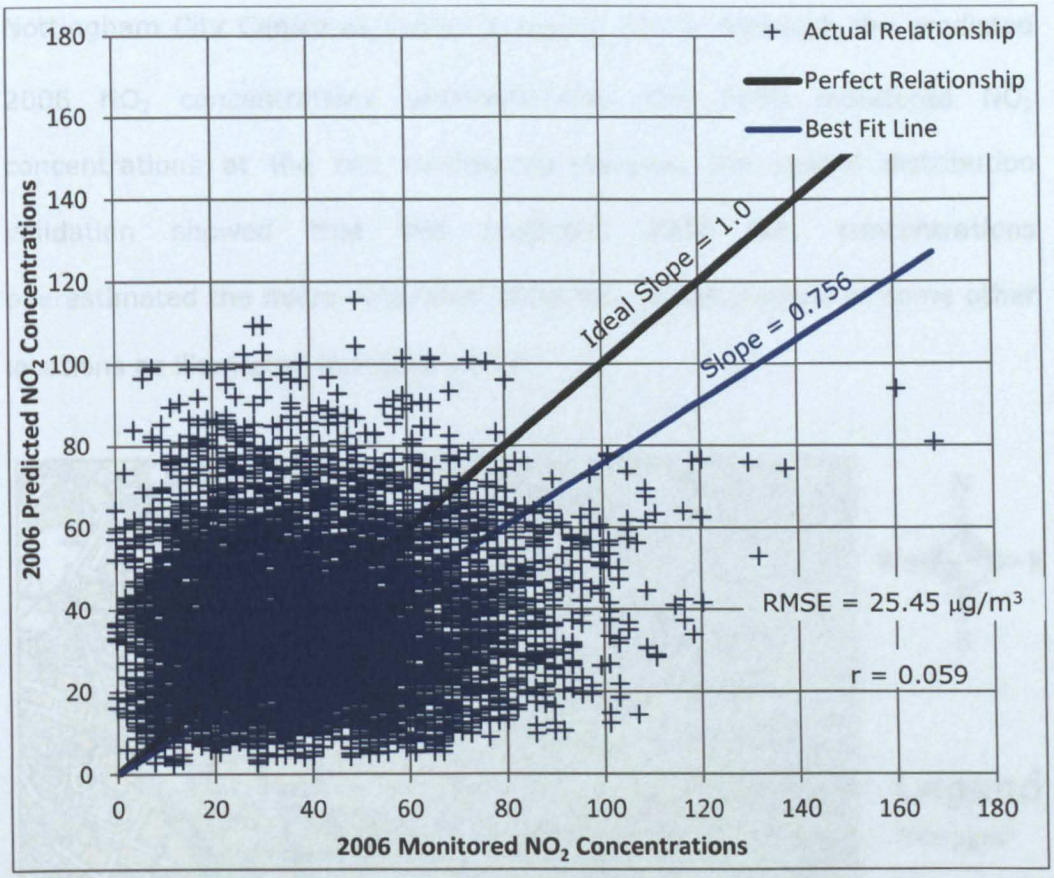

Figure 10.14 Scatter Diagram of Hourly 2006 NO_2 Concentrations at the Carter Gate Station

The predicted *2006 annual mean NO_2 concentrations* were calculated at the output grid receptors described in Section 10.6 in order to create the predicted 2006 ground-level contour map of the annual mean NO_2 concentrations as shown in Figure 10.15. The comparison between Figure 10.11 and Figure 10.15 indicated that the decline in future background concentrations would effectively decrease the exceedances of the AQO for annual mean NO_2 concentrations around the roads not directly by the implementation of the Turning Point North scheme, despite the future traffic growth. The 2006 ground-level contour map of the predicted annual mean NO_2 concentrations in Figure 10.15 was compared to the 2006 ground-level contour map of the micro-calibrated NO_2 concentrations in Figure 9.19 in order to validate the spatial distribution of NO_2 predictions in

Nottingham City Centre as shown in Figure 10.16. Although the predicted 2006 NO_2 concentrations underestimated the 2006 monitored NO_2 concentrations at the two monitoring stations, the spatial distribution validation showed that the predicted 2006 NO_2 concentrations overestimated the micro-calibrated 2006 NO_2 concentrations at some other locations as illustrated in Figure 10.16.

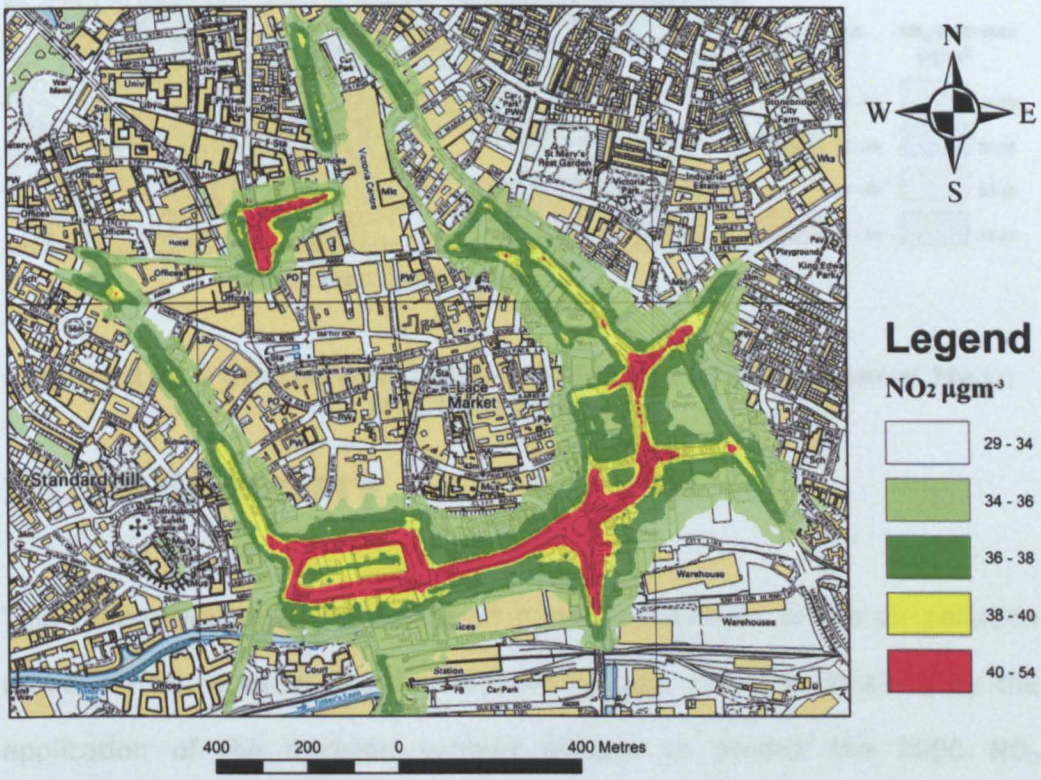

Figure 10.15 Contour Map of Predicted 2006 Ground-level Annual Mean NO_2 Concentrations in the City Centre

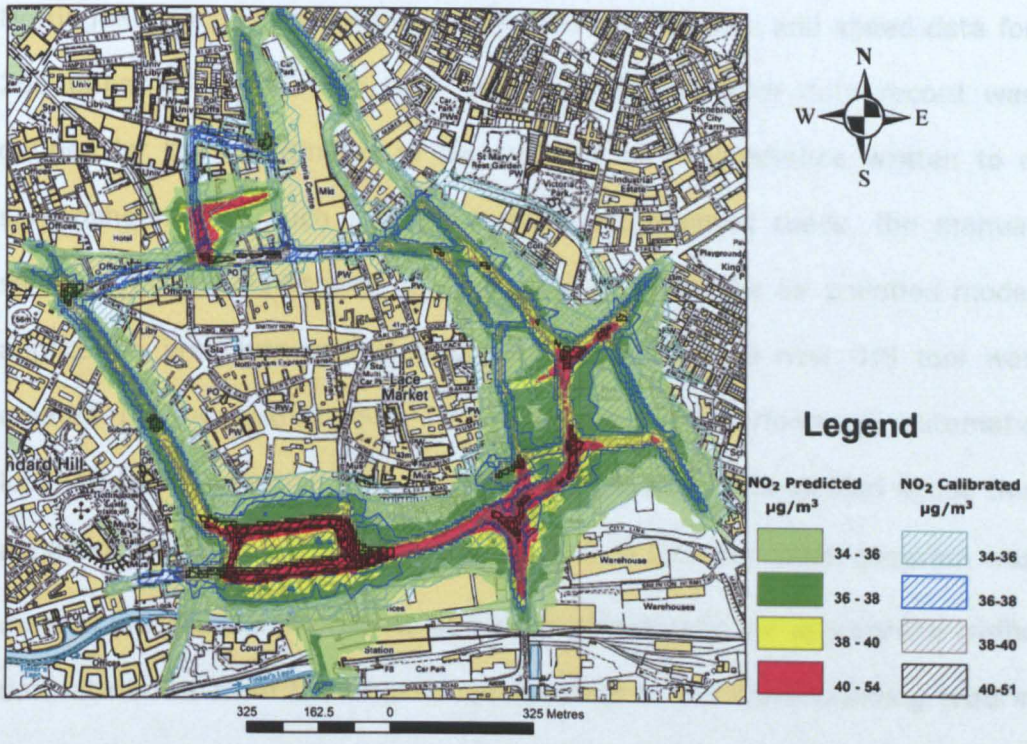

Figure 10.16 Spatial Distribution Validation of 2006 Annual Mean NO_2 Concentrations

10.10 Summary

This chapter validated the future air quality predictions of the air pollution model of the research decision-support system. This was attained by the application of the decision support system to predict the 2006 NO_2 concentrations in Nottingham City Centre after the implementation of the Turning Point North transport scheme. The base case year was 2003, before the implementation of this transport scheme, and the model application area was selected as the final air pollution model application area in Figure 9.1. Using this air pollution model application area allowed the comparison between the spatial distribution of the predicted 2006 NO_2 concentrations and the spatial distribution of the base year micro-calibrated 2006 NO_2 concentrations from Chapter 9.

Nottingham City Council provided the 2003 traffic flow and speed data for 206 unnamed roads. The road corresponding to each data record was defined by the coordinates of the vertices of its centreline written to a spreadsheet. With such a large number of unnamed roads, the manual selection and/or digitisation of roads located inside the air pollution model application area was almost impossible. Therefore, a new GIS tool was created by the author with Python in order to perform an automatic location-based selection of the road centreline segments located inside this application area as explained in Figure 10.2. A VBA computer program was created in MS Excel in order to append automatically the appropriate traffic data attributes from the original spreadsheet to the corresponding road in the tool's output roads subset. The tool's output road centrelines were exported to Google Earth in a KML file format where the width of each road was measured for input into the air pollution model.

The 2003 background concentrations of NO_X, NO_2 and O_3, monitored by the Rochester air quality monitoring station, were downloaded from NAEI (2009). Many records were missing in these hourly background concentrations which interrupted the running of the air pollution model. Therefore, a VBA computer program was created in MS Excel in order to fill the missing records automatically with the average of the last and first available hourly background concentrations before and after the missing records.

The base case scenario model underestimated the 2003 annual mean of monitored NO_2 and NO_X concentrations, and overestimated the 2003 annual mean of the monitored O_3 concentrations at the AURN monitoring station. Therefore, the input background concentrations of the base case scenario model were calibrated using 2003 monitoring data from the AURN monitoring station, downloaded from the UK Air Quality Archive. The

application of equations (6.1), (6.2) and (6.3), derived from the macro-calibration of the Dunkirk AQMA air pollution model, greatly improved the macro-validation results of the City Centre base case scenario model at the AURN monitoring station, as indicated by the results of run 2 in Table 10.1. The application of the micro-calibration equations, (6.8), (10.1) and (6.10) improved the micro-validation results of the City Centre base case scenario model as shown in Figure 10.9. The application of the VBA computer program, for which the flowchart was illustrated in Figure 9.14, eliminated the error described in Section 9.5.2 and improved further the micro-validation results of the City Centre base case scenario model as shown in Figure 10.10.

A 1.4% annual average traffic growth rate was recommended by Nottingham City Council in order to project the traffic flows of the 2003 base case scenario to the 2006 Do-Something scenario. For the roads directly affected by the implementation of the Turning Point North scheme, a 90% reduction was applied to their projected 2006 traffic flows. The 2003 traffic speeds of the roads expected to be largely unaffected by the Turning Point North scheme were kept the same for 2006. The potential traffic speed rise due to the large reduction in the traffic flow for the roads directly affected by the Turning Point North scheme was limited to the urban speed limit in Nottingham City Centre.

The micro-calibrated background concentrations based on run 17 adjusted and the traffic-induced emissions of the City Centre base case scenario model were projected from 2003 to 2006 as described in Section 8.2. The 2003 NO_X as NO_2 industrial emission rates were used in the 2006 Do-Something air quality scenario as recommended by Nottingham City Council. The predicted 2006 NO_2 concentrations underestimated, on the

macro and micro levels, the monitored 2006 NO_2 concentrations at both the AURN and Carter Gate monitoring stations as shown in Table 10.3, Figure 10.13 and Figure 10.14.

The projection of the 2003 base case scenario to the 2006 Do-Something scenario worsened the macro-validation of NO_2 concentrations at the AURN monitoring station by 1.35 $\mu g/m^3$. In addition, this projection increased the RMSE between the hourly calculated and monitored NO_2 concentrations at the AURN monitoring station by 15.63 $\mu g/m^3$ as implied by the comparison between Figure 10.10 and Figure 10.13. Moreover, this projection increased the drift of the actual relationship between the hourly calculated and monitored NO_2 concentrations from the perfect straight-line relationship by 86.66%, as indicated by the values of r in Figures 10.1 and 10.13. Furthermore, this projection increased the underestimation tendency on the micro level by 23.4%, as indicated by the slopes of the regression through the origin best fit lines in Figures 10.1 and 10.13. Although the predicted 2006 NO_2 concentrations underestimated the 2006 monitored NO_2 concentrations at the two monitoring stations, the spatial distribution validation showed that the predicted 2006 NO_2 concentrations overestimated the micro-calibrated 2006 NO_2 concentrations at some other locations as illustrated in Figure 10.16.

Chapter 11

Conclusions and Recommendations for Further Work

11.1 Evaluation of the Aim and Objectives

As stated in the introduction, this research has attempted to create an effective decision-support system to assist air quality-related transport planning. This decision-support system is based on three main elements integrated with each other: firstly, automatic collection and processing algorithms for traffic flow, and geospatial, data for input to the air pollution model; secondly, a calibrated air pollution model for the prediction of the air quality impacts of a proposed urban transport scheme; and thirdly, a 3D air pollution dispersion interface for the intuitive visualisation of the air quality predictions. The decision-support system can be used for choosing between numerous alternative designs for a proposed urban transport scheme, based on the modelled potential air quality impacts. It can also be used for the development of future traffic scenarios for a proposed urban transport scheme to assist the development of the design of the transport scheme in order to maximise air quality benefits and/or minimise adverse air quality impacts.

Section 1.3 lists a number of objectives which required addressing in order to achieve the research aim. These are recalled below and conclusions are drawn from the research results presented in this thesis.

11.1.1 Evaluation of the State-of-the-art in Air Pollution Modelling and Visualisation

Many challenges have been identified in the recent air pollution dispersion modelling research in terms of lack of calibration of air pollution models, the laborious manual collection and processing of input data for air pollution models and the very long air pollution model runtime, as discussed in Section 1.1. Currently, the results of air pollution dispersion modelling are usually displayed by overlaying 2D coloured contour maps of air pollution concentrations over 2D digital maps of the interest area in a GIS. The few attempts so far to give a 3D representation of the air pollution modelling results have not achieved a very good 3D visualisation. Furthermore, these few attempts displayed only the air pollution modelling results at a single height, thus excluding the air pollution at other heights above the ground surface, and identified the true 3D visualisation of air pollution as a challenge ahead as described in Section 3.6.

11.1.2 Evaluation of Algorithms Developed to Automate the Processing of Traffic and Geospatial Input Data

ADMS-Roads requires the AADT flow, the monthly traffic profiles, and the hourly traffic profiles for Saturdays, Sundays and weekdays, but has no internal algorithm for creating this data from traffic count data. Namdeo et al. (2002) developed a computer function that can create hourly traffic flow profiles from the AADT flow data, excluding the monthly profiles. In fact, these hourly profiles are created from modelled hourly traffic flows from the SATURN model, not actual traffic flows that may be observed over sub-

hour time intervals. Therefore, the mathematical algorithm implemented by VBA computer programming in Section 5.4 was necessary for the processing of large files of primary traffic flow count data that were recorded every five minutes for all of the year 2006. The computer program outputs for each road in the Dunkirk AQMA the AADT flow, and the hourly and monthly traffic profiles for the base case scenario. The application of this computer program significantly reduced the processing time and effort, which may allow an increase in the number of road links that can be modelled in air pollution dispersion models. This improves the model accuracy, and thus increases the reliability of air quality predictions.

The application of the VBA computer program also helps to avoid the potential human errors that may arise during the manual processing of large files of traffic flow input data, which may further increase the reliability of air pollution dispersion models. The high resolution of the primary traffic flow data for which the program can start the processing makes this computer program suitable for a broad range of other road links with similar or less traffic flow data resolution.

Well-developed air pollution models are integrated with GIS systems to enable the digitisation of the modelled road network centrelines on a digital map of the area of interest (CERC, 2006a). This requires a massive amount of labour and time, particularly for study areas with a dense road network. Therefore, the two new GIS tools, developed and implemented by the computer programming in this research project, were extremely useful for automating the collection and processing of geospatial data of road sources for input to the air pollution dispersion model. Hence it was possible to avoid the laborious digitisation of the dense road network in Nottingham City Centre, and to introduce a new consistent GIS-based approach to

generate the road network geospatial data for an air pollution model run (see Sections 9.4 and 10.4 for details).

The LOD algorithm, implemented in these two new GIS tools as shown in Figures 9.2b and 10.2b, was essential to meet the technical requirements of ADMS-Roads to ensure that the vertices of each road centreline are at least 1 metre apart. The implementation of the output table maintenance computer algorithm in the new GIS tools was helpful to automate the removal of the single-vertex roads from the output table after the implementation of the LOD algorithm (see Figures 9.2c and 10.2c for details). The graphical user interface designed for the input data entry and the runtime console of the new GIS tools may enable users who are unfamiliar with GIS to use the new tools and give them insight into the processing.

11.1.3 Evaluation of the Air Pollution Model Set-up

The five selection criteria, used in Table 4.1, were extremely useful to select the transport schemes used as case studies for the set-up of the air pollution model in different stages of the development of the decision-support system. Sections 8.3, 9.1010.9 and 10.9 explain the air quality impacts of these transport schemes.

The selection of NO_2 to model before and after the implementation of the transport schemes was helpful to assess their air quality impacts. As NO_2 is mainly a traffic-related air pollutant, the modelling of NO_2 can potentially be helpful to assess the air quality impacts of a broad range of other transport schemes. The selection of NO_X and O_3 to model in the base case scenario was essential to model the atmospheric chemical reactions of NO_X

that affect the calculated NO_2 concentrations. In addition, modelling NO_X and O_3 was required for the macro-calibration and micro-calibration of the base case scenario model.

The hourly sequential meteorological data and background concentrations of NO_2, NO_X and O_3 were essential for the micro-calibration and micro-validation of the base case scenario NO_2 results. The output grid design was suitable for capturing the rapidly changing NO_2 concentrations' gradient close to the main roads in the air pollution model application area while optimising the model runtime. The height limit and height step determination strategy was suitable for capturing the vertical dispersion of NO_2 concentrations above the ground surface which is necessary in order to attain a true 3D visualisation of NO_2 dispersion in the 3D city model. However, this strategy was applied to identify the height limit and step at only one or two locations in the air pollution model application area. The application of this strategy at two different locations in Nottingham City Centre showed that the height limit may change from one location to another in the model application area (see Figure 9.17 and Figure 9.18).

11.1.4 Evaluation of the Developed Calibration and Validation Strategies

The macro-calibration is the process of minimising the error between the calculated and monitored annual mean air pollution concentrations. The micro-calibration is the process of minimising the error between not only the annual means but also the hourly calculated and monitored NO_2 concentrations. The macro-validation evaluates the error between the annual means of calculated and monitored concentrations and was helpful to decide the final acceptable iteration of the macro-calibration. The micro-

validation statistics were used to evaluate the error between the hourly calculated and monitored NO_2 concentrations. This helped to identify the final acceptable iteration of the micro-calibration.

Neither increasing the primary NO_2 emissions from the traffic, nor decreasing the surface roughness and the minimum Monin-Obukhov length of the air pollution model application area, was effective for the macro-calibration. Adjusting the rural background concentrations of NO_X, NO_2 and O_3, conducted by trial and error during the initial development, was effective for the macro-calibration of the base case scenario model. The results of the trial and error approach were used to derive equations (6.1), (6.2) and (6.3), which were found applicable to macro-calibrate the base case scenario model of other case studies. However, the macro-calibration did not significantly minimise the error between the hourly calculated and monitored NO_2 concentrations of the base case scenario model.

The iterative application of the micro-calibration equations (6.8), (6.9) and (6.10), initially developed for the Dunkirk AQMA air pollution model, effectively minimised the error between both the annual mean, and the hourly, calculated and monitored NO_2 concentrations. These equations were found applicable to micro-calibrate the rural background concentrations of NO_X, NO_2 and O_3 of the 2006 base case scenario of the Nottingham City Centre air pollution model. However, equation (6.9) needed to take the general form of equations (6.8) and (6.10), and thus was replaced with equation (10.1), in order to micro-calibrate the rural background concentrations of the 2003 base case scenario of the Nottingham City Centre air pollution model.

For the hours with missing monitored air pollution concentrations, the micro-calibration equations were unusable. This was addressed by using the macro-calibrated background concentrations for these hours, as discussed in Section 6.4.2.2. As the macro-calibrated background concentrations give less precise calculated concentrations on the hourly level (see Sections 6.4.2.2, 9.5.2 and 10.5.2 for details), such a strategy may reduce the reliability of the number of exceedances and percentiles predicted by the air pollution model. The micro-calibration iterations were conducted manually which slowed down the micro-calibration development of the base case scenario model.

The inclusion of the hourly and monthly traffic profiles in the Dunkirk AQMA air pollution model did not have a significant impact on the error between the annual means of calculated and monitored concentrations. On the other hand, the inclusion of these traffic profiles did reduce the RMSE between the hourly calculated and monitored NO_2 concentrations by 28.4% (see Section 6.4.3 for details). The data required to produce these traffic profiles for modelling Nottingham City Centre was not available for the research project, and thus the traffic profiles were not considered in the Nottingham City Centre air pollution modelling.

In terms of the error between the annual means of calculated and monitored NO_2 concentrations, using ADMS-Roads with only the macro or micro-calibrated background concentrations was more accurate than using ADMS-Urban with a grid source and rural background concentrations. Moreover, in terms of the error between the hourly calculated and monitored NO_2 concentrations, using ADMS-Roads with only the micro-calibrated background concentrations was much more accurate, although slightly less accurate with only macro-calibrated background concentrations

(see Section 6.4.4 for details). Using the trajectory model of CRS in ADMS-Urban did not significantly change the error between the monitored and calculated concentrations otherwise obtained, and so effectively did not change the comparative results between using ADMS-Roads and ADMS-Urban.

Replacing the grid source with either the macro or micro-calibrated background concentrations can save up to 9.41 months of the model runtime in order to generate the air pollution data required to build the 3D air pollution dispersion interface for a certain modelling year. The micro-calibration mathematical model did not require any input data to start the iterations, apart from the monitored air pollution concentrations. In comparison, the grid air pollution sources require precise input data for the air pollution emissions which may impede their usage in air pollution modelling of areas without a precise emissions inventory.

The use of the street canyon module in ADMS-Roads, based on the Danish Operational Street Pollution Model (OSPM) (Berkowicz, 2000), did not effectively increase the calculated annual mean NO_2 concentrations inside a 6 metre height canyon (see Section 6.4.5.1). Altering the traffic flow and speed effectively increased the calculated annual mean NO_2 concentrations inside the canyon; however it worsened the balance between the calculated and monitored concentrations outside the canyon (see Section 6.4.5.2). Therefore, using GIS techniques to input the digital boundary of the canyon to the VBA computer program described in Section 6.4.5.3 was extremely useful to increase the calculated annual mean NO_2 concentrations inside the canyon without adversely affecting the well estimated annual mean NO_2 concentrations outside the canyon.

The mathematical algorithm, implemented by VBA in MS Excel as shown in Figure 9.14, was helpful to eliminate the increase in the error between the calculated and monitored NO_2 concentrations at some hours after the micro-calibration at these hours. Such unexpected increase in the error with the micro-calibration was possibly due to either the imprecise model simulation of actual atmospheric chemical reactions between NO_X and O_3 or the imprecise monitoring data at these hours. The application of this mathematical algorithm after the final development stage of the micro-calibration improved further the micro-validation of the base case scenario model. The mathematical algorithm, initially developed for the 2006 base case scenario of the Nottingham City Centre air pollution model, was found applicable to the 2003 base case scenario of the Nottingham City Centre air pollution model.

The methods used in this research to project the input data for the air pollution model base case scenario, to after the implementation of urban transport schemes, were required in order to predict the future air quality impacts of these transport schemes. The modelled air quality benefits of the envisaged reduction in the future background levels, due to improved vehicle technology and better fuel standards, significantly outweighed the adverse air quality impacts of the future traffic growth. Such a reduction in the future background levels can significantly decrease the area in which the AQO of annual mean NO_2 concentrations is exceeded without the implementation of urban transport schemes (see Section 8.5 and 9.10 for details).

The projection of the air pollution input data from 2003 to 2006 did not significantly increase the error between the annual means of predicted and actual NO_2 concentrations (see Table 10.2 and Table 10.3). However, it

significantly increased the error between the hourly predicted and actual NO_2 concentrations (see Figure 10.10 and Figure 10.13). The spatial distribution validation was extremely useful to identify the discrepancy between the predicted and micro-calibrated 2006 NO_2 concentrations throughout the model application area (see Figure 10.16).

11.1.5 Evaluation of the Developed 3D Air Pollution Dispersion Interface

The selected LOD to represent the 3D buildings of the Dunkirk AQMA in its 3D city model was suitable to achieve smooth navigation while maintaining a good level of location recognition and orientation in the 3D city model. The virtual traffic animation and the representation of road network features in the 3D city model both improved the location recognition and orientation and compensated for the absence of 3D residential buildings; were these residential buildings represented in the 3D city model, they would obscure the air pollution within and underneath. However, it has not been feasible to increase the number of displayed virtual vehicles in the 3D city model, in order to simulate properly the actual traffic conditions in the Dunkirk AQMA, so that the observer can intuitively understand the relationship between the traffic and the displayed air pollution. Such an increase in the number of displayed virtual vehicles in the 3D city model overburdened the model and impeded smooth navigation through the virtual scene.

The representation of the NET Phase 2 infrastructure in the Dunkirk AQMA 3D city model, requiring real integration of CAD and virtual reality, which was identified as a challenge by Whyte et al. (2000), was done so as to create a contrast between present and future infrastructure in the Dunkirk

AQMA. However, the animation of the virtual tram object over the curved parts of the NET Phase 2 viaduct is not fully realistic. As the virtual tram is a long object without hinges, the virtual tram partially leaves the track when traversing the curved parts of the NET Phase 2 viaduct.

The 3D point array interfaces, shown in Figure 7.14 and Figure 7.16, displayed NO_2 concentrations at and above the ground surface in a single 3D virtual scene, which was identified as a challenge ahead by Wang et al. (2008). However this development was found not to be particularly intuitively meaningful, so the research was progressed further to the representation of the NO_2 concentrations by 3D volumetric clouds, as shown in Figure 7.22, which, given the analogy with weather clouds mentioned in Section 1.5, may assist human visualisation of air pollution.

In terms of maintaining a good level of location recognition and orientation, the representation of the 3D models of all the buildings in the Nottingham City Centre 3D city model was helpful to compensate for the availability of these models in a low LOD, as shown in Figure 9.44. The low LOD of these models allowed the representation of all the buildings in the 3D city model without impeding smooth navigation through the virtual scene.

The 3D volumetric clouds air pollution dispersion interface was found applicable to visualise NO_2 dispersion at and above the ground surface in the 3D city model of Nottingham City Centre (see Figure 9.28, Figure 9.42 and Figure 9.45). However, as the base elevations of 3D points, which were wrapped with a 3D volumetric mesh to create each 3D volumetric cloud, were interpolated from the DTM, the low resolution DTM of the Nottingham City Centre 3D city model resulted in assigning some of these points, located at the same height above the ground surface, the same total elevation. This excluded these points from the wrapped volumetric

cloud as Geomagic Studio version 10 does not support wrapping 3D volumetric meshes around planar point sets.

A specific investigation and the development of additional output receptor points, described in Section 9.7, were needed to give the 3D volumetric clouds representing the critical NO_2 concentrations, exceeding the AQO of annual mean NO_2 concentration, realistic vertical and horizontal shapes in the Nottingham City Centre 3D air pollution dispersion interface.

The developed 3D air pollution dispersion interface displayed calculated annual mean NO_2 concentrations, using a roof-top roughness coefficient, at an output grid of receptor points, repeated vertically at many heights above the ground surface. This did not display the impact of additional circulation, which happens in street-canyons, on calculated annual mean concentrations, which may reduce the reliability of displayed air pollution levels in the 3D interface.

11.1.6 Evaluation of the Developed Future Traffic Scenarios for the Proposed Transport Scheme

Neither an increase nor a reduction in the traffic speeds of the 2021 Do-Something traffic scenario was helpful to increase the air quality benefits of a proposed urban transport scheme (see Figure 8.13). The reduction in the traffic flows of the 2021 Do-Something traffic scenario, as shown in Figure 8.14 to Figure 8.17 for after the implementation of NET Phase 2 through the Dunkirk AQMA, could be helpful to increase the air quality benefits of a proposed urban transport scheme. In addition, increasing the traffic speeds in conjunction with the reduction in the traffic flows could attain the same

air quality benefits with 4% less reduction in the traffic flows as shown in Figure 8.18 to Figure 8.21. Therefore, the reduction in urban traffic congestion, corresponding to the reduction in traffic density, can improve the air quality if its effect on traffic flow is not eroded by the increase in traffic speed, and hence was capable of reducing the traffic flow.

Colouring the roads in the 3D air pollution dispersion interfaces for the developed alternative traffic scenarios was useful to simplify the visualisation of all the different reductions to the original forecast traffic flows considered for the same future traffic scenario (see Figure 8.28 to Figure 8.35). This further increased the information retention and reduced the comprehension time of the 3D air pollution dispersion interfaces for these traffic scenarios.

11.2 Recommendations for Further Work

The achieved results lead to recommendations for future work to be proposed, which are presented in three parts. The first part is about possible applications and enhancements of the developed algorithms to automate the collection and processing of traffic flow and geospatial data for input to the air pollution model. The second part discusses possible improvements to both the calibration mathematical model and the future projection of air pollution input data that can further improve the reliability of air quality predictions. The third part is on testing and enhancing the 3D air pollution dispersion interface which may encourage its adoption in actual public consultations about proposed urban transport schemes.

11.2.1 Input Data Processing and Collection Algorithms

ADMS-Roads version 2.3 has introduced a new functionality in terms of providing a way of entering traffic emission factors based on the traffic flow for each hour in the modelled year. These emission factors are applied to the average emissions of road sources and are more detailed than the monthly and hourly traffic profiles used in the Dunkirk AQMA air pollution model in this research. Therefore, further research is recommended to modify the traffic flow data processing VBA computer program so that it can automatically produce this form of emission factors from the sub-hour traffic flow count data. Then, the impact of using such high resolution emission factors on the macro-validation, micro-validation and runtime of the air pollution model can be investigated.

The application of the LOD algorithm of the new GIS tools is recommended to generate many different LODs for the same road network. Further research is then recommended to investigate the impact of varying the LOD on the macro-validation, micro-validation and runtime of the air pollution model so that the optimum range for the LOD of a modelled road network can be identified.

11.2.2 Calibration of Air Pollution Models and Future Projection of Air Pollution Input Data

For the hours with missing monitored air pollution concentrations, further research is needed to investigate the impact of using the macro-calibrated background concentrations on the reliability of the predicted number of

exceedances and percentiles by the air pollution model. In case of a significant adverse impact, further research is recommended into the micro-calibration of the rural background concentrations of these hours, based on the meteorological data and the micro-calibrated background concentrations of other hours with monitored concentrations.

Further research is recommended to automate the micro-calibration of the rural background concentrations. This may be conducted by getting access to the source code of ADMS-Roads in order to add an additional module for the micro-calibration of the input background concentrations before running the air pollution model. Alternatively, this may be conducted by integrating ADMS-Roads with optimisation software that can automate the micro-calibration process such as modeFRONTIER (ESTECO, 2010). The automation of the micro-calibration iterations may speed up this process and increase the number of possible iterations, which may improve further the micro-validation of the NO_2 results for the base case scenario modelling.

Further research is recommended to investigate the impact of including the monthly and hourly traffic profiles on the micro-validation of an air pollution model that has a large number of road sources, such as the Nottingham City Centre air pollution model. This is to correlate between the number of road sources with traffic profiles in the air pollution model and the possible reduction in the RMSE between the hourly calculated and monitored NO_2 concentrations.

Further research is needed to investigate the impact of including the calculation of air pollution dispersion around buildings on the macro-validation, micro-validation and runtime of the air pollution model. This

may lead to a recommendation for the optimum range of the LOD of buildings that are considered in the air pollution model.

Further investigation into the validation of the future NO_2 predictions in Nottingham City Centre is needed to identify the contribution of each projected item of the air pollution input data to the identified error between the predicted and monitored NO_2 concentrations. This may lead to the calibration of the future projection methods of this research and/or the adoption of other more accurate methods which may further improve the reliability of future air quality predictions.

Further research is required to adapt the macro-calibration and micro-calibration equations for modelling the air pollution dispersion of inert pollutants, e.g. CO and PM. As chemical reactions will not be considered, the calibration equations may reduce to one equation for the macro-calibration, and one equation for the micro-calibration, of the input background concentrations.

11.2.3 3D Air Pollution Dispersion Interface

Further development for the 3D air pollution dispersion interface is recommended to allow the number of displayed virtual vehicles in the 3D city model to be increased without impeding smooth navigation through the virtual scene. Moreover, further research is needed to improve the animation realism of long objects, e.g. the virtual tram, over curved paths in the 3D city model. These may require either the development of 3D Analyst of ArcGIS 9.2 by computer programming or switching the 3D air pollution dispersion interface to another 3D visualisation package.

Extending the functionality of Geomagic Studio version 10 by computer programming is recommended to enable wrapping a 3D volumetric mesh

around a group of 3D points which all lie in a single plane. This may improve the 3D volumetric clouds air pollution dispersion interface in areas with a low resolution DTM.

Further studies should identify the optimum number and distribution of locations in the air pollution model application area that can be used to work out accurately the height limit of the air pollution plume above the ground surface. This may further improve the 3D visualisation of air pollution dispersion in 3D city models.

It is recommended to use the 3D air pollution *dispersion interface for the* 3D visualisation of percentiles of pollutant concentration and exceedance statistics which are used as benchmarks in air quality standards. Furthermore, as it was not possible in this research project to do formal user-centred testing, as discussed in Section 7.2, it is recommended to test the 3D air pollution dispersion interface on many of the sorts of people who participate in actual public consultation exercises about proposed urban transport schemes. Then, the feedback of all the different participants may contribute to further development of the 3D air pollution dispersion interface.

After the potential further development of the 3D air pollution dispersion interface, it is recommended to make the interface accessible through the web to all the general public. One possibility to do so is by the representation of the 3D air pollution volumetric clouds and the transport scheme infrastructure in Google Earth, which is a freely available web-based application that is commonly used nowadays to view the 2D and/or 3D built environment. Then, further research is recommended to develop new controls for Google Earth, by computer programming, that enable the user to switch the 3D view between before and after the implementation of

the proposed urban transport scheme. These new controls may also enable the user to switch on or off the volumetric clouds of any air pollution concentration band and/or interpolate the 3D volumetric clouds for a new concentration band from the existing clouds.

References

ABDULHAI, B. & KATTEN, L. 2004. Traffic Engineering Analysis. *Handbook of Transportation Engineering* McGraw-Hill Professional Publishing.

AEA. 2008. *UK National Air Quality Archive: LAQM Tools* [Online]. Available: http://www.airquality.co.uk/archive/laqm/tools.php?tool=background04 [Accessed 08/05/2008].

AEA 2009. UK air quality modelling for annual reporting 2007 on ambient air quality assessment under Council Directives 96/62/EC, 1999/30/EC and 2000/69/EC.

APPLETON, K., LOVETT, A., SUNNENBERG, G. & DOCKERTY, T. 2002. Rural landscape visualisation from GIS databases: a comparison of approaches, options and problems. *Computers, Environment and Urban Systems,* 26, 141-162.

AQEG 2007. Trends in Primary NO_2 in the United Kingdom. Department for Environment, Food and Rural Affairs (DEFRA), http://www.defra.gov.uk/environment/quality/air/airquality/publications/.

ATHANASSIADOU, M., BAKER, J., CARRUTHERS, D., COLLINS, W., GIRNARY, S., HASSELL, D., HORT, M., JOHNSON, C., JOHNSON, K., JONES, R., THOMSON, D., TROUGHT, N. & WITHAM, C. 2010. An assessment of the impact of climate change on air quality at two UK sites. *Atmospheric Environment,* In Press, Corrected Proof.

BARRETT, S. R. H. & BRITTER, R. E. 2008. Development of algorithms and approximations for rapid operational air quality modelling. *Atmospheric Environment,* 42, 8105-8111.

BARRETT, S. R. H. & BRITTER, R. E. 2009. Algorithms and analytical solutions for rapidly approximating long-term dispersion from line and area sources. *Atmospheric Environment,* 43, 3249-3258.

BBC 2006. AIR QUALITY UPDATING AND SCREENING ASSESSMENT. Broxtowe Borough Council.

BBC 2009. AIR QUALITY UPDATING AND SCREENING ASSESSMENT. Broxtowe Borough Council.

BBC. 2010. *Air Pollution* [Online]. Broxtowe Borough Council. Available: http://www.broxtowe.gov.uk/index.aspx?articleid=1292 [Accessed 01/06/ 2010].

BELL, M. C. 2006. Environmental factors in intelligent transport systems. *Intelligent Transport Systems, IEE Proceedings,* 153, 113-128.

BENG, S. A. S. 2002. *THE INTEGRATION OF CFD AND VR METHODS TO ASSIST AUXILIARY VENTILATION PRACTICE.* PhD, THE UNIVERSITY OF NOTTINGHAM.

BENSON, P. E. 1992. A review of the development and application of the CALINE3 and 4 models. *Atmospheric Environment. Part B. Urban Atmosphere,* 26, 379-390.

BERKOWICZ, R. 2000. OSPM - A Parameterised Street Pollution Model. *Environmental Monitoring and Assessment,* 65, 323-331.

BERKOWICZ, R., HERTEL, O., SORENSEN, N. N. & MICHELSEN, J. A. 1994. Modelling air pollution from traffic in urban areas. *Proceedings of the IMA Conference on Flow and Dispersion Through Groups of Obstacles.* University of Cambridge.

BILDSTEIN, F. Year. 3D City Models for Simulation and Training Requirements on Next Generation 3D City Models. *In:* Next Generation City Models, 2005 Bonn. European Spatial Data Research (EuroSDR).

BRIGGS, D. J. 2007. The use of GIS to evaluate traffic-related pollution. *Occupational and Environmental Medicine,* 64, 1-2.

BRIGGS, D. J., HOOGH, C. D., GULLIVER, J., WILLS, J., ELLIOTT, P., KINGHAM, S. & SMALLBONE, K. 2000. A regression-based method for mapping traffic-related air pollution: application and testing in four contrasting urban environments. *The Science of the Total Environment,* 253, 151-167.

CAI, H. & XIE, S. D. 2010. A modelling study of air quality impact of odd-even day traffic restriction scheme before, during and after the 2008 Beijing Olympic Games. *Atmospheric Chemistry and Physics Discussions,* 10, 5135-5184.

CARSLAW, D. C., BEEVERS, S. D. & BELL, M. C. 2007. Risks of exceeding the hourly EU limit value for nitrogen dioxide resulting from increased road transport emissions of primary nitrogen dioxide. *Atmospheric Environment,* 41, 2073-2082.

CARTER, D. 2007. Evidence of David Carter: Forecasting and Appraisal – Main Proof NET.P3/A. mva consultancy.

CASA & ERG. 2008. *3-D Map of Air Pollution in London* [Online]. London: The London Air Quality Network. Available: http://www.londonair.org.uk/london/asp/virtualmaps.asp?view=maps [Accessed 18/07/ 2010].

CERC 2003. Validation and Sensitivity Study of ADMS-Urban For London.

CERC 2006a. ADMS-Roads Version 2.2 User Guide. *An Air Quality Management System.* Cambridge Environmental Research Consultants Ltd.

CERC 2006b. ADMS-Urban Version 2.2 User Guide. *An Air Quality Management System.* Cambridge Environmental Research Consultants Ltd.

CERC 2009. Using ADMS-Urban and ADMS-Roads and the latest government guidance. *In:* MCHUGH, C. (ed.) *UK tools for modelling NO_X and NO_2.* ADMS-Urban and Roads User Group Meeting.

CERC. 2010. *Air quality forecasting* [Online]. Available: http://www.cerc.co.uk/air-quality-forecasting/united-kingdom.html [Accessed 1st May 2010].

CHENG, K. & CHANG, N.-B. 2009. Assessment of the impact of biogenic VOC emissions in a high ozone episode via integrated remote sensing and the CMAQ model. *Frontiers of Earth Science in China,* 3, 182-197.

CURTIS, L., REA, W., SMITH-WILLIS, P., FENYVES, E. & PAN, Y. 2006. Adverse health effects of outdoor air pollutants. *Environment International,* 32, 815-830.

DAVISON, L. J. & KNOWLES, R. D. 2006. Bus quality partnerships, modal shift and traffic decongestion. *Journal of Transport Geography,* 14, 177-194.

DEFRA 2003. Technical Guidance on Local Air Quality Management LAQM.TG(03).

DEFRA 2009. Technical Guidance on Local Air Quality Management LAQM.TG(09).

DETR 2006. NATIONAL ROAD TRAFFIC FORECASTS (GREAT BRITAIN) 1997. Department of the Environment, Transport and the Regions.

DMRB 2007. ENVIRONMENTAL ASSESSMENT TECHNIQUES. *Design Manual for Roads and Bridges, Volume 11, Section 3.*

DÖLLNER, J. & BUCHHOLZ, H. 2005. Continuous level-of-detail modeling of buildings in 3D city models. *Proceedings of the 13th annual ACM international workshop on Geographic information systems.* Bremen, Germany: ACM.

DOWLING, R. 1997. Planning techniques to estimate speeds and service volumes for planning applications. United States. Federal Highway Administration, American Association of State Highway and Transportation Officials: Washington, DC: National Academy Press.

EDINA 2009. OS Land-Form PANORAMA DTM, [DXF geospatial data], Scale: 1:50,000, Tiles: sk42 and sk44, Ordnance Survey, GB. Using: EDINA Digimap Ordnance Survey Service, <http://edina.ac.uk/digimap>, Downloaded: June 2009.

EERENS, H. C., SLIGGERS, C. J. & VAN DEN HOUT, K. D. 1993. The CAR model: The Dutch method to determine city street air quality. *Atmospheric Environment. Part B. Urban Atmosphere,* 27, 389-399.

ELLIS, K., MCHUGH, C., CARRUTHERS, D. & STIDWORTHY, A. 2001. Comparison of ADMS-Roads, CALINE4 and UK DMRB Model Predictions for Roads. *7th International Conference on Harmonisation within Atmospheric Dispersion Modelling for Regulatory Purposes.* Belgirate (Lake Maggiore), Italy: Cambridge Environmental Research Consultants Ltd.

ESTECO. 2010. *Software for engineering design optimization, process integration and multidisciplinary optimiz* [Online]. Available: http://www.esteco.com/products.jsp [Accessed 16/05 2010].

EVANS, S., HUDSON-SMITH, A. & BATTY, M. 2007. 3-D GIS : Virtual London and beyond. *Cybergeo, Sélection des meilleurs articles de SAGEO 2005.*

GBC 2003. Air Quality Progress Report. Gedling Borough Council.

GBC 2007. Air Quality Detailed Assessments. Gedling Borough Council.

GINNEBAUGH, D. L., LIANG, J. & JACOBSON, M. Z. 2010. Examining the temperature dependence of ethanol (E85) versus gasoline emissions on air pollution with a largely-explicit chemical mechanism. *Atmospheric Environment,* 44, 1192-1199.

GOOGLE 2009. Google Earth (Version 5.1.3533.1731) Available on: http://earth.google.co.uk/download-earth.html.

HANNA, S. R., CHANG, J. C. & STRIMAITIS, D. G. 1993. Hazardous gas model evaluation with field observations. *Atmospheric Environment. Part A. General Topics,* 27, 2265-2285.

HANNA, S. R., STRIMAITIS, D. G. & CHANG, J. C. 1991. Hazard response modeling uncertainty (a quantitative method). Vol. 1, User's guide for software for evaluating hazardous gas dispersion models. Tech. Rep. prepared for Engineering and Services Laboratory, Air Force Engineering and Services Center, Tyndall Air Force Base, and American Petroleum Institute, by Earth Tech, 58 pp.

HIRTL, M. & BAUMANN-STANZER, K. 2007. Evaluation of two dispersion models (ADMS-Roads and LASAT) applied to street canyons in Stockholm, London and Berlin. *Atmospheric Environment,* In Press, Corrected Proof.

HOCHADEL, M., HEINRICH, J., GEHRING, U., MORGENSTERN, V., KUHLBUSCH, T., LINK, E., WICHMANN, H.-E. & MER, U. K. 2006. Predicting long-term average concentrations of traffic-related air pollutants using GIS-based information. *Atmospheric Environment,* 40, 542–553.

HOEK, G., BEELEN, R., DE HOOGH, K., VIENNEAU, D., GULLIVER, J., FISCHER, P. & BRIGGS, D. 2008. A review of land-use regression models to assess spatial variation of outdoor air pollution. *Atmospheric Environment,* 42, 7561-7578.

JAIN, S. & KHARE, M. 2010. Adaptive neuro-fuzzy modeling for prediction of ambient CO concentration at urban intersections and roadways. *Air Quality, Atmosphere & Health.*

JALALUDIN, B. B., O'TOOLE, B. I. & LEEDER, S. R. 2004. Acute effects of urban ambient air pollution on respiratory symptoms, asthma

medication use, and doctor visits for asthma in a cohort of Australian children. *Environmental Research,* 95, 32-42.

KANJI, G. K. 2006. *100 STATISTICAL TESTS*, SAGE Publications.

LANDMAP 2009. Building Heights, [2D shape file geospatial data]. Using: University of Manchester Landmap Service, http://landmap.mimas.ac.uk, Downloaded: June 2009.

LAXEN, D. & WILSON, P. 2002. A New Approach to Deriving NO_2 from NO_x for Air Quality Assessments of Roads. Defra and the Devolved Administrations: Air Quality Consultants Ltd. http://www.airquality.co.uk/reports/reports.php?action=category&section_id=6.

LEICA 2009. Leica Photogrammetry Suite Project Manager User's Guide. United States of America: Leica Geosystems Geospatial Imaging, LLC.

LINDER, W. 2006. Aerial Triangulation. *Digital Photogrammetry: A Practical Course* 2nd ed.: Springer.

MADSEN, C., CARLSEN, K. C. L., HOEK, G., OFTEDAL, B., NAFSTAD, P., MELIEFSTE, K., JACOBSEN, R., NYSTAD, W., CARLSEN, K.-H. & BRUNEKREEF, B. 2007. Modeling the intra-urban variability of outdoor traffic pollution in Oslo, Norway--A GA2LEN project. *Atmospheric Environment,* Volume 41, Issue 35, Pages 7500-7511, ISSN 1352-2310, DOI: 10.1016/j.atmosenv.2007.05.039.

MAJUMDAR, B., DUTTA, A., CHAKRABARTY, S. & RAY, S. 2009. Assessment of vehicular pollution in Kolkata, India, using CALINE 4 model. *Environmental Monitoring and Assessment,* 10.1007/s10661-009-1212-2, http://dx.doi.org/10.1007/s10661-009-1212-2.

NAEI. 2009. *the UKs National Atmospheric Emissions Inventory* [Online]. Available: http://www.naei.org.uk/ [Accessed 18/07/ 2009].

NAMDEO, A., MITCHELL, G. & DIXON, R. 2002. TEMMS: an integrated package for modelling and mapping urban traffic emissions and air quality. *Environmental Modelling & Software,* 17, 177-188.

NAMDEO, A. K. & COLLS, J. J. 1996. Development and evaluation of SBLINE, a suite of models for the prediction of pollution concentrations from vehicles in urban areas. *Science of The Total Environment,* 189-190, 311-320.

NCC 2007. A 612 Gedling Transport Improvement Scheme. Nottinghamshire County Council.

NCC. 2009a. *Broadmarsh Shopping Centre Planning Application* [Online]. Available: http://plan4.nottinghamcity.gov.uk/WAM/pas/showCaseFile.do;jsessionid=375CD1B76918C6EF266569A976DAA972?councilName=Nottingham+City+Council&appNumber=07%2F00117%2FPVAR3 [Accessed 29/05/ 2010].

NCC. 2009b. *Turning Point East : Nottingham City Council* [Online]. Available: http://www.nottinghamcity.gov.uk/index.aspx?articleid=1722 [Accessed 29/05/ 2010].

NCC. 2010. *NET Phase Two* [Online]. Nottingham City Council. Available: http://www.nottinghamcity.gov.uk/netphase2/index.aspx?articleid=7487 [Accessed 18/07/ 2010].

NCC & NCC 2006. Local Transport Plan for Greater Nottingham 2006/7 to 2010/11. Nottingham City Council and Nottinghamshire County Council.

NCC & NCC 2009. Congestion Delivery Plan. Nottingham City Council and Nottinghamshire County Council.

NOYES, P. D., MCELWEE, M. K., MILLER, H. D., CLARK, B. W., VAN TIEM, L. A., WALCOTT, K. C., ERWIN, K. N. & LEVIN, E. D. 2009. The

toxicology of climate change: Environmental contaminants in a warming world. *Environment International,* 35, 971-986.

OLESEN, H. R. 2001. Ten years of harmonization activities: past, present, and future. *7th International Conference on Harmonisation within Atmospheric Dispersion Modelling for Regulatory Purposes.* Belgirate, Italy, National Environmental Research Institute, Roskilde, Denmark: www.harmo.org.

PARRA, M. A., SANTIAGO, J. L., MARTÍN, F., MARTILLI, A. & SANTAMARÍA, J. M. 2010. A methodology to urban air quality assessment during large time periods of winter using computational fluid dynamic models. *Atmospheric Environment,* 44, 2089-2097.

PCS 2001. Second and Third Stage of Air Quality Review and Assessment Report. Nottingham City Council (Pollution Control Section).

PCS 2003. Stage Four Review and Assessment of Nottingham's Air Quality Management Areas July 2003. Nottingham City Council (Pollution Control Section).

PCS 2004. Detailed Assessment v1a October 2004. Nottingham City Council (Pollution Control Section).

PCS 2006. Updating and Screening Assessment Report. Nottingham City Council (Pollution Control & Envirocrime Section).

PCS 2008. Detailed Assessment Consultation Document. Nottingham City Council (Pollution Control & Envirocrime Section).

PCS 2010. Detailed Assessment 2009. Nottingham City Council (Pollution Control & Envirocrime Section).

POOLEY, C. G. & TURNBULL, J. 2005. Coping with congestion: responses to urban traffic problems in British cities c.1920-1960. *Journal of Historical Geography,* 31, 78-93.

RBC 2005. Second Round Review and Assessment of Local Air Quality Rushcliffe Borough Council.

RBC. 2010a. *Air Quality Management Areas* [Online]. Rushcliffe Borough Council. Available: http://www.rushcliffe.gov.uk/doc.asp?cat=9659 [Accessed 01/06/ 2010].

RBC 2010b. Air Quality Progress Report. Rushcliffe Borough Council.

RUCHIRAWAT, M., SETTACHAN, D., NAVASUMRIT, P., TUNTAWIROON, J. & AUTRUP, H. 2007. Assessment of potential cancer risk in children exposed to urban air pollution in Bangkok, Thailand. *Toxicology Letters,* 168, 200-209.

SANDSTROM, T. & BRUNEKREEF, B. 2007. Traffic-related pollution and lung development in children. *The Lancet,* 369, 535-537.

SEARS, A. & JACKO, J. A. 2008. *The Human-Computer Interaction Handbook: Fundamentals, Evolving Technologies, and Emerging Applications*, Lawrence Erlbaum Associates.

SMIT, R., NTZIACHRISTOS, L. & BOULTER, P. 2010. Validation of road vehicle and traffic emission models - A review and meta-analysis. *Atmospheric Environment,* 44, 2943-2953.

SPSS 2008. SPSS Base 17.0 for Windows User's Guide. Chicago IL.

USEPA 1998. Revised draft users' guide for the AMSrEPA regulatory model - AERMOD. Research Triangle Park, North Carolina.

VAN VLIET, D. 1982. SATURN — a modern assignment model. *Traffic Engineering and Control,* 23 (12), 578–581.

VENEGAS, L. E. & MAZZEO, N. A. 2006. Modelling of urban background pollution in Buenos Aires City (Argentina). *Environmental Modelling & Software,* 21, 577-586.

VIENNEAU, D., DE HOOGH, K., BEELEN, R., FISCHER, P., HOEK, G. & BRIGGS, D. 2010. Comparison of land-use regression models between Great Britain and the Netherlands. *Atmospheric Environment,* 44, 688-696.

VIENNEAU, D., DE HOOGH, K. & BRIGGS, D. 2009. A GIS-based method for modelling air pollution exposures across Europe. *Science of The Total Environment*.

WANG, X. 2005. Integrating GIS, simulation models, and visualization in traffic impact analysis. *Computers, Environment and Urban Systems,* 29, 471-496.

WANG, X., SHI, J. & HUANG, H. 2008. Traffic-related air quality analysis and visualisation. *Civil Engineering and Environmental Systems,* 25, 157 - 166.

WHYTE, J., BOUCHLAGHEM, N., THORPE, A. & MCCAFFER, R. 2000. From CAD to virtual reality: modelling approaches, data exchange and interactive 3D building design tools. *Automation in Construction,* 10, 43-55.

ZHU, Q., LI, F. & ZHANG, Y. 2005. Unified Representation of Three Dimensional City Models. *In:* JIANG, J. (ed.) *Proceedings of the ISPRS Hangzhou 2005 Workshop.* Hangzhou, China.